

**Targeting Tumour Angiogenesis in
Colorectal Cancer Liver Metastases**

Peter John Webster

Submitted in accordance with the requirements for the degree of
Doctor of Philosophy

The University of Leeds
Faculty of Medicine and Health

December 2016

The candidate confirms that the work submitted is his own and that appropriate credit has been given where reference has been made to the work of others.

This copy has been supplied on the understanding that it is copyright material and that no quotation from the thesis may be published without proper acknowledgement.

The right of Peter John Webster to be identified as Author of this work has been asserted by him in accordance with the Copyright, Designs and Patents Act 1988.

© 2016 The University of Leeds and Peter John Webster

Acknowledgements

I would like to thank the following people, without whom this work would not have been possible:

Professor David Beech for the opportunity to conduct research in his laboratory as well as all his sound advice, support and guidance throughout my studies.

Mr Dermot Burke for all his supervision both in my academic studies and clinical work. I hope it has not been too difficult supervising your first PhD student!

Dr Richard Young, Dr Jing Li, Dr Heather Martin and Dr Darren Tomlinson for their RNA interference screening work, which helped form the basis for this project.

Dr Sally Boxall for all her knowledge and help with flow cytometry studies.

Leeds Teaching Hospitals Charitable Foundation for their generous funding to enable me to undertake this research.

All patients who selflessly donated tissue at St. James's University Hospital, Leeds. Sadly, some of these patients have already passed away and I hope that through their donations this research will help improve outcomes for future patients.

Mr Raj Prasad and Professor Peter Lodge, without whom I would not have been able to acquire patient tissue samples.

Hannah Gaunt for all her help. From accidentally throwing my cells in the bin to teaching me how to do the perfect western blot, I have really appreciated her support and friendship throughout this PhD.

Dr Baptiste Rode for his help with the Piezo1 mice and love of all things Yorkshire!

Anna Littlejohns for all her work and enthusiasm as an intercalating medical student and keen WEE1 investigator.

Elizabeth Gabriel for helping to rationalise the proteomics data.

Nicola (Nikki) Blythe, Katie Musialowski, Elizabeth (Beth) Evans, Adam Hyman, Dr Nick Moss, Dr Hollie Appleby and Dr Lara Morley who themselves are all at various stages of the PhD process. They have all helped make this PhD a great experience.

Mum, Dad, James and Murts for their love, support and never-ending encouragement in everything I do. My Gran sadly passed away during my PhD studies and were she still alive I know she would be happily telling everyone about this work and what I've achieved!

Sarah for all her love and unwavering support as my girlfriend. Although you going away to New Zealand to work for a year enabled me to complete most of this PhD, it was also a lonely time and I couldn't wait for you to come back! I hope that when you read this you are proud and finally understand what WEE1 is all about.

Abstract

Colorectal cancer liver metastases (CLM) remain a significant cause of cancer-related morbidity and mortality. Central to their survival and growth is the process of tumour angiogenesis. Current clinical anti-angiogenic therapies target vascular endothelial growth factor signalling, but resistance to therapy is problematic. The aim of this study was to identify proteins critical for CLM endothelial cell (CLMEC) survival that could be targeted for the development of new anti-angiogenic therapies.

CLMECs and endothelial cells of normal adjacent liver (LECs) were isolated from patients undergoing curative resection. The two cell types were superficially similar, exhibiting markers and functional characteristics expected of endothelial cells. However, a number of differences in protein expression were identified, one of which was the previously unrecognised upregulation of the WEE1 checkpoint-kinase, a target of the small molecule WEE1 inhibitor AZD1775, currently in clinical trials. AZD1775 monotherapy was shown to inhibit proliferation and migration of CLMECs. Investigation of the underlying mechanism suggested induction of double-stranded DNA (DS-DNA) breaks due to a critical nucleotide shortage, which then led to caspase-3 dependent apoptosis. The implication for CLMEC tube formation was striking, with AZD1775 inhibiting branching tube formation by 83%. AZD1775 also had direct anti-cancer activity in a p53-mutated colorectal cancer cell line (HT29). In combination with 5-FU it caused increased caspase-3 dependent apoptosis because of DS-DNA breaks, not premature mitosis, which is thought to be the mechanism of AZD1775 toxicity when used in combination with DNA-damaging agents.

Proteomic screening of matched LECs and CLMECs identified a further 157 differentially expressed proteins, including up-regulation of the established endogenous angiogenesis inhibitors thrombospondin-1 and vascular endothelial growth factor receptor-1. The mechanosensitive, Ca²⁺ permeable ion channel Piezo1 was identified as another potential anti-angiogenic target in CLMECs. Modulation of the Piezo1 channel with the newly discovered Piezo1 activator Yoda1 is demonstrated for the first time in CLMECs and shown to induce phosphorylation of endothelial nitric oxide synthase.

This study has identified a number of proteins that are differentially expressed in CLMECs, which could be targeted for the development of anti-angiogenic therapies in the treatment of CLM. AZD1775 has anti-angiogenic activity in CLMECs and Piezo1 represents another target which can be investigated in future studies.

Table of Contents

Acknowledgements	iii
Abstract	v
Table of Contents	vii
List of Tables	xiv
List of Figures	xv
List of Publications and Communications	xviii
Abbreviations	xxi
Chapter 1: Introduction	1
1.1 Historical Perspective	1
1.2 Current Treatment of Colorectal Cancer	3
1.3 Failure of Treatment	7
1.3.1 Local Recurrence	7
1.3.2 Metastatic Disease	7
1.4 Development of Colorectal Cancer Liver Metastases	8
1.4.1 Colorectal Cancer Biology	8
1.4.2 The Metastatic Cascade	10
1.4.3 Progression of Colorectal Cancer Liver Metastases	13
1.5 Treatment of Colorectal Cancer Liver Metastases	16
1.5.1 Conservative	16
1.5.2 Surgical Resection	16
1.5.3 Systemic Neoadjuvant Chemotherapy.....	17
1.5.4 Systemic Adjuvant Chemotherapy.....	17
1.5.5 Regional Adjuvant Chemotherapy	18
1.5.6 Systemic Palliative Chemotherapy	18
1.5.7 Radiofrequency Ablation	19
1.5.8 Transarterial Chemoembolisation	19
1.5.9 Microwave Hyperthermia and Interstitial Laser Ablation	20
1.5.10 Percutaneous Ethanol Injection	21
1.5.11 Cryotherapy.....	21
1.5.12 Hepatic Transplant	21
1.5.13 Biological Agents.....	23

1.6 Angiogenesis.....	25
1.6.1 The Cardiovascular System	25
1.6.2 The Endothelium	26
1.6.3 Sprouting Angiogenesis.....	28
1.6.3.1 The Role of Hypoxia	28
1.6.3.2 The Role of Vascular Endothelial Growth Factor	29
1.6.3.3 Endothelial Tip, Stalk and Phalanx Cells	31
1.6.3.4 DLL4-Notch Signalling.....	32
1.6.3.5 Maturation of Blood Vessels	34
1.6.4 Intussusceptive Angiogenesis	36
1.6.5 Tumour Angiogenesis	37
1.6.5.1 Characteristics of Tumour Blood Vessels	37
1.6.5.2 Tumour Endothelial Cells.....	39
1.6.5.3 Vasculogenic Mimicry.....	41
1.6.5.4 Vessel Co-option	41
1.6.5.5 Angiogenesis in Colorectal Cancer Liver Metastases.....	42
1.7 Anti-Angiogenic Agents	43
1.7.1 Endogenous Angiogenesis Inhibitors.....	43
1.7.2 Anti-Angiogenic Drugs used in Metastatic Colorectal Cancer	45
1.7.3 Toxicity Associated with Anti-Angiogenic Therapy.....	49
1.7.4 Failure of Anti-Angiogenic Therapy	51
1.8 Summary.....	53
Aims and Objectives	54
Chapter 2: Materials and Methods	55
2.1 Cell Lines and Cell Culture	55
2.2 Human Liver Endothelial Cell Isolation	56
2.3 Mouse Liver Endothelial Cell Isolation.....	60
2.3 Drugs and Reagents	61
2.3.1 Drugs	61
2.3.1.1 AZD1775	61
2.3.1.2 RO-3306.....	61

2.3.1.3 5-Fluorouracil	62
2.3.1.4 Oxaliplatin	62
2.3.1.5 Irinotecan	62
2.3.1.6 Yoda1	63
2.3.1.7 Ionomycin	63
2.3.2 VEGF	65
2.3.3 ATP	65
2.3.4 Matrigel®	65
2.3.5 Nucleosides	65
2.4 Transfections	66
2.5 Western Blotting	68
2.5.1 Solutions	68
2.5.2 Cell Lysis	68
2.5.3 Protein Quantification	69
2.5.4 Western Blotting	69
2.5.5 Protein Visualisation	70
2.6 WST-1 Proliferation Assay	72
2.7 Vybrant® DyeCycle™ Green Proliferation Assay	72
2.8 Migration Assays	73
2.9 In vitro Co-Culture Tube Formation Assay	75
2.10 Matrigel® Tube Formation Assay	77
2.11 Flow Cytometry	78
2.11.1 General Principles	78
2.11.2 Sample Preparation	81
2.11.3 Cell Cycle Analysis	81
2.11.4 γH2AX Detection	84
2.11.5 pHH3 Detection	87
2.11.6 Data Analysis	87
2.12 Intracellular Ca ²⁺ Measurement	88
2.13 Immunocytochemistry	90
2.14 Caspase-3 Measurement	92
2.15 Endothelial Cell Alignment	94

2.16 RNA Interference Screening.....	94
2.17 Proteomic Studies	95
2.17.1. Sample Preparation.....	95
2.17.2 TMT- Labelling and High pH reversed-phase chromatography	95
2.17.3 Nano-LC Mass Spectrometry	96
2.17.4 Data Analysis	97
2.18 Generation of Endothelial Specific Piezo1 Knockout Mice.....	98
2.19 Data Analysis	99
Chapter 3: Characterisation of Colorectal Cancer Liver Metastases	
 Endothelial Cells	100
3.1 Endothelial Cells Isolated from Colorectal Cancer Liver Metastases Express Recognised Endothelial Markers	101
3.2 VEGF Evokes Ca ²⁺ Entry in LECs and CLMECs.....	104
3.3 CLMECs Have Endothelial Specific Functional Properties	106
3.4 RNA Interference Screen Reveals WEE1 to have Critical Role in Regulating Endothelial Cell Proliferation.....	109
3.5 Genetic and Chemical Inhibition of WEE1 Inhibits HUVEC Proliferation.....	111
3.6 Genetic and Chemical Inhibition of WEE1 Regulates Phosphorylation of CDK1	114
3.7 WEE1 is Upregulated in CLMECs	116
3.8 Summary of Findings	118
3.9 Discussion.....	119
3.9.1 Characterisation of CLMECs	119
3.9.2 The VEGF-VEGFR-2 Signalling Pathway in CLMECs	121
3.9.3 WEE1 Inhibition as an Anti-Angiogenic Target	123
3.9.3.1 WEE1 Function and Regulation.....	123
3.9.3.2 WEE1 Inhibition as an Anti-Cancer Therapy.....	124
3.9.3.3 The Role of WEE1 in the Endothelium.....	126
3.9.4 RNA interference Screening Results	127
3.9.5 Conclusion	129

Chapter 4: WEE1 Inhibition has Anti-Angiogenic Effects in Endothelial Cells of Colorectal Cancer Liver Metastases	130
4.1 Genetic and Chemical Inhibition of WEE1 Inhibits Proliferation in CLMECs.....	131
4.2 AZD1775 Inhibits Angiogenic Processes in CLMECs	134
4.3 AZD1775 Changes the Cell Cycle Distribution in CLMECs as a Result of Altered CDK1 Phosphorylation	138
4.4 AZD1775 Induces DS-DNA Breaks in CLMECs	141
4.5 AZD1775 Induced DS-DNA Breaks in CLMECs can be Prevented if Co-Treated with RO-3306 or Exogenous Nucleosides	144
4.6 AZD1775 Causes Caspase-3 Dependent Apoptosis in CLMECs which can be Rescued with Exogenous Nucleoside Supplementation	147
4.7 Summary of Findings	149
4.8 Discussion.....	150
4.8.1 Functional Importance of WEE1 in CLMECs	150
4.8.2 In Vitro Angiogenesis Assays	151
4.8.3 Mechanism of Action of WEE1 Inhibition	153
4.8.4 Implications of AZD1775 as an Anti-Angiogenic Drug	155
4.8.5 Conclusion	159
Chapter 5: AZD1775 Induces Toxicity Through DS-DNA Breaks Independently of Chemotherapeutic Agents in p53 Mutated Colorectal Cancer Cells	160
5.1 AZD1775 Enhances 5-FU Toxicity in HT29 cells, but only Enhances Other Colorectal Cancer Chemotherapeutic Agents at Low Concentrations.....	163
5.2 AZD1775 Decreases pCKD1-Y15 in 5-FU Treated HT29 Cells and Increases the Number of Cells in S Phase and G2/M Phase.....	165
5.3 5-FU and AZD1775 Combination Therapy Causes Increased Mitosis and DS-DNA Breaks in HT29 Cells	168
5.4 AZD1775 Causes DS-DNA Breaks in HT29 Cells when used as a Monotherapy	171
5.5 AZD1775 and 5-FU Combination Therapy Causes DS-DNA Breaks and Caspase-3 Dependent Apoptosis that can be Rescued by Exogenous Nucleoside Addition	173
5.6 Summary of Findings	176

5.7 Discussion.....	177
5.7.1 Dosing Strategies	177
5.7.2 AZD1775 Mechanism of Action	178
5.7.3 Importance of p53 Status	181
5.7.4 Implications for Ongoing Clinical Trials.....	182
5.7.5 Conclusion	183
Chapter 6: Identifying New Anti-Angiogenic Targets in Colorectal Cancer Liver Metastases using a Proteomics Screen	184
6.1 LECs and CLMECs Express Numerous Endothelial Cell Markers.....	185
6.2 Quantitative Proteomics Reveals Differentially Expressed Proteins in CLMECs and LECs	190
6.3 Validation of Proteomic Results.....	193
6.4 Thrombospondin-1 as an Anti-Angiogenic Target.....	197
6.5 Piezo1 as an Anti-Angiogenic Target	201
6.5.1 Yoda1 Causes Ca ²⁺ Entry Specifically Through Piezo1	204
6.5.2 Yoda1 Causes eNOS Phosphorylation in CLMECs	208
6.6 Summary of Findings	210
6.7 Discussion.....	211
6.7.1 Validation of LECs and CLMECs.....	211
6.7.2 Results of The Proteomics Study	212
6.7.3 Identification of Further Anti-Angiogenic Targets in CLM	216
6.7.3.1 Thrombospondin-1	216
6.7.3.2 VEGFR-1/sVEGFR-1.....	217
6.7.3.3 Piezo1	219
6.7.4 Conclusion	223
Chapter 7: Conclusions and Future Work.....	224
7.1 Summary of Key Findings	225
7.2 Future Directions.....	229
7.2.1 The Functional Importance of WEE1 in the Endothelium in vivo	229
7.2.2 Optimal Dosing Strategy for AZD1775.....	230
7.2.3 Investigation of Piezo1 as an Anti-Angiogenic Target.....	231

7.2.4 Interrogation of Proteomic Data and Investigation of Further Hits	232
7.2.4 Future Clinical Implications	232
7.3 Conclusion	234
References	235
Appendix I: Differentially Expressed Proteins in the Proteomics Screen.....	279

List of Tables

Table 1 The Tumour Node Metastasis (TNM) Classification System.....	4
Table 2 The AJCC Colorectal Cancer Staging System	5
Table 3 Endogenous Inhibitors of Angiogenesis.....	44
Table 4 Summary of Clinical Trials Investigating Anti-Angiogenic Agents in Metastatic Colorectal Cancer	48
Table 5 Pooled WEE1 siRNA Sequences	67
Table 6 Summary of Primary Antibodies used for Western Blotting....	71
Table 7 Summary of Primary Antibodies used for Immunocytochemistry	91
Table 8 Patient Characteristics of the Matched LEC and CLMEC Samples Submitted for Proteomic Studies	187
Table 9 Colorectal Cancer History for Each Patient Investigated with Proteomic Studies.....	188
Table 10 Differentially Expressed Proteins in LECs and CLMECs	192
Table 11 Validated Alterations in Protein Expression in CLMECs	228

List of Figures

Figure 1 The Adenoma Carcinoma Sequence.....	9
Figure 2 The Metastatic Cascade.....	12
Figure 3 The Hepatic Sinusoid.....	14
Figure 4 The Vascular Endothelium	27
Figure 5 Vascular Endothelial Growth Factors and their Receptors	30
Figure 6 DLL4-Notch Signalling.....	33
Figure 7 Pericyte Stabilisation Through Ang-1/Tie-2 Signalling.....	35
Figure 8 VEGF/VEGFR-2 Signalling and Consequences of Inhibition.....	50
Figure 9 Immuno-Magnetic Selection of CD31-Positive Cells.....	59
Figure 10 Chemical Structures of Chemotherapeutic Agents	64
Figure 11 Incucyte™ Kinetic Imaging System and Essen Woundmaker™.....	74
Figure 12 In vitro Co-Culture Tube Formation Assay.....	76
Figure 13 Components of a Flow Cytometer.....	78
Figure 14 Forward and Side Scatter	80
Figure 15 Measurement of Fluorescence	80
Figure 16 Eliminating Doublets from Cell Cycle Analysis.....	83
Figure 17 Fluorescence Emission Profiles for Alexa 488 and PI.....	85
Figure 18 Gating Strategy for the Detection of γ H2AX Positive Cells	86
Figure 19 Flexstation II (Molecular Devices).....	89
Figure 20 NucView™ 488 Caspase-3 Assay.....	93
Figure 21 Isolated LECs and CLMECs Express CD31	102
Figure 22 CLMECs Express Recognised Endothelial Markers	103
Figure 23 CLMEC VEGF-Evoked Ca^{2+} Entry is Decreased Compared to Matched LECs.....	105
Figure 24 CLMECs Align in Response to Shear Stress.....	107
Figure 25 CLMECs Form Tubular Structures when Grown on Matrigel®	108
Figure 26 RNA Interference Screen Identifies WEE1 as a Regulator of HUVEC Proliferation	110

Figure 27 Genetic Inhibition of WEE1 Decreases Proliferation in HUVECs	112
Figure 28 Chemical Inhibition of WEE1 Decreases Proliferation in HUVECs	113
Figure 29 Genetic and Chemical Inhibition of WEE1 Decreases pCDK1-Y15 in HUVECs	115
Figure 30 WEE1 is Upregulated in CLMECs Compared to Matched LECs.....	117
Figure 31 Genetic Inhibition of WEE1 Decreases Proliferation in CLMECs	132
Figure 32 AZD1775 Inhibits CLMEC Proliferation	133
Figure 33 AZD1775 Inhibits CLMEC Migration.....	135
Figure 34 AZD1775 Inhibits CLMEC Tube Formation	136
Figure 35 AZD1775 Does Not Affect Fibroblast Bed Integrity.....	137
Figure 36 AZD1775 Increases the Number of CLMECs in S Phase and G2/M Phase	139
Figure 37 Genetic and Chemical Inhibition of WEE1 Decreases pCDK1-Y15 in CLMECs.....	140
Figure 38 AZD1775 Induces DS-DNA Breaks in CLMECs	142
Figure 39 AZD1775 Does Not Increase Mitosis in CLMECs	143
Figure 40 AZD1775 Induced DS-DNA Breaks in CLMECs Can be Prevented if Co-treated with RO-3306	145
Figure 41 AZD1775 Induced DS-DNA Breaks in CLMECs Can be Prevented if Co-treated with Exogenous Nucleoside Addition....	146
Figure 42 AZD1775 Causes Caspase-3 Dependent Apoptosis in CLMECs	148
Figure 43 AZD1775 Enhances the Cytotoxicity of 5-FU.....	164
Figure 44 Combination Therapy Decreases pCDK1-Y15 compared to 5-FU Treatment Alone.....	166
Figure 45 5-FU and AZD1775 Combination Therapy Increases the Number of HT29 Cells in S Phase and G2/M Phase	167
Figure 46 AZD1775 Causes Progressive DS-DNA Breaks Over 24 hrs in HT29 Cells Pre-Treated with 5-FU.....	169
Figure 47 AZD1775 Causes An Early Peak in Mitosis in HT29 Cells Pre-Treated with 5-FU	170
Figure 48 AZD1775 Monotherapy Inhibits Proliferation of HT29 Cells and Causes DS-DNA Breaks	172

Figure 49 DS-DNA Breaks Caused by AZD1775 and 5-FU Combination Therapy can be Prevented by Adding Exogenous Nucleosides.....	174
Figure 50 AZD1775 and 5-FU Combination Therapy Induces Caspase-3 Dependent Apoptosis, which can be Prevented with Exogenous Nucleoside Addition	175
Figure 51 LECs and CLMECs Express a Range of Endothelial Markers	189
Figure 52 Heat Map of the Total LEC and CLMEC Proteome Determined by Proteomic Studies	191
Figure 53 vWF is Down-Regulated in CLMECs	194
Figure 54 VEGFR-1 and sVEGFR-1 are Up-Regulated in CLMECs	195
Figure 55 Fibronectin is Down-Regulated in CLMECs	196
Figure 56 Thrombospondin-1 is Up-Regulated in CLMECs	198
Figure 57 TSP-1 Knockdown Increases Proliferation in CLMECs	199
Figure 59 Piezo1 Expression is not Altered in CLMECs.....	202
Figure 60 Yoda1 evokes Ca²⁺ Entry in LECs and CLMECs	203
Figure 61 Yoda1 does not Evoke Ca²⁺ Entry in Mouse Liver Endothelial Cells with Piezo1 Knockout.....	206
Figure 62 Endothelial Piezo1 Knockout Does Not Effect ATP and Ionomycin Evoked Ca²⁺ Entry in Mouse Liver Endothelial Cells	207
Figure 63 Yoda1 Induces Phosphorylation of eNOS at Ser-1177 in CLMECs	209
Figure 64 Proposed Mechanism of Action of AZD1775 in CLMECs	227

List of Publications and Communications

Published Manuscripts

1) Li J, Bruns AF, Hou B, Rode B, **Webster PJ**, Bailey MA, Appleby HL, Moss NK, Ritchie JE, Yuldasheva NY, Tumova S, Quinney M, McKeown L, Taylor H, Prasad KR, Burke D, O'Regan D, Porter KE, Foster R, Kearney MT, Beech DJ. Orai3 Surface Accumulation and Calcium Entry Evoked by Vascular Endothelial Growth Factor. *Arterioscler Thromb Vasc Biol.* 2015 Sep;35(9):1987-94.

2) **Webster PJ**, Littlejohns AT, Gaunt HJ, Young RS, Rode B, Ritchie JE, Stead LF, Harrison S, Droop A, Martin HL, Tomlinson DC, Hyman AJ, Appleby HL, Boxall S, Bruns AF, Li J, Prasad KR, Lodge JPA, Burke DA, Beech DJ. Upregulated WEE1 protects endothelial cells of colorectal cancer liver metastases. *Oncotarget (In Press)*

3) **Webster PJ**, Littlejohns AT, Gaunt HJ, Prasad KR, Beech DJ, Burke DA. AZD1775 Induces Toxicity Through Double-Stranded DNA Breaks Independently of Chemotherapeutic Agents in p53 Mutated Colorectal Cancer Cells. *Submitted to Cell Cycle (In Press)*

Manuscripts in Preparation

1) Rode B, Shi J, Drinkhill MJ, **Webster PJ**, Bailey MA, Yuldasheva NY, Ludlow MJ, Cubbon RM, Endesh N, Li J, Morley L, Gaunt HJ, Baxter PD, Wheatcroft SB, Kearney MT, Beech DJ. Specialised Piezo1 channels sense whole body physical activity to reset cardiovascular homeostasis and enhance performance. Submitted to Nature Communications

2) Gaunt HJ, Cuthbertson K, Endesh N, Evans E, **Webster PJ**, Tanahashi Y, Li J, Rode B, Viswambharan H, Blythe N, Ludlow MJ, Bruns A, Burke DA, Kearney MT, Foster R, Beech DJ. CaMKII[δ] tightly couples Piezo1 channels to nitric oxide production.

Oral Presentations

1) **Webster PJ**, Littlejohns AT, Beech DJ, Burke DA. AZD1775 Induces Toxicity Through Double-Stranded DNA Breaks Independent of 5-FU Activity in p53 Mutated Colorectal Cancer Cells. Oncology Session. SARS, Dublin, January 2017.

2) Gaunt HJ, Endesh N, **Webster PJ**, Cuthbertson K, Evans E, Rode B, Viswambharan H, Tanahashi Y, Li J, Foster R, Beech DJ. Piezo1 Mechanosensor Signalling in the Endothelium. Northern Vascular Biology Forum, Hull, December 2016.

3) Littlejohns AT, **Webster PJ**, Beech DJ, Burke DA. AZD1775 Kills Colorectal Cancer Cells Through Nucleotide Exhaustion and Double-Stranded DNA Breaks Independent of p53 Status. The 6th Christie International Student Cancer Conference, Manchester, September 2016.

4) **Webster PJ**, Burke DA, Beech DJ. Exhausted to Death. AZD1775 Inhibits Angiogenesis in Colorectal Liver Metastases Through Nucleotide Depletion. Basic and Applied Science Session, ASGBI, Belfast, May 2016.

5) **Webster PJ**. AZD1775 Inhibits Endothelial Cell Remodelling in Colorectal Liver Metastases *in vitro*. 4th Endothelial Retreat, Ullswater, January 2016.

6) **Webster PJ**, Burke DA, Prasad KR, Beech DJ. AZD1775 Inhibits Endothelial Cell Remodelling in Colorectal Liver Metastases in Vitro. Burnand-Williams Prize Session, SARS, London, January 2016.

7) **Webster PJ**, Burke DA, Prasad KR, Beech DJ. Not so WEE...Targeting the G2/M Checkpoint Kinase as an Anti-Angiogenic Therapy for Colorectal Liver Metastases. Oral Prize Session, Yorkshire and Humber Academic Day, Sheffield, June 2015.

8) **Webster PJ**. Inhibition of the G2/M Checkpoint Kinase WEE1 as an Anti-Angiogenic Therapy for Colorectal Liver Metastases. 3rd Endothelial Retreat, Ullswater, January 2015.

9) **Webster PJ**, Young RS, Martin HL, Harrison S, Stead LF, Tomlinson DC, Prasad KR, Burke DA, Beech DJ. Inhibition of the G2/M Checkpoint Kinase WEE1 as an Anti-Angiogenic Therapy for Colorectal Liver Metastases. RSM Future Projects Prize Session, SARS, Durham, January 2015.

Poster Presentations

1) **Webster PJ**, Young RS, Martin HL, Harrison S, Stead LF, Prasad KR, Burke DA, Beech DJ. Not so WEE...Targeting the G2/M Checkpoint Kinase as an Anti-Angiogenic Therapy for Colorectal Liver Metastases. Yorkshire and Humber Academic Day, Sheffield, June 2015 (**Awarded Runner Up Poster Presentation Prize**)

Abbreviations

AJCC	American Joint Committee on Cancer
APC	Adenomatous Polyposis Coli
BSA	Bovine Serum Albumin
CDK1	Cyclin Dependent Kinase 1
CLM	Colorectal Cancer Liver Metastases
CLMEC	Colorectal Cancer Liver Metastases Endothelial Cell
DAG	Diacyl Glycerol
DLL4	Delta-Like Ligand 4
DMSO	Dimethyl Sulfoxide
DS-DNA	Double-Stranded DNA
dTTP	Deoxythymidine Triphosphate
EBM-2	Endothelial Cell Basal Medium
EGFR	Epidermal Growth Factor Receptor
eNOS	Endothelial Nitric Oxide Synthase
ER	Endoplasmic Reticulum
EPC	Endothelial Progenitor Cell
FCS	Foetal Calf Serum
FOLFIRI	5-FU, Irinotecan, Leucovorin
FOLFOX	5-FU, Oxaliplatin, Leucovorin
HIA	Hepatic Intra-Arterial
HIF-1	Hypoxia-Inducible Factor 1
HRE	Hypoxia Response Element
IFL	Irinotecan, 5-FU, Leucovorin
IMS	Immune-Magnetic Sorting
IP ₃	Inositol Triphosphate
HUVEC	Human Umbilical Vein Endothelial Cell
KRAS	V-Ki-ras2 Kirsten rat sarcoma viral oncogene homolog
LEC	Liver Endothelial Cell

LYVE-1	Lymphatic Vessel Endothelial Hyaluronan Receptor 1
MACS	Magnetically-Activated Cell Sorting
mLEC	Mouse Liver Endothelial Cell
MRI	Magnetic Resonance Imaging
NHDF	Normal Human Dermal Fibroblasts
PIP ₂	Phosphatidylinositol 4,5-biphosphate
PBS	Phosphate Buffered Saline
PDPN	Podoplanin
PDGF-β	Platelet-Derived Growth Factor-β
PGF	Placental Growth Factor
PI	Propidium Iodide
PLK1	Polio-Like Kinase 1
PROX1	Prospero Homeobox Protein 1
RPM	Revolutions Per Minute
RWD	Relative Wound Density
RFA	Radiofrequency Ablation
SBS	Standard Bath Solution
sVEGFR-1	Soluble Vascular Endothelial Growth Factor Receptor 1
TACE	Transarterial Chemoembolisation
TEC	Tumour Endothelial Cell
TEM	Tumour Endothelial Marker
TNM	Tumour Node Metastases
TS	Thymidylate Synthase
TSP	Thrombospondin
TSRs	Thrombospondin Type-1 Repeats
VEGF	Vascular Endothelial Growth Factor
VEGFR	Vascular Endothelial Growth Factor Receptor
vWF	von Willebrand Factor
5-FU	5-Fluorouracil

Chapter 1: Introduction

Colorectal cancer is a global health problem with an estimated 1.4 million cases and 693,900 deaths occurring per year (Torre et al., 2015). In the United Kingdom, over 41,000 people are diagnosed with colorectal cancer annually, a trend that has slowly increased over the last 50 years (Cancer Research UK, 2016). Advancing diagnostic technology, increasing resources and the introduction of a national screening program have helped improve disease detection, however, outcomes for patients with metastatic colorectal cancer remain poor.

This chapter will review the biology of colorectal cancer and how this has shaped current treatment options. Reasons for treatment failure, including metastatic spread to the liver, will be considered and how angiogenesis and tumour endothelial cells are essential to this process. Finally, current anti-angiogenic treatments will be reviewed including their efficacy in metastatic colorectal cancer and associated side effects.

1.1 Historical Perspective

Cancer appears in the medical literature as early as 1600 BC in the Edwin Smith papyrus, where the oldest description of the disease exists. However, the origin of the word cancer is attributed to ancient Greece and the Hippocratic physicians who used the word *karkinoma*, meaning “crab”, to describe non-healing “cancer” (Weiss, 2000). This is thought to refer to the distension of localised veins in advanced breast cancer that had the appearance of the legs of a crab.

With regard to colorectal cancer, its signs and symptoms were observed as early as the 14th century by the English surgeon John of Arderne. He recognised the progressive and destructive nature of the disease “*so this sickness lurks within in the beginning, but after the passage of time it ulcerates and emerges eroding the anus*”. Despite this, no form of excisional surgery was performed for at least 400 years. It was not until the eighteenth century when Giovanni Morgagni proposed excision of the rectum for rectal cancer that surgery was considered a therapeutic option (Galler et al., 2011). In 1826 Jacques LisFranc performed the first successful excision of a rectal tumour. He went on to perform nine more resections, but haemorrhage and sepsis were common and mortality rates were high (Galler et al., 2011).

With the advent of anaesthesia and asepsis there was an explosion of surgical techniques for excising rectal cancer, but recurrent disease was problematic and seemed inevitable. In England, William Ernest Miles noted the problems of local recurrence in his own patients. Out of 57 perineal resections, 54 patients (95%) developed local recurrence, most commonly within the first 6 months of resection (Miles, 1908). Through postmortem dissections he noted the pattern of recurrence and designed an operation to remove the rectum and the “upward direction of spread” that he coined the “radical abdominoperineal resection”. In a 1908 *Lancet* article Miles reported 12 procedures (Miles, 1908). He calculated a 42% mortality rate (5 deaths) with 7 survivors tumour-free at one year.

Subsequent surgical developments have been focused on improving excisional techniques to limit local recurrence and metastatic disease. The most significant of these being the anterior resection with “total mesorectal excision” developed by

Richard Heald. Based on the embryological development of the hindgut, this sphincter preserving operation involves resection of the tumour and mesorectum en bloc to the level of the levator muscles. Heald's technique led to local recurrence rates of 3.6% (Heald and Ryall, 1986).

1.2 Current Treatment of Colorectal Cancer

Surgical excision remains the mainstay of treatment for colorectal cancer. The twenty-first century has seen the advent of laparoscopic and robotic colorectal cancer surgery techniques with comparable oncological outcomes to open surgery (Green et al., 2013, Mak et al., 2014, Vennix et al., 2014, Feroci et al., 2016). Improvements in anaesthesia, peri- and post-operative care have also led to significant reductions in operative morbidity and mortality. However, the long-term prognosis for patients with colorectal cancer has only modestly improved over the last 30 years. In 1985, 58.1% of patients diagnosed with colorectal cancer were still alive at 5-years, compared to 67.2% in 2008 (Surveillance Epidemiology and End Results (SEER) Program, 2016).

Once a diagnosis of colorectal cancer is established the local and distant extent of the disease must be determined to provide a framework for planning treatment (Table 1). The Tumour Node Metastasis (TNM) staging system from the American Joint Committee on Cancer (AJCC) is the preferred staging system for colorectal cancer (Table 2). Broadly speaking, patients are divided into four stages, with stage IV (distant metastatic disease at the time of diagnosis) carrying the worst prognosis with a five-year survival of just 5.7% (Edge et al., 2010).

Primary Tumour (T)	Regional Lymph Node (N)	Distant Metastasis (M)
T0: No tumour	N0: No regional lymph node metastases	M0: No distant metastases
T1: Invades submucosa	N1a: Metastasis in one regional lymph node	M1a: Metastases confined to one organ
T2: Invades muscularis propria	N1b: Metastases in two-three regional nodes	M1b: Metastases in more than one organ
T3: Invades into pericorectal tissues	N1c: Tumor deposit(s) in the subserosa, mesentery, or nonperitonealised peri-colic or peri-rectal tissues without regional nodal metastasis	
T4a: Penetrates visceral peritoneum	N2a: Metastases in four-six regional nodes	
T4b: Invades/Adherent to other organs	N2b: Metastases in seven or more regional nodes	

Table 1 The Tumour Node Metastasis (TNM) Classification System

The TNM classification system is used for staging colorectal cancers. “T” refers to the size or direct extent of the primary tumour, “N” refers to the amount of regional lymph node involvement and “M” refers to the presence or absence of metastatic disease.

Stage	T	N	M
I	T1	N0	M0
	T2	N0	M0
IIa	T3	N0	M0
IIb	T4a	N0	M0
IIc	T4b	N0	M0
IIIa	T1-2	N1	M0
	T1	N2a	M0
IIIb	T3-T4a	N1	M0
	T2-3	N2a	M0
	T1-2	N2b	M0
IIIc	T4a	N2a	M0
	T3-4a	N2b	M0
	T4b	N1-N2	M0
IVa	Any T	Any N	M1a
iVb	Any T	Any N	M1b

Table 2 The AJCC Colorectal Cancer Staging System

Patients diagnosed with colorectal cancer are given a stage based upon their TNM score. Staging is important in deciding what treatment strategy is most appropriate. A higher stage indicates more advanced disease and therefore a worse prognosis.

For patients with colorectal cancer the aim of surgery is complete excision of the tumour, the major vascular pedicle, and the lymphatic drainage basin of the affected colonic segment. Post-operative (adjuvant) chemotherapy may also be used to eradicate micro-metastases, thereby reducing the likelihood of disease recurrence. This is most beneficial to patients with stage III (lymph node positive) disease. The survival benefit of adding oxaliplatin to fluoropyrimidines, such as 5-Fluorouracil (5-FU), a regime known as FOLFOX, has been demonstrated in multiple randomised controlled clinical trials, with an approximate 30% reduction in the risk of disease recurrence and a 22-32% reduction in mortality compared to surgery alone (Benson, 2005, Kuebler et al., 2007, Andre et al., 2009).

Neoadjuvant chemoradiotherapy is an increasingly used strategy for patients with rectal adenocarcinoma. However, the only definitive indication for neoadjuvant chemoradiotherapy is T3/T4 disease. The seminal German Rectal Cancer Study reported at 46 months median follow-up that pre-operative chemoradiotherapy was associated with a significantly lower pelvic relapse rate than post-operative chemoradiotherapy (6% vs. 13%) (Sauer et al., 2004). The difference persisted with longer follow-up, although it was of a lower magnitude at 10 years (7% vs. 10%) (Sauer et al., 2012). The benefit of adjuvant chemotherapy in patients receiving neoadjuvant chemoradiotherapy is unclear (Bujko et al., 2010, Kiran et al., 2012).

1.3 Failure of Treatment

1.3.1 Local Recurrence

Despite radical surgery with or without adjuvant therapy, up to 15% of patients with colorectal cancer will experience a local recurrence within 5 years (Palmer et al., 2007). Recurrent rectal cancer carries significant morbidity in the form of severe pain, bleeding, discharge and poor quality of life (Camilleri-Brennan and Steele, 2001). Untreated, the prognosis is poor with a median survival of just 7 months (Nielsen et al., 2011). Selected patients with locally recurrent disease can be treated with curative intent using multimodality therapy. Five-year survival rates of 35-50% with acceptable morbidity have been reported with this approach in recurrent rectal cancer (Harji et al., 2012).

1.3.2 Metastatic Disease

Colorectal cancer can spread by lymphatic and hematogenous dissemination, as well as by contiguous and transperitoneal routes. The intestinal tract drains via the portal venous system and therefore the first site of hematogenous dissemination is usually the liver. From there other metastatic sites include the lungs and the brain.

Half of patients undergoing curative treatment for colorectal cancer ultimately die from the disease and liver metastases remain the major cause of death (Oliphant et al., 2013). Approximately 25% of colorectal cancer patients will present with synchronous liver metastases and up to 50% will develop metachronous liver metastases, most commonly within the first three years of diagnosis (Vatandoust et al., 2015). Unlike other solid tumours, metastatic disease is often confined to the liver and 30% of patients with stage IV colorectal cancer have metastases limited to

the liver. This pattern of metastatic disease provides a unique opportunity for treatment with curative intent that is not often possible with other advanced cancers.

1.4 Development of Colorectal Cancer Liver Metastases

1.4.1 Colorectal Cancer Biology

The luminal surface of the large intestine is lined by epithelial cells that form invaginations called crypts. At the base of each crypt are intestinal stem cells that differentiate into specialised epithelial cells including columnar absorptive cells and mucus-secreting goblet cells. Colorectal cancer results from the progressive accumulation of genetic and epigenetic changes that lead to the transformation of normal colonic epithelium to colonic adenocarcinoma (Kheirlesei et al., 2013). In 1990, Fearon and Vogelstein proposed the multistep genetic hypothesis for colorectal tumourigenesis (Fearon and Vogelstein, 1990). In this, a progression from normal bowel mucosa to adenoma to carcinoma is supported by accumulating mutations in known oncogenes and tumour suppressor genes (Figure 1). Phenotypically, the resulting cancerous cells have six common hallmarks; self-sufficiency in growth signals, insensitivity to anti-growth signals, the ability to evade apoptosis, limitless replicative potential, sustained angiogenesis and the ability to invade and metastasise (Hanahan and Weinberg, 2000).

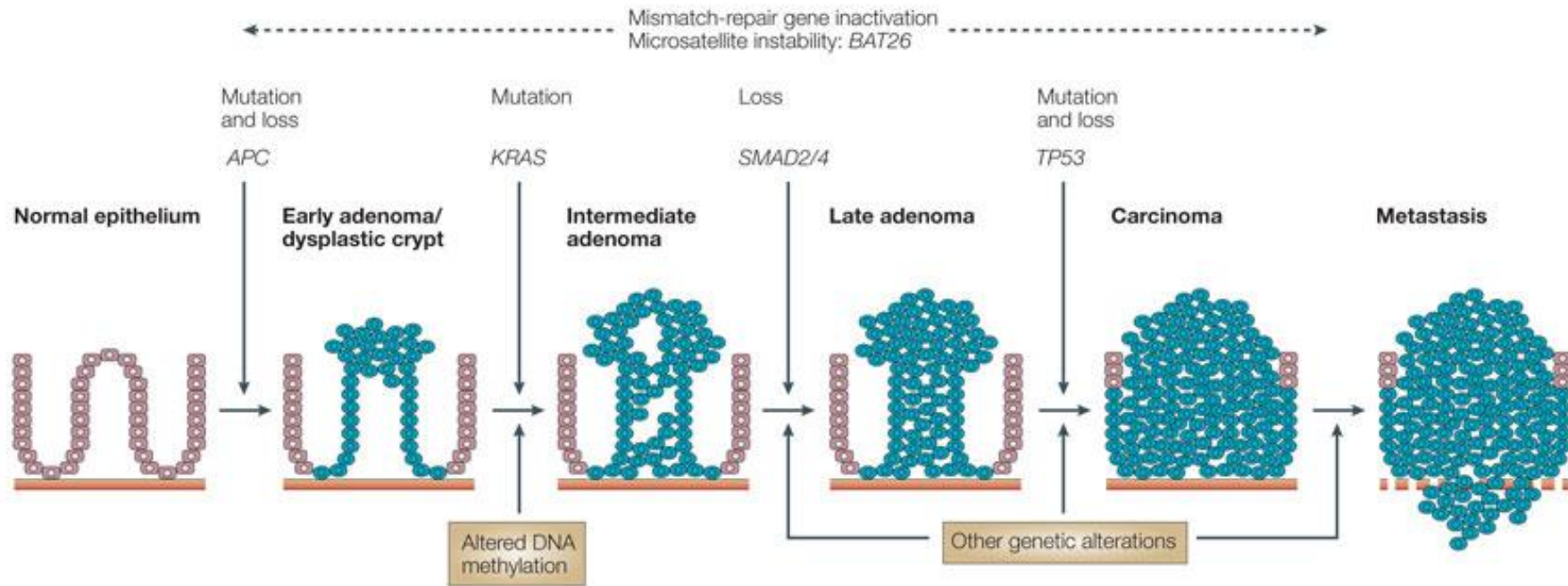


Figure 1 The Adenoma Carcinoma Sequence

The progression from normal epithelium to adenoma to carcinoma is accompanied by increasing genetic and epigenetic alterations in known tumour suppressor genes and oncogenes. Adapted from Davies et al (2005). *APC*= Adenomatous Polyposis Coli, *KRAS*= V-Ki-ras2 Kirsten rat sarcoma viral oncogene homolog

1.4.2 The Metastatic Cascade

The defining histopathological characteristic of a carcinoma is invasion across the basement membrane, an extracellular network of proteins and collagen. This signals the invasive nature and metastatic potential of a carcinoma. In order for a cancer to metastasise a sequence of five steps must successfully take place (Figure 2). The steps are invasion, intravasation, survival in the circulation, extravasation and metastatic colonisation (Mina and Sledge, 2011). Cancers are biologically heterogeneous containing genotypically diverse subpopulations of tumour cells, each of which has the potential to undertake the five steps to metastasise (Fidler, 2003). Comparisons have been made between the successful metastatic cell and a decathlon champion, who must be proficient in all the steps and not just a few to succeed (Fidler, 1990).

Metastatic colonisation is not a random process. The “seed and soil” hypothesis was proposed in 1889 by the English surgeon Stephen Paget to explain the pattern of metastatic spread in breast cancer (Paget, 1889). He suggested that tumour cells (“the seed”) preferentially grow in the microenvironment of select organs (“the soil”). His view was challenged in 1928 by the American pathologist James Ewing, who proposed that metastatic dissemination was limited by mechanical factors resulting from the anatomical structure of the vascular system (Ewing, 1928). Nearly a century later however, it was Paget’s hypothesis that was proven to be correct (Hart and Fidler, 1980).

Only a small number of primary tumour cells that enter the circulation give rise to metastases. Fidler reported that 24 hrs after injection of ¹²⁵iodine-iodo-deoxyuridine labelled B16 melanoma cells into C57BL/6J mice, less than 0.1% of tumour cells

were still viable, and that less than 0.01% of these cells survived to produce metastases (Fidler, 1970). This prompted the question of whether metastatic disease represents the fortuitous survival and growth of a few neoplastic cells or whether it represents the selective growth of unique subpopulations of malignant cells that are endowed with special properties (Fidler, 2003).

Several molecular and cellular observations support the “seed and soil” hypothesis. This includes the fact that endothelial cells lining the blood vessels of different organs express different adhesion molecules (Nicolson, 1988) and that tumour cells expressing the corresponding receptor may therefore bind and arrest in specific tissues. Furthermore, there is evidence supporting a role for chemokines in the chemo-attraction of tumour cells (Muller et al., 2001).

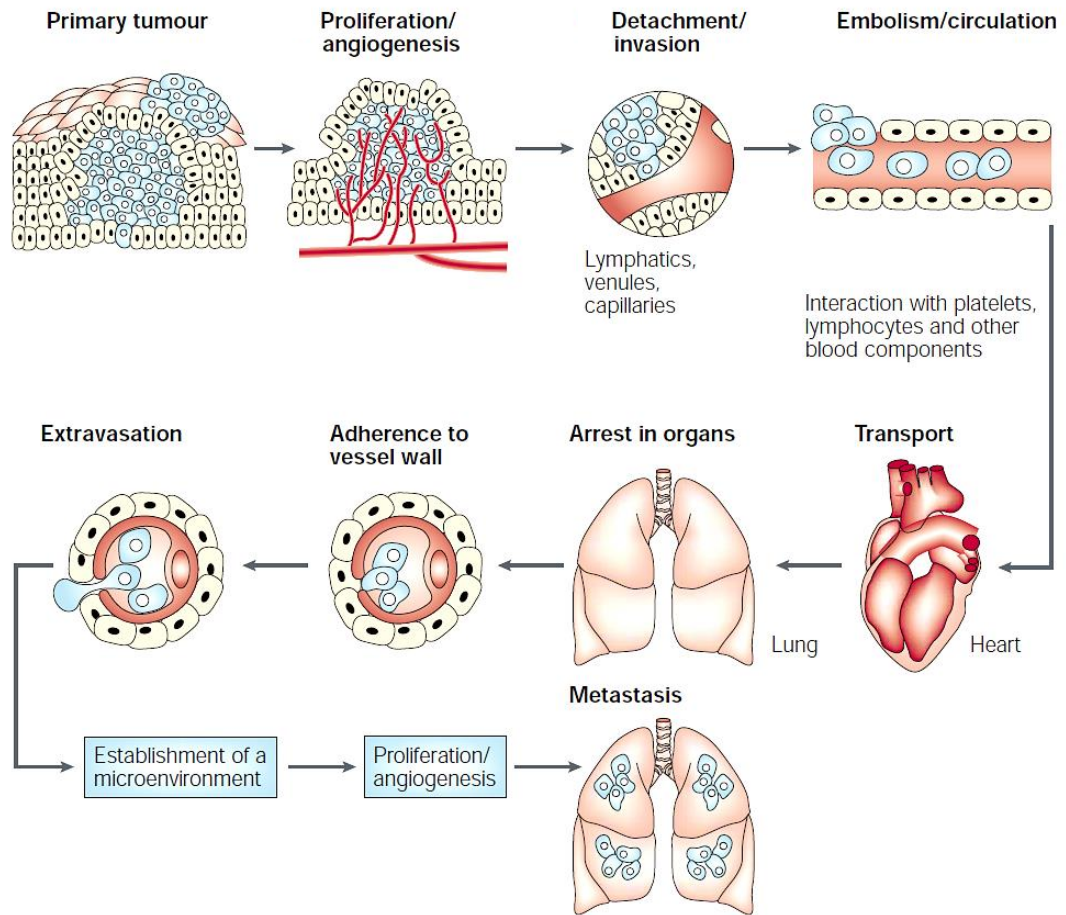


Figure 2 The Metastatic Cascade

In order for a cancer to metastasise a series of events must all successfully take place. After a period of growth in the primary cancer, tumour cells enter thin walled venules and gain access to the circulation. Most circulating tumour cells are rapidly destroyed, however, a small number are able to travel to distant organs where they become trapped as they adhere to endothelial cells within the capillary bed. Extravasation occurs as the tumour cells pass into the organ parenchyma. Finally, the tumour cells must proliferate within the parenchyma to complete metastatic colonisation. Adapted from Fidler (2003).

1.4.3 Progression of Colorectal Cancer Liver Metastases

Colorectal cancer most commonly metastasises to the liver. Once detached from the primary colorectal cancer, tumour cells are transported through the hepatic-portal circulatory system to reach the liver. They arrest in the hepatic sinusoids, which are specific hepatic capillary networks (Figure 3). Located within the sinusoidal lumen, or in close proximity to the sinusoidal wall are cells that play a key role in extravasation; sinusoidal endothelial cells, Kupffer cells and hepatic stellate cells. The progression of colorectal cancer liver metastases (CLM) is divided into four phases (Paschos et al., 2014):

- 1) Microvascular phase of liver-infiltrating malignant cells
- 2) Interlobular micrometastases phase
- 3) Angiogenic micrometastases phase
- 4) Established hepatic metastases phase

The first phase mainly occurs within sinusoids and is predominantly mediated by sinusoidal endothelial cells. During this phase they produce both tumouricidal and tumourigenic effects that result in either colorectal cancer cell destruction or liver colonisation. For instance, they form a major scavenger cell system and accomplish receptor-mediated endocytosis and pinocytosis (Smedsrod et al., 2009), but are also capable of expressing adhesion molecules, such as E-selectin, which mediate colorectal cancer cell attachment, facilitating extravasation into the hepatic parenchyma (Laferriere et al., 2001).

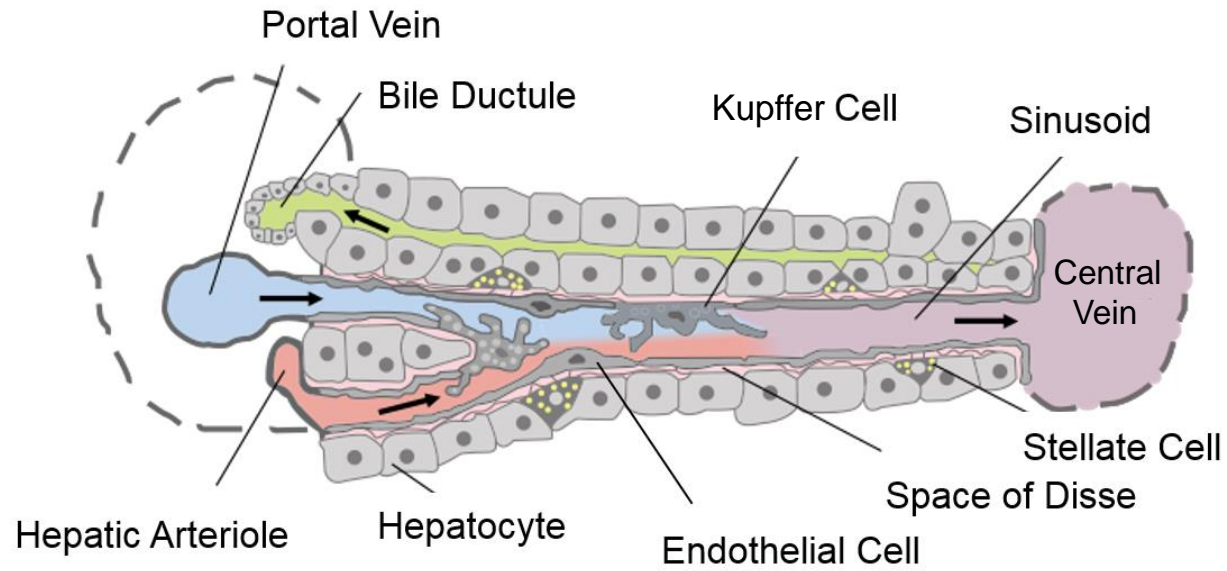


Figure 3 The Hepatic Sinusoid

Pictorial representation of a hepatic sinusoid, which mixes oxygen-rich blood from the hepatic artery with nutrient-rich blood from the portal vein. A single layer of endothelial cells line the hepatic sinusoids and they are separated from hepatocytes by the space of Disse. Adapted from Frevert et al (2005).

The adherence of colorectal cancer tumour cells to liver sinusoidal endothelial cells is critical for extravasation and hepatic colonisation. Although colorectal cancer tumour cells bind to selectins in hepatic sinusoids, the bonds are weak and do not guarantee stable cell adhesion (Paschos et al., 2014). Integrin-mediated tumour cell adhesion and changes in the binding affinity of integrins are necessary for stable tumour cell adhesion and subsequent migration and colonisation (Haier and Nicolson, 2001). These stronger bonds overcome the force of hydrodynamic blood flow. Shortly after adhesion, colorectal cancer cells begin to migrate through the pores of sinusoidal endothelial cells and the space of Disse to reach hepatocytes within 48 hrs (Shimizu et al., 2000). At the point of extravasation, immunological cells including cytotoxic T-cells, monocytes and macrophages are activated in the extra-sinusoidal space. Ultimately, a few colorectal cancer tumour cells evade the host response and successfully cause micro-metastases in the hepatic parenchyma. The transition to macroscopic metastases may take weeks or months and is reliant on the process of angiogenesis to create new blood vessels to supply the oxygen and nutrients required for increased growth. Recent evidence suggests that CLM themselves are also able to shed intact tumour cells with invasive potential, suggesting that the “seed” may be able to leave the “soil” once again (Rahbari et al., 2016).

1.5 Treatment of Colorectal Cancer Liver Metastases

1.5.1 Conservative

The majority of patients with CLM are not amenable to curative surgery. Conservative treatment includes symptom control (analgesia, anti-emetics) and nutritional support. Median survival is just 8 months (Rocha and Helton, 2012).

1.5.2 Surgical Resection

The only curative treatment for CLM is surgical resection. In surgical case series, five-year survival rates of up to 58% have been reported when combined with adjuvant chemotherapy (Choti et al., 2002, Abdalla et al., 2004, Fernandez et al., 2004). The percentage of patients suitable for resection is a moving target as surgeons have differing views of what is resectable. Nevertheless, the majority of patients with CLM are not surgical candidates because of the tumour size, location, multifocality, or inadequate hepatic reserve.

Even when hepatic resection with curative intent is performed, 70-80% of patients will experience a recurrence, most commonly within the first two years (Tomlinson et al., 2007). Recurrence occurs equally at intrahepatic and extrahepatic sites (Misiakos et al., 2011). Repeat resection is feasible in 10-15% of patients with intrahepatic recurrence and five-year survival rates of 29% have been reported (Adair et al., 2012).

Criteria for hepatic resection have changed over the last decade, with increasing focus on what should be left after the resection. Previous criteria, including size,

location and number of tumours and presence of extrahepatic disease have largely been abandoned. Current criteria include a complete resection with tumour-free surgical margins (R0 resection), sparing at least two liver segments having an independent inflow, outflow, and biliary drainage. The size of the liver remnant after resection should not be less than 20% of the total liver volume (Misiakos et al., 2011). This can be accurately predicted pre-operatively with magnetic resonance imaging (MRI).

1.5.3 Systemic Neoadjuvant Chemotherapy

“Conversion therapy” describes the use of induction chemotherapy in patients with initially unresectable CLM. Up to 36% of patients with initially unresectable disease who receive induction chemotherapy can go on to have a complete R0 resection (Falcone et al., 2007, Malik et al., 2015) with five-year survival rates of 30-35% (Rivoire et al., 2002, Adam et al., 2004).

1.5.4 Systemic Adjuvant Chemotherapy

Evidence of a survival benefit for patients receiving adjuvant chemotherapy following surgery is lacking. Two multi-centre randomised clinical trials in the 1990s, the FFCD and ENG trials, compared six months of post-operative systemic 5-FU and leucovorin versus observation alone following hepatic resection. In a combined analysis of both trials, although there were improvements in median progression-free survival and overall survival with the adjuvant chemotherapy group, the results were not statistically significant (Mitry et al., 2008).

The chemotherapeutic agents used in the above trials are considered inferior by today's standards. The combination of newer drugs including oxaliplatin, irinotecan, bevacizumab and cetuximab have improved survival in patients with unresectable metastatic colorectal cancer (as will be discussed later), however, there are limited data on their use in an adjuvant setting for resected CLM.

1.5.5 Regional Adjuvant Chemotherapy

As CLM derive their blood supply from the hepatic artery, regional hepatic intra-arterial (HIA) chemotherapy following metastasectomy offers a potential advantage in drug delivery. Unfortunately results from randomised clinical trials have been poor. A German trial in 1998 was closed prematurely when interim analysis showed that patients who received HIA chemotherapy (5-FU and leucovorin) after surgery had a worse median survival compared to surgery alone (Lorenz et al., 1998). More recent studies have combined HIA chemotherapy with systemic chemotherapeutic agents with promising results (House et al., 2011, Bolton et al., 2012). Randomised controlled clinical trials are ongoing assessing the efficacy of combined HIA and systemic chemotherapy, however at present the routine use of HIA chemotherapy after hepatic resection has not gained widespread acceptance.

1.5.6 Systemic Palliative Chemotherapy

For patients with unresectable CLM, chemotherapy can be used in a palliative setting to extend survival. Initially 5-FU and leucovorin afforded patients a median survival of 14 months, but this was increased to 19 months with the sequential use of newer cytotoxic agents including oxaliplatin and irinotecan (de Gramont et al., 2000, Goldberg et al., 2004). The introduction of biologically targeted therapies,

such as bevacizumab and cetuximab, has further prolonged survival rates up to 30 months (Hurwitz et al., 2004, Van Cutsem et al., 2011, Loupakis et al., 2014).

1.5.7 Radiofrequency Ablation

Radiofrequency ablation (RFA) uses a needle electrode to deliver high frequency alternating current from the tip of the electrode to the surrounding tissue. Ions within the tissue follow the change in the direction of the current causing frictional heating of the tissue up to 60°C resulting in coagulative necrosis. RFA can be applied via open, laparoscopic or percutaneous approaches.

A wide range of five-year survival rates (14-55%) and recurrence rates (4-60%) have been reported for RFA treatment of CLM (Wong et al., 2010). RFA is well tolerated, however the reported mortality rate is 0-2% and major complication rate is 6-9% (Wong et al., 2010). There have been no randomised clinical trials comparing RFA with surgical resection with or without adjuvant chemotherapy for patients with resectable CLM. A 2012 Cochrane review concluded there is insufficient evidence to recommend RFA as a radical oncological treatment for CLM (Cirocchi et al., 2012).

1.5.8 Transarterial Chemoembolisation

Transarterial chemoembolisation (TACE) is a minimally invasive procedure that combines cytotoxic drug infusion with embolisation of the tumour's blood supply. Small embolic particles coated with chemotherapeutic agents are injected through a catheter into the arteries feeding CLMs under radiological guidance.

In a multi-centre randomised trial, 74 patients with unresectable CLM were assigned to TACE in the form of drug-eluting beads preloaded with irinotecan (DEBIRI) or systemic irinotecan, fluorouracil and leucovorin (FOLFIRI). The DEBIRI group had a significantly higher overall survival compared to the FOLFIRI group (22 vs. 15 months) (Fiorentini et al., 2012). Further larger randomised trials are needed to confirm TACE provides superior outcomes to systemic chemotherapy regimens including oxaliplatin. No trials to date have compared surgical resection with TACE.

1.5.9 Microwave Hyperthermia and Interstitial Laser Ablation

Also known as microwave coagulation, the surgical technique of microwave hyperthermia was first reported in 1979 and uses a microwave coagulator, which simultaneously cuts and coagulates the tumour tissue (Tabuse, 1979). It can be applied using an open technique or percutaneously. In a randomised clinical trial, 30 patients with resectable CLM were assigned to laparotomy and ultrasound-guided microwave hyperthermia or hepatic resection. One-, two- and three-year survival rates were similar between the two groups, with the microwave hyperthermia group having significantly less intra-operative blood loss (Shibata et al., 2000).

Interstitial laser ablation use is limited to specialist centres. Nevertheless, there are several reports of success in treating CLM (Christophi et al., 2004, Vogl et al., 2004, Pech et al., 2007). In the largest series, 603 patients underwent MRI-guided laser-induced interstitial thermotherapy for CLM. The reported five-year survival rate was 37% (Vogl et al., 2004).

1.5.10 Percutaneous Ethanol Injection

Percutaneous ethanol injection techniques have been widely used for the treatment of small hepatocellular carcinomas and have been shown to be effective in causing complete tumour necrosis in 30-56% of CLM (Giovannini and Seitz, 1994, Giorgio et al., 1998). However, there are limitations to the technique including the inability to access some lesions.

1.5.11 Cryotherapy

Cryotherapy involves the delivery of liquid nitrogen or argon gas directly into CLM. This is achieved under ultrasound guidance using a specially designed probe and results in the formation of ice crystals causing destruction of tumour cells. A Cochrane review of one randomised clinical trial with a high degree of bias concluded that cryotherapy should not be used for the treatment of CLM outside the context of clinical trials (Bala et al., 2013).

1.5.12 Hepatic Transplant

Liver transplant was conceived as an ideal curative treatment for CLM as it leads to an R0 resection and eliminates the potential of recurrence in the liver remnant. This is particularly valuable in patients with unresectable disease. The SECA study was an open, prospective pilot study where 21 patients with unresectable CLM underwent liver transplant. Five-year overall survival rates were impressive, with a reported estimate at 60% (Hagness et al., 2013). However, extra-hepatic disease recurrence rates were high, with 19 out of 21 patients experiencing a recurrence after a median time of 6 months, most commonly in the lungs (17 patients). There

were also a number of major complications. Two patients had hepatic artery thrombosis requiring re-transplantation and there were five re-operations for post-operative haemorrhage/haematoma.

In a comparative analysis, the results of the SECA study were analysed against results of the NORDIC VII study, a randomised multi-centre clinical trial assessing first-line chemotherapy regimes in patients with unresectable CLM. Disease free survival in both groups was similar (8-10 months), however the overall five-year survival rate was 56% in patients undergoing transplantation compared to just 9% in patients receiving first-line chemotherapy (Dueland et al., 2015). The extraordinary differences in overall survival were attributed to the pattern of disease recurrence. In patients undergoing liver transplant the primary site of recurrence was the lungs, whereas the patients who received first-line chemotherapy most commonly had progressive liver metastases. Furthermore, the pulmonary metastases in patients occurring in patients who had undergone transplant were small, slow growing and often amenable to further treatment including pulmonary resection and ablation.

Hepatic transplant for CLM is controversial. Critics point out that donor livers are a scarce resource (Chapman, 2013, Martins et al., 2015). Furthermore, with nearly 100% of transplanted patients experiencing recurrence, is liver transplant for CLM truly a curative procedure or merely a procedure to extend life? If it is the latter, should patients with unresectable CLM be offered liver transplants with the same priority as patients with conventional indications for hepatic transplant? Hagness and colleagues point out that liver grafts are currently allocated for patients with recurrent hepatitis C, which has a five-year survival rate of less than 50% (Hagness

et al., 2013). Is it justifiable to perform hepatic re-transplant in patients with recurrent hepatitis C cirrhosis, while denying patients with unresectable CLM a liver transplant, knowing that the outcome is at least similar, if not superior? Clearly hepatic transplant for CLM as a treatment is in its infancy. Not only are more multi-centre, prospective, randomised trials required for validation of these results, but further work on risk-stratification for patient selection and cost-effectiveness must also be undertaken.

1.5.13 Biological Agents

Cetuximab (Erbix[®]) and panitumumab (Vectibix[®]) are monoclonal antibodies that bind with high affinity to the extracellular domain of the human epidermal growth factor receptor (EGFR). As their affinity for the EGFR is up to ten-fold higher than endogenous ligands, they block their binding, inhibiting receptor function. EGFR activation leads to stimulation of several intracellular signalling pathways including Ras-Raf-MEK-ERK and PI3K-AKT-mTOR, which ultimately result in increased cellular proliferation and decreased apoptosis (Scaltriti and Baselga, 2006). Up to 75% of colorectal cancer cells express EGFR (Goldstein and Armin, 2001), however it is not fully clear if this level of expression is translated to metastatic cells also (Tol and Punt, 2010). Resistance to anti-EGFR therapy is found in patients with KRAS mutations, as this results in constitutive activation of the Ras-Raf-MEK-ERK signalling pathway, which is independent of EGFR activation by ligand binding (Benvenuti et al., 2007). For this reason the use of cetuximab and panitumumab is limited to patients with wildtype KRAS metastatic colorectal cancer.

The CRYSTAL trial reported the benefit of adding cetuximab to first-line irinotecan containing therapy for patients with EGFR-positive, wildtype KRAS, unresectable

metastatic colorectal cancer. Patients receiving FOLFIRI and cetuximab had significantly better overall survival (23.5 vs 20 months). Furthermore, an increased number of patients also underwent metastasectomy with R0 margins (Van Cutsem et al., 2011). The benefit of cetuximab with oxaliplatin based regimes is less clear as results from randomised clinical trials are mixed. The OPUS trial reported that patients with wildtype KRAS had a significantly improved response rate (57% vs. 34%) and median progression-free survival, (8.3 vs. 7.2 months) when cetuximab was added to FOLFOX4 compared to FOLFOX4 alone (Bokemeyer et al., 2011). However, the MRC COIN (Maughan et al., 2011) and NORDIC VII (Tveit et al., 2012) trials found no progression-free survival benefit with the addition of cetuximab to patients with wildtype KRAS metastatic colorectal cancer receiving oxaliplatin based chemotherapy.

A number of biological anti-angiogenic agents have been shown to improve outcomes in metastatic colorectal cancer. Angiogenesis and its potential for targeted therapeutics will be discussed in more detail in the subsequent sections.

1.6 Angiogenesis

1.6.1 The Cardiovascular System

The cardiovascular system consists of the heart, arteries, arterioles, capillaries, venules and veins, which together circulate blood and transport nutrients, oxygen, carbon dioxide and hormones throughout the body. It is the first organ system to develop and become functional in the embryo. This, in part, reflects the fundamental need for a vascular system that can deliver nutrients and remove catabolic products from growing organs and tissues. The de novo formation of blood vessels, termed vasculogenesis, results from the differentiation of mesoderm-derived endothelial precursor cells and predominates in early embryological life (Risau et al., 1988). In adult life, blood vessels form from pre-existing blood vessels in a process termed angiogenesis.

Angiogenesis is a complex, tightly regulated process that involves the interaction of multiple cell types. During adulthood most blood vessels remain quiescent, however, endothelial cells retain the ability to “turn on” and rapidly divide in response to a physiological stimulus. Physiological angiogenesis does occur in adult life in the cycling ovary, wound healing and in the placenta during pregnancy (Carmeliet, 2005). However, when these stimuli are excessive pathological conditions can arise, notably malignant, ocular and inflammatory disorders (Carmeliet, 2005).

1.6.2 The Endothelium

The structure of a blood vessel varies depending upon its function. For example, arteries have thick vessel walls to cope with high arterial pressure, whereas veins contain valves to prevent the backflow of low pressure blood. All blood vessels are lined on their inner surface by a monolayer of endothelial cells (Figure 4). Described as the foundation stones of the vascular system, they have important roles in physiological processes including the regulation of blood flow and blood pressure, but are also implicated in several pathological processes including atherosclerosis, hypertension and cancer (Khazaei et al., 2008).

Much of our knowledge regarding endothelial cell physiology and function has developed from in vitro studies of Human Umbilical Vein Endothelial Cells (HUVECs). The culture of endothelial cells was first reported over forty years ago (Jaffe et al., 1973).

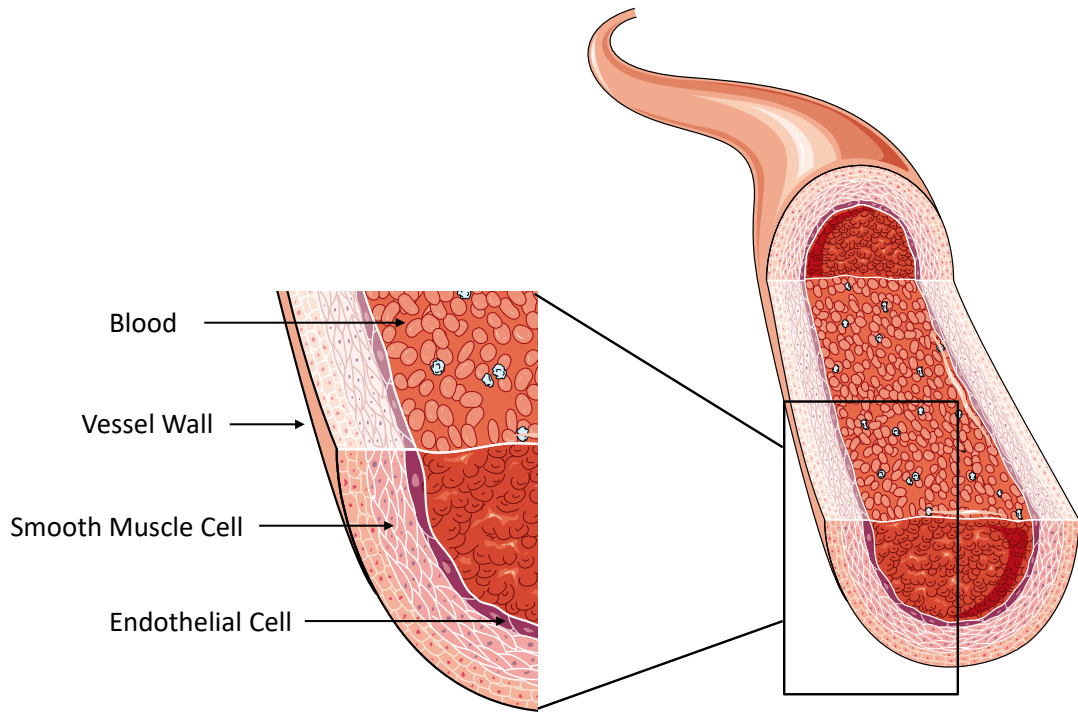


Figure 4 The Vascular Endothelium

The vascular endothelium consists of a monolayer of endothelial cells that line the inner surface of blood vessels. *Image created through Servier Medical Art.*

1.6.3 Sprouting Angiogenesis

As implied by its name, sprouting angiogenesis is characterised by sprouts of endothelial cells that grow towards an angiogenic stimulus. The basic steps of sprouting angiogenesis include; enzymatic degradation of the capillary basement membrane, endothelial cell proliferation, migration of endothelial cells, endothelial cell tube formation, vessel fusion, vessel pruning, and pericyte stabilization (Adair and Montani, 2010).

1.6.3.1 The Role of Hypoxia

Hypoxia is an important stimulus for sprouting angiogenesis and central to this is the transcription factor hypoxia-inducible factor 1 (HIF-1). HIF-1 is an $\alpha\beta$ heterodimer that was first recognised as a DNA-binding factor that mediates hypoxia-inducible transcription of erythropoietin. Both HIF- α and HIF- β exist as a series of isoforms. HIF-1 β subunits are constitutive nuclear proteins, whereas HIF-1 α subunits are inducible by hypoxia (Pugh and Ratcliffe, 2003). Of the three HIF- α isoforms, HIF-1 α and HIF-2 α are closely related. Both HIF-1 α and HIF-2 α are able to interact with hypoxia response elements (HREs) in promoter regions of genes to induce transcriptional activity (Tian et al., 1997). The third isoform, HIF-3 α , appears to be involved in the negative regulation of this response (Makino et al., 2001). In normoxic conditions hydroxylation at conserved proline residues on HIF- α subunits mediates interaction with the von Hippel-Lindau E3 ubiquitin ligase complex. This complex targets HIF- α for proteosomal destruction (Ivan et al., 2001). In hypoxic conditions HIF prolyl-hydroxylase, the enzyme responsible for the hydroxylation of the conserved proline residues, is inhibited since it utilises oxygen as a co-substrate. This allows HIF-1 α to escape inactivation in hypoxic conditions

1.6.3.2 The Role of Vascular Endothelial Growth Factor

HIFs upregulate many genes, however, the induction of vascular endothelial growth factor (VEGF) is the most striking, increasing thirty-fold within minutes (Semenza, 1999, Carmeliet, 2003). The VEGF signalling pathway has been established as the major regulator of angiogenesis. There are five protein members of the VEGF family; VEGF-A, VEGF-B, VEGF-C, VEGF-D and placental growth factor (PGF). These signal proteins bind to three tyrosine kinase receptors; VEGFR-1 (Flt1), VEGFR-2 (KDR/Flk1) and VEGFR-3 (Flt4) (Figure 5). VEGF-A is commonly referred to as VEGF and is considered the main inducer of angiogenesis by signalling through the VEGFR-2 receptor (Ferrara et al., 2003).

VEGFR-2 is a 200-230 kDa tyrosine kinase receptor with a high-affinity for VEGF. It is expressed in vascular and lymphatic endothelial cells as well as other cell types such as megakaryocytes. Upon activation by VEGF, VEGFR-2 receptor dimerization occurs which facilitates auto-phosphorylation of multiple tyrosine residues along the cytoplasmic domains of each monomer (Schlessinger, 2000). Auto-phosphorylation is crucial for the recruitment of a variety of signalling proteins including those responsible for angiogenic activity.

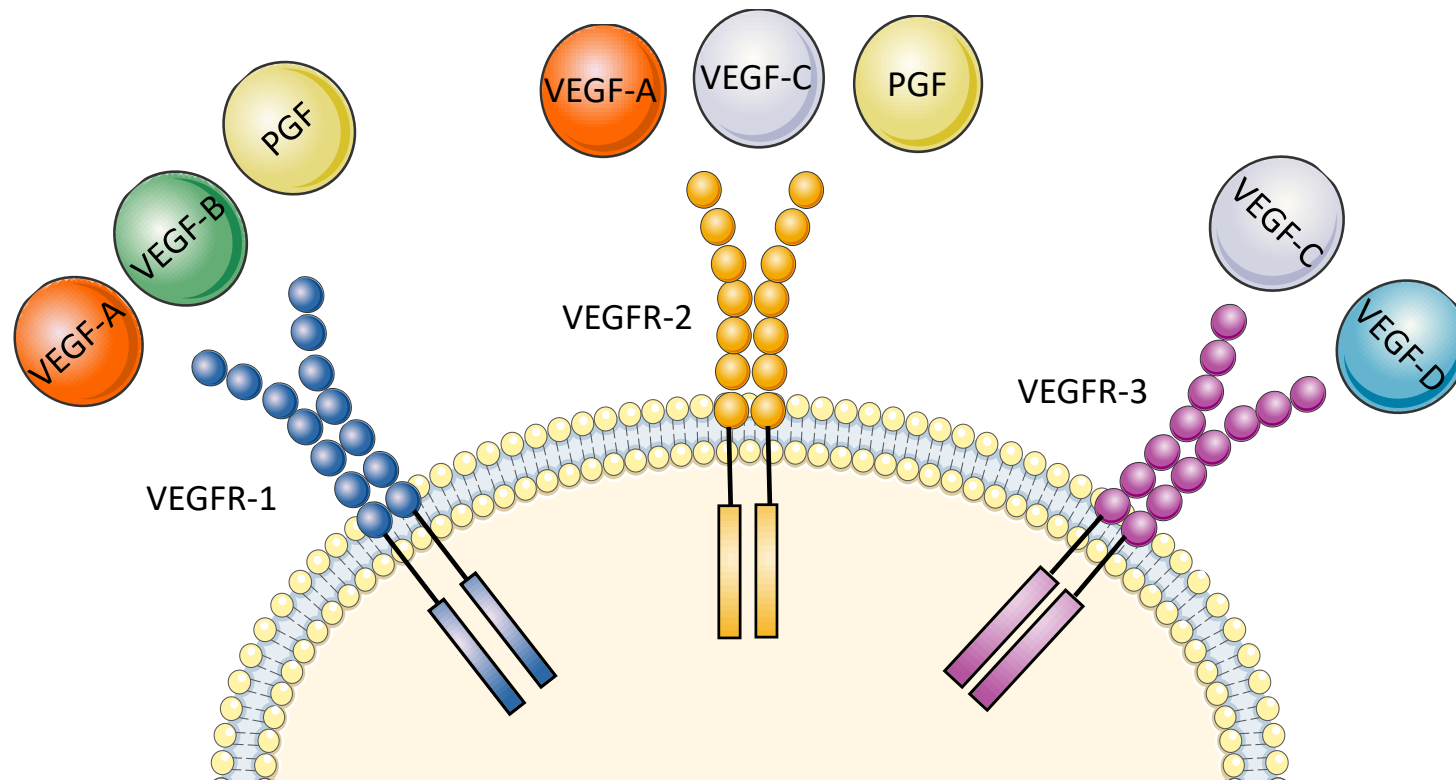


Figure 5 Vascular Endothelial Growth Factors and their Receptors

The five protein members of the VEGF family bind to different VEGF receptors. VEGF-A is commonly referred to as VEGF and via VEGFR-2 is the main inducer of angiogenesis. *Image created through Servier Medical Art.*

1.6.3.3 Endothelial Tip, Stalk and Phalanx Cells

During angiogenesis endothelial cells within the vessel wall are selected for sprouting. This is controlled by a balance of pro-angiogenic factors, including VEGF and anti-angiogenic factors that promote quiescence including tight pericyte contact, certain extracellular matrix molecules and VEGF inhibitors. Favourable angiogenic conditions lead to the specification of endothelial cells into tip and stalk cells having different morphologies and functional properties. The description of “tip” and “stalk” cells was first made in 2003 (Gerhardt et al., 2003). Tip cells are polarised, primarily migrate and proliferate very little. They can adopt a proteolytic phenotype and break down the basement membrane (Hughes, 2008). This results in a loss of contact with the basement membrane laminin and exposes the cells to interstitial collagen. This triggers signalling cascades and cytoskeletal reorganisation resulting in sprouting morphogenesis (Rhodes and Simons, 2007). Tip cells express high levels of Delta-like ligand 4 (DLL4), platelet derived growth factor- β (PDGF- β), VEGFR-2 and VEGFR-3 and have low levels of notch signalling. Consistent with the prominent expression of VEGFR-2 in tip cells, endothelial cell guidance is controlled by VEGF (Adams and Alitalo, 2007).

Stalk cells are phenotypically and functionally distinct from tip cells. They are highly proliferative, form tubes and branches and form a vascular lumen (Thurston and Kitajewski, 2008). They also establish junctions with neighbouring cells and synthesise basement membrane components (Phng and Gerhardt, 2009). As endothelial cells transition from active sprouting to quiescence they adopt a “phalanx” phenotype, resembling a phalanx formation of ancient Greek soldiers. They are immobile and non-proliferative promoting vessel integrity and stabilisation (Bautch, 2009).

1.6.3.4 DLL4-Notch Signalling

VEGF induces the expression of DLL4 in tip cells that binds to its receptors notch1 and notch4 on adjacent stalk cells (Figure 6). DLL4-notch signalling is important in determining how endothelial cells decide both spatially and temporally when to adopt tip or stalk phenotypes (Dufraine et al., 2008). DLL4 in tip cells signals through notch1 in the adjoining stalk cells to initiate a VEGF feedback loop, limiting sprouting by downregulation of VEGFR-2 (Dufraine et al., 2008). The signalling pathway functions as a dampening mechanism for preventing excess angiogenesis and promoting the orderly development of new vessels (Chung et al., 2010). This is evidenced by decreasing levels of DLL4 or blocking notch-signalling both resulting in increased sprouting, branching and fusion of endothelial tubes (Sainson et al., 2005, Ridgway et al., 2006, Noguera-Troise et al., 2006).

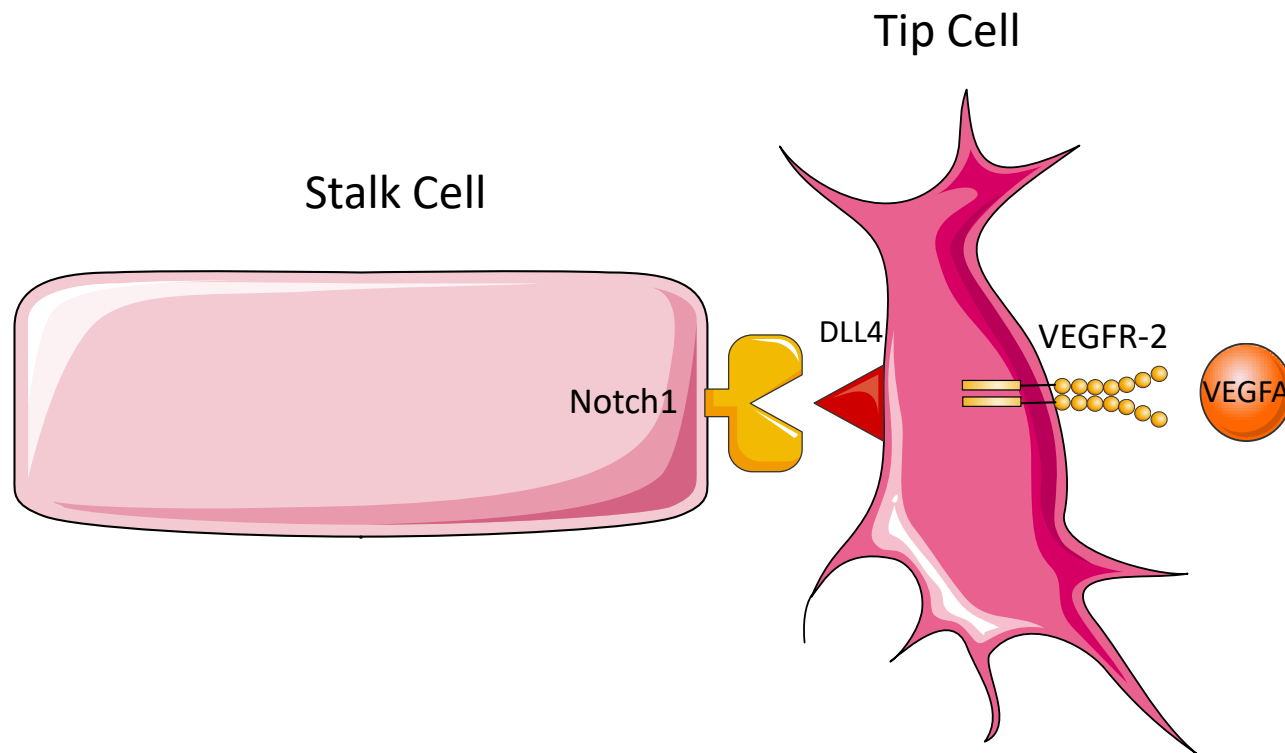


Figure 6 DLL4-Notch Signalling

VEGF induces expression of DLL4 in tip cells which binds to notch receptors on adjacent stalk cells and is an important mechanism for determining tip and stalk cell phenotypes. *Image created through Servier Medical Art.*

1.6.3.5 Maturation of Blood Vessels

To form new vascular connections, tip cells need to suppress their motile, explorative behaviour upon encountering the tips of other sprouts or existing capillaries (Adams and Alitalo, 2007). After the establishment of a vascular plexus, a maturation process follows which involves enhancement of tight junctions, secretion of basement membrane components and recruitment of perivascular cells. The recruitment of pericytes, thought to be the functional equivalent of vascular smooth muscle cells, is essential for the maturation of endothelial tubes into blood vessels. This is achieved through PDGF- β , which is secreted by endothelial cells.

Pericytes signal to endothelial cells to maintain quiescence and regulate vascular permeability through Tie/Angiopoietin signalling. The Tie/Ang signalling system comprises of two Ang ligands (Ang-1 and -2) and two Tie tyrosine kinase receptors (Tie-1 and -2). Pericytes express Ang-1 on their surface that binds to Tie-2 receptors on the surface of endothelial cells (Figure 7). This tight interaction mediates blood vessel stabilisation. Ang-2 expression has antagonistic effects. In the switch from quiescent to activated phenotype, the release of Ang-2 from endothelial cells antagonises Ang-1 function increasing basement membrane degradation and endothelial cell migration (Adams and Alitalo, 2007).

Upon maturation of the blood vessel, blood flows to the newly vascularised area increasing oxygen levels and decreasing VEGF levels, bringing an end to angiogenesis.

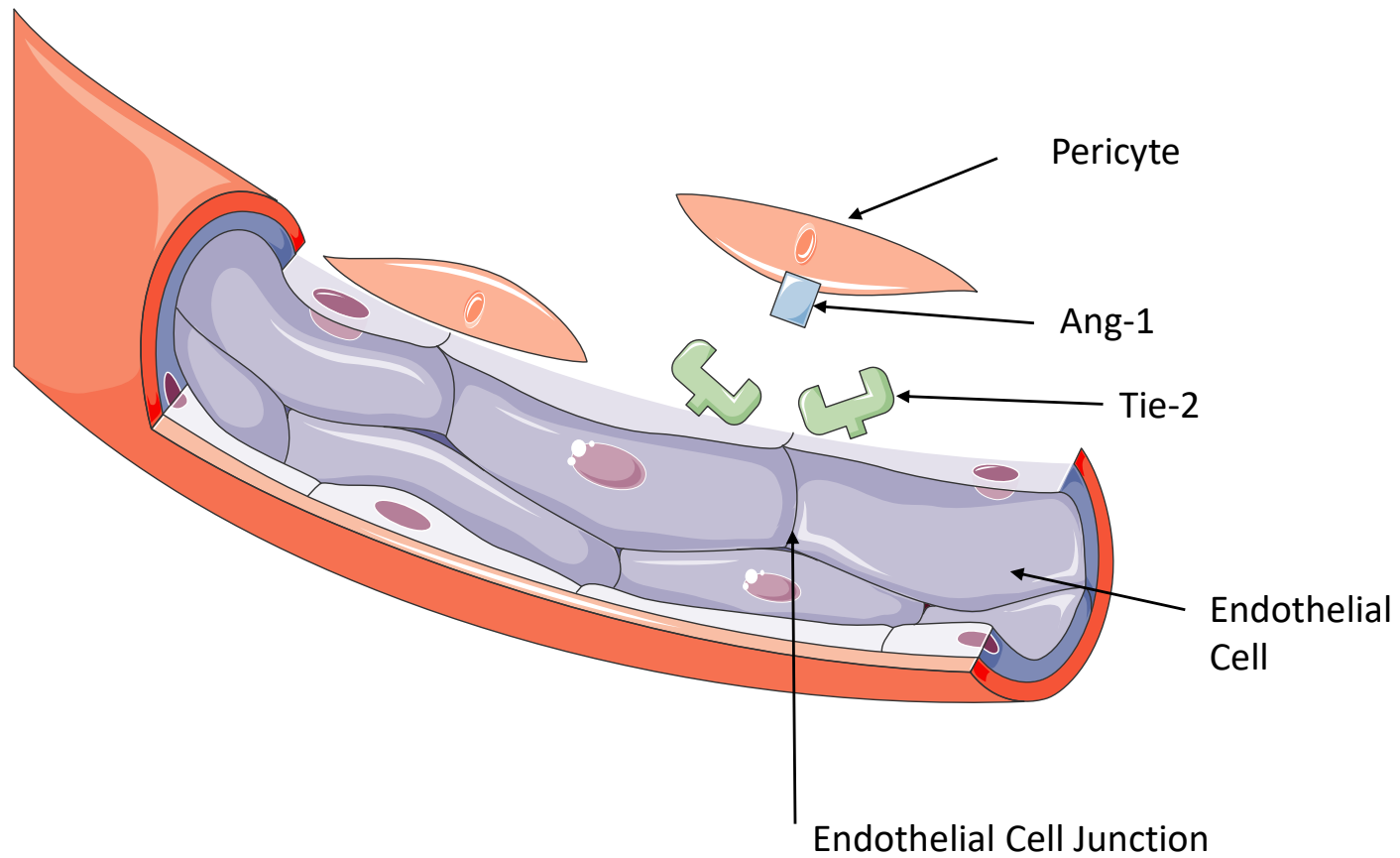


Figure 7 Pericyte Stabilisation Through Ang-1/Tie-2 Signalling

Pericytes express Ang-1 on their surface that binds to Tie-2 receptors on the surface of endothelial cells. This tight interaction mediates blood vessel stabilisation. *Image created through Servier Medical Art.*

1.6.4 Intussusceptive Angiogenesis

An alternative, rapid mechanism for new blood vessel formation is through intussusceptive angiogenesis. It was first observed in the rapidly expanding pulmonary capillary bed of neonatal rats (Caduff et al., 1986). Here, 1-2 μm holes within vascular corrosion casts were shown to correspond to intraluminal trans-capillary tissue pillars where the capillary wall had invaginated into the vessel lumen. The process of intussusceptive angiogenesis is fast, taking minutes to hours, as there is no need for endothelial cell proliferation. Instead, endothelial cells are remodelled, increasing in volume and becoming thinner.

Typically there are four phases to pillar formation (Djonov et al., 2003). In phase I a zone of contact is created between opposing capillary walls. In phase II there is reorganisation of the inter-endothelial cell junctions and central perforation of the bilayer. In phase III an interstitial pillar core is formed that is invaded by pericytes and myofibroblasts that then lay down collagen fibrils. Finally in phase IV the pillars increase in girth without undergoing any further change in their basic structure. Although the molecular mechanisms behind intussusceptive angiogenesis are not fully understood, there are thought to be several key factors that can influence pillar formation (Hillen and Griffioen, 2007).

Changes in blood flow dynamics may stimulate the process of intussusceptive angiogenesis and has been observed in chick chorioallantoic membranes (Djonov et al., 2002). Furthermore, changes in shear stress on endothelial cells can activate a biochemical cascade which may lead to cytoskeletal rearrangements. It is hypothesised that inhibition of sprouting angiogenesis may stimulate

intussusceptive angiogenesis, therefore, it could be a means of drug resistance against anti-angiogenic agents (Hillen and Griffioen, 2007).

1.6.5 Tumour Angiogenesis

In 1971 Judah Folkman published in the "*New England Journal of Medicine*" hypothesising that tumour growth was dependent on angiogenesis and that inhibition of angiogenesis could be therapeutic (Folkman, 1971). Referred to as "The Father of Angiogenesis", Folkman was initially criticised for his theories as the prevailing opinion of the time was that tumour growth did not depend on angiogenesis, rather that tumour vascularity was nonspecific inflammation. Today, it is widely accepted that tumours can grow to a size of 1-2 mm³ before their metabolic demands are restricted due to the diffusion limit of oxygen and nutrients (Hillen and Griffioen, 2007).

1.6.5.1 Characteristics of Tumour Blood Vessels

It has long been known that tumour blood vessels are morphologically abnormal. The vessels are tortuous with irregular branching patterns and lack the normal hierarchical arrangement of artery-arteriole-capillary (Konerding et al., 1999). They also have poor stability due, in part, to defects in pericytes, which are loosely attached (Morikawa et al., 2002). These changes can affect blood flow, with some vessels having bidirectional flow and some having no blood flow at all.

Functionally, tumour vessels are inappropriately permeable to large macromolecules. They are inefficient at both delivering oxygen to the tumour and removing waste products. This results in the creation of a hostile tumour

microenvironment that is both hypoxic and acidic. Tumours must activate signalling pathways that allow adaptation. The expression of growth factors, such as VEGF, results in more inefficient angiogenesis that in turn makes the tumour microenvironment even more hostile. This vicious circle ensures that a microenvironment is created that selects tumours with the most aggressive phenotype.

Abnormalities in the tumour vasculature may also lead to tumour progression. Fragile, permeable vessels may allow tumour cells to enter the circulation and disseminate to distant sites. Deficient pericyte coverage is associated with increased metastases in human cancers (Yonenaga et al., 2005). Furthermore, correction of these abnormalities in mouse models suppresses tumour invasion and metastases (Welen et al., 2009, Mazzone et al., 2009).

The abnormal tumour vasculature makes drug delivery difficult. Hypoxia itself can cause resistance to radiation and certain chemotherapeutic agents. Jain hypothesised that the increased permeability impairs the ability of chemotherapeutic agents to reach the tumour site. Therefore, blocking VEGF may “normalise” blood flow and improve drug delivery (Jain, 2005). This is supported in mouse models where a single dose of bevacizumab (a monoclonal antibody targeted against VEGF) decreased microvessel density, vascular permeability and interstitial pressure and improved intratumoural perfusion (Dickson et al., 2007). Furthermore, clinical studies support the concept of combining bevacizumab with chemotherapeutic agents to improve outcomes in patients with advanced colorectal cancer (Hurwitz et al., 2004). These findings have led to two conflicting schools of thought regarding anti-angiogenic strategies (Carmeliet and Jain, 2011). Should

tumour vessels be destroyed resulting in tumour shrinkage due to oxygen starvation, or should they be normalised to limit metastatic spread from oxygen-enriched tumours and improve responses to conventional anticancer treatments?

1.6.5.2 Tumour Endothelial Cells

Although HUVECs were first isolated in 1973, it was well over twenty-five years before tumour endothelial cells (TECs) could be successfully isolated and cultured. Several technical limitations have made the study of the biology of TECs difficult. TECs are most commonly isolated using an immune-magnetic sorting (IMS) technique in which small magnetic beads are coated with endothelial cell surface marker antibodies. The most commonly used markers are CD31 and CD146, but these are common to endothelial cells from all vessel types (capillary, venous etc.). This means cultures are likely a heterogeneous population of endothelial cells. Also, IMS is not 100% efficient and contamination with other cell types such as fibroblasts is a possibility. Furthermore, the optimal conditions for culturing TECs has not been established. In vivo, TECs may be adapted to the toxic tumour microenvironment which is hypoxic and acidotic and where they are exposed to aberrant forces from chaotic blood flow. Therefore, TECs in vitro may not be an accurate representation of TECs in vivo. Nevertheless, it is well known that TECs are irregular in shape and size, have ruffled margins and long, fragile cytoplasmic projections extending across the vessel lumen (Dudley, 2012). In one of the first reports of successful isolation TECs maintained their phenotype, expressed growth factor receptors, and were stimulated by typical endothelial cell mitogens (Alessandri et al., 1999).

More recent studies have shown that tumour angiogenesis is not simply driven by pre-existing endothelial cells and that tumour endothelial cells can arise from novel sources (Dudley, 2012). VEGF and the hypoxic tumour microenvironment recruits endothelial progenitor cells (EPCs) from the bone marrow and/or activates tumour resident EPCs. EPCs then either differentiate into endothelial cells or produce angiogenic growth factors to stimulate angiogenesis (Marçola and Rodrigues, 2015). Many aspects of the role played by EPCs in tumour angiogenesis however, remain unclear.

St. Croix published the first comprehensive genetic screening of human TECs from malignant colorectal cancer tissue (St Croix et al., 2000). Serial analysis of gene expression identified 46 transcripts elevated in TECs and 9 novel transcripts thought to be specific tumour endothelial cell markers (TEM 1-9). However, subsequent studies suggested TEM expression is not restricted to TECs, occurring also in normal vascular beds (Seaman et al., 2007), developing tissue (Opavsky et al., 2001), fibroblasts and perivascular cells (MacFadyen et al., 2007), the brain (Lee et al., 2005) and osteosarcoma cell lines (Halder et al., 2009). Collated transcript profiles from multiple studies and multiple tumour types have shown only a few overexpressed transcripts to be shared by different tumours including MMP9, HEYL and SPARC (Aird, 2009). A number of studies have compared gene expression between cultured colorectal cancer derived endothelial cells and normal colonic endothelial cells (van Beijnum et al., 2006, Schellerer et al., 2007, Jayasinghe et al., 2009, Mesri et al., 2013). No studies to date have analysed endothelial cells from CLM.

1.6.5.3 Vasculogenic Mimicry

Vasculogenic mimicry was first reported in 1999 and describes the ability of tumour cells to masquerade as endothelial cells (Maniotis et al., 1999). Occurring mainly in aggressive tumours, tumour cells are able to de-differentiate to an endothelial phenotype and make tube-like structures. This provides tumours with a secondary circulatory system independent of angiogenesis. The exact mechanism underlying vasculogenic mimicry is yet to be resolved. Several molecules appear to be involved including PI3 kinase, VE-Cadherin and tissue factor pathway inhibitor 2 (Hillen and Griffioen, 2007).

1.6.5.4 Vessel Co-option

Although it is generally accepted that tumours start as an avascular mass and induce angiogenesis to grow beyond a few millimetres in size, it has been suggested that many tumours can grow in an avascular stage in well vascularised tissue like the brain and lungs. Known as vessel co-option, tumours can grow along existing vessels without inducing an angiogenic response (Holmgren et al., 1995, Pezzella et al., 1997). The first evidence for this process was reported in 1999 (Holash et al., 1999). In vivo studies reported that 2 weeks after implantation of C6 glioma cells in rat brains, tumours were well vascularised with vessels that had characteristics of normal blood vessels, suggesting vessel co-option. However, after 4 weeks, blood vessels had undergone a dramatic regression resulting in a secondary avascular tumour mass with massive tumour cell loss. The tumours were then rescued by robust angiogenesis at the tumour periphery. The Tie-2 receptor antagonist Ang-2 and pro-angiogenic VEGF appear to be key regulators of this process.

1.6.5.5 Angiogenesis in Colorectal Cancer Liver Metastases

The liver is a highly vascularised organ and three different patterns of growth of CLM have been identified with differing levels of angiogenesis (Vermeulen et al., 2001). In “pushing-type” growth, metastases compress the surrounding liver parenchyma and there is a high level of angiogenic activity. In “desmoplastic” growth, metastases are separated from the surrounding liver parenchyma by a rim of desmoplastic stroma containing a dense lymphocytic infiltrate and numerous capillaries. In “replacement” type growth, tumour cells replace hepatocytes maintaining the liver architecture with minimal inflammatory reaction. They have low levels of angiogenesis instead co-opting hepatic sinusoids. A combination of these growth patterns may exist in patients with multiple liver metastases (Nielsen et al., 2014).

Understanding the biology of CLM and variability in levels of angiogenesis is important and may help predict which patients will respond best to anti-angiogenic therapy.

1.7 Anti-Angiogenic Agents

1.7.1 Endogenous Angiogenesis Inhibitors

Tumour angiogenesis represents an attractive treatment target for cancer therapeutics. Disrupting an essential process necessary for tumour growth and spread is a logical approach. A number of endogenous angiogenesis inhibitors exist (Table 3) and attempts have been made to develop anti-angiogenic agents based on these substances. An exhaustive review of each individual substance is beyond the scope of this work, however, key substances will be briefly considered.

Endostatin is a 20 kDa c-terminal fragment derived from Type XVIII collagen that has broad-spectrum anti-angiogenic activity (Nyberg et al., 2005). This includes; 1) Inhibition of cyclin-D1 causing G1 cell cycle arrest and apoptosis, 2) Alteration of fibroblast growth factor (FGF) signal transduction inhibiting migration of endothelial cells, 3) Blocking VEGF-mediated signalling through direct interaction with VEGFR-2, 4) Binding to integrin $\alpha 5\beta 1$ on endothelial cells inhibiting their migration by blocking signalling pathways via Ras and Raf, 5) Binding to and inactivating matrix metalloproteinases and 6) Blocking tumour necrosis factor-induced activation of c-Jun NH2-terminal kinase and c-Jun NH2-terminal kinase-dependent proangiogenic gene expression. In a phase III clinical trial, the addition of endostar (a recombinant human endostatin) to conventional platinum based chemotherapy resulted in a significantly increased response rate and median overall survival in patients with locally advanced or non-small cell lung cancer (Sun et al., 2013)

Matrix Derived	Non-Matrix Derived
Arresten	Angiostatin
Canstatin	Antithrombin III
Endorepellin	Chondromodulin
Endostatin	Interferons
Fibronectin	Interleukins
Fibulin	Prolactin Fragments
Thrombospondin-1 and -2	Tissue Inhibitor of Metalloproteinases (TIMPs)
Tumstatin	Troponin I
	Vasostatin

Table 3 Endogenous Inhibitors of Angiogenesis

A number of natural endogenous substances are capable of inhibiting angiogenesis. They have been divided into matrix-derived and non-matrix derived.

Thrombospondins (TSPs) are a family of secreted glycoproteins with anti-angiogenic functions. There are five family members with TSP-1 and -2 being potent inhibitors of angiogenesis. TSP-1 was the first protein to be shown to play a critical role as a naturally occurring inhibitor of angiogenesis (Lawler and Lawler, 2012). The mechanisms by which TSPs regulate angiogenesis are complex, with direct and indirect activity. For instance, it can inhibit endothelial cell migration and induce endothelial cell apoptosis, but also has indirect effects on growth factors, cytokines and proteases that regulate angiogenesis. Surprisingly, a phase II clinical trial assessing ABT-510 (a synthetic analogue of TSP-1) for the treatment of metastatic melanoma failed to demonstrate any clinical efficacy (Markovic et al., 2007).

1.7.2 Anti-Angiogenic Drugs used in Metastatic Colorectal Cancer

Bevacizumab (Avastin[®]) is a humanised monoclonal antibody targeted against VEGF-A. Binding of bevacizumab prevents VEGF from binding to its receptors. Two randomised clinical trials have shown that bevacizumab improves overall survival in patients with metastatic colorectal cancer when used in conjunction with first- and second-line chemotherapeutic agents. In the first study, median overall survival improved from 15.6 months in patients with metastatic colorectal cancer receiving IFL (5-FU, leucovorin and irinotecan) to 20.3 months in patients who received IFL and bevacizumab (Hurwitz et al., 2004). The E3200 trial showed the benefit of using bevacizumab as part of a second-line therapy when combined with FOLFOX. Median overall survival increased from 10.8 to 12.9 months with the addition of bevacizumab compared to FOLFOX alone (Giantonio et al., 2007).

Aflibercept (Zaltrap[®]) is a recombinant fusion protein with receptor components of VEGFR-1 and VEGFR-2, which binds multiple ligands including VEGF-A, VEGF-B and PGF. It binds to circulating VEGF preventing it from binding to VEGFR-2. Aflibercept in combination with FOLFIRI improved overall survival (13.5 vs 12.06 months), and progression-free survival (6.9 vs. 4.67 months) compared to FOLFIRI alone in patients with metastatic colorectal cancer who had progressed with FOLFOX therapy (Van Cutsem et al., 2012).

Ramucirumab (Cyramza[®]) is a human monoclonal antibody directed against the extracellular domain of the VEGFR-2 receptor and functions as a VEGFR-2 receptor antagonist. Ramucirumab in combination with FOLFIRI improved median overall survival (13.3 vs. 11.7 months) compared to FOLFIRI alone in patients with metastatic colorectal cancer who had disease progression following first-line therapy with bevacizumab, oxaliplatin, and a fluoropyrimidine (Tabernero et al., 2015).

Regorafenib is an oral multikinase inhibitor that targets protein kinases involved in tumour angiogenesis (VEGFR1-3, Tie-2), oncogenesis (KIT, RET and RAF) and the tumour microenvironment (platelet-derived growth factor receptor- β and fibroblast growth factor receptor) (Wilhelm et al., 2011). The CORRECT trial, an international, multi-centre phase III trial, showed the benefit of regorafenib monotherapy in patients with metastatic colorectal cancer who had progressed on standard first-line therapy, including bevacizumab. Regorafenib improved median overall survival (6.4 vs. 5.0 months) and progression-free survival (1.9 vs. 1.7 months) compared to placebo (Grothey et al., 2013).

Agents that target other parts of the angiogenesis pathway are under investigation in clinical trials. For instance, EZN-9628 is an anti-sense oligonucleotide inhibitor of HIF-1 α currently being investigated in patients with liver metastases from advanced solid tumours (Clinical trials identifier: NCT01120288). Unfortunately a number of agents that showed promising anti-angiogenic activity have had negative results in phase III clinical trials. This includes the tyrosine kinase inhibitors sunitinib and vatalanib (Hecht et al., 2011, Carrato et al., 2013). A summary of anti-angiogenic agents and their efficacy in metastatic colorectal cancer are provided in Table 4.

Indication	Therapy	Trial	Outcome	Citation
First line	FOLFIRI +/- Bevacizumab	AV2119	Improvement in OS and PFS.	Hurwitz et al., 2004
	FOLFOX or XELOX +/- Bevacizumab	NO16966	No Improvement in OS. Improvement in PFS.	Saltz et al., 2008
	Capecitabine +/- Bevacizumab	AVEX	Improvement in PFS. OS N/A.	Cunningham et al., 2013
	FOLFIRI +/- Sunitinib	SUN1122	No improvement in PFS.	Carrato et al., 2011
	FOLFOX +/- Vatalanib	CONFIRM1	No improvement in OS and PFS.	Hecht et al., 2013
Second Line	FOLFOX +/- Bevacizumab	E3200	Improvement in OS and PFS.	Giantonio et al., 2007
	FOLFIRI +/- Afibercept	VELOUR	Improvement in OS and PFS.	Van Cutsem et al., 2012
	Regorafenib vs. Placebo	CORRECT	Improvement in OS.	Grothey et al., 2013
	FOLFIRI +/- Ramucirumab	RAISE	Improvement in OS and PFS.	Tabernero et al., 2015

Table 4 Summary of Clinical Trials Investigating Anti-Angiogenic Agents in Metastatic Colorectal Cancer

A number of randomised clinical trials have been undertaken investigating the benefit of anti-angiogenic therapy in the treatment of metastatic colorectal cancer. In the table, trials have been separated into first-line (no previous chemotherapy) or second line (failed conventional chemotherapy). Overall survival (OS) and progression-free survival (PFS) outcomes are included.

1.7.3 Toxicity Associated with Anti-Angiogenic Therapy

As angiogenesis in the adult is a rare process, it was initially presumed that anti-angiogenic agents would have limited side effects. However, clinical experience has revealed a number of adverse events associated with these drugs. The most common adverse events are experienced in the cardiovascular system (hypertension, arterial thromboembolic events, ventricular dysfunction, congestive heart failure) and urinary system (proteinuria, renal thrombotic microangiopathy). Other reported adverse events include haemorrhage, wound complications, gastrointestinal perforation, venous thromboembolism and hypothyroidism (Chen and Cleck, 2009). Excessive toxicity may necessitate dose reductions or treatment breaks, which can limit anti-angiogenic efficacy.

Adverse events generally arise as a direct consequence of VEGFR-2 inhibition. For instance, in the case of hypertension, the best documented cardiovascular adverse effect with anti-VEGF therapy, VEGFR-2 signalling normally generates nitric oxide and prostaglandin I₂, which induce endothelial cell dependent vasodilatation in vessels. Inhibition of this signalling pathway has the opposite effect, causing vasoconstriction. Physiological functions of VEGF/VEGFR-2 signalling and consequences of inhibition are summarised in Figure 8.

An obvious concern with the use of anti-angiogenic agents for patients undergoing curative liver resection for CLM is what impact they have upon liver regeneration and wound healing. However, numerous case-control studies have found no difference in post-operative morbidity or mortality with their use (Tamandl et al., 2010, Chaudhury et al., 2010).

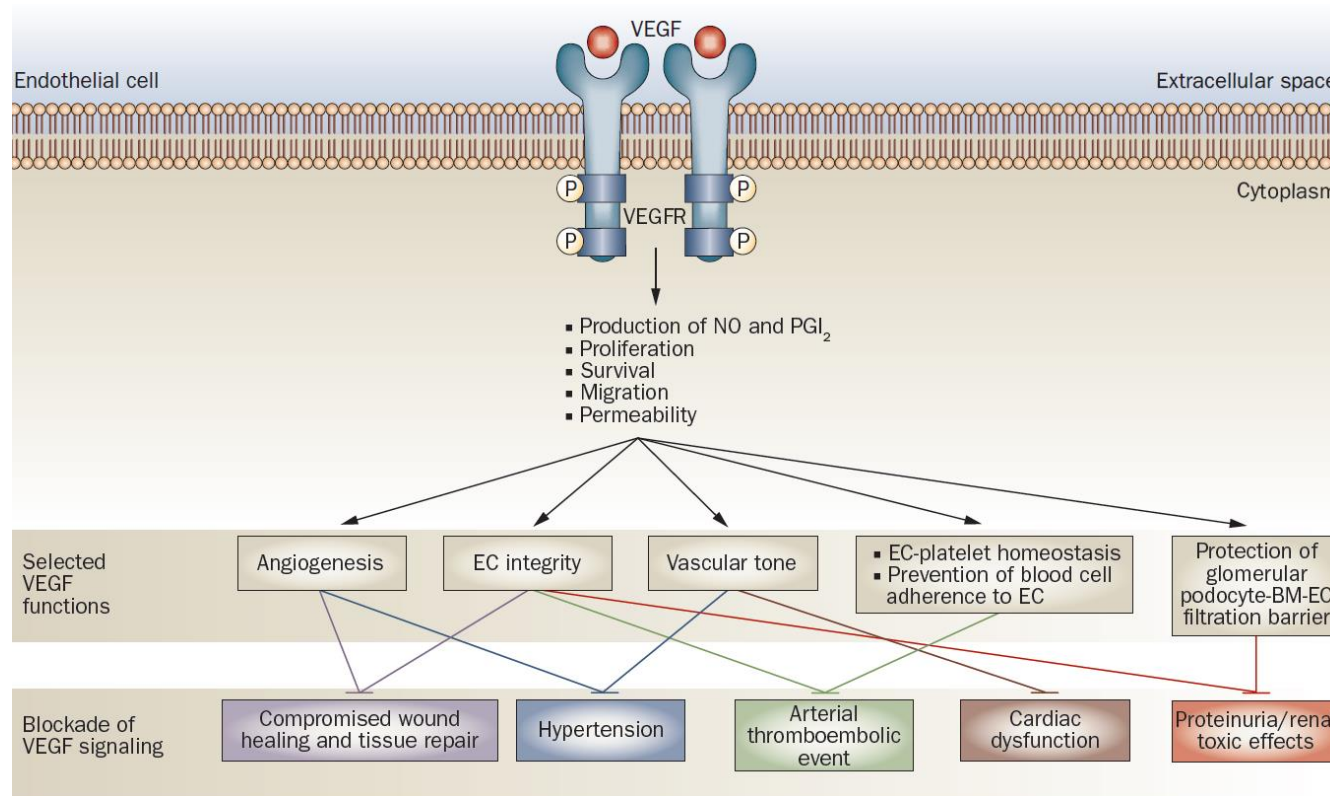


Figure 8 VEGF/VEGFR-2 Signalling and Consequences of Inhibition

VEGF signalling via VEGFR-2 leads to downstream molecular and cellular events including nitric oxide production, endothelial cell proliferation and migration. This is important in the regulation of a number of process including angiogenesis and vasodilatation. Blockade of VEGF signalling can therefore disrupt a number of physiological processes with pathological consequences including impaired wound healing, hypertension, arterial thromboembolic events and cardiac dysfunction. BM= basement membrane, EC= endothelial cells, P= phosphorylated residues; PGI₂= prostaglandin I₂, NO= nitric oxide. Adapted from Chen and Cleck (2009).

1.7.4 Failure of Anti-Angiogenic Therapy

Resistance to anti-angiogenic therapy is a problematic issue that, in part, explains the variable results observed in randomised clinical trials with anti-angiogenic agents. The tumour vasculature is heterogeneous in its response to anti-angiogenic agents, with some vessels being sensitive to treatment whilst others are resistant. Pre-clinical studies have demonstrated that anti-VEGF therapy can inhibit tumour vessel angiogenesis, but is less effective upon established tumour vasculature. This is believed to be due to the dependence of nascent tumour vessels on VEGF that is lost once the vessel undergoes maturation (Helfrich et al., 2010).

The ability of tumours to signal via alternative angiogenic pathways once the VEGF pathway is blocked can also contribute to treatment resistance. Pre-clinical studies have identified numerous up-regulated candidates including angiopoietins, EGF, fibroblast growth factor 1 and 2 and the delta-notch pathway (Vasudev and Reynolds, 2014). Although the logical approach would be to block other signalling pathways in conjunction with VEGF, this has yet to be validated clinically and some multi-targeted drugs, such as sunitinib, have had negative results in clinical trials (Carrato et al., 2013).

Although anti-angiogenic agents should reduce oxygen and nutrient delivery to the tumour, there is pre-clinical evidence that tumours can adapt to survive in stressful conditions. This may be driven by genetic abnormalities such as mutated p53 (Yu et al., 2002). Alternatively, tumours may recruit other mechanisms of tumour vascularisation, such as intussusceptive angiogenesis, vasculogenic mimicry and vessel co-option. These mechanisms may be independent of VEGF signalling and so the tumour can “switch” mechanism once VEGF signalling is blocked. For

instance, treatment of mice breast carcinoma allografts with vatalinib significantly reduced tumour vascularisation, but upon cessation of therapy the tumour vasculature expanded predominantly by intussusceptive angiogenesis (Hlushchuk et al., 2008).

Anti-angiogenic agents are expensive. A single dose of bevacizumab costs in excess of £1000 (National Institute for Health and Care Excellence, 2010). At present the National Institute for Health and Clinical Excellence (NICE) do not recommend bevacizumab in combination with oxaliplatin and either 5-FU plus leucovorin or capecitabine for patients with metastatic colorectal cancer (National Institute for Health and Care Excellence, 2010). Similarly bevacizumab in combination with non-oxaliplatin (fluoropyrimidine-based) chemotherapy is not recommended for the treatment of patients with metastatic colorectal cancer that have progressed after first-line chemotherapy (National Institute for Health and Care Excellence, 2012). This is because, in their opinion, it does not provide enough benefit to patients to justify its high costs. NICE also do not recommend the use of aflibercept with FOLFIRI for metastatic colorectal cancer that is resistant to or has progressed after an oxaliplatin containing regimen (National Institute for Health and Care Excellence, 2014).

Concerns regarding the safety and efficacy of current anti-angiogenic agents perhaps suggest that interference with the VEGF/VEGFR-2 signalling mechanism is not the best approach for designing future therapeutics. Instead, agents which directly kill tumour endothelial cells may be preferential. This will require the identification of new novel targets important to tumour endothelial cell growth and survival.

1.8 Summary

Colorectal cancer liver metastases are a significant cause of cancer-related morbidity and mortality. Although an increasing number of patients are undergoing curative surgery, the vast majority of patients are treated palliatively. Furthermore, for patients that do undergo curative surgery, recurrence rates are high. Central to CLM growth and survival is the process of tumour angiogenesis, which is regulated by VEGF/VEGFR-2 signalling. Targeting tumour angiogenesis is an attractive treatment strategy, whereby tumour blood vessels are destroyed resulting in the starvation of oxygen and nutrients leading to tumour shrinkage. Licensed anti-angiogenic agents target the VEGF/VEGFR-2 signalling pathway and although they have had promising results in pre-clinical studies, this has not really translated into meaningful improvements in outcomes for metastatic colorectal cancer. This, in part, is due to anti-angiogenic therapy resistance, as tumours appear to be able to switch to alternative angiogenic mechanisms.

Tumour blood vessels are morphologically abnormal and are lined on their inner surface by tumour endothelial cells. Tumour endothelial cells are genetically and phenotypically distinct from other endothelial cell types. Endothelial cells of CLM have never been isolated or characterised before. Knowledge of their molecular make-up may help better understand the mechanisms associated with anti-angiogenic therapy resistance. Furthermore, identification of proteins critical to their survival may lead to the development of new anti-angiogenic therapies that have direct tumour endothelial cell cytotoxicity.

Aims and Objectives

Aim

The overall aim of this research is to identify novel protein targets in endothelial cells of colorectal cancer liver metastases that could be used for the development of anti-angiogenic therapies for the treatment of CLM.

Hypothesis

Compared to normal liver endothelial cells, endothelial cells of colorectal cancer liver metastases differentially express proteins that can be therapeutically targeted to inhibit tumour angiogenesis.

Objectives

- Isolate and culture endothelial cells from CLM.
- Characterise endothelial cells from CLM using endothelial cell markers and functional assays.
- Analyse RNA interference screening data to identify proteins critical to CLM endothelial cell survival.
- Perform in vitro angiogenesis studies to determine the anti-angiogenic potential of identified protein targets.
- Perform mechanistic studies to determine how identified protein targets inhibit angiogenesis.
- Perform in vitro studies to determine if the identified protein targets have direct anti-cancer activity.
- Use proteomic studies to identify differences in protein expression between normal liver endothelial cells and endothelial cells of CLM.

Chapter 2: Materials and Methods

2.1 Cell Lines and Cell Culture

Human Umbilical Vein Endothelial Cells (HUVECs)

HUVECs were purchased from Lonza and maintained in Endothelial Cell Basal Medium (EBM-2) supplemented with a BulletKit™. The BulletKit™ contained 2% foetal calf serum (FCS) and the following growth factors; 10 ng.ml⁻¹ VEGF, 5 ng.ml⁻¹ human basic fibroblast growth factor, 1 µg.ml⁻¹ hydrocortisone, 50 ng.ml⁻¹ gentamicin, 50 ng.ml⁻¹ amphotericin B, and 10 µg.ml⁻¹ heparin. Experiments were performed on cells from passage 2-8.

Human Liver Endothelial Cells

Human liver endothelial cells were obtained fresh from patients undergoing curative liver resection for CLM at St. James's University Hospital, Leeds Teaching Hospitals NHS Trust. Matched endothelial cells from CLM and normal liver tissue were both grown in EBM-2 supplemented with a Bulletkit™. Cells were passaged once 95% confluent and used from passage 1-5.

Mouse Liver Endothelial Cells

Mouse liver endothelial cells were obtained fresh from mice livers harvested by Dr Baptiste Rode (University of Leeds). Cells were plated directly into experimental dishes, grown in EBM-2 supplemented with a Bulletkit™ and never passaged.

Normal Human Dermal Fibroblasts (NHDF)

NHDF were purchased from Lonza. These cells were cultured in EBM-2 growth medium supplemented with a Bulletkit™. Cells were passaged once 95% confluent and used from passage 1-8.

HT29 Colorectal Adenocarcinoma Cells

HT29 cells (ATCC® HTB-38™) were purchased from Sigma. This cell line was established in 1964 from the primary tumour of a 44-year-old caucasian female with colorectal adenocarcinoma. They have a mutated p53 (Arg-273 to His). Cells were cultured in Dulbecco's Modified Eagle Medium GlutaMAX (Invitrogen) supplemented with 10% FCS and 100 units.ml⁻¹ penicillin-streptomycin.

All cells were grown in a 5% CO₂ incubator at 37°C.

2.2 Human Liver Endothelial Cell Isolation

Ethical approval for tissue collection was granted by Yorkshire and the Humber - Leeds East Research Ethics Committee (REC Reference No: 14/YH/1001). Approval was also granted by Leeds Teaching Hospitals NHS Trust Research and Development Department to undertake this research in their hospitals (Reference: GS14/1121) and by the Histopathology Department (Reference: 300/PATHRES/14). Patients undergoing curative liver resection for CLM provided fully informed written consent to take part in the study. Each participant was assigned a study number, and a form containing medical history was generated.

Tissue was taken immediately following surgical resection in the operating theatres at St. James's University Hospital, Leeds. Tumours were visually and manually located within the specimen. A 2.5 cm x 2.5 cm x 2.5 cm incision was made into the tumour avoiding the centre and any obvious areas of necrosis. A similar slice of macroscopically normal liver tissue was also taken at least 2.5 cm away from the tumour. The tissue samples were stored in separate 50 mL falcon tubes containing EBM-2 supplemented with a BulletKit™ and transported on ice.

Isolation of endothelial cells was undertaken in a sterile manner in a tissue culture hood assigned for use with human tissues. The protocol was adapted from a previously published technique (van Beijnum et al., 2008). Tissue was minced using two scalpel blades and re-suspended in a dissociation solution consisting of 9 mL 0.1% Collagenase II, 1 mL 2.5 units.mL⁻¹ Dispase, 1 µM Calcium Chloride and 1 µM Magnesium Chloride in Hanks Buffer solution per sample. The tissue-dissociation mix was incubated at 37°C for 45 mins in a MACSMix Tube Rotator (Miltenyi Biotech) to provide continuous agitation.

Following enzymatic digestion, the samples were passed through 100 µm and 40 µm cell strainers to remove any undigested tissue. Cells were washed twice in magnetically-activated cell sorting (MACS) buffer consisting of; Phosphate Buffered Saline (PBS), EDTA 2 mM and 0.1% Bovine Serum Albumin (BSA) pH 7.2. The washed pellets were suspended in 20 mL red blood cell lysis buffer consisting of 0.206 g Tris base, 0.749 g NH₄Cl in 100 mL PBS pH 7.2 for 10 mins. Cells were washed for a final time in MACS buffer before the pellet was incubated with 200 µL of dead cell removal paramagnetic microbeads per 1 x10⁷ cells (Miltenyi Biotec) in MACS buffer at room temperature for 15 mins. After incubation, the cells were

passed through an LS column prepared with 1 x binding buffer (Miltenyi Biotec) in a magnetic field (MiniMACS Separator, Miltenyi Biotec). The column retains apoptotic and dead cells, meaning the eluate consists of live cells only.

IMS was used to select CD31 positive cells (Figure 9). Live cells were incubated with 30 μ L FcR blocking reagent and 30 μ L CD31-conjugated paramagnetic microbeads for 15 mins at 4 °C under continuous agitation. After incubation, the solution was passed through an MS column prepared with MACS buffer. CD31 positive cells were retained in the column and CD31 negative cells passed through as eluate. CD31 positive cells were washed through with warm EBM-2 media supplemented with a BulletKitTM and the CD31 selection process was repeated for a second time to help reduce contamination with other cell types. After the second selection, cells were placed in one well of a 6-well plate and incubated in a 5% CO₂ incubator at 37°C. Medium was changed at 12 hrs and then every 48 hrs until confluent. Cells were used from passage 1-5.

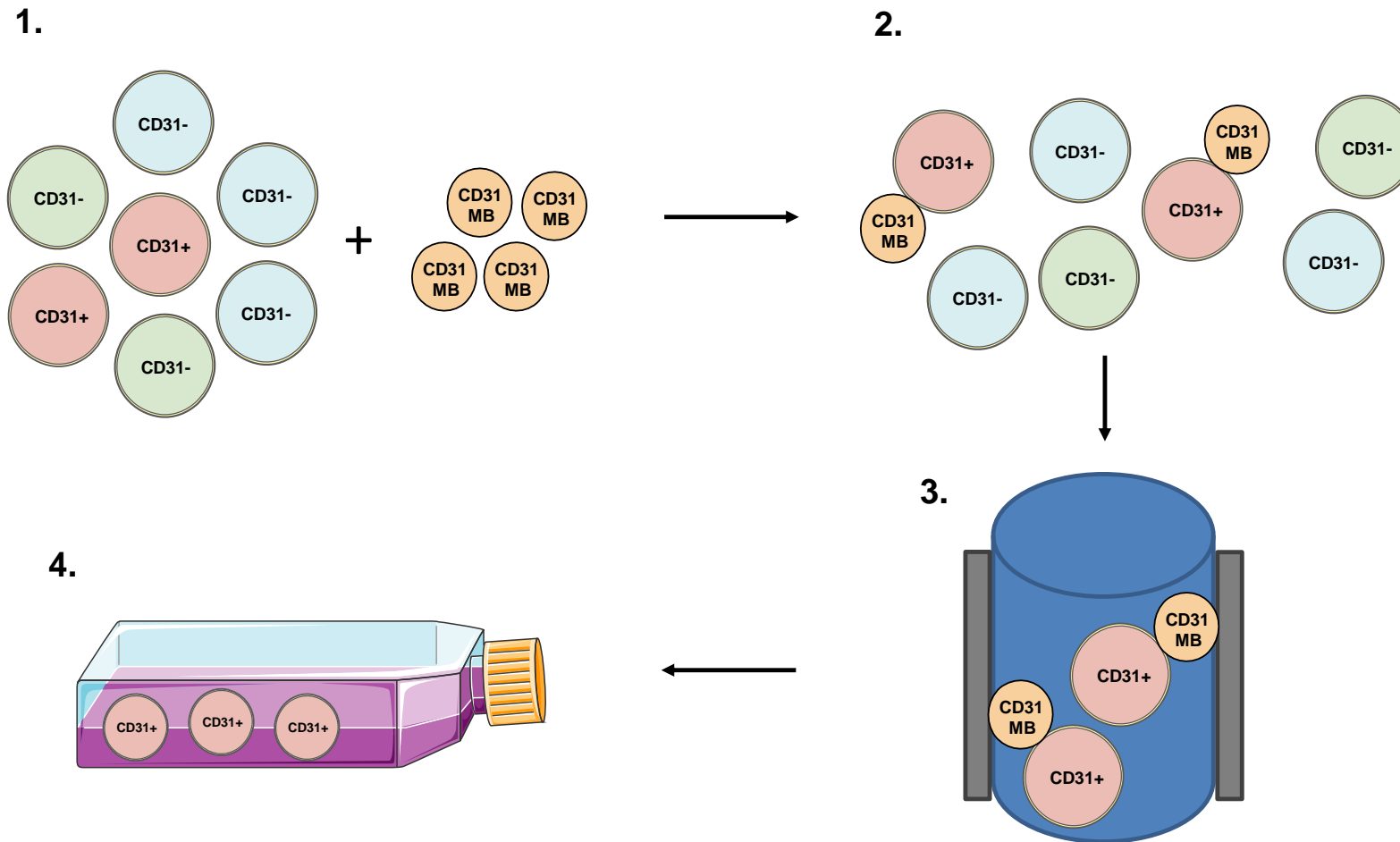


Figure 9 Immuno-Magnetic Selection of CD31-Positive Cells

1. After the generation of a single-cell suspension, cells are incubated with CD31-magnetic beads. 2. The CD31-magnetic beads bind to CD31 positive cells only. 3. The suspension is passed through a column in a magnetic field where CD31-positive cells are retained and CD31-negative cells pass through as eluate. 4. CD31-positive cells are flushed through and cultured. MB = Magnetic beads. *Image created through Servier Medical Art.*

2.3 Mouse Liver Endothelial Cell Isolation

Mouse liver endothelial cell isolation also used an IMS technique similar to human liver endothelial cell isolation. Mouse livers were harvested by Dr Baptiste Rode (University of Leeds). The entire liver was minced using 2 scalpel blades and re-suspended in a dissociation solution consisting of 9 mL 0.1% Collagenase II, 1 mL 2.5 units.mL⁻¹ Dispase, 1 µM Calcium Chloride and 1 µM Magnesium Chloride in Hanks Buffer solution per sample. The tissue-dissociation mix was incubated at 37°C for 45 mins in a MACSMix Tube Rotator (Miltenyi Biotec) to provide continuous agitation.

Following enzymatic digestion, the samples were passed through 100 µm and 40 µm cell strainers to remove any undigested tissue. Cells were washed twice in PEB buffer consisting of PBS, EDTA 2 mM and 0.5% BSA pH 7.2. The washed pellets were suspended in 200 µL of dead cell removal paramagnetic microbeads per 1 x10⁷ cells (Miltenyi Biotec) in PEB buffer at room temperature for 15 mins. After incubation, the cells were passed through an LS column prepared with 1 x binding buffer (Miltenyi Biotec) in a magnetic field (MiniMACS Separator, Miltenyi Biotec). The eluates were incubated with 20 mL red blood cell lysis buffer consisting of 0.206 g Tris base, 0.749 g NH₄Cl in 100 mL PBS pH 7.2 for 10 mins and then washed a final time in PEB buffer.

IMS was used to select CD146 positive cells. Live cells were incubated with 30 µL CD146-conjugated paramagnetic microbeads for 15 mins at 4 °C under continuous agitation. After incubation, the solution was passed through an MS column prepared with PEB buffer. CD146 positive cells were retained in the column and

CD146 negative cells passed through as eluate. CD146 positive cells were washed through with warm EBM-2 media supplemented with a BulletKit™ and the CD146 selection process was repeated for a second time to help reduce contamination with other cell types. After the second selection cells were plated directly onto experimental dishes in a 5% CO₂ incubator at 37°C. Medium was changed at 12 hrs and then every 48 hrs until experiments were performed.

2.3 Drugs and Reagents

2.3.1 Drugs

2.3.1.1 AZD1775

AZD1775 (Active Biochem) is a small molecule WEE1 inhibitor, which inhibits WEE1-activity in an ATP-competitive manner and has an IC₅₀ of 5.2 nM. It is a pyrazolo-pyrimidine derivative and has high specificity for WEE1, inhibiting only eight out of 223 other serine/threonine or tyrosine kinases tested (Hirai et al., 2009). Of these eight, AZD1775 only had high affinity for Yamaguchi sarcoma virus oncogene with an IC₅₀ value of 14 nM. It was reconstituted in dimethyl sulfoxide (DMSO) which in experiments is referred to as the vehicle control.

2.3.1.2 RO-3306

RO-3306 (Sigma) is a quinolinyl thiazolinone derivative and selective ATP-competitive inhibitor of CDK1. It inhibits cyclin B-CDK1 activity with Ki of 35 nM. It has nearly 10-fold selectivity relative to cyclin E-CDK2 and over 50-fold relative to cyclin D-CDK4 (Vassilev et al., 2006).

2.3.1.3 5-Fluorouracil

5-FU (Sigma) is a chemotherapeutic agent used clinically for the treatment of colorectal cancer. Its primary mechanism of action is as a thymidylate synthase (TS) inhibitor, inhibiting the synthesis of the critical pyrimidine thymidine. TS is an enzyme that normally catalyzes the reductive methylation of deoxyuridine monophosphate to deoxythymidine monophosphate (dTMP). Depletion of dTMP results in subsequent depletion of deoxythymidine triphosphate (dTTP), which induces perturbations in the levels of the other deoxynucleotides (dATP, dGTP and dCTP) through various feedback mechanisms (Longley et al., 2003). Deoxynucleotide pool imbalances (in particular, the dATP/dTTP ratio) are thought to severely disrupt DNA synthesis and repair, resulting in lethal DNA damage (Houghton JA et al., 1995). The chemical structures of all chemotherapeutic agents used in this study are shown in Figure 10.

2.3.1.4 Oxaliplatin

Oxaliplatin (Sigma) is a platinum-based chemotherapy used clinically for the treatment of colorectal cancer. It forms inter- and intra-strand cross links in DNA, preventing DNA replication and transcription, resulting in cell death (Graham et al., 2004).

2.3.1.5 Irinotecan

Irinotecan (Sigma) is used in combination with other chemotherapeutic agents for the treatment of colorectal cancer. It is a derivative of camptothecin, which inhibits the action of topoisomerase I, a nuclear enzyme that has a critical role in DNA replication and transcription. Topoisomerase I normally causes transient breaks in a

single strand of DNA that helps release the torsional strain caused by synthesis of a new strand of DNA or RNA around the double helix. Irinotecan binds to the topoisomerase I-DNA complex stabilising it and preventing the reannealing of the parent DNA. Collision of replication forks with the stabilized complex during cell division leads to double-stranded DNA breaks and tumour cell death.

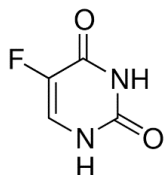
2.3.1.6 Yoda1

Yoda1 is a recently discovered activator of Piezo1 (Syeda et al., 2015). Concentrations of up to 10 μM were used for experiments, at which point Yoda1 becomes insoluble.

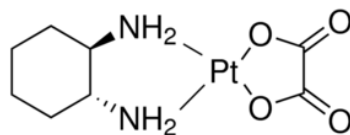
2.3.1.7 Ionomycin

Ionomycin (Sigma) is a selective Ca^{2+} ionophore produced by the bacterium *Streptomyces conglobatus*. Ionomycin was used at a final concentration of 1 μM for experiments.

5-FU



Oxaliplatin



Irinotecan

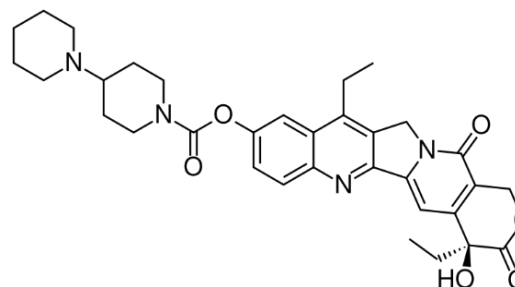


Figure 10 Chemical Structures of Chemotherapeutic Agents

5-FU is a TS inhibitor that disrupts the synthesis of the pyrimidine thymidine, which is necessary for DNA replication. It contains a fluorine atom on the 5th carbon of a uracil ring. Oxaliplatin is a platinum-based chemotherapy that interferes with DNA cross-linking. It contains a square central planar platinum, a bidentate ligand, 1,2-diaminocyclohexane and a bidentate oxalate group. Irinotecan is a topoisomerase I inhibitor, preventing the co-ordinated unwinding of DNA during replication. It is a semisynthetic analogue of camptothecin and is characterised by a bulky piperidino side-chain at the Carbon 10 position.

2.3.2 VEGF

VEGF (Sigma) was used to mediate increases in cytosolic Ca^{2+} and stimulate endothelial cell migration. VEGF was prepared as a $30 \mu\text{g.mL}^{-1}$ stock solution in distilled water and was used at a concentration of 30 ng.mL^{-1} during experiments.

2.3.3 ATP

ATP (Sigma) is a key signalling molecule that causes Ca^{2+} entry in endothelial cells through a number of mechanisms. ATP was prepared as a 100 mM stock solution in distilled water and used at a concentration of 20 μM during experiments.

2.3.4 Matrigel[®]

Matrigel[®] (Corning) is a gelatinous protein mixture secreted by Engelbreth-Holm-Swarm (EHS) mouse sarcoma cells. It acts as an artificial basement membrane upon which endothelial cells form lattice like structures. Matrigel[®] was diluted with EBM-2 media supplemented with a BulletKitTM to a concentration of 10 mg.mL^{-1} for experiments.

2.3.5 Nucleosides

Nucleosides (EmbryoMax) were applied exogenously in experiments to rescue nucleotide shortage. Their dilution factor is stated in each experiment.

2.4 Transfections

Knockdown of WEE1 was achieved using a transient transfection method. Endothelial cells were seeded overnight on a 6-well plate and transfected once 90% confluent. For transfection of one well, 100 μ L of Optimem containing 3% Lipofectamine 2000 was added to 100 μ L Optimem containing 250 nM pooled WEE1 siRNA (Dharmacon On-Targetplus) and left at room temperature for 20 mins. The individual siRNA sequences are provided in (Table 5). The 200 μ L transfection mix was added to 800 μ L fresh EBM-2 media supplemented with a BulletKitTM and added to the well, giving a final WEE1 siRNA concentration of 50 nM. This was applied and incubated in a 5% CO₂ incubator at 37°C. After 3.5 hrs, the transfection mix was removed and replaced with fresh EBM-2 media supplemented with a BulletKitTM. Cells were incubated for a further 24 hrs and were used in experiments from 48 hrs onwards. WEE1 knockdown was confirmed by western blot. Transfection of Thrombospondin-1 was also achieved using pooled siRNA (Dharmacon On-Targetplus) using the same method.

siRNA	Target Sequence
WEE1 (J-005050-05)	AAUAGAACAUCUCGACUUA
WEE1 (J-005050-06)	AAUAUGAAGUCCCGUAUA
WEE1 (J-005050-07)	GAUCAUAUGCUUAUACAGA
WEE1 (J-005050-08)	CGACAGACUCCUCAAGUGA

Table 5 Pooled WEE1 siRNA Sequences

2.5 Western Blotting

2.5.1 Solutions

Lysis Buffer

10 mM Tris, pH 7.4, 150 mM NaCl, 0.5 mM EDTA, 0.5 % NP-40, MiniComplete protease inhibitors (Roche 1:500), and PhosSTOP phosphatase inhibitors (Roche 1:500).

Sample (Loading) Buffer

200 mM Tris pH 6.8, 8% SDS, 40% glycerol, 8% mercaptoethanol, 0.1% bromophenol blue.

Running (Electrophoresis) Buffer

25 mM Tris, 192 mM glycine and 0.1% SDS, pH 8.3.

Semi-dry transfer buffer

48 mM Tris, 39 mM glycine and 20% methanol, pH 9.2.

TBS-T

145 mM NaCl, 20 mM Tris-base, 0.5% Tween 20, pH 7.5.

2.5.2 Cell Lysis

Cells were grown to confluence in a 6-well culture plate and harvested in lysis buffer. Cells were washed with PBS twice before 0.1 mL of lysis buffer was added and the cells incubated for 1 min. Cells were then scraped off the dish and collected into an eppendorf. The lysate was centrifuged at 13,000 revolutions per minute (RPM) at 4 °C for 10 mins and the soluble protein-containing layer aspirated.

2.5.3 Protein Quantification

Protein was quantified using the Bio-Rad Protein Assay (Bio-Rad). This is a dye-binding assay in which a differential colour change occurs in response to various concentrations of protein. Absorbance was measured in a microtitre plate reader at 570 nm wavelength. Comparison was made to a BSA standard curve and the protein concentrations were derived from this.

2.5.4 Western Blotting

Equal quantities of test and control protein samples were mixed with sample buffer and heated to 90°C for 5 mins to ensure complete denaturation. Samples were loaded alongside markers (Bio-Rad) into sodium dodecyl sulphate (SDS) polyacrylamide gels and electrophoresis was carried out for 90 mins at 160 V. SDS is an anionic detergent that disrupts the secondary structures of proteins to create linear, negatively charged structures. Application of an electrical charge across the gel results in the movement of negatively charged proteins towards the positively charged electrode. The distance each protein travels is inversely proportional to its size and molecular weight.

Following gel electrophoresis, the protein was transferred to a polyvinylidene fluoride membrane using semi-dry transfer buffer and electrophoresis at a constant current of 0.05 A for 90 mins. The membrane was then incubated in either 5% non-fat milk solution or 5% BSA solution (dependent on primary antibody) to reduce non-specific background antibody binding. Following this, the membrane was incubated with primary antibody at appropriate dilutions at 4 °C for 12 hrs (Table 6). The membrane was then washed in TBS-T and the secondary HRP-conjugated

antibody was added at 1:5,000 dilution in 5% non-fat milk solution. After a 1 hr incubation at room temperature, the membrane was washed for a final time in TBS-T.

2.5.5 Protein Visualisation

To detect protein bands, membranes were treated with SuperSignal Femto detection reagent (Perbio Science). Membranes were imaged using a G:BOX (Syngene). Data were analysed using Image J software.

Antibody	Host Species	Dilution	MW (kDa)	Dilution	Supplier
Anti-WEE1	Mouse	1:300	96	5% Non-Fat Milk	Santa Cruz Biotechnology (sc-5285)
Anti-YH2AX	Rabbit	1:1000	15	5% BSA	Cell Signalling Technology (#9718)
Anti-pCDK1-Y15	Rabbit	1:1000	34	5% BSA	Cell Signalling Technology (#9111)
Anti-CDK1	Mouse	1:1000	34	5% Non-Fat Milk	Cell Signalling Technology (#9116)
Anti- β -Actin	Mouse	1:2000	42	5% Non-Fat Milk	Santa Cruz Biotechnology (sc-47778)
Anti-CD31	Mouse	1:1000	130	5% Non-Fat Milk	Dako (M0823)
Anti-VEGFR1	Goat	1:1000	180	5% Non-Fat Milk	R&D Systems (AF321)
Anti-VEGFR2	Goat	1:1000	250	5% Non-Fat Milk	R&D Systems (AF357)
Anti-eNOS	Rabbit	1:1000	133	5% Non-Fat Milk	Cell Signalling Technology (#9572)
Anti-peNOS	Rabbit	1:1000	133	5% BSA	Cell Signalling Technology (#9571)
Anti-TSP-1	Rabbit	1:1000	180	5% Non-Fat Milk	GeneTex (GTX130967)
Anti-Fibronectin	Rabbit	1:1000	263	5% Non-Fat Milk	Abcam (ab2413)
Anti-vWF	Mouse	1:1000	250	5% Non-Fat Milk	Dako (M0616)

Table 6 Summary of Primary Antibodies used for Western Blotting

2.6 WST-1 Proliferation Assay

WST-1 [(2-(4-iodophenyl)-3-(4-nitrophenyl)-5-(2,4-disulfophenyl)-2H-tetrazolium)] is a tetrazolium salt. It is broken down to formazan by the mitochondrial dehydrogenase succinate-tetrazolium reductase, which is present in metabolically active cells. Cells were plated onto a 96-well plate at an optimised seeding density and grown overnight. The following morning cells were drugged and allowed to grow for the duration of the experiment. Upon completion of the experiment WST-1 was added to media in each well in accordance with the manufacturer's protocol. The absorbance of the formazan salt was measured at 440 nm using a microtiter plate reader. A second reading at 630 nm was recorded and subtracted from the 440 nm reading to control for artefacts. Drug effect on proliferation was quantified by measuring the absorbance of treated cells and comparing this to vehicle control cells.

2.7 Vybrant[®] DyeCycle[™] Green Proliferation Assay

Vybrant[®] DyeCycle[™] Green (Molecular Probes, Invitrogen) is an inert, membrane permeable, fluorescent, double-stranded DNA dye. It is excited at 488 nm with emission ~520 nm. As with the WST-1 assay, cells were plated onto a 96-well plate at an optimized seeding density and grown overnight. The following morning cells were drugged and allowed to grow for the duration of the experiment. At the end of the experiment, 1 μ M Vybrant[®] DyeCycle[™] Green was added to each well as per the manufacturer's instructions and the plate was imaged on an Incucyte[™] Kinetic Imaging System (Essen Bioscience, Michigan) in phase-contrast and fluorescence mode using a x10 objective. The total number of fluorescent cells in each well was calculated using inbuilt algorithms.

2.8 Migration Assays

Migration was analysed using the Incucyte™ Kinetic Imaging System (Essen Bioscience, Michigan). This consists of a microscope inside an incubator and permits long-term live content imaging of cells (Figure 11). For migration assays, cells were plated onto a 96-well plate (Essen Imagelock, Essen) and grown overnight to confluence. The following morning a linear scratch (wound) was made in every well using the Essen Woundmaker™ (Essen). Following the scratch, cells were drugged before being placed in the Incucyte™ Kinetic Imaging System. Cells were imaged every hour for 24 hrs or until they had fully migrated across the scratch wound.

Migration was measured automatically by the Incucyte™ Kinetic Imaging System, which calculates Relative Wound Density (RWD). This measures the spatial density in the scratch wound relative to the spatial density of cells outside of the scratch wound. It is 0% at 0hrs and reaches 100% once the spatial density inside the scratch is the same as outside. This allows data to be self-normalised against changes in cell density that occur outside of the wound due to cell proliferation. For endothelial cell migration, cells were treated with media that contained a higher concentration of VEGF (20 ng.mL⁻¹) and lower concentration of serum (0.2%) compared to normal EBM-2 media supplemented with a BulletKit™. This was to stimulate migration and reduce proliferation.



Figure 11 Incucyte™ Kinetic Imaging System and Essen Woundmaker™

The Incucyte™ Kinetic Imaging System (left) consists of a microscope inside an incubator and permits long-term live content imaging of cells. The Essen Woundmaker™ (right upper and lower) is capable of making a linear scratch in each well of a 96-well plate.

2.9 In vitro Co-Culture Tube Formation Assay

In vitro tube formation was studied using an endothelial/fibroblast co-culture assay (Figure 12). Normal Human Dermal Fibroblasts (NHDF, Lonza) were seeded at 6,000 cells per well in a 96 well plate (Greiner Bio-one) and allowed to grow to a confluent monolayer over 4 days. On day 5, endothelial cells were seeded on top of the fibroblast monolayer at 6,000 cells per well and allowed to grow overnight. Over the next 5 days endothelial cells reliably grew into tube structures and were treated daily with either AZD1775 (1 μ M) or vehicle control (days 6-10). On day 11 cells were stained for CD31 to assess tube formation.

For staining, cells were fixed in 4% paraformaldehyde and permeabilised with 0.1% TritonX-100 at room temperature. After three washes in PBS the cells were blocked in donkey serum for 30 mins at 37°C. Cells were then incubated with 1% BSA in PBS containing mouse anti-human CD31 (Dako, Clone JCT0A) at 1:300 dilution for 1 hr at 37°C. Following washing, cells were incubated with Alexa 488-conjugated Affinipure Donkey anti-Mouse IgG (Jackson Immuno Research Laboratories) at 1:300 dilution for 45 mins at 37°C. After this cells were incubated with 100 μ L PBS and imaged on the Incucyte™ FLR Kinetic Imaging System in phase-contrast and fluorescence mode using a x10 objective. Tube length, number of branch points and tube surface area were calculated using inbuilt algorithms.

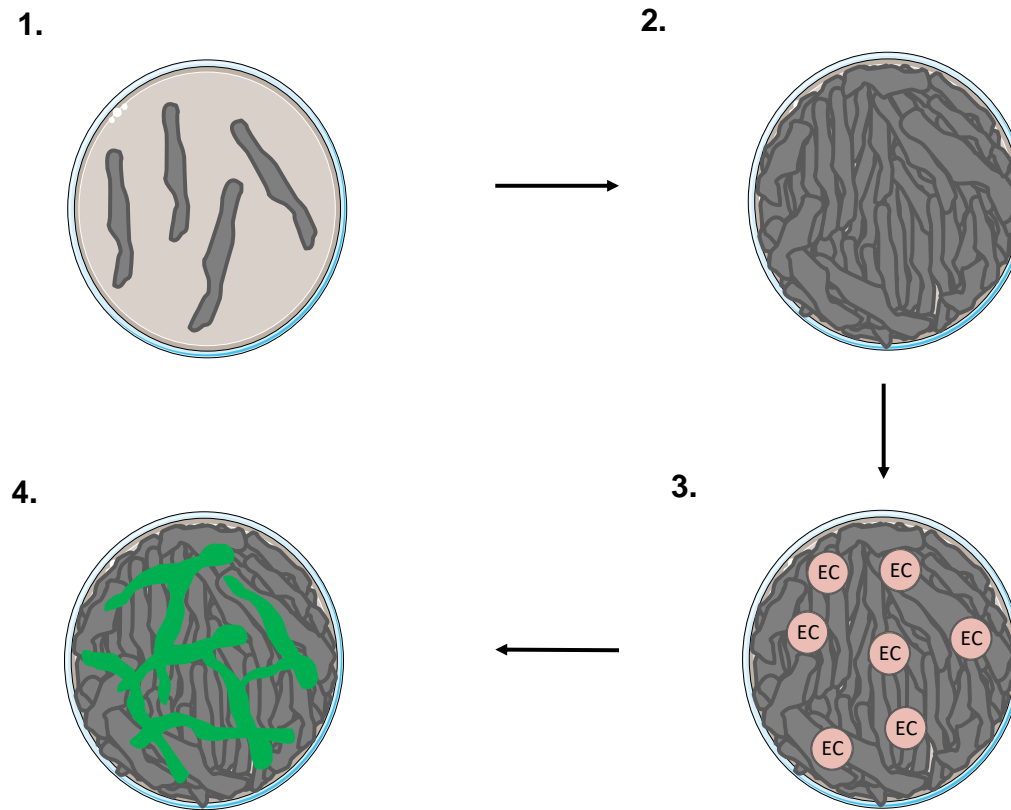


Figure 12 In vitro Co-Culture Tube Formation Assay

1. 6,000 normal human dermal fibroblasts are plated into a well of a 96 well plate 2. After 4 days they reach confluence 3. 6,000 endothelial cells are plated on top of the confluent normal human dermal fibroblasts 4. Over the next 5 days the endothelial cells grow into tube like structures that can be stained with Alexa 488 conjugated CD31 and imaged on the Incucyte™ Kinetic Imaging System.

2.10 Matrigel[®] Tube Formation Assay

An alternative way to assess tube formation is by the use of Matrigel[®]. When applied to Matrigel[®], endothelial cells form tube-like structures. Matrigel[®] (Corning) was plated onto each well of a 96-well plate (Nunc) at a concentration of 10 mg.mL⁻¹ and incubated at 37°C overnight. The following morning 20,000 endothelial cells were plated into each well containing Matrigel[®]. Over the space of 24 hrs the endothelial cells reliably grew into tube-like structures and plates were imaged on the Incucyte[™] FLR Kinetic Imaging System. To assess tube formation the number of complete loops were counted and compared to conditions when Matrigel[®] was not present.

2.11 Flow Cytometry

2.11.1 General Principles

Flow cytometry is an analytical technique that utilizes light to count and profile cells. It can be used to measure multiple parameters of individual cells within a heterogeneous population. It performs this analysis by passing thousands of cells through a laser beam, capturing the light that emerges from each cell as it passes through. There are several components to a flow cytometer, including a fluidics system, lasers, optics, detectors and an electronic processing system (Figure 13).

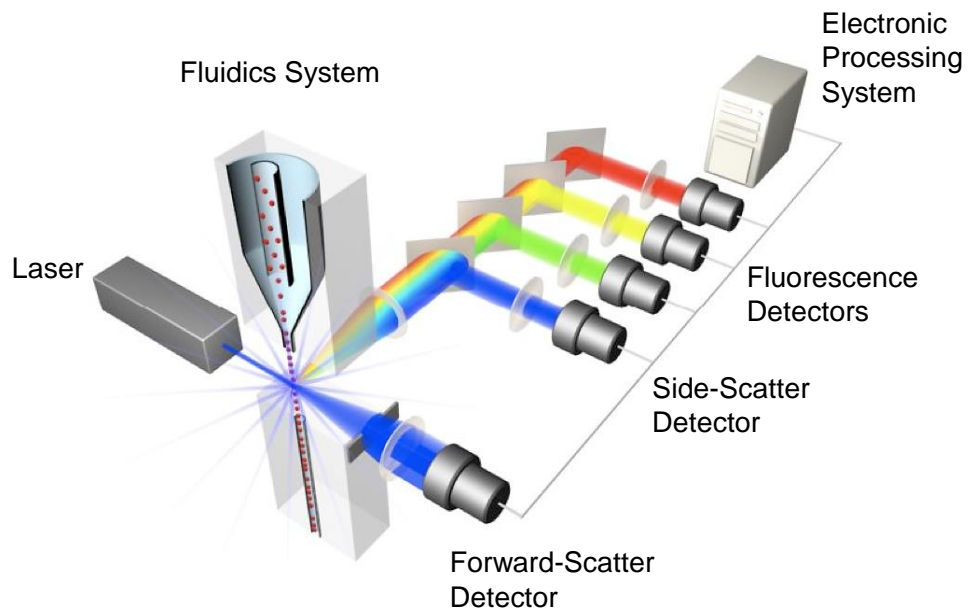


Figure 13 Components of a Flow Cytometer

A fluidics system delivers cells in a single file to a laser. As the cells pass through the laser it causes light to scatter which can be registered by detectors. The detectors convert light intensity into a voltage pulse which is processed by the electronic processing system. Adapted from ThermoFisher Scientific (2016).

During flow cytometry, it is important that cells are analysed one at a time, therefore an injected cell suspension must be converted into a stream of fluid consisting of single cells only. To achieve this, sheath fluid is used to haemodynamically focus the cell suspension through a small nozzle. Once in single file, cells progress towards the laser. As a cell passes through a laser it will refract (“scatter”) light at all angles. There are two important measures of scatter; “forward-scatter” and “sideward-scatter” (Figure 14). Forward-scatter is the amount of light that is scattered in the forward direction and is approximately proportional to the size of the cell. Side-scatter is caused by structural complexity within the cell. It is focused through a lens system to a separate detector. Both detectors convert the light intensity into a voltage pulse, which is recorded by the electronic processing system.

In addition to light scatter detectors, flow cytometers have fluorescence detectors. Characteristics of cells can be analysed using fluorophore labelled antibodies (Figure 15). Laser light of a specific wavelength excites fluorophores to a higher energy level. This is followed by the return of the fluorophore to its ground state with the emission of light. The energy in the emitted light is dependent upon the energy level to which the fluorophore is excited. The emission light will have a specific wavelength and a specific colour. This is directed to the appropriate detector where it is also converted into a voltage pulse and recorded by the electronic processing system.

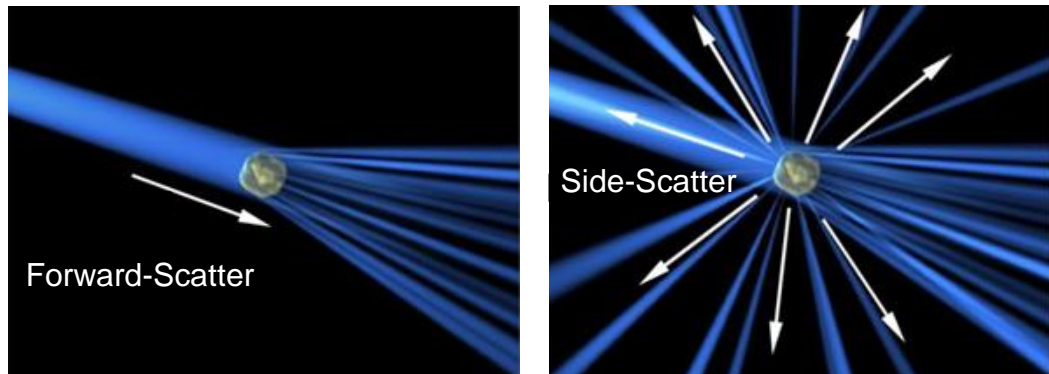


Figure 14 Forward and Side Scatter

As a cell passes through the laser beam it will scatter the light. Forward scatter is the amount of light scattered in the forward direction and provides a measurement of cell size (left). Side scatter reveals structural complexity within the cell (right). Adapted from ThermoFisher Scientific (2016).

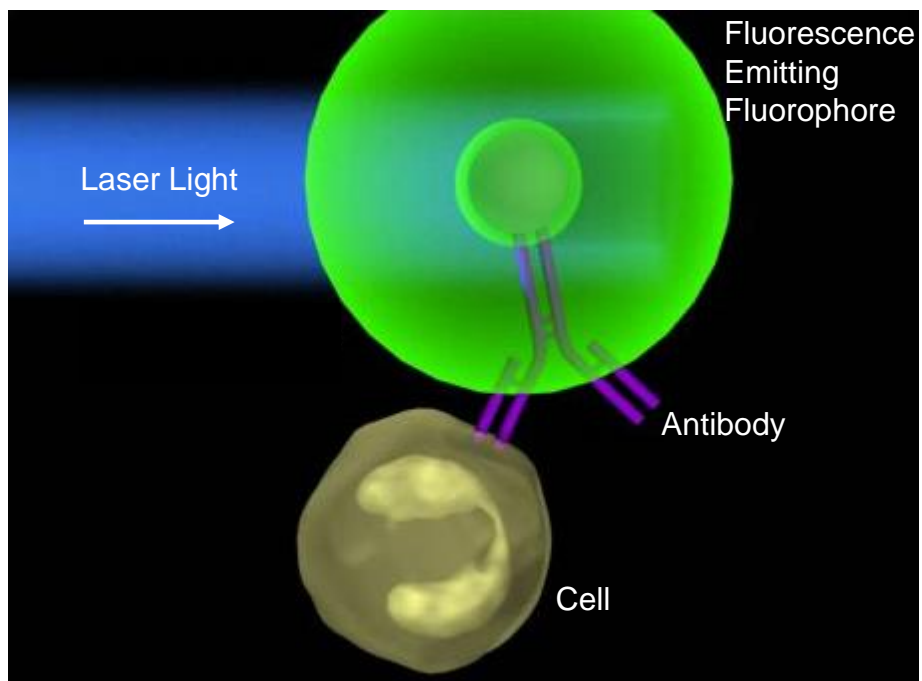


Figure 15 Measurement of Fluorescence

Fluorophores bound to specific antibodies are excited to a higher energy level by laser light of a specific wavelength. As it returns to its ground state it emits light, the colour and energy of which can be registered by detectors and converted to voltage pulses. Adapted from ThermoFisher Scientific (2016).

2.11.2 Sample Preparation

All experiments were undertaken on 6-well plates. Cells were seeded overnight and treated the following morning. At the end of the experiment, cells, media and drugs were removed and washed with PBS. Following this, the cells were trypsinised and placed in a 15 mL falcon tube with fresh media. The samples were centrifuged at 1,000 RPM for 5 mins. All medium was then removed and 0.5 mL ice cold 70% ethanol was added dropwise to each sample under continuous agitation. Ethanol allows permeabilisation of the cells. The samples were immediately frozen at -20°C until analysis was performed.

2.11.3 Cell Cycle Analysis

Propidium Iodide (PI) is a fluorescent dye that intercalates with DNA and RNA in a stoichiometric fashion. As PI binds to both DNA and RNA, the latter must be removed by digestion with ribonucleases. Forty-eight hours after freezing samples with ethanol they were retrieved and centrifuged at 1,000 RPM for 5 mins. The samples were then washed in PBS and re-centrifuged before 0.5 mL PI-RNase Staining Buffer (BD Biosciences) was added per 1×10^6 cells. Samples were incubated at room temperature for 15 mins before being run on the flow cytometer.

DNA histograms can provide information about how cells in a sample are distributed throughout the cell cycle. They are generated by plotting the PI fluorescence (measured as the voltage pulse area and assigned an arbitrary channel number) on the x-axis against the number of cells per channel number on the y-axis (Figure 16 upper left). Normal diploid cells in G0 or G1-phase contain 2N

DNA. Cells in G2/M phase contain double the amount of DNA (4N). Cells with DNA contents between 2N and 4N are in S phase.

Cell clumping was eliminated from the dataset by gating. If 2 cells in the G0 or G1-Phase were clumped together ("doublet") and passed through the laser they would register as having 4N, incorrectly labelling the cell as being in G2/M phase. Doublets were eliminated by gating cells based on the voltage pulse width versus the voltage pulse area of the PI signal (Figure 16 upper right). This takes into account the fact that it takes longer for a doublet to pass through the laser beam than a single cell. This makes the width of the signal larger for doublets than single cells, whilst the area is the same (Figure 16 bottom). Only single cell events are highlighted in the gate.

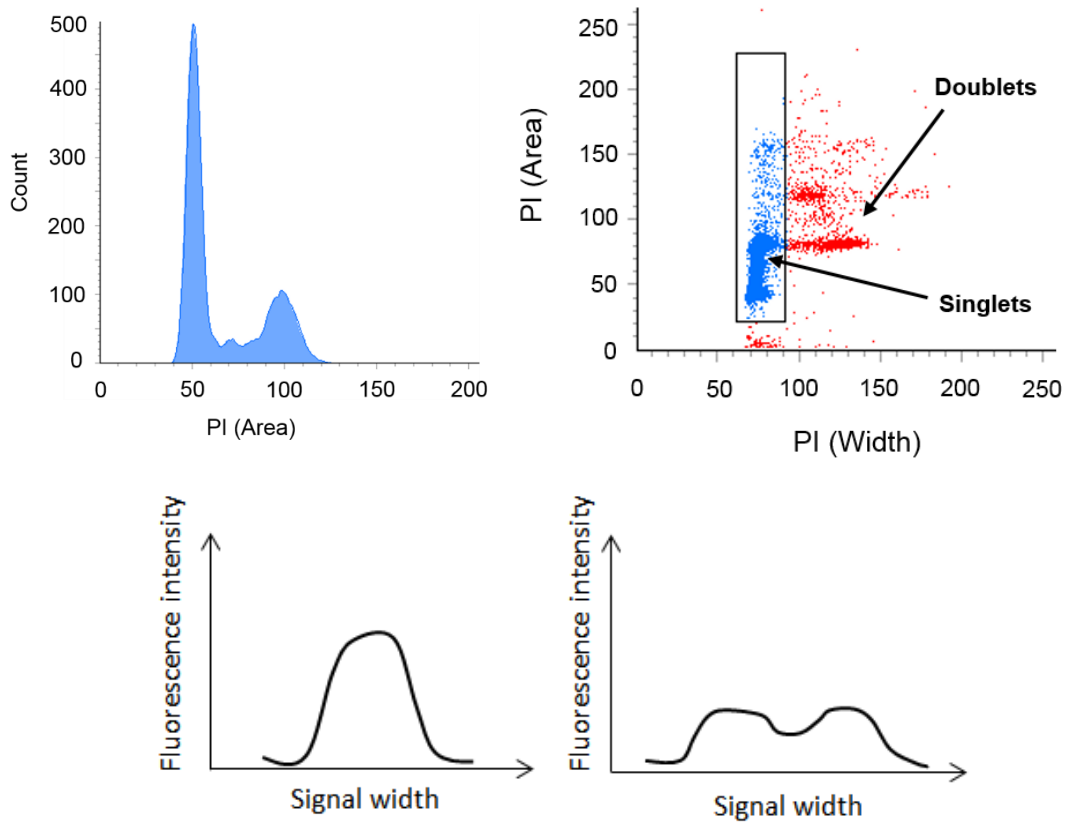


Figure 16 Eliminating Doublets from Cell Cycle Analysis

DNA histograms (upper left) are generated by measuring the PI signal against cell count and follows that cells in G2/M phase have twice the DNA content (4N) compared to G1 Phase (2N). By plotting PI width vs PI area doublets can be excluded from analysis (upper right). This is because although singlets and doublets have the same area signal, it takes longer for a doublet to pass through the laser resulting in a larger width signal (bottom).

2.11.4 γ H2AX Detection

Histones are highly basic proteins that complex with DNA to form chromatin. The H2AX histone belongs to the H2A histone family. Members of this family are components of nucleosomal histone octamers. Double-stranded DNA breaks resulting from a magnitude of processes, including replication errors and cytotoxic agents, lead to the phosphorylation of H2AX on serine 139. Phosphorylation specifically at this site is termed γ H2AX. γ H2AX recruits and localises proteins to repair DNA, maintaining genomic stability and preventing oncogenic transformation. Thus, γ H2AX can be used as a specific marker to measure double-stranded DNA breaks.

To detect γ H2AX, samples were defrosted, washed twice with 1 mL PBS and then incubated with 5 μ L Alexa Fluor 488 Mouse anti-H2AX (BD Biosciences) in 50 μ L PBS per test for 20 mins at room temperature. Following incubation, samples were washed again with 1 mL PBS before adding 0.5 mL PI-RNAse Staining Buffer per 1×10^6 cells. Samples were incubated at room temperature for 15 mins before analysis on the flow cytometer.

As two fluorophores were used in this experiment compensation needed to be made for the spectral overlap of the fluorescence emission profiles. Figure 17 shows the fluorescence emission profiles for Alexa 488 and PI, showing overlap between 560 nm and 600 nm. If this were not compensated for, filters for one fluorophore could capture fluorescence emitted by the other fluorophore at these wavelengths. To eliminate this, samples were run with a single fluorophore (e.g. Alexa 488) and the mean fluorescence values for both the positive (fluorophore

present in sample) and negative (no fluorophore in sample) populations were corrected to be equal in the other fluorophore channel (e.g. PI).

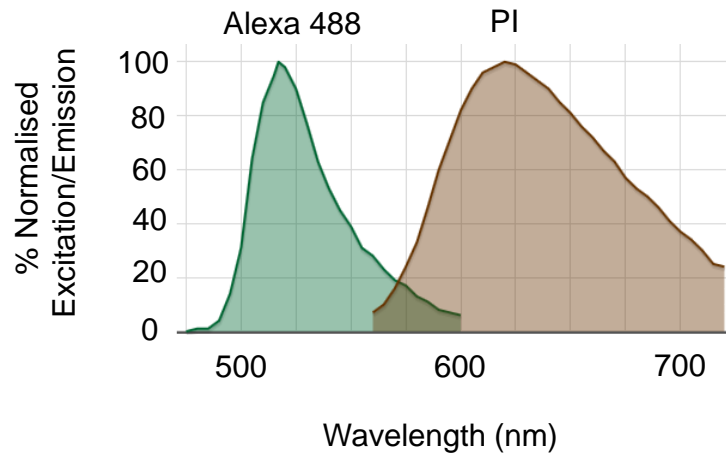


Figure 17 Fluorescence Emission Profiles for Alexa 488 and PI

Alexa 488 and PI have a small area of fluorescence emission overlap. If not, corrected filters for PI could detect fluorescence emitted by Alexa 488 and vice versa. Adapted from ThermoFisher Scientific (2016).

To identify the subset of γ H2AX positive cells a specific gating strategy was employed. Firstly a plot of forward-scatter versus side-scatter was created to ensure one population of cells (Figure 18 upper left). Next, a plot of PI width versus PI area was created to separate singlet and doublet events (Figure 18 upper right). To identify γ H2AX positive cells a negative and positive control were used to set the threshold fluorescence intensity (Figure 18 bottom left). Finally, PI-area was plotted against Alexa 488-area (Figure 18 bottom right) with the gate indicating cells positive for γ H2AX.

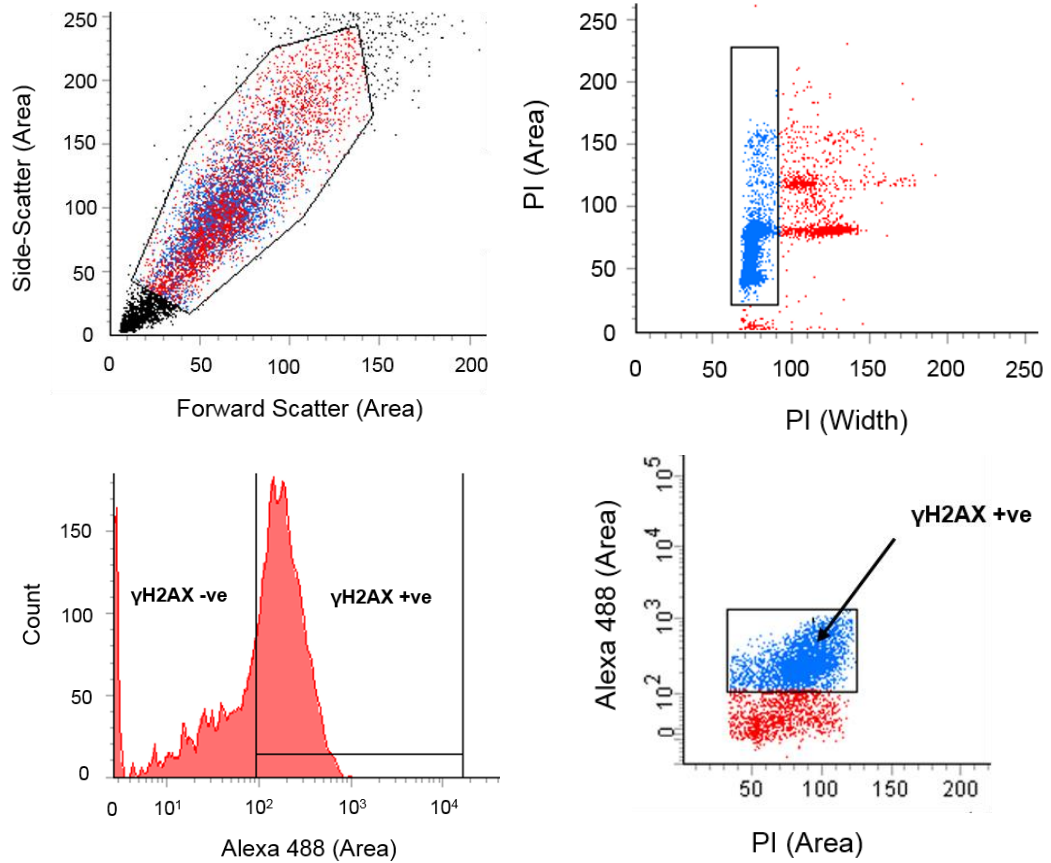


Figure 18 Gating Strategy for the Detection of γ H2AX Positive Cells

To ensure one population of cells were studied a plot of forward-scatter versus side-scatter was created (upper left). Next doublets were removed by gating PI width versus PI area (upper right). The gate highlights singlets only. To identify γ H2AX positive cells a negative and positive control were used to set the threshold fluorescence intensity (bottom left). Finally γ H2AX cells were identified by plotting PI-area against Alexa 488-area (bottom right). The blue dots in the gate are γ H2AX positive cells. The red dots outside the gate are γ H2AX negative cells

2.11.5 pHH3 Detection

Detection of pHH3 followed broadly the same principles as γ H2AX detection. Histone H3 is phosphorylated at serine 28 during mammalian cell mitosis and meiosis, specifically in the transition from prophase to anaphase.

To detect pHH3 samples were defrosted, washed twice with 1 mL PBS and then incubated with 20 μ L Alexa Fluor 647 Rat anti-Histone H3 (pS28) (BD Biosciences) in 80 μ L PBS for 20 mins at room temperature. Following incubation, samples were washed again with 1 mL PBS before adding 0.5 mL PI-RNAse Staining Buffer per 1×10^6 cells. Samples were incubated at room temperature for 15 mins before analysis on the flow cytometer.

2.11.6 Data Analysis

All flow cytometry work was undertaken on a BD-LSR Fortessa Flow Cytometer. All pHH3 and γ H2AX analysis was undertaken using BD FACSDiva v6.2 software. Cell cycle analysis was performed using ModFit LT software.

2.12 Intracellular Ca²⁺ Measurement

Fura-2 is a ratiometric Ca²⁺ indicator dye which permits the measurement of intracellular Ca²⁺. It is excited at 340 nm and 380 nm and the ratio of emission at 510 nm calculated. Once bound to Ca²⁺ there is a spectral shift in Fura-2 absorption which is proportional to the intracellular concentration of Ca²⁺. This causes a change in the ratio which can be measured (ΔF Ratio).

To test changes in intracellular Ca²⁺ concentration, a FlexStation II³⁸⁴ (Molecular Devices, California) bench-top fluorometer was used (Figure 19). This can be utilised for kinetic fluorescence experiments using a 96-well based assay. Endothelial cells were grown to confluence in a 96-well plate overnight. The following morning medium was removed and cells in each well were incubated with 50 μ L Fura-2 loading solution for 1 hr at 37 °C in a 5% CO₂ incubator. The Fura-2 loading solution consisted of 2 μ M Fura-2 AM and 0.01% Pluronic Acid in Standard Bath Solution (Ca²⁺-SBS) consisting of 130 mM NaCl, 5 mM KCl, 1.2 mM MgCl₂, 1.5 mM CaCl₂, 8 mM D-Glucose and 10 mM HEPES. After 1 hr the loading solution was removed and 80 μ L of Ca²⁺-SBS was added to each well and left at room temperature for 10 mins. A compound plate was prepared containing drugs to be tested (VEGF/Yoda1/ATP/Ionomycin) at twice the final concentration in Ca²⁺-SBS. The FlexStation II³⁸⁴ was set to add 80 μ L of the compound solution to each well on the test plate containing 80 μ L of Ca²⁺-SBS. Baseline fluorescence ratios were recorded before the addition of the compound solution to the cell plate after 60 seconds, with regular recordings thereafter for a total of 5-10 mins.

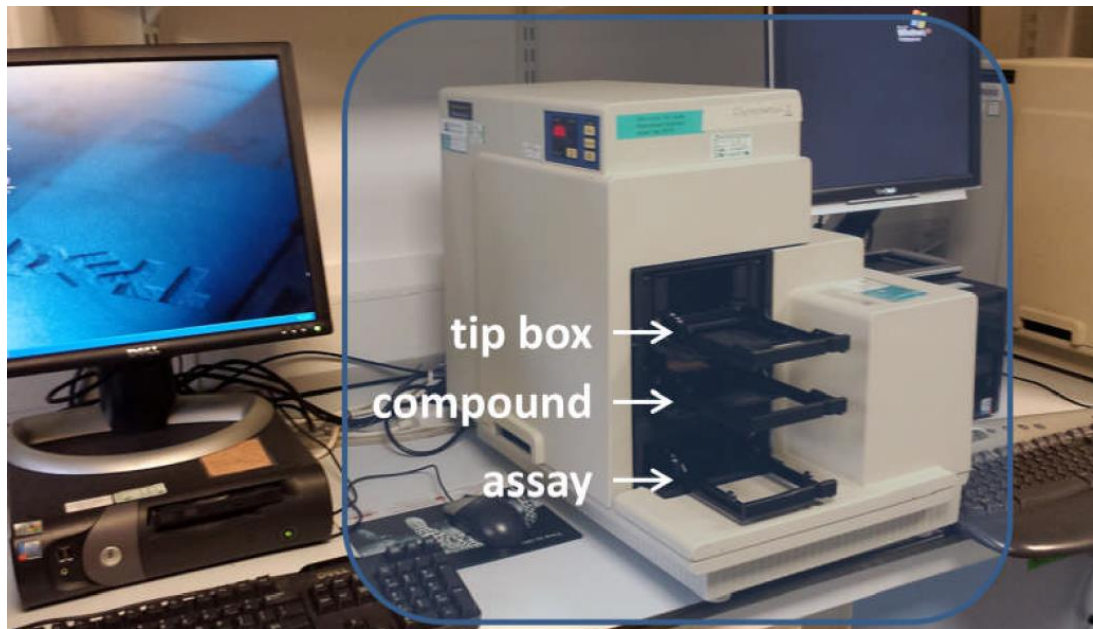


Figure 19 Flexstation II (Molecular Devices)

Flexstation II device with areas of interest highlighted. The assay plate consisted of a confluent monolayer of endothelial cells loaded with the intracellular Ca^{2+} indicator Fura-2 AM. The tip box area contained pipette tips that transferred drugs from the compound plate to the assay plate. The SoftMax Pro program was used to acquire data.

2.13 Immunocytochemistry

Endothelial cells were seeded and grown to 80% confluence on glass coverslips in a 24 well plate. After removal of media, cells were washed in PBS and fixed in 4% paraformaldehyde solution at room temperature for 5 mins. To permeabilise cells, 0.1% Triton X-100 was applied for 5 mins at room temperature. To prevent non-specific antibody binding, cells were blocked with 300 μ L 5% donkey serum for 1 hr. Primary antibodies were prepared at the appropriate concentrations by diluting in 1% BSA solution (Table 7). Cells were incubated with primary antibody at room temperature for 1 hr. After washing, cells were incubated with the relevant species-specific secondary antibodies conjugated with appropriate fluorophores at room temperature for 30 mins. Following incubation, cells were washed and the coverslips were mounted on glass slides using Prolong Gold Antifade Reagent (Invitrogen). This contains DAPI which was used to counterstain the nuclei of cells. Slides were kept at room temperature overnight and imaged the following day using an LSM 880 confocal microscope (Zeiss).

Antibody	Host Species	Dilution	Supplier
Anti-WEE1	Mouse	1:50	Santa Cruz Biotechnology (sc-5285)
Anti-SM α	Mouse	1:100	Sigma (C6198)
Anti- γ H2AX	Mouse	1:50	BD Biosciences (560445)
Anti-CD31	Mouse	1:100	Dako (M0823)
Anti-CD31	Rabbit	1:100	abcam (ab28364)
Anti-vWF	Mouse	1:100	Dako (M0616)
Anti-VEGFR2	Goat	1:200	R+D Systems (AF357)
Anti-eNOS	Rabbit	1:100	Cell Signalling Technology (#9572)
Anti-VE-Cadherin	Rabbit	1:200	Invitrogen (36-1900)

Table 7 Summary of Primary Antibodies used for Immunocytochemistry

2.14 Caspase-3 Measurement

Caspases (cysteine-aspartic proteases) are a family of protease enzymes playing essential roles in programmed cell death including apoptosis. Caspases are generally divided into two distinct classes: “initiator caspases”, which include caspase-2, -8, -9 and -10 and “effector caspases”, which include caspases-3, -6 and -7. All caspases are produced in cells as inactive zymogens and undergo proteolytic activation in response to stimuli. Effector caspases cause proteolytic cleavage of several cellular targets, leading to cell death. Caspase-3 is activated by the extrinsic (death ligand) and intrinsic (mitochondrial) apoptotic pathways. NucView™ 488 Caspase-3 substrate is a novel cell membrane-permeable fluorogenic caspase substrate designed for detecting caspase-3 activity within live cells in real time (Figure 20). It consists of a fluorogenic DNA dye and a DEVD (Aspartic Acid - Glutamic Acid - Valine - Aspartic Acid) substrate moiety specific for caspase-3. The DEVD substrate is non-fluorescent and non-functional as a DNA dye. It is able to cross the cell membrane into the cytoplasm where, in the presence of caspase-3 it is cleaved to a high affinity DNA-dye that stains the nucleus green. To assess apoptosis, cells were plated onto a 6-well plate and grown overnight. The following morning they were treated with the relevant drugs and 5 µM NucView™488 caspase-3 substrate (Biotium) was added to each well according to the manufacturer’s instructions. Cells were placed in the Incucyte™ FLR and imaged every hr for 24 hrs in phase contrast and fluorescence mode using a x10 objective. At 24 hrs, the number of apoptotic cells (fluorescent green) was calculated using inbuilt software. Subsequently the total number of cells were calculated by staining with 5 µM Vybrant DyeCycle Green® (Molecular Probes, Invitrogen). The Apoptotic Index was calculated as the percentage of caspase-3 positive cells divided by the total number of cells.

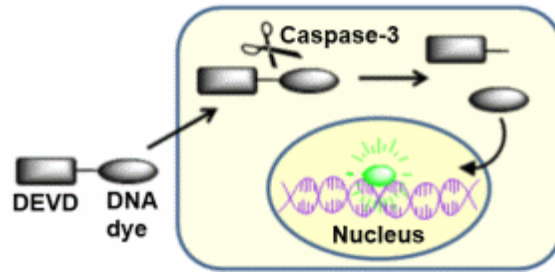


Figure 20 NucView™ 488 Caspase-3 Assay

The NucView™ 488 Caspase-3 substrate consists of a non-functional fluorogenic DNA dye and a DEVD substrate moiety specific for caspase-3. In the presence of caspase-3 it is cleaved to a high affinity DNA-dye. Adapted from Biotium (2016).

2.15 Endothelial Cell Alignment

Endothelial cells align in response to shear stress. To investigate this, endothelial cells were grown to 80% confluence in a 6-well plate. Shear stress was achieved by placing the cells on an orbital shaker for 48 hrs (180 RPM). The swirling motion of the media around the edge of the wells produces tangential shear stress, resulting in cell elongation and alignment. After 48 hrs, cells were imaged using the Incucyte™ Kinetic Imaging System (Essen Bioscience, Michigan). Images were analysed using ImageJ software to determine the degree of alignment. To do this, images were rotated to the direction of applied shear stress and were processed using a Difference of Gaussian plugin to define cell edges (<http://www.sussex.ac.uk/gdsc/intranet/microscopy/imagej/utility>). Quantification of cell orientation relative to the direction of shear stress was determined using OrientationJ software (<http://bigwww.epfl.ch/demo/orientation/>). OrientationJ generates a histogram of all local angles in each image and a Gaussian distribution curve was fitted. From this, the baseline-subtracted frequency maximum at the mode of the distribution was determined.

2.16 RNA Interference Screening

RNA Interference screening was performed by Dr Heather Martin (University of Leeds) and involves high-throughput imaging combined with siRNA gene silencing. Briefly, reverse transfection was undertaken on a 96-well plate using Dharmacon siGenome siRNA (50 nM per well), 0.1 µL RNAiMAX and 5,000 HUVECs per well. siRNA from ion channel, GPCR, Kinase, Phosphatase and Apoptosis libraries was transfected. Cells were incubated for 72hrs before being stained with Hoescht (1:1000). Cells were then fixed, imaged and analysed with plate-wise robust Z

scores (sample median - plate median / median absolute deviation). In a second validation screen reverse transfection was undertaken on a 96-well plate using Dharmacon On-Target Plus siRNA (50 nM per well) with other steps remaining unchanged. Genes with a robust Z-score of >2 or <-2 on the RNA interference screen corresponded to a p-value of <0.05 and were deemed significant.

2.17 Proteomic Studies

2.17.1. Sample Preparation

Matched human liver endothelial cells and endothelial cells from colorectal cancer liver metastases were culture expanded in T25 flasks up to passage 3. Cells were lysed in filter-aided sample preparation buffer which consisted of 100 mM Tris-HCl (pH 7.6), 4% w/w SDS, MiniComplete protease inhibitors (Roche 1:500), and PhosSTOP phosphatase inhibitors (Roche 1:500). The lysate was centrifuged at 13,000 RPM 4 °C for 10 mins and the soluble protein layer aspirated. Samples were quantified using the Bio-Rad Protein Assay (Bio-Rad) and immediately frozen at -80°C. Once all samples were collected, they were sent on dry ice to Dundee Cell Products for proteomic analysis.

2.17.2 TMT-Labeling and High pH reversed-phase chromatography

All proteomic experiments were performed by Dundee Cell Products. Aliquots of 100 µg of six samples per experiment were digested with trypsin (2.5 µg trypsin per 100 µg protein; 37°C, overnight), labelled with Tandem Mass Tag (TMT) ten-plex reagents according to the manufacturer's protocol (Thermo Fisher Scientific) and the labelled samples pooled.

An aliquot of the pooled sample was evaporated to dryness and re-suspended in buffer A (20 mM ammonium hydroxide, pH 10) prior to fractionation by high pH reversed-phase chromatography using an Ultimate 3000 liquid chromatography system (Thermo Fisher Scientific). In brief, the sample was loaded onto an XBridge BEH C18 Column (130Å, 3.5 µm, 2.1 mm X 150 mm, Waters, UK) in buffer A and peptides eluted with an increasing gradient of buffer B (20 mM Ammonium Hydroxide in acetonitrile, pH 10) from 0-95% over 60 mins. The resulting fractions were evaporated to dryness and re-suspended in 1% formic acid prior to analysis by nano-LC MSMS using an Orbitrap Fusion Tribrid mass spectrometer (Thermo Scientific).

2.17.3 Nano-LC Mass Spectrometry

High pH RP fractions were further fractionated using an Ultimate 3000 nanoHPLC system in line with an Orbitrap Fusion Tribrid mass spectrometer (Thermo Scientific). In brief, peptides in 1% (vol/vol) formic acid were injected onto an Acclaim PepMap C18 nano-trap column (Thermo Scientific). After washing with 0.5% (vol/vol) acetonitrile 0.1% (vol/vol) formic acid peptides were resolved on a 250 mm × 75 µm Acclaim PepMap C18 reverse phase analytical column (Thermo Scientific) over a 150 min organic gradient, using 7 gradient segments (1-6% solvent B over 1min., 6-15%B over 58min., 15-32%B over 58min., 32-40%B over 5min., 40-90%B over 1min., held at 90%B for 6min and then reduced to 1%B over 1min.) with a flow rate of 300 nL.min⁻¹. Solvent A was 0.1% formic acid and Solvent B was aqueous 80% acetonitrile in 0.1% formic acid. Peptides were ionized by nano-electrospray ionization at 2.0 kV using a stainless steel emitter with an internal diameter of 30 µm (Thermo Scientific) and a capillary temperature of 275°C.

All spectra were acquired using an Orbitrap Fusion Tribrid mass spectrometer controlled by Xcalibur 1.9 software (Thermo Scientific) and operated in data-dependent acquisition mode using an SPS-MS3 workflow. FTMS1 spectra were collected at a resolution of 120 000, with an automatic gain control (AGC) target of 400 000 and a max injection time of 100 ms. The TopN most intense ions were selected for MS/MS. Precursors were filtered according to charge state (to include charge states 2-6) and with monoisotopic precursor selection. Previously interrogated precursors were excluded using a dynamic window (40s +/-10 ppm). The MS2 precursors were isolated with a quadrupole mass filter set to a width of 1.2m/z. ITMS2 spectra were collected with an AGC target of 5000, max injection time of 70 ms and CID collision energy of 35%.

For FTMS3 analysis, the Orbitrap was operated at 30 000 resolution with an AGC target of 50 000 and a max injection time of 105 ms. Precursors were fragmented by high energy collision dissociation (HCD) at a normalised collision energy of 55% to ensure maximal TMT reporter ion yield. Synchronous Precursor Selection (SPS) was enabled to include up to 10 MS2 fragment ions in the FTMS3 scan.

2.17.4 Data Analysis

The raw data files were processed and quantified using Proteome Discoverer software v1.4 (Thermo Scientific) and searched against the UniProt Human database (downloaded 08/11/14: 126385 entries) using the SEQUEST algorithm. Peptide precursor mass tolerance was set at 10 ppm, and MS/MS tolerance was set at 0.6Da. Search criteria included oxidation of methionine (+15.9949) as a variable modification and carbamidomethylation of cysteine (+57.0214) and the addition of the TMT mass tag (+229.163) to peptide N-termini and lysine as fixed

modifications. Searches were performed with full tryptic digestion and a maximum of 1 missed cleavage was allowed. The reverse database search option was enabled and all peptide data was filtered to satisfy false discovery rate (FDR) of 5%.

2.18 Generation of Endothelial Specific Piezo1 Knockout Mice

All animal work including organ harvesting was performed by Dr Baptiste Rode (University of Leeds). All animal work was approved by the University of Leeds Animal Ethics Committee and by The Home Office, UK (Ref: 40/3557 and P606320FB). All animals were maintained in GM500 individually ventilated cages (Animal Care Systems), at 21°C 50–70% humidity, light/dark cycle 12/12 hrs on RM1 diet (SpecialDiet Services, Witham,UK) ad libitum and bedding of Pure'ο Cell[®] (Datesand, Manchester, UK). All animal use was authorised by the University of Leeds Animal Ethics Committee and The Home Office, UK. Genotypes were determined using real-time PCR with specific probes designed for each gene (Transnetyx, Cordova, TN).

To generate tamoxifen inducible deletion of the Piezo1 gene in endothelial cells of adult mice, C57BL/6 Piezo1^{flox} mice were crossed with C57BL/6 mice expressing cre recombinase under the Cadherin5 promoter (Tg(Cdh5-cre/ERT2)1Rha) and inbred to obtain C57BL/6 Piezo1^{flox/flox}/Cdh5-cre mice. Tamoxifen (Sigma-Aldrich) was dissolved in corn oil (Sigma-Aldrich) at 20 mg.mL⁻¹. Adult male mice (aged 12 to 16 weeks) were injected intra-peritoneal with 75 mg.kg⁻¹ tamoxifen for 5 consecutive days and liver tissues was harvested 10 to 14 days following the last tamoxifen injection. Piezo1^{flox/flox}/Cdh5-cre mice that received tamoxifen injections

and therefore had Piezo1 deleted from their endothelial cells were referred as Piezo1^{ΔEC}, Piezo1^{flox/flox} littermates that received tamoxifen injections and therefore retained endothelial cell Piezo1 were referred as Control.

2.19 Data Analysis

Origin[®] 8.6 software was used for data analysis and presentation. Data are expressed as mean +/- standard error of the mean. Data were checked for normality using the Shapiro-Wilk test. If normally distributed, statistical comparisons were made using the Student's T-Test. Data sets with more than two groups were compared using a one-way ANOVA test with a post-hoc Bonferroni correction. Statistical significance is indicated by * (p<0.05), ** (p<0.01) and *** (p<0.001). No significant difference is indicated by NS (p>0.05). The number of independent experiments is indicated by 'n'. For multiwell assays, the number of replicate wells is indicated by 'N'.

Chapter 3: Characterisation of Colorectal Cancer Liver Metastases Endothelial Cells

Much of our understanding about the biology of tumour angiogenesis is based upon experiments undertaken in HUVECs. Although easy to culture and study, it is important to note that tumour angiogenesis most commonly involves the microvasculature rather than the macrovasculature. Furthermore, there is increasing evidence that TECs are genetically and phenotypically distinct from normal endothelial cells (Dudley, 2012). Therefore, conclusions derived from in vitro studies using HUVECs may lead to inaccurate assumptions about true tumour angiogenesis.

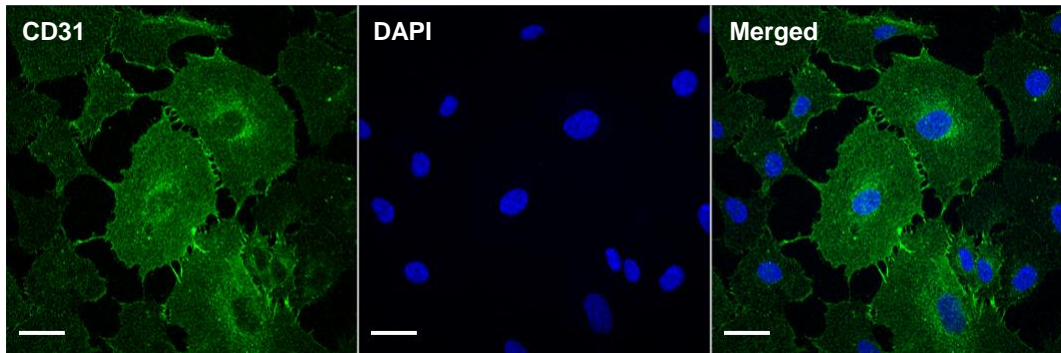
Anti-angiogenic agents have been utilised in the treatment of metastatic colorectal cancer for over a decade. However, promising pre-clinical studies have not really translated into radical improvements in patient outcomes. The majority of licensed therapeutics target the VEGF-VEGFR-2 signalling pathway, which has been established as the main regulator of angiogenesis, but it appears that tumours can resort to other mechanisms to result in treatment resistance. These pathways are not fully understood, in part, due to a lack of specific knowledge about the properties and molecular mechanisms of CLM endothelial cells. Another approach to inhibiting CLM angiogenesis would be to directly target mechanisms essential to TEC survival. Identification of these critical mechanisms would involve the isolation and detailed study of CLM endothelial cells, a feat which has not yet been achieved.

The aim of this chapter was to successfully isolate and characterise CLM endothelial cells and identify a new anti-angiogenic target relevant for their survival.

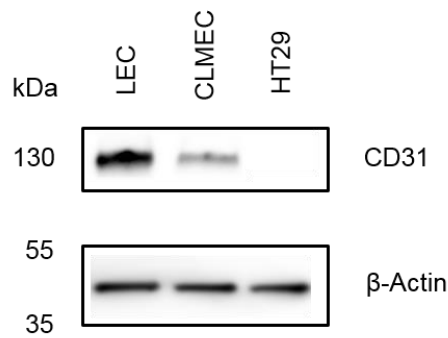
3.1 Endothelial Cells Isolated from Colorectal Cancer Liver Metastases Express Recognised Endothelial Markers

Endothelial cells were isolated and cultured from CLM and surrounding macroscopically normal liver in patients undergoing curative hepatic resection. Immunofluorescent staining of CLM endothelial cells (CLMECs) confirmed expression of the endothelial intercellular-junction protein CD31 (Figure 21a). Western blotting also confirmed the presence of CD31 in healthy liver endothelial cells (LECs) as well as CLMECs, but not in the colorectal cancer cell line HT29 (Figure 21b). Quantification of the CD31 band intensity relative to the β -actin loading control in matched samples revealed the expression of CD31 to be 64% lower in CLMECs (Figure 21c). To further validate the endothelial nature of CLMECs, immunofluorescent staining of additional endothelial markers was performed. CLMECs stained positively for VE-Cadherin, VEGFR-2, von Willebrand Factor (vWF) and endothelial Nitric Oxide Synthase (eNOS) (Figure 22).

a



b



c

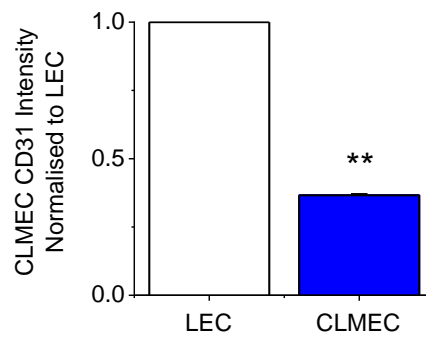


Figure 21 Isolated LECs and CLMECs Express CD31

a. Immunofluorescence images of CLMECs stained with anti-CD31 antibody (green) and DAPI to label nuclei (blue). Scale bars 20 μ m **b.** Example western blot labelled with anti-CD31 and anti- β -actin antibodies for matched LECs and CLMECs and a human colorectal adenocarcinoma cell line (HT29) **c.** Quantification of the CLMEC CD31 band intensity relative to β -actin and normalised to LEC (n=3 each).

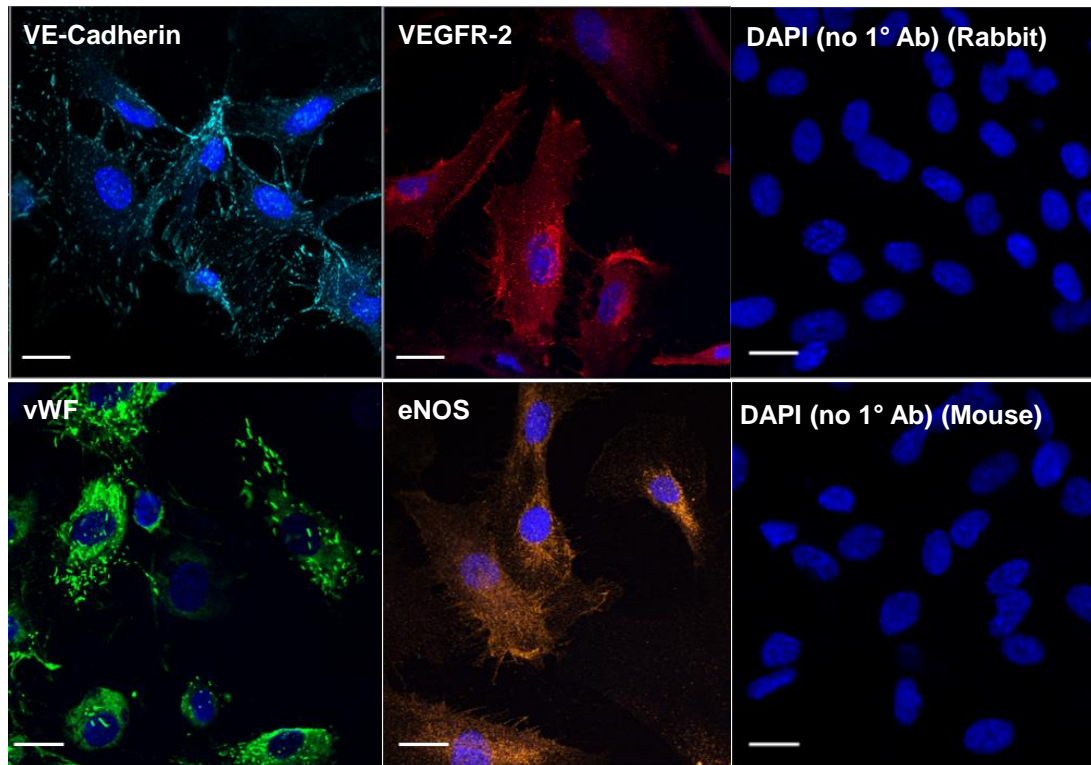


Figure 22 CLMECs Express Recognised Endothelial Markers

Immunofluorescence images of CLMECs stained with anti-VE-Cadherin (turquoise), anti-Vascular Endothelial Growth Factor Receptor 2 (VEGFR-2, red), anti-von Willebrand Factor (vWF, green) and anti-endothelial Nitric Oxide Synthase (eNOS, orange). In each image nuclei were labelled with DAPI (blue). Control images in the absence of the primary antibodies are shown on the right. Scale bars 20 μm .

3.2 VEGF Evokes Ca²⁺ Entry in LECs and CLMECs

The VEGF-VEGFR-2 signalling pathway has been established as the main regulator of angiogenesis. To establish the presence of this pathway, firstly, western blotting was performed to confirm VEGFR-2 expression in matched LECs and CLMECs (Figure 23a). Quantification of the VEGFR-2 band intensity relative to the β -actin loading control revealed the expression of VEGFR-2 to be 55% lower in CLMECs (Figure 23b).

Intracellular Ca²⁺ elevation is an early event in the action of VEGF acting through VEGFR-2 in endothelial cells (Li et al., 2015). To elicit this response, matched LECs and CLMECs were stimulated with a physiological concentration of VEGF (30 ng.mL⁻¹) in the presence of extracellular Ca²⁺ and intracellular Ca²⁺ concentrations were recorded. In both LECs and CLMECs, application of VEGF resulted in an increase in intracellular Ca²⁺ that reached a peak after 220 seconds followed by a sustained phase that remained above the baseline for at least 600 seconds (Figure 23c). The peak intracellular Ca²⁺ response in CLMECs was 53% lower than in matched LECs (Figure 23d). There was less difference in the sustained response, which was 31% lower in CLMECs (Figure 23d).

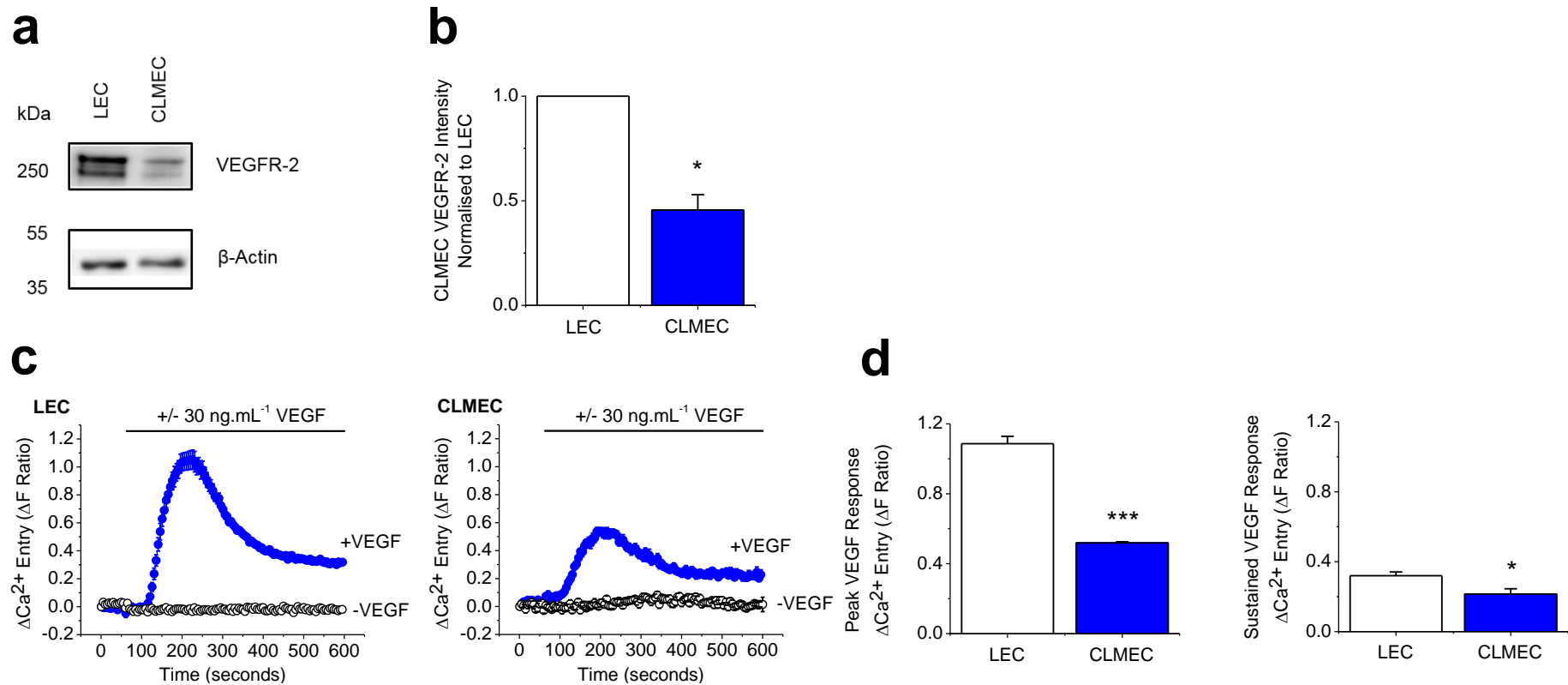


Figure 23 CLMEC VEGF-Evoked Ca^{2+} Entry is Decreased Compared to Matched LECs

a. Example western blot labelled with anti-VEGFR-2 and anti- β -actin antibodies for matched LECs and CLMECs **b.** Quantification of the CLMEC VEGFR-2 band intensity relative to β -actin and normalised to LEC (n=3 each) **c.** Intracellular Ca^{2+} measurement data from matched LECs (left) and CLMECs (right). Traces show averaged responses to 30 ng.mL⁻¹ VEGF across multiple wells of a 96-well plate compared to control (N=5 wells each) **d.** Mean data for the peak (200 s) and sustained (600 s) responses to VEGF of the type exemplified in c (n=3, N=15 each).

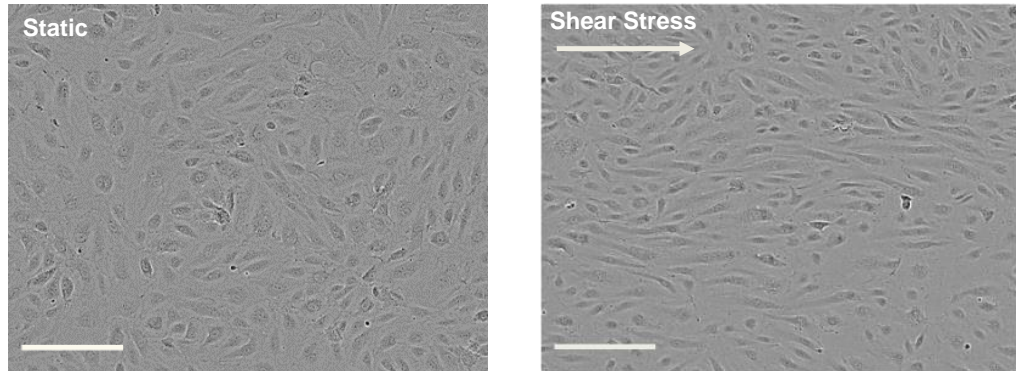
3.3 CLMECs Have Endothelial Specific Functional Properties

To determine if CLMECs behaved functionally like endothelial cells, alignment in response to shear stress and tube formation in the presence of Matrigel® was investigated.

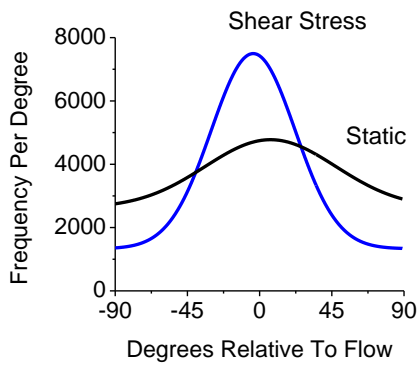
Endothelial cells align in response to shear stress, a process occurring physiologically in blood vessels as a result of blood flow (Li et al., 2014). In static conditions, CLMECs grew into a “cobblestone” monolayer, typical for endothelial cell growth in vitro. In contrast, after 48 hrs of shear stress, CLMECs appeared to align to the direction of flow (Figure 24a). Analysis of CLMECs exposed to shear stress revealed a peak in the number of cells orientated to the direction of flow (0°) confirming alignment (Figure 24b,c).

The formation of capillary-like structures on the artificial basement membrane extracellular matrix Matrigel® is a behaviour specific to endothelial cells (Arnaoutova et al., 2009). In the presence of Matrigel®, CLMECs rapidly formed capillary-like structures in less than 12 hrs (Figure 25a). The number of capillary-like structures were quantified by counting the number of complete loops. With Matrigel®, 25 complete loops were observed, whereas in the absence of Matrigel®, CLMECs grew into a confluent monolayer and no capillary-like structures were observed (Figure 25b).

a



b



c

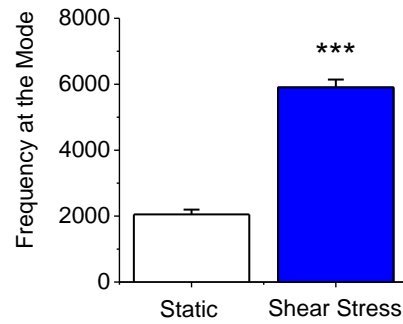
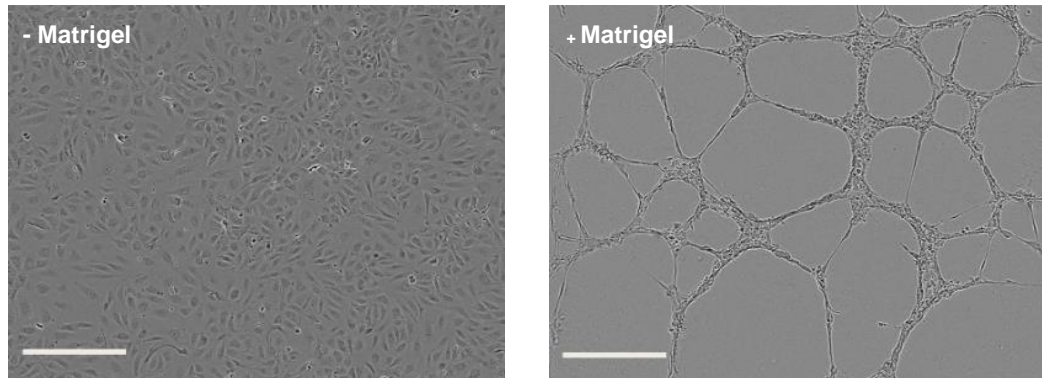


Figure 24 CLMECs Align in Response to Shear Stress

- a.** Images of CLMECs in static condition and after shear stress. Scale bars 80 μ m
- b.** Example orientation analysis for the images shown in **a**
- c.** Mean data for the analysis shown in **b** (n=3, N=18).

a



b

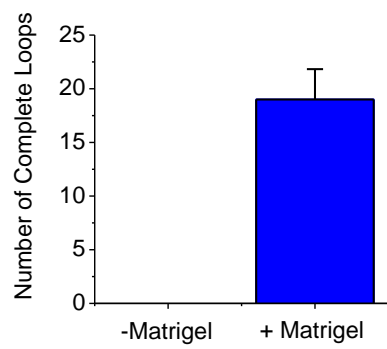


Figure 25 CLMECs Form Tubular Structures when Grown on Matrigel®

a. Images of CLMECs in the absence and presence of Matrigel®. Scale bars 250 μm **b.** Quantification of the number of complete loops seen in images of the type shown in a (n=4, N=12).

3.4 RNA Interference Screen Reveals WEE1 to have Critical Role in Regulating Endothelial Cell Proliferation

To help determine which proteins are important for CLMEC proliferation, results of an unbiased RNA interference screen in HUVECS performed by Dr Heather Martin (University of Leeds) were analysed. The screen was performed prior to the commencement of this research project and consisted of an initial screen followed by a validation screen with different siRNA chemistry. To identify potential anti-angiogenic targets, plate wide robust Z-scores were calculated for each gene with a robust Z-score of -2 or less indicating a significant inhibition of proliferation. In total, 12 genes were identified to significantly inhibit HUVEC proliferation (Figure 26a). A review of the literature indicated two related proteins involved in cell cycle regulation, WEE1 and CDK1.

WEE1 is a tyrosine kinase that forms a crucial component of the G2/M checkpoint, preventing cells from entering mitosis with unrepaired DNA damage by regulating the phosphorylation of cyclin B bound cyclin dependent kinase 1 (CDK1) at Tyr15. As WEE1 regulates CDK1 activity and had a clear anti-proliferative effect (Figure 26b) that was greater than CDK1 (mean robust Z-score -4.05 vs -2.52) it was selected for further investigation.

a

Gene	Initial Screen Z Score	Validation Screen Z Score
PLK1	-2.85	-9.43
PPP1R12B	-2.75	-5.73
WEE1	-2.72	-5.37
KCNS2	-3.36	-4.77
TNFRSF1B	-2.37	-3.92
PIK3C2A	-2.99	-3.82
FN3KRP	-3.03	-3.58
MAPK1	-3.10	-3.42
ALPP	-2.08	-3.26
NT5E	-2.96	-3.06
CDK1	-2.34	-2.70
PPP5C	-2.42	-2.09

b

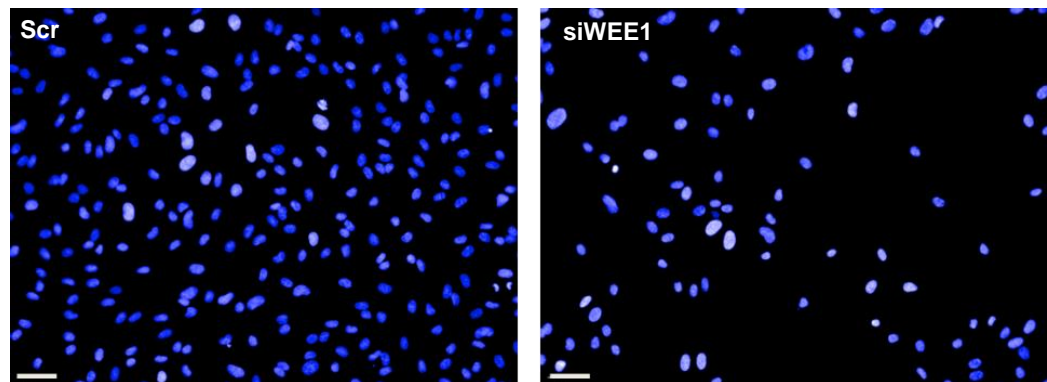


Figure 26 RNA Interference Screen Identifies WEE1 as a Regulator of HUVEC Proliferation

a. Table of results for the RNA interference screen in HUVECs performed by Dr Heather Martin (University of Leeds). All proteins that significantly inhibited proliferation are displayed. Plate wise robust Z-scores are provided for the initial and validation screens. A Z-score of less than -2 suggests the protein significantly inhibits HUVEC proliferation ($p < 0.05$) **b.** Example images of Hoechst staining of HUVECs 72 hrs after transfection with scrambled siRNA (Scr) or with siGENOME WEE1 siRNA (siWEE1) as part of the initial RNA interference screen. Scale bars 50 μm .

3.5 Genetic and Chemical Inhibition of WEE1 Inhibits HUVEC Proliferation

To validate the RNA interference results, transfection of HUVECs was performed with pooled WEE1 siRNA and its effects on proliferation were measured using a Vybrant® DyeCycle™ Green proliferation assay. In non-transfected HUVECs, western blotting confirmed a single band the expected size for WEE1 (96 kDa) (Figure 27a). Knockdown of WEE1 by siRNA decreased the single band intensity (Figure 27a). Quantification of the WEE1 band intensity relative to the β -actin loading control revealed the expression of WEE1 to be 66% lower in HUVECs transfected with WEE1 siRNA compared to scrambled siRNA (Figure 27b). Proliferation was measured 48 hrs after transfection using the nuclear dye Vybrant® Green (Figure 27c). Transfection with siRNA against WEE1 inhibited proliferation by 53% compared to scrambled siRNA (Figure 27d).

AZD1775, a small molecule WEE1 inhibitor, was used to achieve chemical inhibition of WEE1 and its effects on proliferation were measured using a WST-1 proliferation assay. After 48 hrs of treatment AZD1775 (1 μ M) inhibited HUVEC proliferation by 83% compared to vehicle control (Figure 28a). A concentration-response curve was constructed for the effect of AZD1775 on HUVEC proliferation. The derived IC₅₀ for AZD1775 against HUVEC proliferation was 365 nM (Figure 28b).

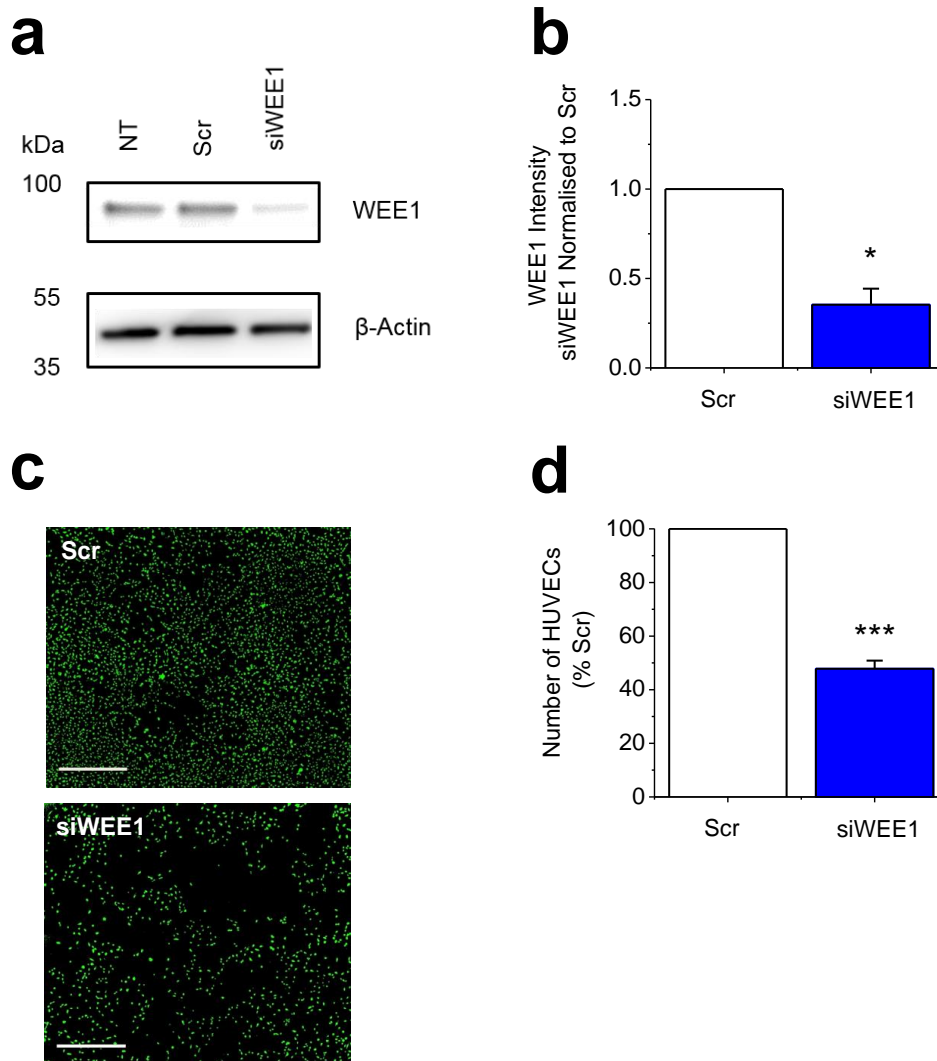


Figure 27 Genetic Inhibition of WEE1 Decreases Proliferation in HUVECs

a. Example western blot labelled with anti-WEE1 and anti- β -actin antibodies for non-transfected (NT) HUVECs and HUVECs transfected with scrambled siRNA (Scr) or ON-TARGETplus WEE1 siRNA (siWEE1) **b.** Quantification of the siWEE1 group WEE1 band intensity relative to β -actin and normalised to the Scr group (n=3 each) **c.** Fluorescence images of HUVECs 48 hrs after transfection with scrambled siRNA (Scr) or ON-TARGETplus WEE1 siRNA (siWEE1). Fluorescence was from cell nuclei stained with Vybrant[®] Dye Cycle[™] (green). Scale bars 400 μ m **d.** Quantification of the number of HUVECs seen in the images of the type shown in c. The siWEE1 group has been normalised to the Scr group (n=3, N=18).

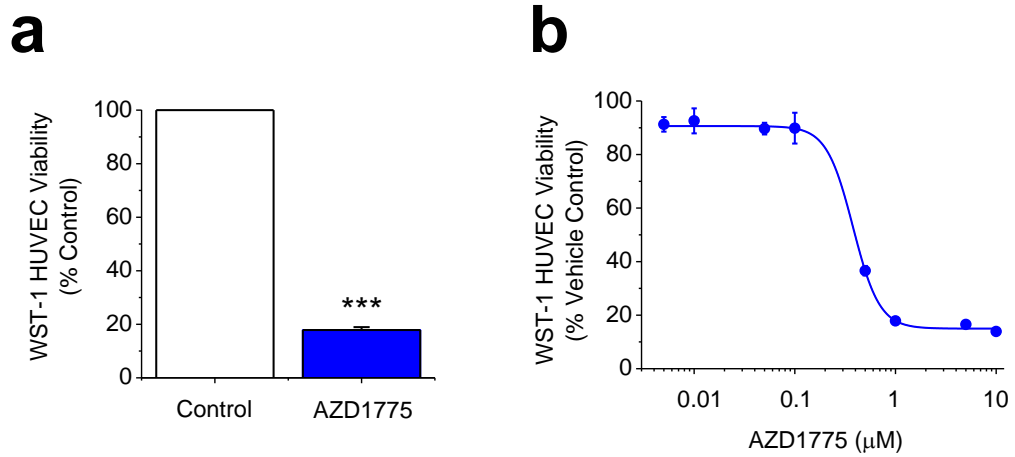


Figure 28 Chemical Inhibition of WEE1 Decreases Proliferation in HUVECs

a. Mean data for HUVEC viability measured using WST-1 reagent after treatment with AZD1775 (1 μM) or vehicle control (Control) for 48 hrs (n=3, N=9) **b.** AZD1775 dose response curve in HUVECs. HUVECs were treated with AZD1775 at the indicated concentrations for 48 hrs and plotted as percentages of the vehicle control (n=3, N=9).

3.6 Genetic and Chemical Inhibition of WEE1 Regulates Phosphorylation of CDK1

WEE1 regulates phosphorylation of cyclin B bound CDK1 at Tyr15. Therefore, western blotting was performed to check target modulation following genetic or chemical inhibition of WEE1. In non-transfected HUVECs, western blotting for pCDK1-Y15 confirmed a single band 34 kDa in size. As expected, knockdown of WEE1 by pooled WEE1 siRNA decreased the single band intensity (Figure 29a). Total CDK1 content was unchanged. Quantification of the pCDK1-Y15 to CDK1 ratio revealed pCDK1-Y15 expression to be reduced in the siWEE1 group compared to scrambled group by 72% (Figure 29b). A similar effect was observed when treating HUVECs with AZD1775. AZD1775 reduced pCDK1-Y15 but not overall CDK1 (Figure 29c). Quantification of the pCDK1-Y15 to CDK1 ratio showed pCDK1-Y15 expression to be reduced with AZD1775 treatment by 78% compared to vehicle control (Figure 29d).

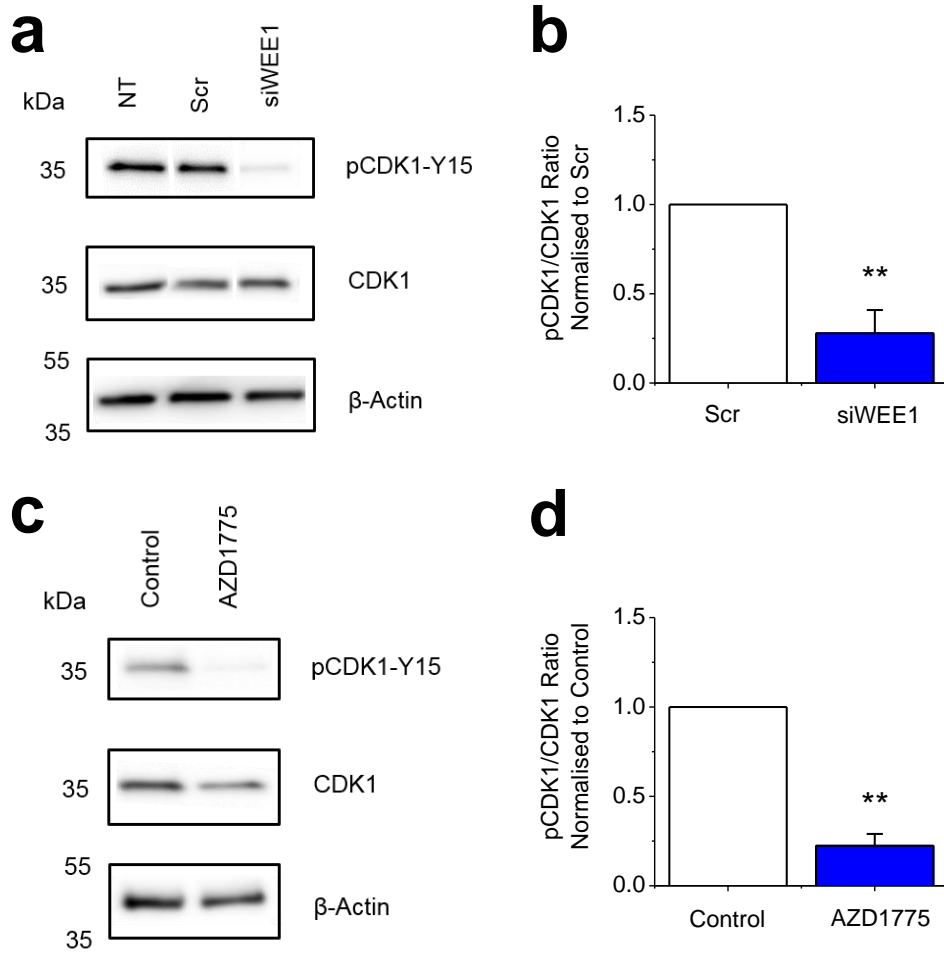


Figure 29 Genetic and Chemical Inhibition of WEE1 Decreases pCDK1-Y15 in HUVECs

a. Example western blot labelled with anti-pCDK1-Y15, anti-CDK1 and anti- β -actin antibodies for non-transfected (NT) HUVECs and HUVECs transfected with scrambled siRNA (Scr) or ON-TARGETplus WEE1 siRNA (siWEE1) **b.** Quantification of the pCDK1-Y15 band intensity divided by the CDK1 band intensity. siWEE1 has been normalised to Scr (n=3 each) **c.** Example western blot labelled with anti-pCDK1-Y15, anti-CDK1 and anti- β -actin antibodies for HUVECs treated with AZD1775 (1 μ M) or vehicle control (Control) for 24 hrs **d.** Quantification of the pCDK1-Y15 band intensity divided by the CDK1 band intensity. AZD1775 has been normalised to Control (n=3 each).

3.7 WEE1 is Upregulated in CLMECs

After identifying WEE1 as a potential anti-angiogenic target in HUVECs, western blotting was performed in matched LECs and CLMECs to confirm the presence of WEE1 and compare its expression between the two cell types. As with HUVECs, a single band 96 kDa in size was detected in both LECs and CLMECs (Figure 30a). Interestingly, quantification of the WEE1 band intensity relative to the β -actin band intensity revealed WEE1 to be significantly upregulated in CLMECs compared to matched LECs (Figure 30b). In contrast, the target protein of WEE1, CDK1, was not upregulated in CLMECs (Figure 30c,d).

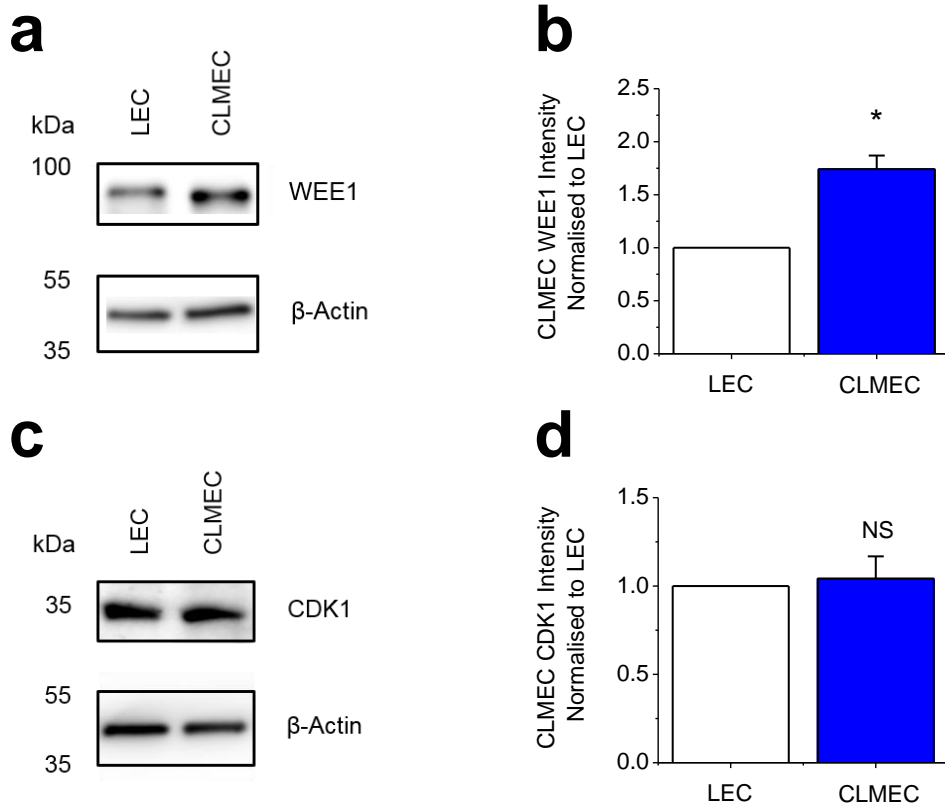


Figure 30 WEE1 is Upregulated in CLMECs Compared to Matched LECs

a. Example western blot labelled with anti-WEE1 and anti- β -actin antibodies for matched LECs and CLMECs **b.** Quantification of the CLMEC WEE1 band intensity relative to β -actin and normalised to LEC (n=3 each) **c.** Example western blot labelled with anti-CDK1 and anti- β -actin antibodies for matched LECs and CLMECs **d.** Quantification of the CLMEC CDK1 band intensity relative to β -actin and normalised to LEC (n=3 each)

3.8 Summary of Findings

- Endothelial cells isolated from colorectal cancer liver metastases behave superficially like other endothelial cells:
 - 1) They express CD31, vWF, VE-Cadherin, eNOS and VEGFR-2
 - 2) They elevate intracellular Ca^{2+} in response to VEGF stimulation
 - 3) They have a “cobblestone” appearance when grown in vitro
 - 4) They align in response to shear stress
 - 5) They form tube-like structures on Matrigel®

- CLMECs have reduced CD31 and VEGFR-2 protein expression compared to matched LECs.

- The VEGF-induced increase in intracellular Ca^{2+} is relatively smaller in CLMECs compared to matched LECs.

- CLMECs have increased WEE1 protein expression compared to matched LECs

- siRNA knockdown of WEE1 inhibits HUVEC proliferation

- AZD1775 inhibits HUVEC proliferation with an IC_{50} of 365 nM.

- WEE1 phosphorylates CDK1 at Tyr15 in HUVECs

3.9 Discussion

The aim of this chapter was to successfully isolate and characterise CLMECs and find a new anti-angiogenic target for the treatment of CLM. CLMECs have been shown to be superficially similar to other types of endothelial cells, including LECs, exhibiting expected markers and functional characteristics. Nevertheless, differences in protein expression have been identified between matched LECs and CLMECs, including the upregulation of WEE1 and downregulation of CD31 and VEGFR-2.

3.9.1 Characterisation of CLMECs

To isolate CLMECs an IMS technique was used with anti-CD31 coated magnetic beads. The liver has a number of endothelial subtypes including those within the conventional vasculature (hepatic artery, arterioles, capillaries, venules, portal vein and hepatic veins) as well as specialised sinusoidal endothelial cells contained within hepatic lobules. These different subtypes have different endothelial marker profiles. CD31 was chosen as it is considered a pan-endothelial marker and would result in the highest yield of endothelial cells (Vermeulen et al., 2002). CD31 expression was found to be lower in CLMECs than matched LECs. CD31 is a cell adhesion protein found at inter-cellular junctions of endothelial cells. It has a critical role in leucocyte trafficking across the endothelial monolayer (Muller, 2014). One possible explanation for downregulation of CD31 in CLMECs could be a tumour defence mechanism. Decreased CD31 expression could abrogate leucocyte extravasation, meaning tumours escape immunological attack. Although there are no previous reports of CD31 down-regulation in tumour endothelial cells, other adhesion molecules, such as ICAM-1 and VCAM-1, have been reported to be

down-regulated in the tumour endothelium (Griffioen et al., 1996, Alessandri et al., 1999).

A range of other endothelial markers have been used to isolate tumour endothelial cells previously including CD146 (St Croix et al., 2000), Endoglin (Xiong et al., 2009) and ICAM2 (Dudley et al., 2008). However, no 100% specific marker exists for normal endothelial cells or tumour endothelial cells. Therefore, to further validate the endothelial nature of CLMECs, other endothelial markers were investigated. CLMECs positively expressed vWF, VE-Cadherin, eNOS and VEGFR-2, strongly suggesting that the isolated cells were endothelial in nature.

Although endothelial cells from primary colorectal cancer have previously been isolated and characterised (van Beijnum et al., 2006, Schellerer et al., 2007, Jayasinghe et al., 2009, Mesri et al., 2013), this is the first time that endothelial cells from CLM have been studied in detail. The formation of tube like structures on the artificial membrane Matrigel[®] has long been used as a method of investigating angiogenesis. Matrigel[®] is a gelatinous protein mixture secreted by Engelbreth-Holm-Swarm (EHS) mouse sarcoma cells. In vivo, the basement membrane regulates endothelial behaviour maintaining endothelial cells in a differentiated state. Rather than grow in a classical cobblestone appearance, the presence of Matrigel[®] resulted in CLMECs migrating across the Matrigel[®], aligning and forming tube like structures within 12 hrs. This complex behaviour is specific to endothelial cells and does not occur with cancer cells or connective tissue cells such as fibroblasts. Tumour derived endothelial cells have previously been reported to be capable of forming chord-like structures on Matrigel[®] within 24 hrs of culture (Alessandri et al., 1999).

The ability of cells to align in response to shear stress is another endothelial specific characteristic and the way in which physical forces, such as blood flow, regulate endothelial vascular structure are complex. The ability of tumour endothelial cells to align in response to shear stress has not been reported. Our laboratory has recently published work on the mechanosensitive Ca^{2+} permeable ion channel Piezo1 (Fam38), which has a critical role in sensing frictional force (shear stress) and determining vascular structure in both development and adult physiology (Li et al., 2014). The role of Piezo1 in the tumour endothelium will be discussed in subsequent chapters of this thesis.

3.9.2 The VEGF-VEGFR-2 Signalling Pathway in CLMECs

VEGFR-2 stimulation by VEGF is thought to be the major regulator of tumour angiogenesis. VEGFR-2 is expressed in CLMECs and was significantly down-regulated compared to matched LECs. The finding of decreased VEGFR-2 expression in CLMECs disagrees with other studies which have reported increased VEGFR-2 expression in tumour derived endothelial cells (Alessandri et al., 1999, Hida et al., 2013).

To examine the VEGF-VEGFR-2 signalling pathway, CLMEC Ca^{2+} entry was investigated in response to VEGF application. Intracellular Ca^{2+} entry is an early consequence of VEGF stimulation in endothelial cells (Li et al., 2015). Upon activation by VEGF, VEGFR-2 dimerization occurs which facilitates auto-phosphorylation of multiple tyrosine residues along the cytoplasmic domains of each monomer (Schlessinger, 2000). This activates binding sites for proteins with Src-homology 2. One such protein is phospholipase C- γ , which upon activation hydrolyses its substrate phosphatidylinositol 4,5-bisphosphate (PIP_2) into two

secondary messengers, inositol triphosphate (IP₃) and diacyl glycerol (DAG). IP₃ diffuses into the endoplasmic reticulum (ER) and binds to the IP₃ receptor. The IP₃ receptor serves as a Ca²⁺ channel, and releases Ca²⁺ from the ER. The reduction in ER [Ca²⁺] is sensed and stimulates the influx of extracellular Ca²⁺ via store-operated channels into the cell cytoplasm (Li et al., 2015). In tumour endothelial cells Ca²⁺ is important in regulating angiogenic processes including proliferation, migration and tube formation (Fiorio Pla and Munaron, 2014). The peak intracellular response (caused by Ca²⁺ release from intracellular stores) was significantly lower in CLMECs compared to matched LECs. Similarly the sustained response (caused by extracellular Ca²⁺ entry) was also significantly lower in CLMECs, although the magnitude of difference was not the same compared to the peak response.

The decreased expression of VEGFR-2 and reduced Ca²⁺ signalling in CLMECs is an unexpected finding. As the main regulatory pathway of tumour angiogenesis, it may be hypothesised that VEGFR-2 would be upregulated. However, downregulation of VEGFR-2 may be a consequence of prolonged exposure to high concentrations of VEGF, which is known to be secreted by tumour cells and cells within the tumour microenvironment such as fibroblasts and macrophages (Goel and Mercurio, 2013). Downregulation of VEGFR-2 is maintained through passage of the cells and although the media that CLMECs were cultured in contained VEGF, this is not thought to be responsible for the downregulation of VEGFR-2, as matched LECs were also cultured in the same media. The downregulation of the VEGF-VEGFR2 signalling pathway in CLMECs could have significant implications upon the efficacy of anti-angiogenic treatments in patients. Tumours are known to be able to develop resistance to anti-VEGF therapy by upregulating alternative pro-angiogenic pathways, however, some patients fail to respond to anti-VEGF therapy from the initiation of treatment. CLM are heterogenous and one possibility is that

VEGF-VEGFR-2 signalling is not as important in the growth of these tumours. This means that agents which target the VEGF-VEGFR-2 axis, such as bevacizumab, ramucirumab and regorafenib will have little benefit.

3.9.3 WEE1 Inhibition as an Anti-Angiogenic Target

The RNA interference screen revealed WEE1 to have a role in HUVEC proliferation. This was validated with separate pooled siRNA and with the small molecule WEE1 inhibitor AZD1775. Furthermore, WEE1 expression was upregulated in CLMECs compared to matched LECs making it a potentially attractive target that could be essential for CLMEC viability.

3.9.3.1 WEE1 Function and Regulation

WEE1 is a tyrosine kinase which forms part of the G2/M cell cycle checkpoint. In response to DNA damage, WEE1 causes phosphorylation of cyclin B bound CDK1 on its Tyr15 residue (Watanabe et al., 1995). CDK1 regulates cell entry into mitosis and phosphorylation by WEE1 negatively regulates mitotic entry, allowing damaged DNA damage to be repaired before the cell divides. Transcriptional synthesis of WEE1 increases during S (DNA synthesis) phase and G2 (Growth 2) phase of the cell cycle and decreases during M (Mitosis) phase (Chow et al., 2011). Once a cell enters mitosis, the exact mechanism by which WEE1 is inactivated is not fully understood, however it appears to occur as a result of hyper-phosphorylation (Perry and Kornbluth, 2007). At the onset of mitosis, WEE1 is phosphorylated by CDK1 at Ser123, which generates a binding motif allowing polio-like kinase 1 (PLK1) to phosphorylate WEE1 at Ser53. Further phosphorylation of WEE1 by Casein Kinase 2 at Ser121 coupled with the phosphorylated Ser123 and Ser53 residues serve as

phosphodegrons that target WEE1 for degradation by the ubiquitin ligase SCF ^{β -TrCP} complex (Chow et al., 2011).

Whilst WEE1 has been known historically as a key component of the G2/M checkpoint, more recently it has been reported to have a critical role in DNA synthesis during S phase (Beck et al., 2010). During replication, DNA is replicated exactly once and it is achieved by thousands of replication forks, which are initiated from replication origins spaced throughout the genome. The number of origins exceeds what is actually needed for replication. Other dormant origins can be fired as a result of replication fork stalling (Alver et al., 2014). Regulation of origin firing by CDKs is important to prevent excessive origin firing and replication stress. Therefore, regulation of CDK1 activity, by WEE1, is critical in regulating DNA synthesis. Recently it has been reported that WEE1 inhibition results in increased CDK1 activity causing increased origin firing (Beck et al., 2012). The increased origin firing results in increased DNA synthesis which exhausts nucleotide stores leading to replication fork stalling and double stranded DNA breaks (Beck et al., 2012).

3.9.3.2 WEE1 Inhibition as an Anti-Cancer Therapy

Due to its functions as a regulator of mitosis and DNA synthesis, WEE1 has been targeted as an anti-cancer agent. Conventional medical therapies for cancer, such as chemotherapy and radiotherapy, cause cell death by inducing lethal DNA damage in cells. In health, DNA damage activates cell cycle checkpoints (G1, S and G2/M) that arrest the cell cycle allowing DNA to be repaired. Understandably this is an essential process in healthy cells in order to preserve genomic integrity,

but in cancerous cells this can limit the efficacy of DNA-damaging treatments. The combination of WEE1 inhibition with DNA damaging agents has emerged as an attractive anti-cancer treatment strategy, whereby cancer cells with lethal DNA damage are forced into premature mitosis with unrepaired DNA damage, resulting in cell death (Medema and Macurek, 2012). This is thought to be particularly effective in cancers with non-functioning p53 as they have a defective G1 cell cycle checkpoint and cannot maintain G1 arrest in response to DNA damage. Therefore, these cancer cells are more reliant on the G2/M checkpoint for DNA repair. Mutation of the tumour suppressor gene p53 is a frequent event in cancer (Rivlin et al., 2011) and therefore this treatment strategy is potentially applicable to a diverse range of cancers. Preclinical studies in several cancer lines, including colorectal cancer, support this treatment strategy (Wang et al., 2001, Hirai et al., 2009, Hirai et al., 2010, Rajeshkumar et al., 2011). At present there are over 25 clinical trials assessing the small molecule WEE1 inhibitor, AZD1775, in combination with DNA damaging agents in a range of cancers (ClinicalTrials.gov Accessed July 2016).

The importance of p53 status in combination therapy has however been questioned after several studies demonstrated that AZD1775 sensitises cancer cells to DNA-damaging agents independent of p53 function (Kreahling et al., 2013, Van Linden et al., 2013, Guertin et al., 2013, Mueller et al., 2014). At the same time, the discovery of the importance of WEE1 in the regulation of DNA synthesis was being made (Beck et al., 2012) and it was hypothesised that WEE1 inhibition in the absence of DNA damaging agents could be a viable anti-cancer strategy. Indeed, a number of studies have shown that AZD1775 is able to induce double-stranded DNA (DS-DNA) breaks in S phase and that cancer cell proliferation could be limited without the need for premature mitosis (Kreahling et al., 2012, Guertin et al., 2013, Pfister et al., 2015). The

first Phase I clinical trial of AZD1775 monotherapy in solid tumours has recently been reported confirming target modulation, safety and efficacy (Do et al., 2015).

Based on the known functions of WEE1, it could be hypothesised that the reduction in HUVEC viability observed with WEE inhibition in this chapter is more likely a consequence of DS-DNA breaks rather than mitosis. This is because WEE1 inhibition was tested in the absence of any DNA-damaging agents and therefore the mechanism of premature mitosis/mitotic catastrophe is not possible.

3.9.3.3 The Role of WEE1 in the Endothelium

The mechanism for WEE1 upregulation in CLMECs is unknown, but whatever the mechanism is it is sustained despite culturing of CLMECs under physiological conditions. One potential stimulus for upregulation is tumour hypoxia. In the only previous piece of research on WEE1 in endothelial cells, hypoxia increased WEE1 mRNA and CDK1 phosphorylation in the MS-1 endothelial cell line (Hong et al., 2011). However, CLMECs were cultured in the same conditions as LECs and this did not revert WEE1 expression in CLMECs back to the levels observed in LECs.

WEE1 has been shown to be upregulated in a number of different cancers including colorectal cancer (Egeland et al., 2016), hepatocellular carcinoma (Masaki et al., 2003), breast cancer (Iorns et al., 2009) and osteosarcoma (PosthumaDeBoer et al., 2011). Expression is shown to increase during carcinogenesis and is highest in metastatic disease (Magnussen et al., 2012). High WEE1 expression has been found to be negatively correlated with disease free survival and primary tumour burden (Magnussen et al., 2012). It is hypothesised that tumour cells have

increased expression of WEE1 to protect themselves from DNA-damage and cell death (Magnussen et al., 2012). This is not only because of its role in controlling mitotic entry, but in ensuring DNA is synthesised in a controlled and co-ordinated manner. In complete contrast, WEE1 has been shown to be down-regulated in non-small cell lung cancer, and loss of WEE was associated with a poorer prognosis (Yoshida et al., 2004). Here investigators hypothesised that decreased WEE1 expression conferred an advantage to neoplastic cells by allowing faster progression through the cell cycle. If this were to be true one could argue that increased WEE1 expression would result in a slower cell cycle in CLMECs compared to LECs. Although proliferation was not formally compared between the two groups, there was no obvious difference in proliferation rate observed during cell culture.

Preliminary work in HUVECs has shown that WEE1 has functional importance in endothelial cells. Pooled WEE1 siRNA generated a good knockdown of WEE1 in HUVECs that had clear effects on HUVEC proliferation. Reassuringly, similar results were observed with the small molecule WEE1 inhibitor, AZD1775. As expected both WEE1 siRNA and AZD1775 inhibited CDK1 phosphorylation at Tyr15 in HUVECs confirming that CDK1 is that target of WEE1 in HUVECs. Therefore, it is likely that the effects on HUVEC proliferation by WEE1 inhibition are mediated through the increased activity of cyclin B-CDK1 complexes.

3.9.4 RNA interference Screening Results

Over the last decade RNA interference screening has become a powerful tool whereby the effects of gene silencing on biological properties, such as cell proliferation, can be systematically explored. RNA interference provided an

unbiased approach in identifying proteins critical to endothelial cell proliferation. The RNA interference screen was performed in HUVECs. Although this means the results of the screen may not directly apply to CLMECs, it does provide a starting point for identifying which genes are important in normal endothelial cell proliferation in vitro. By using two independent sets of RNA interference chemistry, hits in the initial screen were able to be validated in a confirmation screen, suggesting that their effect on HUVEC proliferation is genuine.

The screen identified twelve genes important in inhibiting HUVEC proliferation. The majority of these have not been reported as critical regulators of cellular proliferation, including a potassium voltage-gated ion channel, fructosamine 3 kinase related protein and a myosin phosphatase subunit. However, two hits were noted to be key regulators of the cell cycle (WEE1 and CDK1) and were selected for further investigation. Small molecule inhibitors of both WEE1 (AZD1775) and CDK1 (R0-3306) have been shown to inhibit tumour cell proliferation (Vassilev et al., 2006, Guertin et al., 2013).

WEE1 was not the most significant hit in the RNA interference screen. It was chosen because its target protein CDK1 also significantly inhibited HUVEC proliferation when knocked down, suggesting this signalling pathway has significant importance. The top hit in the screen was Polio-like kinase 1 (PLK1), which is also implicated in the regulation of cyclin B-CDK1 activity and mitotic entry. PLK1 promotes mitotic entry in two ways. Firstly it is able to phosphorylate CDC25C which activates phosphatases capable of de-phosphorylating (and thereby activating) the cyclin B-CDK1 complex, promoting mitosis (Roshak et al., 2000). Secondly, as previously discussed, it is able to phosphorylate and deactivate

WEE1, which normally keeps cyclin B-CDK1 complexes in an inhibited state by phosphorylation of the Tyr15 residue on CDK1. Although PLK1 promotes mitotic entry, its primary role in mammalian cells is the control of mitotic progression, particularly the regulation of proteins that are involved in the metaphase-anaphase transition and mitotic exit. Inhibition of PLK1 with a small molecule PLK1 inhibitor results in mitotic arrest and apoptosis in tumour cells (Steegmaier et al., 2007). As a result, Volasertib (also known as BI 6727), is currently being investigated in clinical trials as an anti-cancer agent. Therefore, in the RNA interference screen it is not surprising that knockdown of PLK1 inhibited the proliferation in HUVECs.

3.9.5 Conclusion

For the first time, CLMECs have successfully been isolated and characterised in vitro. Although they share functional properties with LECs, differences in protein expression are apparent. Both CD31 and VEGFR-2 are down-regulated in CLMECs, the latter significantly impacting upon VEGF-VEGFR-2 induced Ca^{2+} signalling. This may, in part, explain the lack of clinical efficacy observed with current anti-VEGF therapy. WEE1 has been identified as a potential anti-angiogenic target which is up-regulated in CLMECs. It has functional importance in HUVECs, with genetic and chemical inhibition significantly inhibiting proliferation. Targeting mechanisms critical to tumour endothelial cell survival represents an alternative approach to anti-angiogenesis therapy, which may help overcome the current problems associated with VEGF-signalling resistance.

Chapter 4: WEE1 Inhibition has Anti-Angiogenic Effects in Endothelial Cells of Colorectal Cancer Liver Metastases

In the previous chapter, WEE1 was identified as a possible anti-angiogenic target that was found to be upregulated in CLMECs. In HUVECs, both genetic inhibition of WEE1 with pooled WEE1 siRNA and chemical inhibition of WEE1 with the small molecule inhibitor AZD1775 inhibited phosphorylation of CDK1 at its Tyr15 residue. In both cases this resulted in a reduction in HUVEC proliferation.

AZD1775, a small molecule WEE1 inhibitor is currently being investigated in a number of oncological clinical trials as both a DNA-damaging sensitiser and as an outright monotherapeutic agent (ClinicalTrials.gov Accessed July 2016). This reflects the ability of WEE1 to regulate CDK1, which has dual functions as a regulator of mitosis and DNA synthesis. As a monotherapy, AZD1775 has been shown to increase CDK1 activity resulting in increased origin firing in cancer cells. This is followed by nucleotide exhaustion, replication fork stalling and DS-DNA breaks (Beck et al., 2012). However, the effects of WEE1 inhibition on endothelial cells, including tumour endothelial cells remain unknown.

Tumour angiogenesis is a complex process involving much more than endothelial cell proliferation. The importance of WEE1 on CLMEC properties such as migration and tube formation are unknown. The aim of this chapter was to determine if WEE1 inhibition has anti-angiogenic activity in CLMECs and identify the mechanism underlying these effects.

4.1 Genetic and Chemical Inhibition of WEE1 Inhibits Proliferation in CLMECs

Although WEE1 had been shown to be important in HUVEC proliferation as a first step it was crucial to determine the importance of WEE1 in CLMEC proliferation. CLMECs were transfected with pooled WEE1 siRNA and its effects on proliferation were measured with the Vybrant® DyeCycle™ Green proliferation assay. Knockdown of WEE1 by siRNA decreased WEE1 band intensity compared to non-transfected CLMECs and CLMECs transfected with scrambled siRNA (Figure 31a). Quantification of the WEE1 band intensity relative to the β -actin loading control revealed the expression of WEE1 to be 85% lower in CLMECs transfected with WEE1 siRNA compared to scrambled siRNA (Figure 31b). Proliferation was measured 48 hrs after transfection using the nuclear dye Vybrant® Green (Figure 31c). Knockdown of WEE1 inhibited proliferation by 41% compared to scrambled siRNA (Figure 31d).

The small molecule WEE1 inhibitor AZD1775 was tested against CLMECs for 48 hrs and cell proliferation was measured using a WST-1 assay. At 1 μ M, AZD1775 inhibited proliferation by 63% compared to vehicle control (Figure 32a). Concentration-response curves were created for AZD1775 in pooled LECs and CLMECs (Figure 32b). The calculated IC_{50} in CLMECs was 267 nM and this was significantly less than the IC_{50} in LECs, which was 414 nM (Figure 32c).

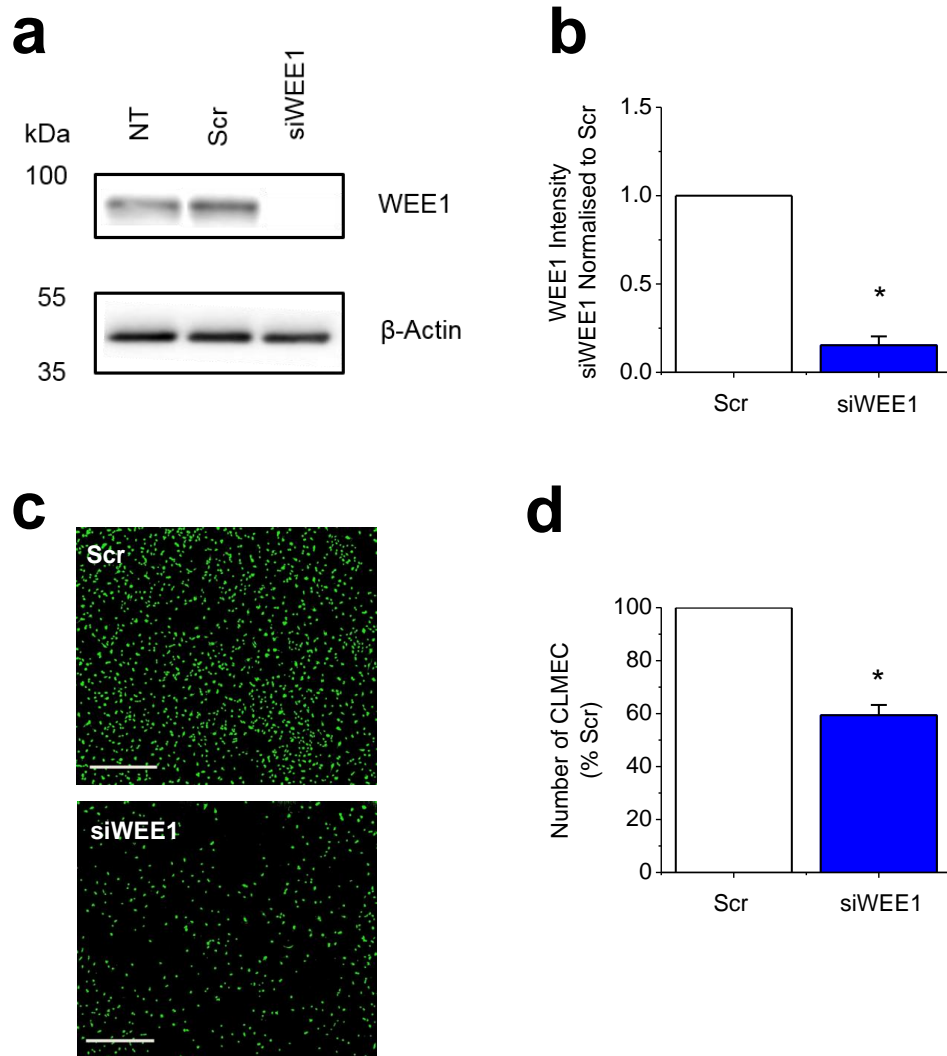


Figure 31 Genetic Inhibition of WEE1 Decreases Proliferation in CLMECs

a. Example western blot labelled with anti-WEE1 and anti- β -actin antibodies for non-transfected (NT) CLMECs and CLMECs transfected with scrambled siRNA (Scr) or ON-TARGETplus WEE1 siRNA (siWEE1) **b.** Quantification of the siWEE1 group WEE1 band intensity relative to β -actin and normalised to the Scr group (n=3 each) **c.** Fluorescence images of CLMECs 48 hrs after transfection with scrambled siRNA (Scr) or ON-TARGETplus WEE1 siRNA (siWEE1). Fluorescence was from cell nuclei stained with Vybrant[®] Dye Cycle[™] (green). Scale bars 400 μ m **d.** Quantification of the number of CLMECs seen in the images of the type shown in c. The siWEE1 group has been normalised to the Scr group (n=3, N=18).

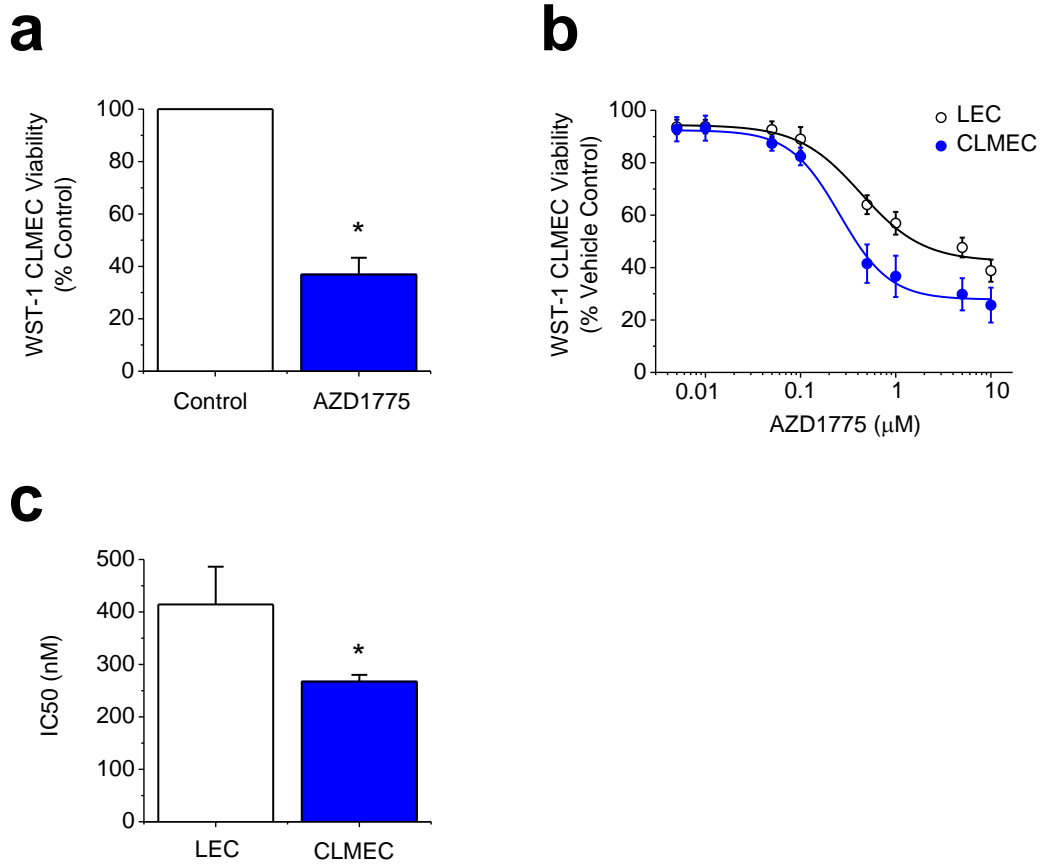


Figure 32 AZD1775 Inhibits CLMEC Proliferation

a. Mean data for CLMEC viability measured using WST-1 reagent after treatment with AZD1775 (1 μM) or vehicle control (Control) for 48 hrs (n=3, N=9) **b.** AZD1775 dose response curve in pooled LECs and CLMECs. LECs and CLMECs were treated with AZD1775 at the indicated concentrations for 48 hrs and plotted as percentages of the vehicle control (n=6, N=18 each) **c.** Mean data for the derived IC₅₀ values of AZD1775 against LECs and CLMECs.

4.2 AZD1775 Inhibits Angiogenic Processes in CLMECs

The process of angiogenesis is not only reliant upon the proliferation of endothelial cells, but also the ability of endothelial cells to migrate and form tube-like structures which will eventually become blood vessels.

To investigate the effects of AZD1775 on CLMEC migration a scratch wound was made in a confluent layer of CLMECs and the cells were subsequently imaged for 24 hrs as they migrated to close the wound (Figure 33a). Media contained low serum (0.2%) and high VEGF concentrations (20 ng.mL⁻¹) to simulate the tumour microenvironment, limit proliferation and ensure migration was the dominant process. The effects of AZD1775 (1 µM) upon CLMEC migration were evident from 4 hrs onwards (Figure 33b). At 24 hrs AZD1775 inhibited migration by 20% compared to vehicle control (Figure 33c).

To assess tube formation a fibroblast/CLMEC co-culture assay was developed. In this, CLMECs were plated onto a confluent layer of fibroblasts and after 5 days reliably grew into tube structures that could be detected with anti-CD31 staining (Figure 34a see *Control*). Treatment with AZD1775 (1 µM) profoundly inhibited tube formation compared to vehicle control (Figure 34a). Specifically, it inhibited the number of branch points, tube length and tube surface area (Figure 34b). The fibroblast bed appeared unaffected by the AZD1775 treatment (Figure 35a). In the absence of CLMECs, AZD1775 (1 µM) did not alter the number of fibroblasts after 5 days of treatment (Figure 35b).

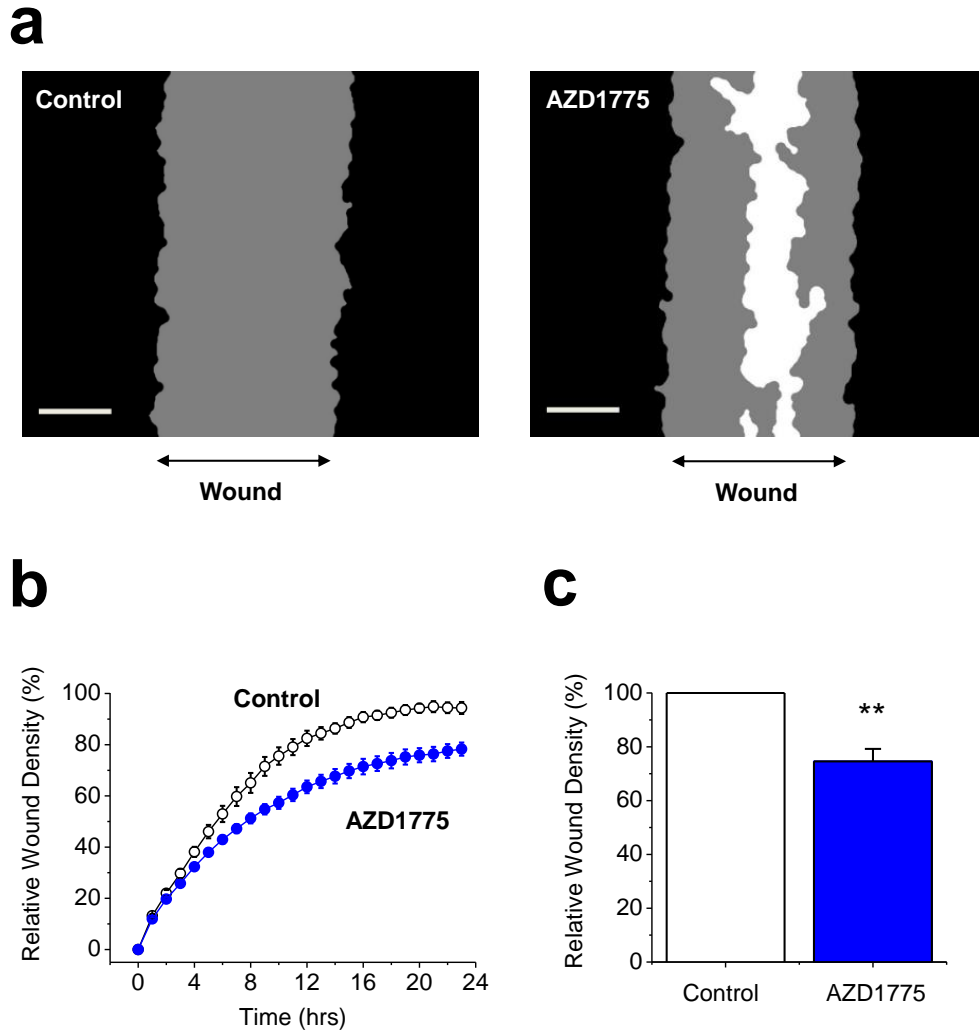
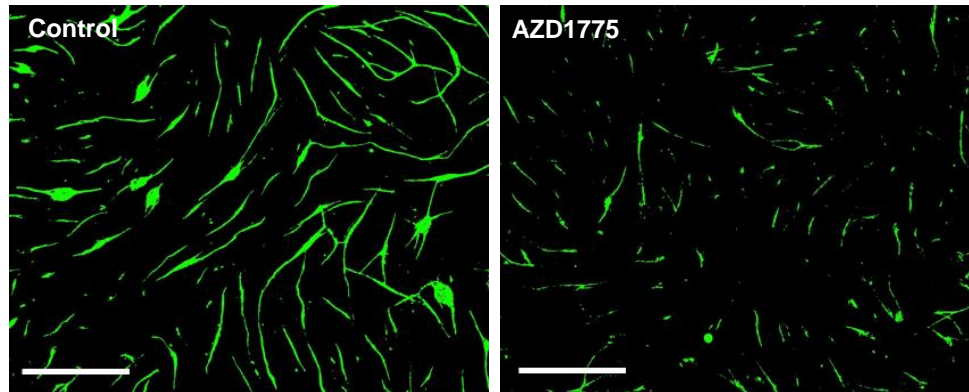


Figure 33 AZD1775 Inhibits CLMEC Migration

a. Example linear wound mask images after 24 hr CLMEC migration in vehicle control (Control) or 1 μ M AZD1775 treated cells. Black represents cells outside the linear wound, grey represents cells which have migrated into the wound, and white represents no cells. Scale bars 200 μ m **b.** Mean RWD at the indicated time points after AZD1775 (1 μ M) or vehicle control (Control) treatment (n=3 each) **c.** Relative wound density at 24 hrs in CLMECs treated with AZD1775 presented as a percentage of Control (n=3, N=9).

a



b

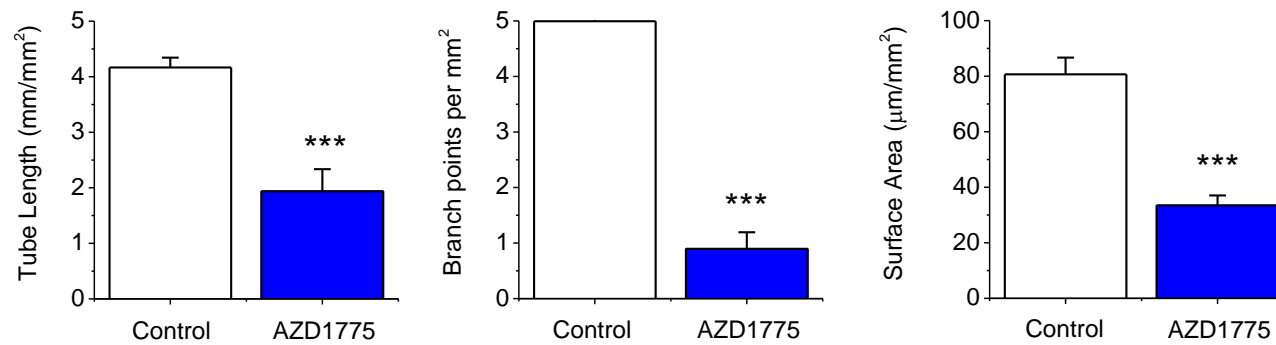
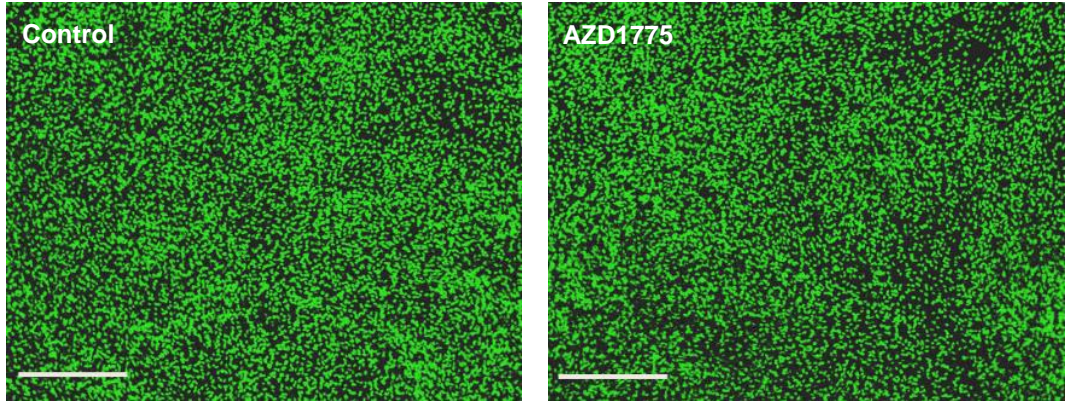


Figure 34 AZD1775 Inhibits CLMEC Tube Formation

a. Fluorescence images of anti-CD31-labelled CLMECs (green) in tube formation on a bed of fibroblasts (the fibroblasts are not visible in the images). The co-cultures were treated daily for 5 days with 1 µM AZD1775 or its vehicle control (Control). Scale bars 800 µm **b.** For experiments of the type exemplified in **a**, mean data for tube length, number of branch points and tube surface area (n=3, N=9)

a



b

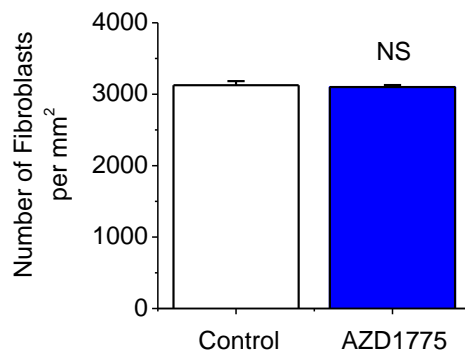


Figure 35 AZD1775 Does Not Affect Fibroblast Bed Integrity

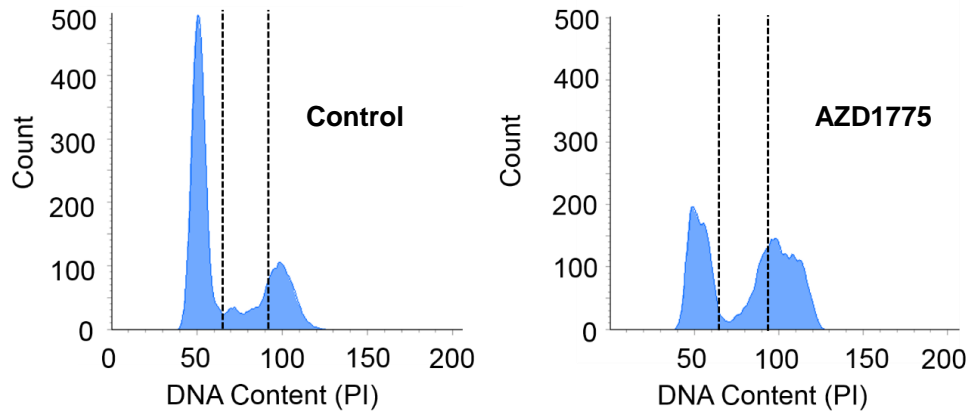
a. Fluorescence images of NHDF cells after 5 days treatment with AZD1775 (1 μ M) or its vehicle control (Control). Fluorescence was from cell nuclei stained with Vybrant[®] Dye Cycle[™] (green). Scale bars 400 μ m **b.** Quantification of the number of NHDF cells seen in the images of the type shown in a.

4.3 AZD1775 Changes the Cell Cycle Distribution in CLMECs as a Result of Altered CDK1 Phosphorylation

WEE1 (through CDK1) is known to regulate cell entry into mitosis and also regulate DNA synthesis. To determine what effect AZD1775 had on the cell cycle, CLMECs were treated for 24 hrs with AZD1775 or vehicle control and CLMEC DNA content was analysed by flow cytometry. CLMECs treated with vehicle control had a large peak at G0/G1 with relatively few cells in S phase and G2/M phase (Figure 36a). In contrast, treatment with AZD1775 (1 μ M) resulted in significantly more cells in S phase (40% vs 18.6%) and G2/M phase (30.6% vs 25.6%) (Figure 36b).

To confirm WEE1 inhibition was preventing CDK1 phosphorylation at Tyr15, western blotting was performed. Firstly an siRNA knockdown approach was used. In non-transfected CLMECs, western blotting for pCDK1-Y15 confirmed a single band 34 kDa in size. As expected, knockdown of WEE1 by pooled WEE1 siRNA decreased the single band intensity (Figure 37a). Total CDK1 content was unchanged. Quantification of the pCDK1-Y15 to CDK1 ratio revealed pCDK1-Y15 expression to be reduced in the siWEE1 group compared to scrambled group by 89% (Figure 37b). A similar effect was observed when treating CLMECs with AZD1775. AZD1775 reduced pCDK1-Y15 but not overall CDK1 band intensity (Figure 37c). Quantification of the pCDK1-Y15 to CDK1 ratio showed pCDK1-Y15 expression to be reduced with AZD1775 treatment by 89% compared to vehicle control (Figure 37d).

a



b

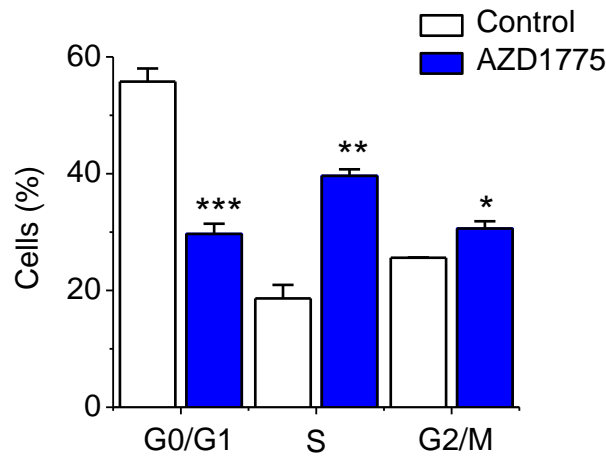


Figure 36 AZD1775 Increases the Number of CLMECs in S Phase and G2/M Phase

a. Example flow cytometry recording for CLMECs 24 hr after treatment with 1 μ M AZD1775 or its vehicle control (Control). The vertical dotted lines separate different phases of the cell cycle **b.** Mean percentage of cells in G0/G1, S and G2/M phases (n=3 each). AZD1775 data are statistically compared with Control data for each phase. * (p<0.05), ** (p<0.01) and *** (p<0.001).

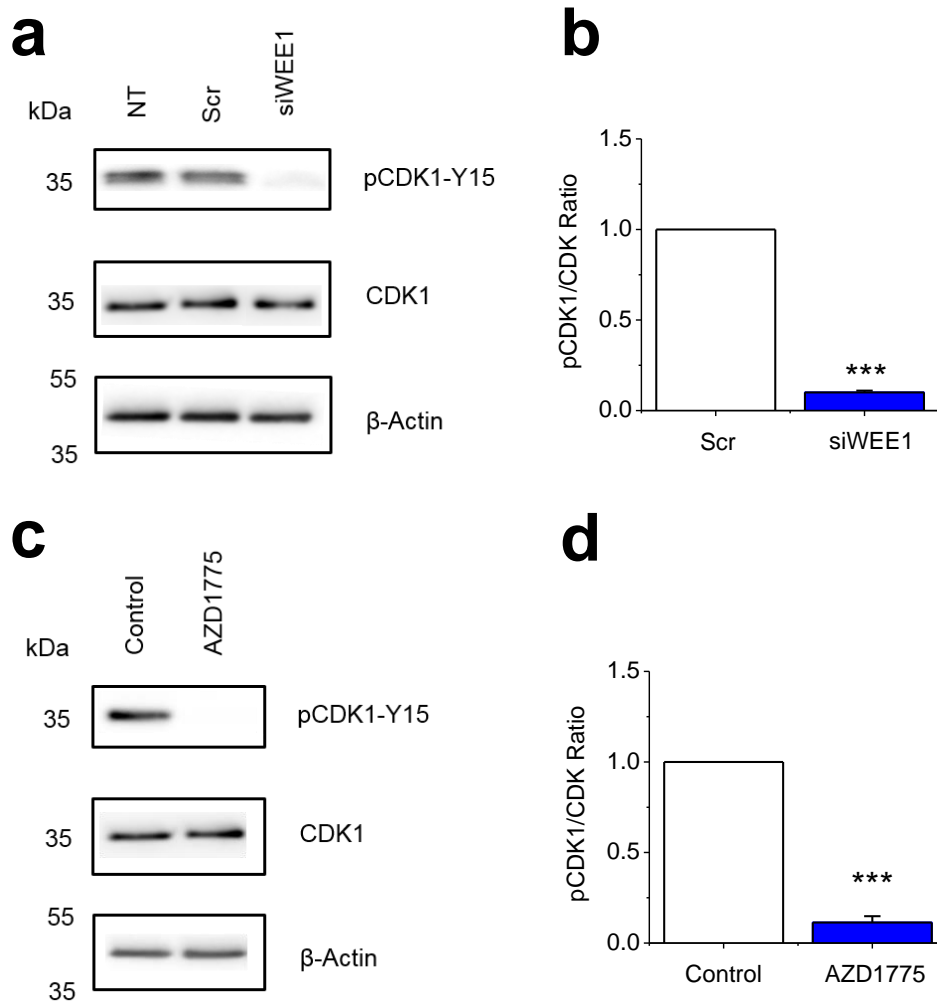


Figure 37 Genetic and Chemical Inhibition of WEE1 Decreases pCDK1-Y15 in CLMECs

a. Example western blot labelled with anti-pCDK1-Y15, anti-CDK1 and anti- β -actin antibodies for non-transfected (NT) CLMECs and CLMECs transfected with scrambled siRNA (Scr) or ON-TARGETplus WEE1 siRNA (siWEE1) **b.** Quantification of the pCDK1-Y15 band intensity divided by the CDK1 band intensity. siWEE1 has been normalised to Scr (n=3 each) **c.** Example western blot labelled with anti-pCDK1-Y15, anti-CDK1 and anti- β -actin antibodies for CLMECs treated with AZD1775 (1 μ M) or its vehicle control (Control) for 24 hrs **d.** Quantification of the pCDK1-Y15 band intensity divided by the CDK1 band intensity. AZD1775 has been normalised to Control (n=3 each).

4.4 AZD1775 Induces DS-DNA Breaks in CLMECs

Studies in cancer cell lines have shown that AZD1775 monotherapy is able to induce DS-DNA breaks. To investigate if the same mechanism of action was occurring in CLMECs, cells were treated with AZD1775 (1 μ M) or its vehicle control for 24 hrs and levels of γ H2AX were measured by western blot and flow cytometry.

In AZD1775 treated CLMECs, western blotting revealed a single band 15 kDa in size consistent with γ H2AX expression (Figure 38a). In contrast, vehicle control treated CLMECs expressed minimal γ H2AX. Quantification of the γ H2AX band intensity relative to the β -actin band intensity revealed γ H2AX expression to be increased 14-fold in the AZD1775 treated cells compared to the vehicle control treated cells (Figure 38b).

To further validate these findings, flow cytometry was performed to measure the percentage of cells that expressed γ H2AX (Figure 38c). As with the western blotting data, relatively few vehicle control treated cells were positive for γ H2AX (0.2%). However, AZD1775 treatment resulted in significantly more CLMECs expressing γ H2AX (14%). Quantification of the flow cytometry data indicated a 70-fold increase in the amount of DS-DNA breaks with AZD1775 treatment (Figure 38d).

WEE1 also negatively regulates mitotic entry, therefore levels of mitosis were analysed after 24 hrs of AZD1775 treatment using the specific mitotic marker pHH3 (Figure 39a). Surprisingly, levels of mitosis were lower in the treatment group after 24 hrs treatment. In the control group relatively few cells were positive for pHH3 (0.6%) and with AZD1775 treatment even fewer were positive (0.05%) (Figure 39b).

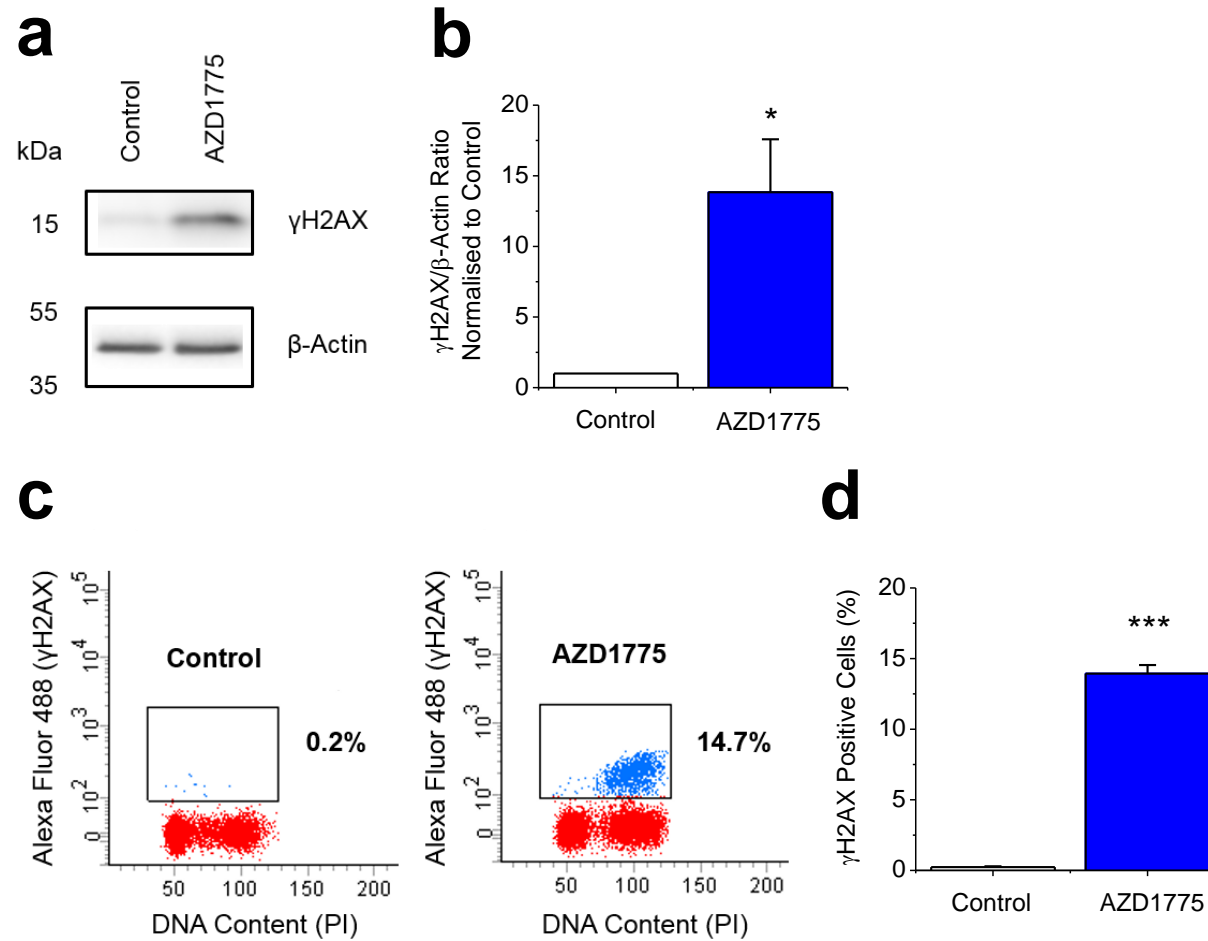


Figure 38 AZD1775 Induces DS-DNA Breaks in CLMECs

a. Example western blot labelled with anti- γ H2AX and anti- β -actin antibodies for CLMECs treated with AZD1775 (1 μ M) or its vehicle control (Control) for 24 hrs **b.** Quantification of the γ H2AX band intensity divided by the β -actin band intensity. AZD1775 has been normalised to Control (n=3 each) **c.** Example flow cytometry dot plots for unlabelled CLMECs (red) and CLMECs labelled with anti- γ H2AX antibody (blue) after 24 hrs treatment with AZD1775 (1 μ M) or its vehicle control (Control) **d.** Mean data for the groups in c (n=3 each).

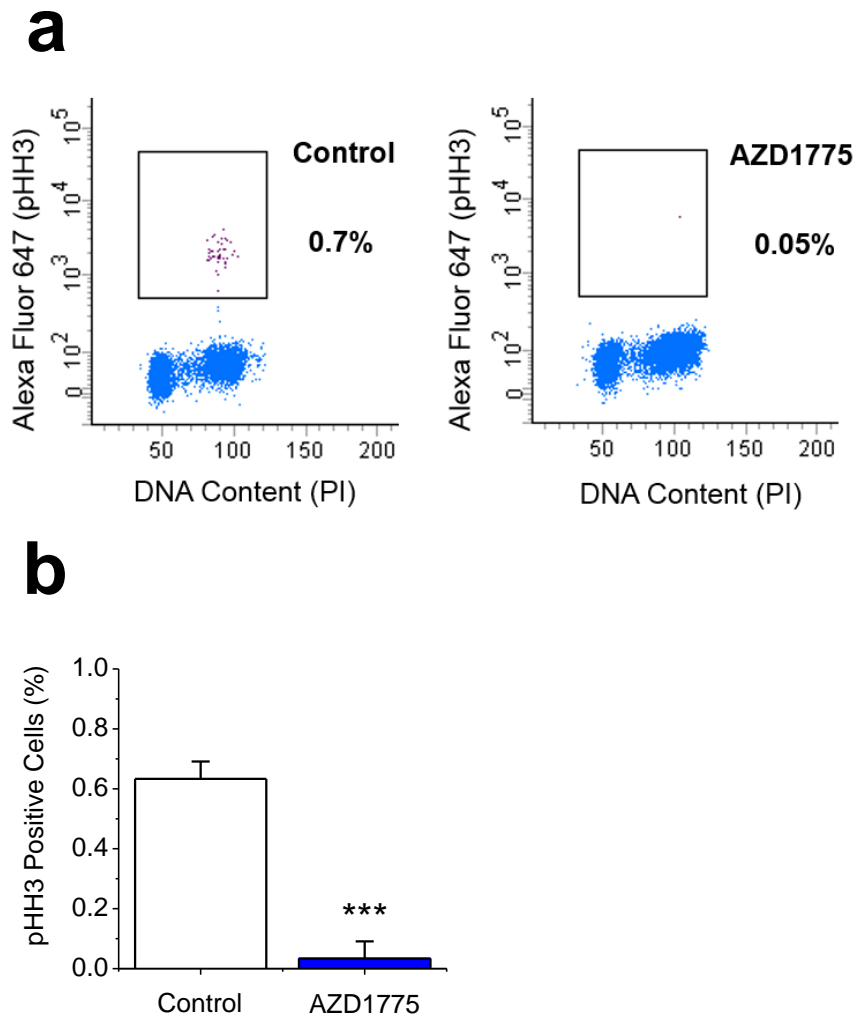


Figure 39 AZD1775 Does Not Increase Mitosis in CLMECs

a. Example flow cytometry dot plots for unlabelled CLMECs (blue) and CLMECs labelled with anti-pHH3 antibody (purple) after 24 hrs treatment with AZD1775 (1 μ M) or its vehicle control (Control) **b.** Mean data for the groups in a (n=3 each).

4.5 AZD1775 Induced DS-DNA Breaks in CLMECs can be Prevented if Co-Treated with RO-3306 or Exogenous Nucleosides

CDK1 regulates origin firing, allowing DNA to be synthesised in a co-ordinated fashion. WEE1 inhibition results in increased CDK1 activity, causing excessive origin firing and ultimately leading to DS-DNA breaks due to nucleotide depletion. To confirm this was occurring in CLMECs treated with AZD1775, the pathway was manipulated at two separate points in an attempt to prevent AZD1775 induced DS-DNA breaks. Firstly RO-3306, a CDK1 inhibitor, was tested in combination with AZD1775 (Figure 40a). After 24 hrs of AZD1775 monotherapy (1 μ M) 12.7% of CLMECs expressed γ H2AX, whereas with RO-3306 monotherapy (10 μ M) only 0.1% of CLMECs expressed γ H2AX. When the treatments were combined, the AZD1775 induced DS-DNA breaks were prevented with only 0.3% of CLMECs expressing γ H2AX (Figure 40b). Combination treatment with a lower dose of RO-3306 (1 μ M) did not fully prevent AZD1775 induced DS-DNA breaks with 8.4% of CLMECs expressing γ H2AX.

In an attempt to prevent AZD1775 induced nucleotide depletion CLMECs treated with AZD1775 were supplemented with exogenous nucleosides (Figure 41a). Nucleosides were used as charged nucleotides cannot readily cross the plasma membrane. Addition of nucleosides to AZD1775 reduced the number of CLMECs expressing γ H2AX from 14.6% to 0.4% (Figure 41b).

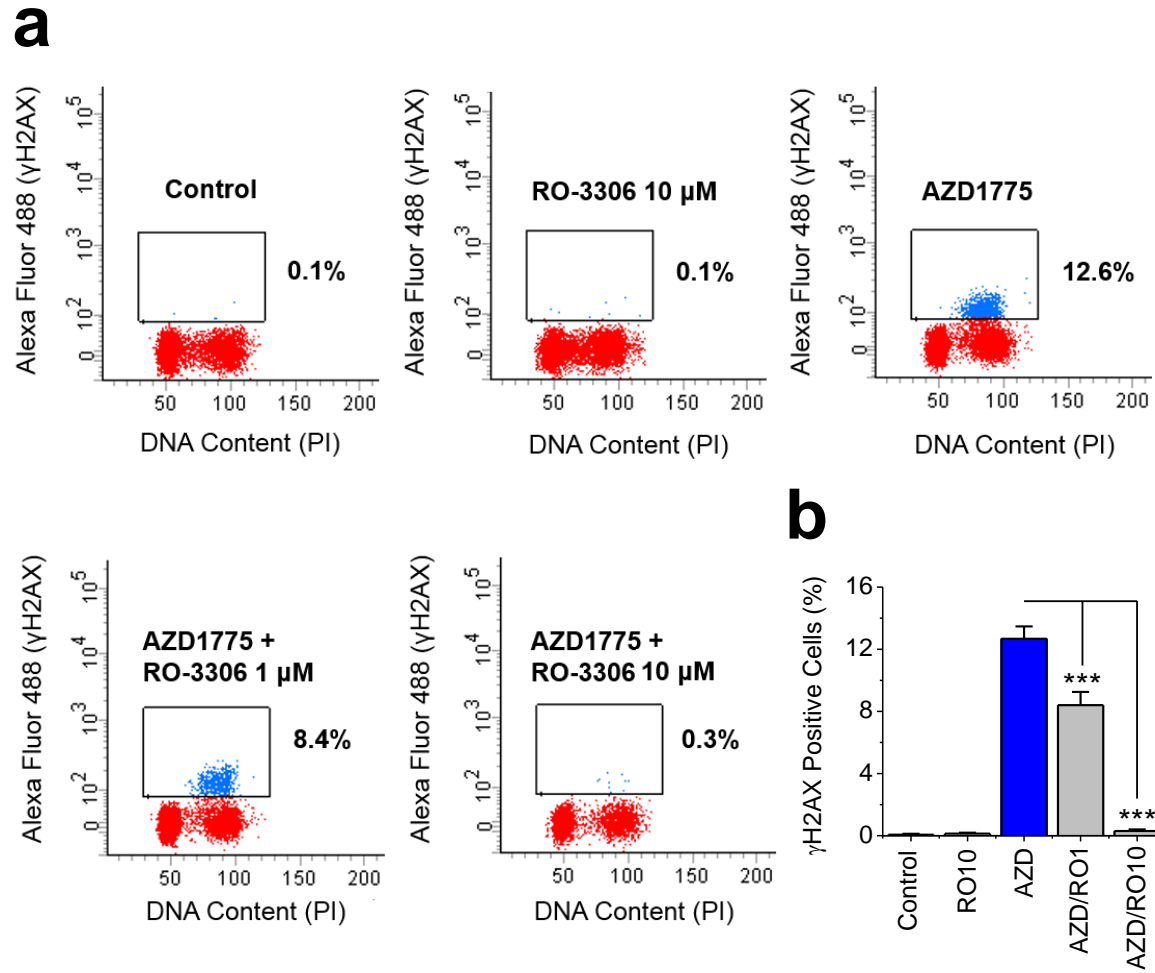


Figure 40 AZD1775 Induced DS-DNA Breaks in CLMECs Can be Prevented if Co-treated with RO-3306

a. Five example flow cytometry dot plots for unlabelled CLMECs (red) and CLMECs labelled with anti- γ H2AX antibody (blue). The five conditions were vehicle control (Control), 10 μ M RO-3306, 1 μ M AZD1775, 1 μ M AZD1775 + 1 μ M RO-3306, and 1 μ M AZD1775 + 10 μ M RO-3306 **b.** Mean data for the five groups in a (n=3 each).

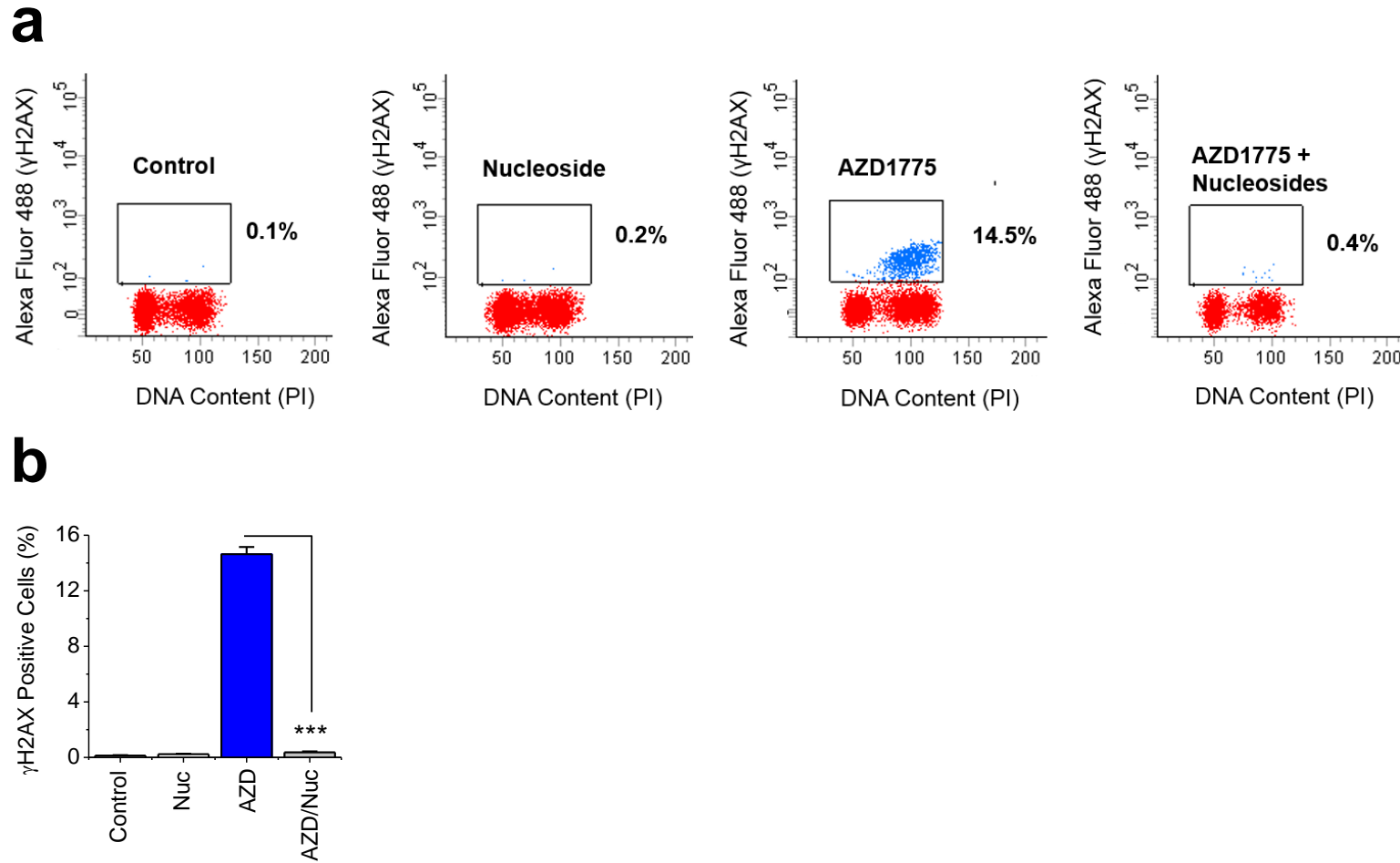


Figure 41 AZD1775 Induced DS-DNA Breaks in CLMECs Can be Prevented if Co-treated with Exogenous Nucleoside Addition

a. Four example flow cytometry dot plots for unlabelled CLMECs (red) and CLMECs labelled with anti- γ H2AX antibody (blue). The four conditions were vehicle control (Control), exogenous nucleosides (Nucleoside) (EmbryoMax[®], 1:5 dilution), 1 μ M AZD1775 and 1 μ M AZD1775 + exogenous nucleosides (Nuc) (EmbryoMax[®], 1:5 dilution) **b.** Mean data for the four groups in a (n=3 each).

4.6 AZD1775 Causes Caspase-3 Dependent Apoptosis in CLMECs which can be Rescued with Exogenous Nucleoside Supplementation

A potential consequence of DS-DNA breaks is increased apoptosis, therefore levels of caspase-3-dependent apoptosis were investigated using a NucView™ 488 Caspase-3 assay. At 24 hrs, levels of apoptosis were very low (0.4%) in vehicle control treated CLMECs (Figure 42a). Treatment with AZD1775 resulted in 10.4% of cells undergoing apoptosis, a 20-fold increase compared to vehicle control treated cells. An increase in apoptosis was evident from 8hrs after treatment and continued to increase up to the end of the experiment at 24 hrs (Figure 42b). As exogenous nucleoside supplementation was able to prevent AZD1775-induced DS-DNA breaks, they were also tested to see if they could prevent apoptotic cell death. Co-treatment with exogenous nucleosides significantly reduced the percentage of Caspase-3 positive cells from 10.4% to 2.6% (Figure 42c).

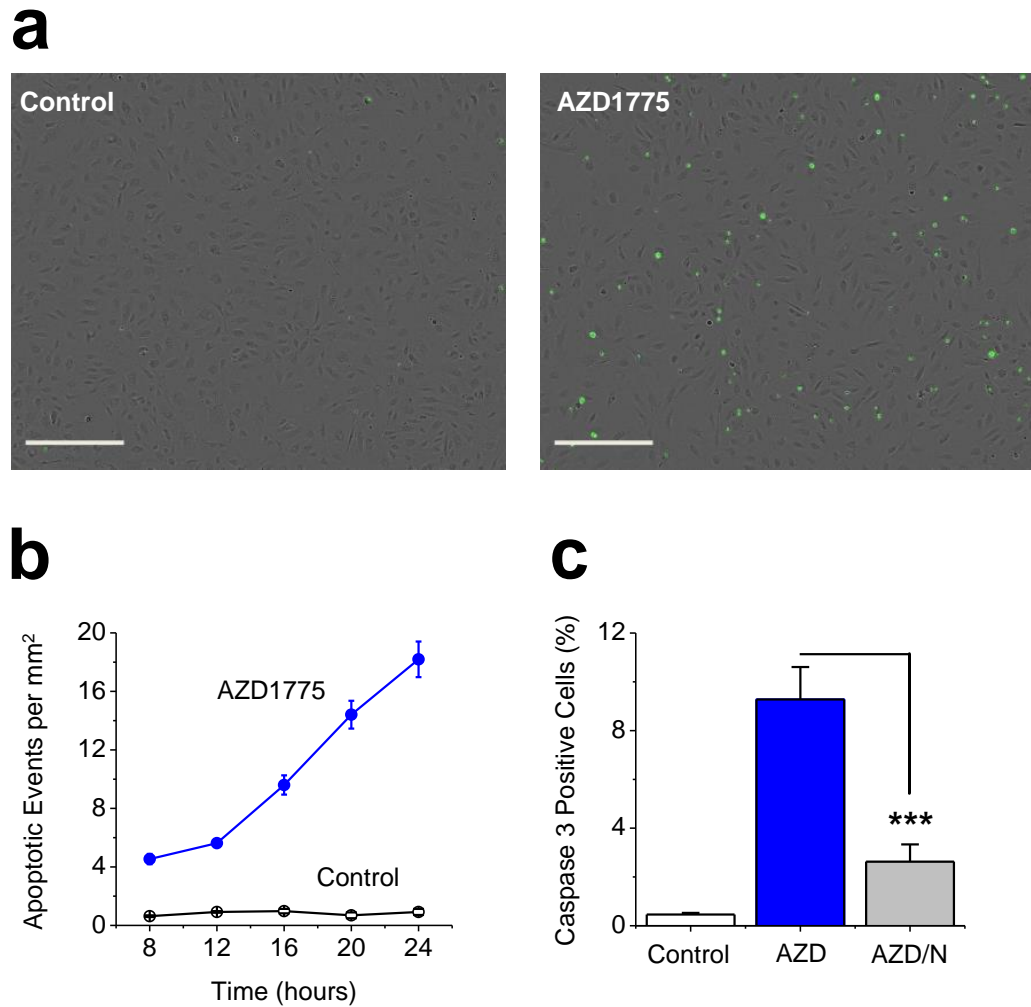


Figure 42 AZD1775 Causes Caspase-3 Dependent Apoptosis in CLMECs

a. Images of fluorescence from caspase-3 activity indicator in CLMECs 24 hrs after treatment with AZD1775 (1 μ M) or its vehicle control (Control). Scale bar 200 μ m **b.** Mean number of caspase-3 positive CLMECs per mm² at the indicated time points after AZD1775 treatment or vehicle control (Control) (n=3 each) **c.** Mean data for experiments of the type shown in a after 24 hr treatment and including a 1 μ M AZD1775 + exogenous nucleoside group (AZD/N) (EmbryoMax[®], 1:5 dilution) (n=3 each).

4.7 Summary of Findings

- Genetic and chemical inhibition of WEE1 inhibits proliferation in CLMECs
- AZD1775 inhibits proliferation in CLMECs with an IC_{50} of 267 nM, significantly less than in LECs
- AZD1775 inhibits CLMEC migration
- AZD1775 inhibits CLMEC tube formation, specifically, tube length, tube surface area and number of branching points.
- WEE1 inhibition decreases pCDK1-Y15 and causes an increase in cells in S Phase and G2/M phase
- AZD1775 induces a 70-fold increase in DS-DNA breaks in CLMECs, which can be rescued if co-treated with RO-3306 or exogenous nucleosides
- AZD1775-induced DS-DNA breaks lead to a 20-fold increase in caspase-3 dependent apoptosis in CLMECs
- AZD1775-induced apoptosis can be rescued if co-treated with exogenous nucleosides

4.8 Discussion

The aim of this chapter was to determine if WEE1 inhibition has anti-angiogenic activity in CLMECs and identify the mechanism underlying these effects. Both AZD1775 and pooled WEE1 siRNA decreased CDK1 phosphorylation at Tyr15 and inhibited CLMEC proliferation. AZD1775 also inhibited other angiogenic processes including CLMEC migration and tube formation. Investigation of the underlying mechanism revealed that AZD1775 was able to induce DS-DNA breaks that lead to caspase-3 dependent apoptosis. Supplementation of CLMECs with exogenous nucleosides rescued DS-DNA breaks and caspase-3 dependent apoptosis induced by AZD1775.

4.8.1 Functional Importance of WEE1 in CLMECs

Tumour angiogenesis is a complex process. For over thirty years sprouting angiogenesis was thought to be the exclusive method of tumour vascularisation. However, the last decade has revealed a number of other important mechanisms including intussusceptive angiogenesis, vessel co-option and vasculogenic mimicry, all of which have made anti-angiogenic treatment strategies more complex than initially thought. Nevertheless, sprouting angiogenesis and VEGF signalling has formed the basis for most tumour angiogenesis research. This has led to the first set of licensed anti-angiogenic therapies which attempt to disrupt VEGF-VEGFR-2 signalling. Sprouting angiogenesis is a complex process that requires endothelial cells to proliferate, migrate and form vessels. AZD1775 was able to inhibit all of these processes and had a particularly striking effect on the ability of tubes to branch, which was reduced by 83% compared to vehicle control. This reduced ability to form branching vessels would restrict the ability of CLM to recruit blood vessels required for growth and survival.

WEE1 protein expression was upregulated in CLMECs compared to LECs. This in itself suggests WEE1 may be important for CLMEC survival. As previously discussed, increased expression of WEE1 may protect CLMECs from DNA-damage and cell death, not only because of its role in controlling DNA repair and mitotic entry, but in ensuring DNA is synthesised in a controlled and co-ordinated manner. Further evidence of the functional importance of WEE1 in CLMECs is illustrated by the lower IC₅₀ value for AZD1775 compared to LECs. Increased sensitivity to AZD1775 infers that CLMECs are more reliant on WEE1 for normal proliferation and survival. Being cancerous in nature, CLMECs may already harbour more DNA damage than LECs and are therefore already more reliant on DNA repair mechanisms. This means a relatively smaller disruption to these DNA repair mechanisms (such as WEE1 inhibition) will result in a relatively greater amount of DNA damage and cell death.

4.8.2 In Vitro Angiogenesis Assays

Assays that stimulate the formation of capillary-like tubules represent the latter stages of angiogenesis and are used extensively to assess novel compounds for pro- or anti-angiogenic activity (Staton et al., 2009). A number of in vitro assays exist and the most basic form involves plating endothelial cells onto a gel matrix such as collagen, fibrin or Matrigel®. Matrigel® causes endothelial cells to differentiate and form capillary-like tubules, although researchers debate as to whether these structures possess lumens or not (Bikfalvi et al., 1991, Grant et al., 1991).

Another method, which was used in this chapter, involves the co-culture of endothelial cells with fibroblasts. The fibroblasts secrete matrix components which

act as a scaffold enabling tube formation. These tubes contain lumens and are heterogeneous in length, more closely resembling capillary beds in vivo (Donovan et al., 2001). Excellent results were achieved using this technique and it is believed that this is the first time this technique has been performed using isolated human tumour endothelial cells. A number of computed modalities were measured (tube length, tube surface area, number of branching points) which eliminated any possibility of human error or bias. AZD1775 significantly inhibited all of these parameters providing strong evidence that it can work as an anti-angiogenic agent. The technique is not without its limitations however. Firstly it is very time consuming, with each assay taking two weeks to perform. Secondly it is not clear what the fibroblasts secrete in their matrix as this has yet to be characterised. Finally, for this assay, normal human dermal fibroblasts were used (non-cancerous cell line) which may not truly reflect what is occurring in tumour angiogenesis. The assay was attempted with tumour fibroblasts also isolated from the patient samples, however these failed to grow into a confluent monolayer, which is necessary for the endothelial cells to form tubes. One potential concern was that AZD1775 could cause cell death in the fibroblast monolayer which is in turn affecting the ability of tubes to form. However, this was ruled out, as five-days treatment of the confluent fibroblast monolayer with AZD1775 resulted in no change in fibroblast cell number.

The next step would be to evaluate AZD1775 in in vivo angiogenesis assays. A number of these exists, each with its own inherent advantages and disadvantages. Commonly used assays include the corneal angiogenesis assay and the chick chorioallantoic membrane assay. Although the anti-angiogenic effects of AZD1775 were not tested in vivo, the in vitro assay worked well and provided strong evidence that WEE1 is necessary for successful tube formation.

4.8.3 Mechanism of Action of WEE1 Inhibition

Work in this chapter has proposed a mechanism by which up-regulated WEE1 in CLMECs could facilitate CLM progression by protecting CLMECs against caspase-3 dependent apoptosis which would otherwise restrict tube formation.

Single agent AZD1775 significantly inhibited CLMEC proliferation and to understand its mechanism of action, WEE1 inhibition in cancer cell studies were reviewed. A number of studies have shown that single agent AZD1775 can inhibit cancer cell proliferation (Kreahling et al., 2012, Guertin et al., 2013, Do et al., 2015, Pfister et al., 2015). In these studies, the activity of AZD1775 has been attributed to its ability to increase CDK1 activity, which is critical for DNA synthesis. WEE1 normally causes an inhibitory phosphorylation of CDK1 at Tyr15. Both AZD1775 and pooled siRNA targeted against WEE1 were able to abolish this inhibitory phosphorylation of CDK1, a finding which is supported in multiple other cell lines (PosthumaDeBoer et al., 2011, Rajeshkumar et al., 2011, Sarcar et al., 2011). CDK1 has two key roles, regulation of origin firing during DNA synthesis and regulation of mitotic entry. The former has been shown to be the key mechanism of action for single agent activity (Beck et al., 2012, Pfister et al., 2015). Excess origin firing culminates in DS-DNA breaks as replication forks stall due to a critical nucleotide shortage. DS-DNA breaks were detectable in CLMECs by measuring levels of γ H2AX through western blotting and flow cytometry. After 24 hrs treatment 14% of CLMECs were positive for γ H2AX compared to 0.2% in the control group with flow cytometry. Although 14% seems like a relatively small amount, it is a 70-fold increase compared to the control group. By comparison, at IC₉₀ concentrations, AZD1775 reportedly caused a 28-fold, 53-fold and 77-fold increase in γ H2AX expression in A2058 lung cancer cells, LoVo colorectal cancer cells and HT29

colorectal cancer cells respectively (Guertin et al., 2013). AZD1775 treatment resulted in apoptotic cell death as determined by measuring levels of caspase-3. With AZD1775 treatment 10.4% of CLMECs were positive for caspase 3, compared to 0.4% in the control group. This suggests that not all CLMECs that sustain DS-DNA breaks undergo apoptosis and that CLMECs may be able to repair some of the DNA damage. Alternatively, the 3.6% difference may indicate the delay between the cell sustaining DS-DNA breaks and the initiation of apoptosis.

Several experiments in this chapter support the hypothesis that the dominant mechanism of action for AZD1775 is through its ability to induce DS-DNA breaks and not premature mitosis. Firstly, when levels of mitosis were measured at 24 hrs they were significantly lower in the AZD1775 treatment group. It may well be that AZD1775 forces cells into mitosis relatively quickly (eg. after 8 hrs) and that by 24 hrs most cells have actually completed mitosis, meaning pHH3 levels are low. However, the CLMEC apoptosis time course showed a linear increase. If early premature mitosis was the dominant mechanism of action an early peak in apoptotic cell death would be expected. The linear increase in apoptotic cell death better reflects accumulating DNA-damage as stalling replication forks lead to DS-DNA breaks. Secondly, supplementation of CLMECs with exogenous nucleosides reversed the AZD1775-induced DS-DNA break levels nearly back to those of the control group. Nucleosides were used because charged nucleotides cannot cross the cell membrane easily. The dose used was based upon reports from previous studies (Beck et al., 2012, Cuneo et al., 2016). Exogenous nucleoside addition also reversed the AZD1775-induced apoptosis levels nearly back to those of the control group. The rescue was not 100%, for either the DS-DNA breaks or caspase-3 dependent apoptosis and may reflect the fact that not enough nucleosides were added. This was difficult to gauge as the measurement of nucleotides is extremely

challenging, with limited techniques available. Other studies have reported difficulty in obtaining a 100% rescue with nucleoside addition (Beck et al., 2012). The supplementation of nucleosides should have no impact upon the toxicity of premature mitosis and therefore by observing a rescue effect this provides further evidence that DS-DNA breaks are the dominant mechanism of action.

RO-3306, a CDK1 inhibitor, was also able to reverse the AZD1775-induced DS-DNA breaks when used at 10 μ M. This dose was used based upon reports from previous studies (Beck et al., 2012). RO-3306 was not used to rescue apoptosis, because CDK1 is relevant to both mechanisms of action and therefore if it did rescue apoptosis it would be unclear if this was because of CDK1 causing DS-DNA breaks or CDK1 causing premature mitosis.

Another possibility is that AZD1775 could be causing both mechanisms of action to work together synergistically. For instance, it could induce DS-DNA breaks in cells and force them into mitosis prematurely resulting in mitotic catastrophe. This could explain why a 100% rescue with exogenous nucleoside addition was not fully possible. However, providing evidence that both these mechanisms were working synergistically would be extremely difficult.

4.8.4 Implications of AZD1775 as an Anti-Angiogenic Drug

WEE1 inhibition has clear anti-angiogenic effects, but what are the potential consequences of using AZD1775 as an anti-angiogenic agent for CLM clinically? Endothelial cells line vessels throughout the body and are pivotal both in health and disease. The relative functional importance of WEE1 inhibition in these contexts is

unknown. Substantial impact upon physiological blood vessels does however seem unlikely because these endothelial cells are normally quiescent. AZD1775 causes DS-DNA breaks in cells that are in the cell cycle and actively replicating (S phase). Results from Phase I clinical trials report no serious vascular complications (Do et al., 2015), however this does not mean that such complications are lacking. Furthermore, not all endothelial cells are quiescent. Physiological angiogenesis occurs in adult life, for instance in the cycling ovary and pregnancy (Carmeliet, 2005). Very relevant to the surgical patient would be the impact of AZD1775 upon angiogenesis required for wound healing after surgery. Designers of future clinical trials involving AZD1775 should include assessments of wound-healing and cardiovascular parameters including those relating to the risk of atherosclerotic disease. However, it is important to note that these concerns will be common amongst any anti-angiogenic agent and current anti-angiogenic agents such as bevacizumab have been used safely in patients. If AZD1775 were to cause systemic problems, techniques to deliver therapy locally, such as HIA infusion could always be considered.

Sustained angiogenesis is one of the six hallmarks of cancer (Hanahan and Weinberg, 2000). It is generally accepted that once tumours grow beyond 1-2 mm³ in size they are reliant upon angiogenesis to provide oxygen and nutrients to meet their increased metabolic demand. Therefore, AZD1775 could be used to treat not only CLM, but all vascularised tumours. The significance of WEE1 in specific vascular tumours such as hemangiomas, hemangioendotheliomas, Kaposi sarcoma, or angiosarcomas is unknown. Anti-angiogenic agents have been used for cancers other than metastatic colorectal cancer. For instance in the US, bevacizumab is also licensed for the treatment of glioblastoma, non-small cell lung cancer and metastatic renal cancer. Sorafenib (Nexvar[®]) is a multi-targeted VEGF

receptor tyrosine kinase inhibitor and is licensed for the treatment of hepatocellular carcinoma and renal cancer. The results from this chapter could mean that AZD1775 could be used as an anti-angiogenic treatment for other types of cancer.

One key question is when exactly would AZD1775 be used in the colorectal cancer patient. It has previously been shown to have direct single agent anti-cancer activity in colorectal cancer cells in vivo (Guertin et al., 2013). It has been reported to improve the efficacy of DNA-damaging agents through premature mitosis (Hirai et al., 2009, Hirai et al., 2010) and in this chapter AZD1775 has also been shown to have anti-angiogenic activity in CLMECs. Therefore AZD1775 has at least three anti-cancer effects and the optimal time and duration to use the drug is difficult to predict. In an anti-angiogenic context, the logical conclusion would be to use AZD1775 in patients diagnosed with CLM to prevent their further growth. However, it could be argued that AZD1775 could be given after the resection of the patient's primary colorectal cancer to prevent metastatic spread.

Clinical trials using AZD1775 have not observed any anti-angiogenic efficacy, but equally they have not been designed to look for one. In current clinical trials, AZD1775 is used for short durations, usually 2-3 days with weekly intervals between each treatment cycle. For instance, in the Phase I single agent trial, AZD1775 was administered orally twice per day (225 mg) over 2.5 days per week for up to 2 weeks per 21-day cycle (Do et al., 2015). This dosing pattern may not be the most appropriate to observe anti-angiogenic activity. An excellent piece of research highlighting "anti-angiogenic scheduling" was published in 2000 and co-authored by Judith Folkmann (Browder et al., 2000). Historically, chemotherapy regimens have been scheduled on a maximum tolerated dose principle. This

schedule, which consists of the highest survivable (minimum lethal) dose, yielded a higher percentage cure rate in in vivo studies, however, such high doses require an extended treatment-free period to allow recovery of normal host cells, such as hematopoietic progenitor cells. Similar to hematopoietic progenitor cells, the tumour endothelial cells may also resume growth during this treatment-free period. Bowder et al., developed an anti-angiogenic schedule for cyclophosphamide dosed at shorter intervals without interruption. This schedule increased apoptosis of tumour endothelial cells and demonstrated long-term suppression of the growth of cyclophosphamide-resistant lung carcinoma and breast carcinoma models in vivo, significantly better than conventional scheduling. Other studies have also confirmed that extended low dose chemotherapy can target cycling endothelial cells (Bocci et al., 2002, Dreves et al., 2004). In this chapter, 5 days uninterrupted AZD1775 significantly inhibited CLMEC tube formation. Therefore, it could be hypothesised that to derive anti-angiogenic benefit clinically, AZD1775 should be dosed for prolonged intervals to prevent tumour endothelial cell recovery. Dosing of AZD1775 in current clinical trials therefore is likely not optimal for anti-angiogenic activity.

Assessing the anti-angiogenic activity of AZD1775 in patients would be difficult as it has direct anti-tumour activity also. It would be difficult to ascertain if any effect on tumour growth was direct, anti-angiogenic or a combination of both. One possible way to determine this could be the generation of an in vivo murine model with an inducible, endothelial specific, WEE1 knockout. After the endothelial WEE1 knockout is induced, tumours could be implanted subcutaneously and allowed to grow. Any deficiency in tumour growth could then be attributed to the genetic inhibition of WEE1 in the endothelial cells. Although it does not specifically involve AZD1775 it would give important information about WEE1 inhibition.

4.8.5 Conclusion

WEE1 has been identified to be both upregulated in CLMECs and critical for their survival. Targeted inhibition of WEE1, with AZD1775, inhibits CLMEC proliferation, migration and tube formation, three processes which are essential for tumour angiogenesis. Treatment with AZD1775 causes a 70-fold increase in DS-DNA breaks in CLMECs which leads to caspase-3 dependent apoptosis because of a critical nucleotide shortage. As AZD1775 is currently under investigation in a number of oncological clinical trials, it is important to investigate its anti-angiogenic efficacy and possible complications that may consequently arise from this.

Chapter 5: AZD1775 Induces Toxicity Through DS-DNA Breaks Independently of Chemotherapeutic Agents in p53 Mutated Colorectal Cancer Cells

In Chapters 3 and 4 WEE1 has been identified as an anti-angiogenic target and the small molecule WEE1 inhibitor AZD1775 has been shown to have clear anti-angiogenic effects in CLMECs. This makes AZD1775 a promising anti-cancer agent which can target both cancer cells and the tumour vasculature. When administered as a monotherapy AZD1775 causes cytotoxicity by causing DS-DNA breaks as a result of excess origin firing and nucleotide shortage. This has been shown here in CLMECs and has also been reported in cancer cells (Guertin et al., 2013, Pfister et al., 2015, Do et al., 2015). However, in the majority of ongoing clinical trials using AZD1775 in combination with DNA-damaging agents, AZD1775 is thought to act by causing premature mitosis in cells with unrepaired DNA damage and not by its ability to induce DS-DNA breaks.

The lack of clarity regarding the dominant mechanism of action for AZD1775 when used in conjunction with DNA-damaging agents is the underlying rationale for this chapter. It is important to determine the main mechanism of action of AZD1775 to ensure an optimal, effective dosing strategy in humans, especially when trying to derive anti-angiogenic benefit. Another factor to consider is the p53 status of cancer cells as some studies have shown that AZD1775 in combination with DNA-damaging agents is only effective in p53-mutated cancer cells (Hirai et al., 2009, Hirai et al., 2010, Rajeshkumar et al., 2011), whereas other studies have shown efficacy independent of p53 status (Kreahling et al., 2012, Van Linden et al., 2013, Mueller et al., 2014). Whether or not AZD1775 increases the sensitivity of p53 deficient/mutant and wildtype cancer cells to DNA-damaging therapies remains one of the outstanding questions regarding AZD1775 therapy (Matheson et al., 2016).

Previous research assessing the mechanism of action of WEE1 inhibition as a treatment for colorectal cancer is conflicting. Evidence of WEE1 inhibition as a radio-sensitising treatment for colorectal cancer was first reported in 2001 (Wang et al., 2001). Irradiation of HT29 (p53 mutant) colorectal cancer cells with 7.5 Gy resulted in an increase in cells arrested at the G2/M checkpoint from 19% to 69%. After a subsequent 4 hrs of treatment with PD0166285 (a less specific WEE1 inhibitor) this was reduced to 37% and resulted in increased cell death. In 2009 Hirai et al., reported that AZD1775 enhanced the cytotoxicity of gemcitabine to treat p53 mutated WiDr colorectal cancer cells in vitro (Hirai et al., 2009). In vivo, AZD1775 (20 mg/kg) given orally 24 hrs following a bolus of gemcitabine (50 mg/kg) in nude rats bearing WiDr colorectal xenografts resulted in significantly reduced tumour growth compared to gemcitabine alone. Also, combination treatment allowed a lower dose of gemcitabine to be administered to obtain similar/improved anti-tumour effects. The following year the same group of authors investigated the ability of AZD1775 to sensitise colorectal cancer cell lines to different types of DNA damaging agents (Hirai et al., 2010). In vitro, AZD1775 enhanced cytotoxic killing of 5-FU in four p53-mutated colorectal cancer cell lines (WiDr, SW948, COLO205 and LS411N), but did not enhance 5-FU cytotoxicity in three p53 wildtype colorectal cancer cell lines (HCT116, COLO678, LS513). Also AZD1775 monotherapy up to 300 nM had no effect.

However, in 2013 evidence first emerged for AZD1775 having monotherapy efficacy against colorectal cancer cell lines (Guertin et al., 2013). In contrast to previous studies this was found to be independent of p53 status. AZD1775 was shown to inhibit proliferation in 66 different colorectal cancer cell lines, irrespective of p53 status, with IC₅₀ values ranging from 0.17 µM to 16.26 µM. In the LoVo and HT29 cell lines, 24 hr AZD1775 treatment induced significant DS-DNA breaks

compared to vehicle control. Only the HT29 cell population showed a significant increase in mitosis as well. In vivo, LoVo bearing xenograft CD-1 nu/nu mice treated with 60 mg/kg AZD1775 twice daily for 13 days had a 13% tumour growth inhibition compared to vehicle control. These results contradicted earlier studies where authors reported no monotherapeutic efficacy of AZD1775 in vivo (Hirai et al., 2009).

The aim of this chapter therefore was to determine the dominant mechanism of action of AZD1775 when used in combination with DNA-damaging agents. To study this, the HT29 colorectal cancer cell line was used which has a mutated non-functional p53 (Arg-273 to His). This meant that both premature mitosis and DS-DNA breaks were possible mechanisms of action.

5.1 AZD1775 Enhances 5-FU Toxicity in HT29 cells, but only Enhances Other Colorectal Cancer Chemotherapeutic Agents at Low Concentrations

In the majority of clinical trials AZD1775 is administered following DNA-damaging therapy in p53-mutated cells to cause mitotic catastrophe and cell death. To investigate the ability of AZD1775 to sensitise p53-mutated colorectal cancer cells to common chemotherapeutic agents (5-FU, irinotecan, oxaliplatin) the HT29 cell line was studied. Concentration-response curves were created by treating cells for 24 hrs with chemotherapy at a range of doses followed by either AZD1775 (300 nM) or vehicle control for a further 24 hrs. An AZD1775 dose of 300 nM was used based on the reports of previous studies (Hirai et al., 2009, Hirai et al., 2010).

5-FU alone had limited effects on HT29 cell viability (Figure 43a), but combination treatment with 300 nM AZD1775 significantly reduced the IC₅₀ from 9.3 µM to 3.5 µM (Figure 43b). When used in combination with oxaliplatin, AZD1775 decreased cell viability at lower doses of oxaliplatin, but not higher doses (Figure 43c). The IC₅₀ was significantly higher in combination treatment than oxaliplatin alone (Figure 43d). Similarly, with irinotecan and AZD1775 combination therapy cell viability was decreased at lower doses of irinotecan but not higher doses (Figure 43e). There was no significant difference in the IC₅₀ values (Figure 43f). Overall, these data suggest that 5-FU cytotoxicity is enhanced with AZD1775 treatment and both oxaliplatin and irinotecan treatments are only enhanced at lower doses.

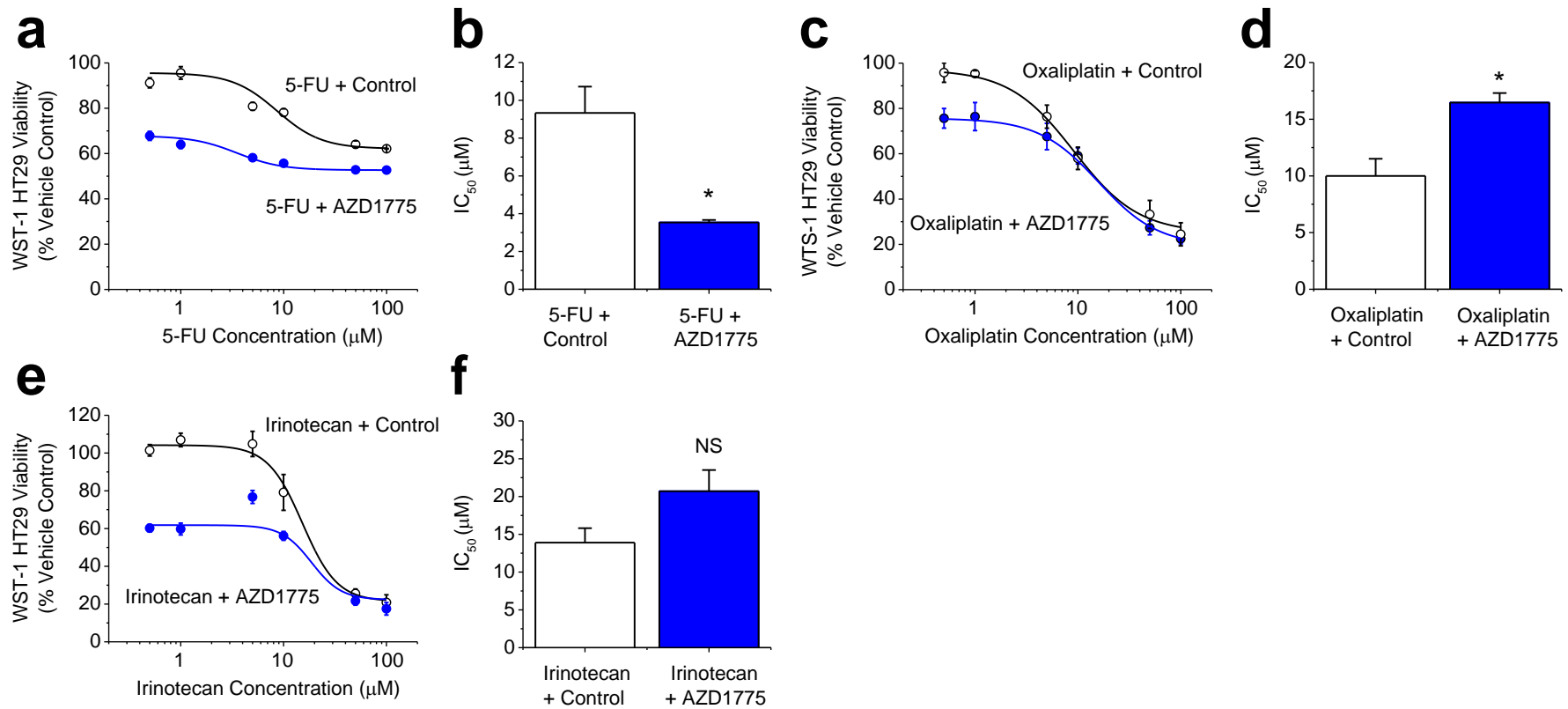


Figure 43 AZD1775 Enhances the Cytotoxicity of 5-FU

a. Dose response curves in HT29 cells for 5-FU with AZD1775 (300 nM) or vehicle control (Control) **b.** Mean data for the derived IC_{50} values for the experiments exemplified in a (n=3, N=9 each condition) **c.** Dose response curves in HT29 cells for oxaliplatin with AZD1775 (300 nM) or vehicle control (Control) **d.** Mean data for the derived IC_{50} values for the experiments exemplified in c (n=3, N=9 each condition) **e.** Dose response curves in HT29 cells for irinotecan with AZD1775 (300 nM) or vehicle control (Control) **d.** Mean data for the derived IC_{50} values for the experiments exemplified in e (n=3, N=9 each condition)

5.2 AZD1775 Decreases pCKD1-Y15 in 5-FU Treated HT29 Cells and Increases the Number of Cells in S Phase and G2/M Phase

To further investigate if a true chemo-sensitisation effect existed subsequent experiments were focused on 5-FU and AZD1775 combination treatment. A dose of 1 μ M 5-FU and 300 nM AZD1775 was studied as this resulted in a large reduction in HT29 viability compared to 5-FU alone. Initially western blotting was performed to ensure AZD1775 was modulating its target, pCDK1-Y15. Combination treatment significantly reduced the pCDK1-Y15 band intensity compared to 5-FU alone (Figure 44a). Quantification of the pCDK1-Y15 band intensity relative to the CDK1 band intensity revealed the expression of pCDK1-Y15 to be 89% lower with combination treatment (Figure 44b). Combination therapy also grossly altered the cell cycle distribution (Figure 45a). The addition of AZD1775 (300 nM) significantly increased the percentage of cells in S phase (40.8% vs 55.7%) and G2/M phase (19.4 vs 35.2%) (Figure 45b).

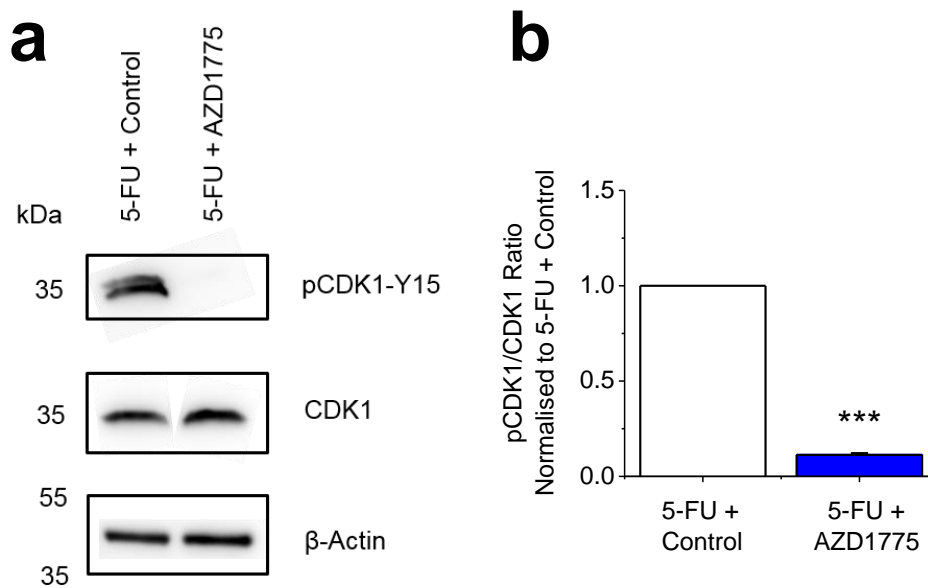


Figure 44 Combination Therapy Decreases pCDK1-Y15 compared to 5-FU Treatment Alone

a. Example western blot labelled with anti-pCDK1-Y15, anti-CDK1 and anti- β -actin antibodies for HT29 cells treated for 24 hrs with 5-FU (1 μ M) and then an additional 24 hrs AZD1775 (300 nM) or vehicle control (Control) **b.** Quantification of the pCDK1-Y15 band intensity divided by the CDK1 band intensity. 5-FU + AZD1775 has been normalised to 5-FU + Control (n=3 each).

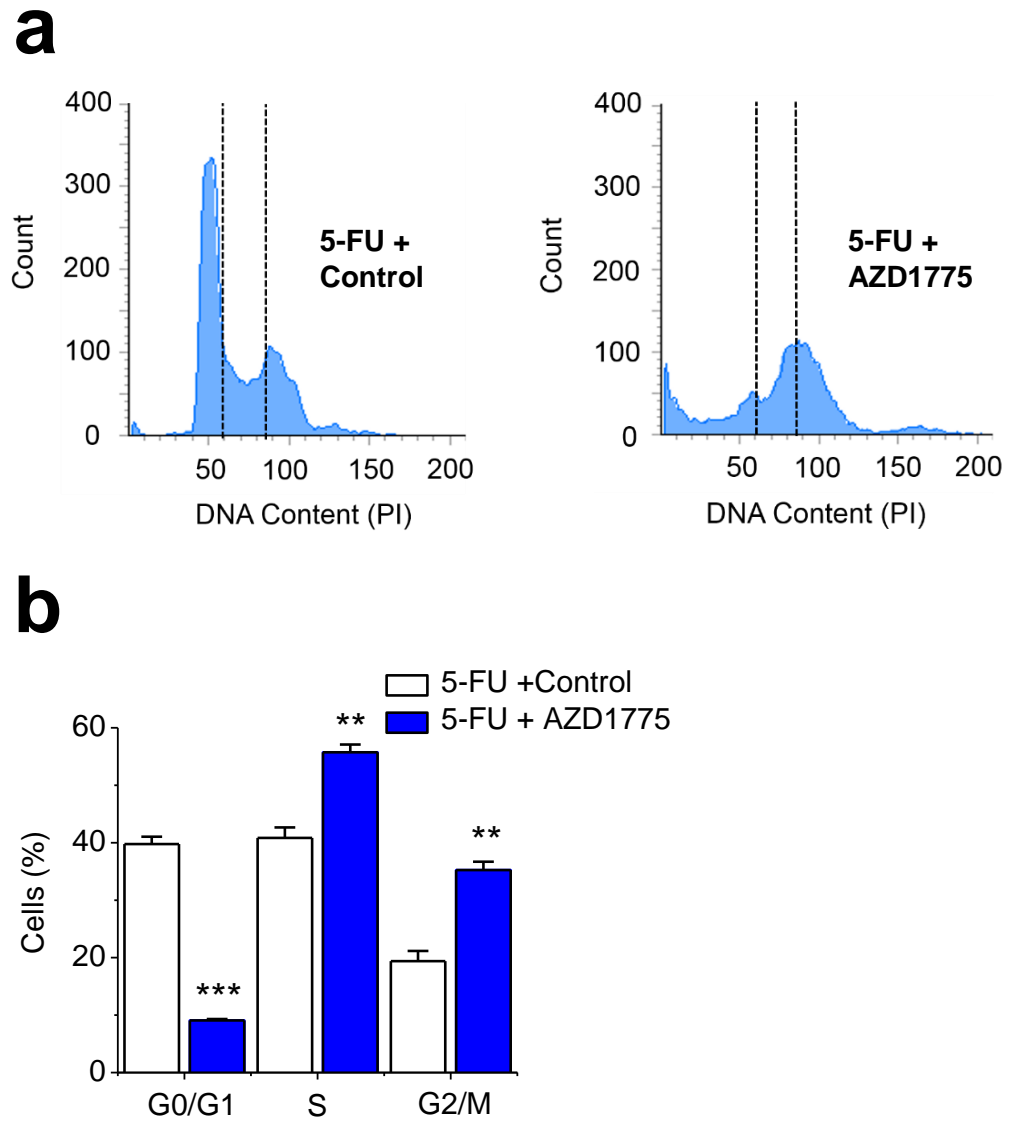


Figure 45 5-FU and AZD1775 Combination Therapy Increases the Number of HT29 Cells in S Phase and G2/M Phase

a. Example flow cytometry recording for HT29 cells after 24 hrs treatment with 5-FU (1 μ M) followed by either AZD1775 (300 nM) or vehicle control (Control). The vertical dotted lines separate different phases of the cell cycle **b.** Mean percentage of cells in G0/G1, S and G2/M phases (n=3 each). 5-FU+AZD1775 data are statistically compared with 5-FU+Control data for each phase.

5.3 5-FU and AZD1775 Combination Therapy Causes Increased Mitosis and DS-DNA Breaks in HT29 Cells

As the HT29 cell line has a mutated p53, both premature mitosis and DS-DNA breaks could be a potential mechanism of action for AZD1775. To investigate this further, a flow cytometry time course assessing levels of DS-DNA breaks (γ H2AX) and mitosis (pHH3) in HT29 cells receiving combination therapy was generated (Figure 46a, Figure 47a). With combination therapy, levels of DS-DNA breaks increased over time to 50.7% 24 hrs after AZD1775 addition, compared to 3.5% in the 5-FU + Control group (Figure 46b). Levels of mitosis followed a slightly different pattern. With combination therapy, the percentage of cells expressing pHH3 peaked 8hrs after the addition of AZD1775 and was significantly higher than in the 5-FU + Control group (55% vs. 3.4%) (Figure 47b). After 8hrs, levels of mitosis in the combination therapy group began to return back to levels in the 5-FU + Control group and 24 hrs after the addition of AZD1775 the two groups were much closer (10.8% vs 2.6%).

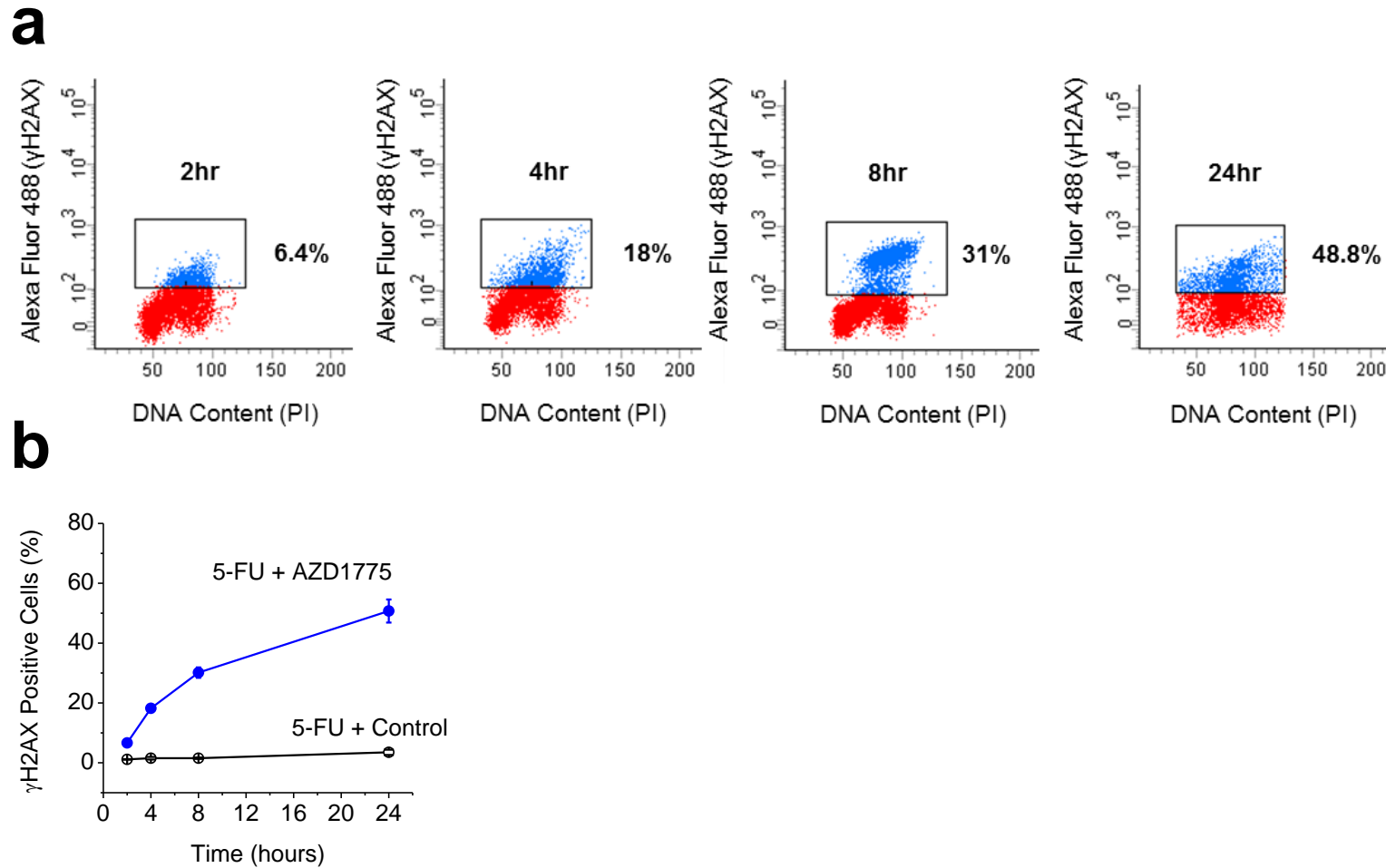


Figure 46 AZD1775 Causes Progressive DS-DNA Breaks Over 24 hrs in HT29 Cells Pre-Treated with 5-FU

a. Example flow cytometry dot plots for unlabelled HT29 cells (red) and HT29 cells labelled with anti- γ H2AX antibody (blue) after 24 hrs treatment with 5-FU (1 μ M) and the addition of AZD1775 (300 nM) for the times indicated **b.** Mean data for the groups in a including a control group (5-FU + Control) where cells were treated for 24 hrs with 5-FU (1 μ M) and vehicle control for the times indicated (n=3 each).

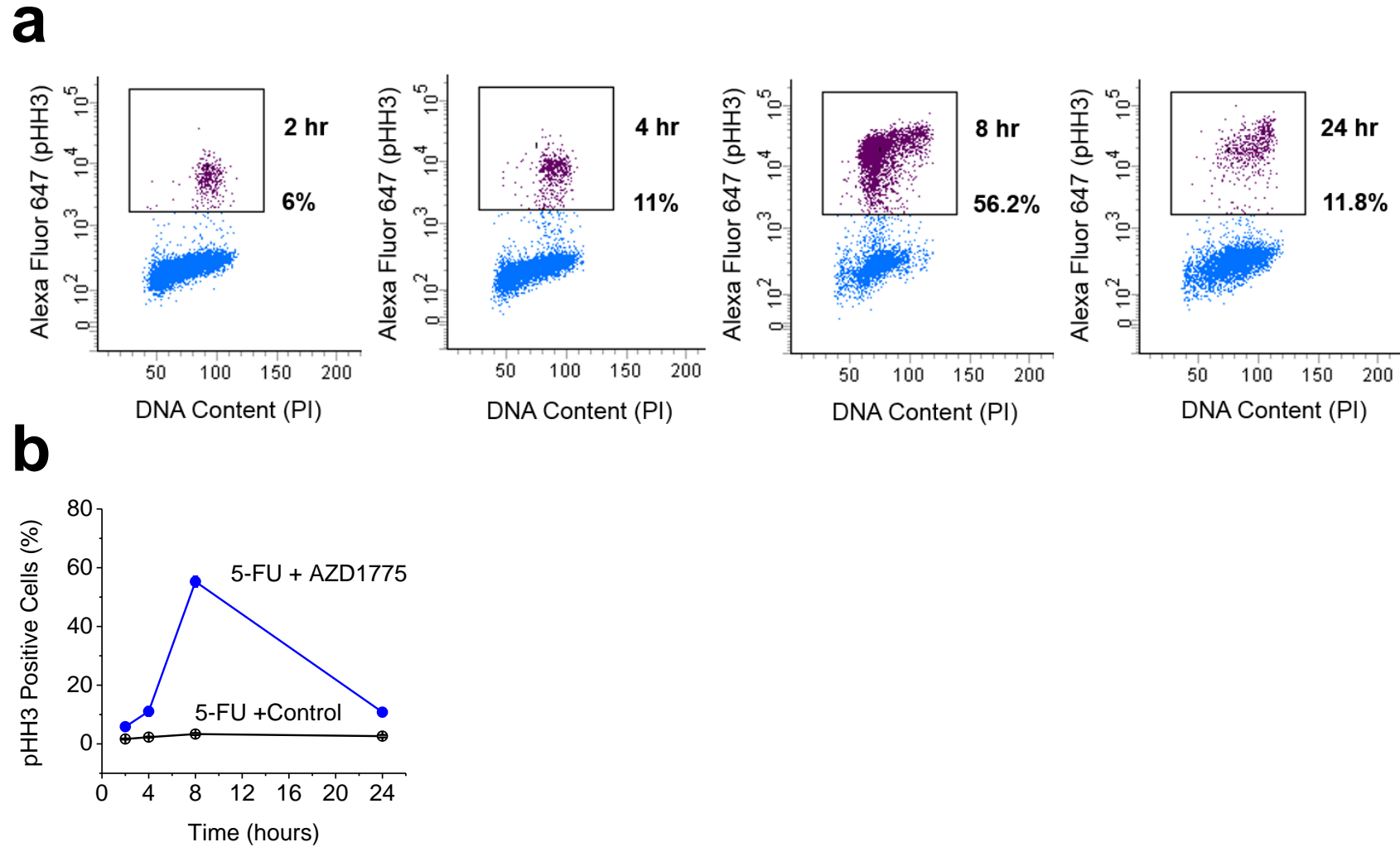


Figure 47 AZD1775 Causes An Early Peak in Mitosis in HT29 Cells Pre-Treated with 5-FU

a. Example flow cytometry dot plots for unlabelled HT29 cells (blue) and HT29 cells labelled with anti-pHH3 antibody (purple) after 24 hrs treatment with 5-FU (1 μ M) and the addition of AZD1775 (300 nM) for the times indicated **b.** Mean data for the groups in a including a control group (5-FU + Control) where cells were treated for 24 hrs with 5-FU (1 μ M) and vehicle control for the times indicated (n=3 each).

5.4 AZD1775 Causes DS-DNA Breaks in HT29 Cells when used as a Monotherapy

To further understand the dominant mechanism of action in HT29 cells the effects of AZD1775 monotherapy were investigated. AZD1775 was tested against HT29 cells for 48 hrs and cell proliferation was measured using a WST-1 assay. At 1 μ M, AZD1775 inhibited proliferation by 69% compared to its vehicle control (Figure 48a). A concentration-response curve was created for AZD1775 in HT29 cells (Figure 48b) and the IC₅₀ value was calculated at 183 nM. To see if AZD1775 monotherapy was able to induce DS-DNA breaks, flow cytometry was used to measure γ H2AX expression (Figure 48c). After 24 hrs treatment AZD1775 (1 μ M) caused 43% of cells to express γ H2AX compared to 0.2% in vehicle control (Control) (Figure 48d).

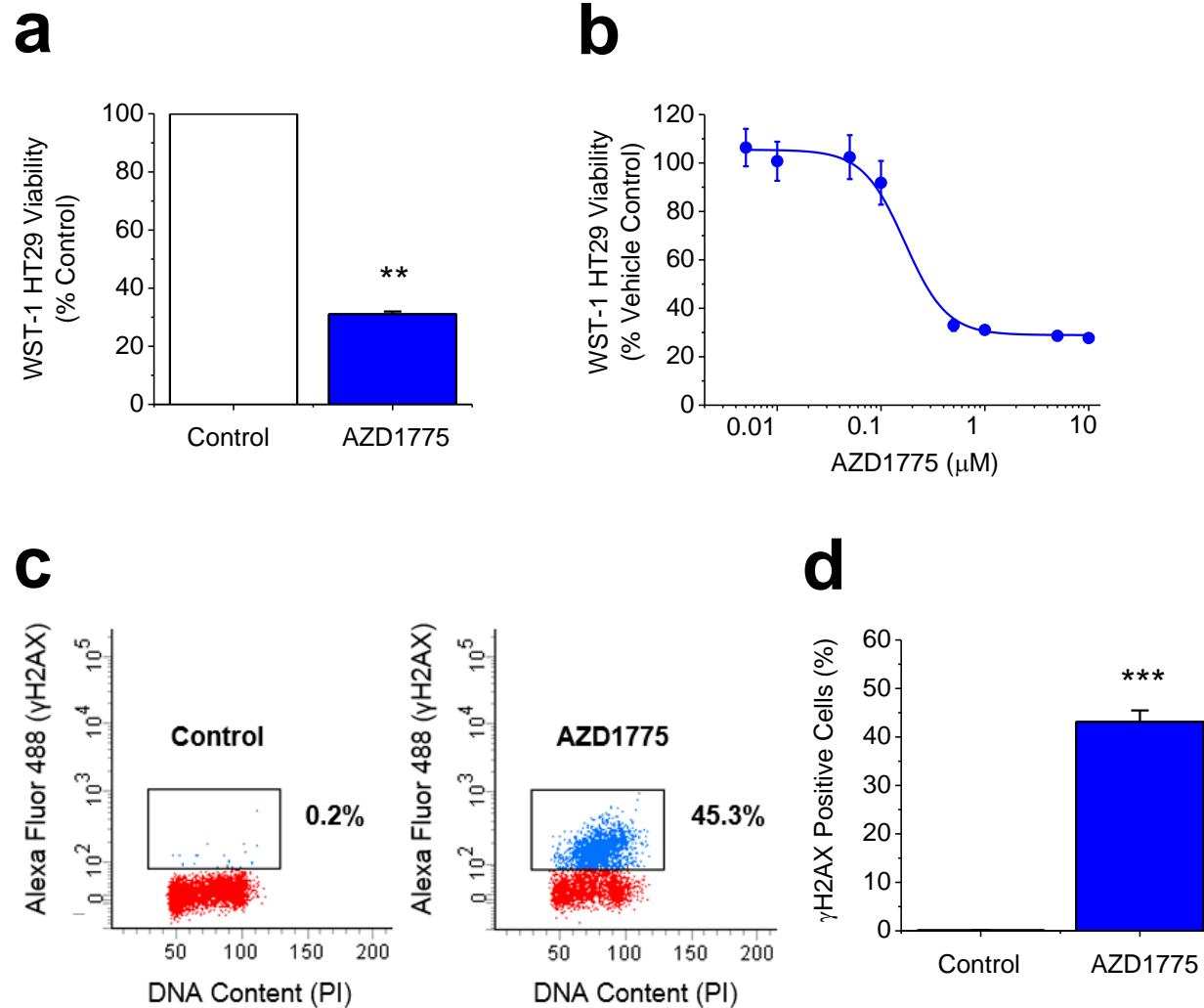


Figure 48 AZD1775 Monotherapy Inhibits Proliferation of HT29 Cells and Causes DS-DNA Breaks

a. Mean data for HT29 viability measured using WST-1 reagent after treatment with AZD1775 (1 μM) or its vehicle control (Control) for 48 hrs (n=3, N=9)
b. AZD1775 dose response curve in HT29 cells. Cells were treated with AZD1775 at the indicated concentrations for 48 hrs and plotted as percentages of the vehicle control (n=3, N=9)
c. Example flow cytometry dot plots for unlabelled HT29 cells (red) and HT29 cells labelled with anti- γH2AX antibody (blue) after 24 hrs treatment with AZD1775 (1 μM) or its vehicle control (Control)
d. Mean data for the groups in c (n=3 each).

5.5 AZD1775 and 5-FU Combination Therapy Causes DS-DNA Breaks and Caspase-3 Dependent Apoptosis that can be Rescued by Exogenous Nucleoside Addition

AZD1775 and 5-FU combination therapy cytotoxicity has previously been attributed to premature mitosis in the presence of unrepaired DNA damage. As AZD1775 monotherapy causes DS-DNA breaks in HT29 cells it was hypothesised that this may actually be the dominant mechanism of action for combination therapy also. Critical to investigating this was the fact that nucleotide shortage is a consequence of excess origin firing and not premature mitosis, both regulated by CDK1, which itself is regulated by WEE1.

Flow cytometry was used to see if exogenous nucleoside addition could reverse DS-DNA breaks induced by combination therapy (Figure 49a). AZD1775 (300 nM) and 5-FU (1 μ M) combination therapy resulted in 44.2% of cells being positive for γ H2AX, whereas 5-FU and vehicle control only caused 4.5% of cells to express γ H2AX. When exogenous nucleosides were added to AZD1775 and 5-FU combination therapy the number of HT29 cells expressing γ H2AX was significantly reduced to 8.7% (Figure 49b).

As DS-DNA breaks can lead to apoptosis, caspase-3 dependent apoptosis was investigated. 5-FU (1 μ M) and vehicle control alone resulted in low levels of apoptosis (4%), whereas 5-FU (1 μ M) and AZD1775 (300 nM) combination therapy significantly increased the apoptotic index up to 13% (Figure 50a,b). The addition of exogenous nucleosides reduced the apoptotic index to 4.7%, which was very similar to levels observed with 5-FU and vehicle control treatment (Figure 50b).

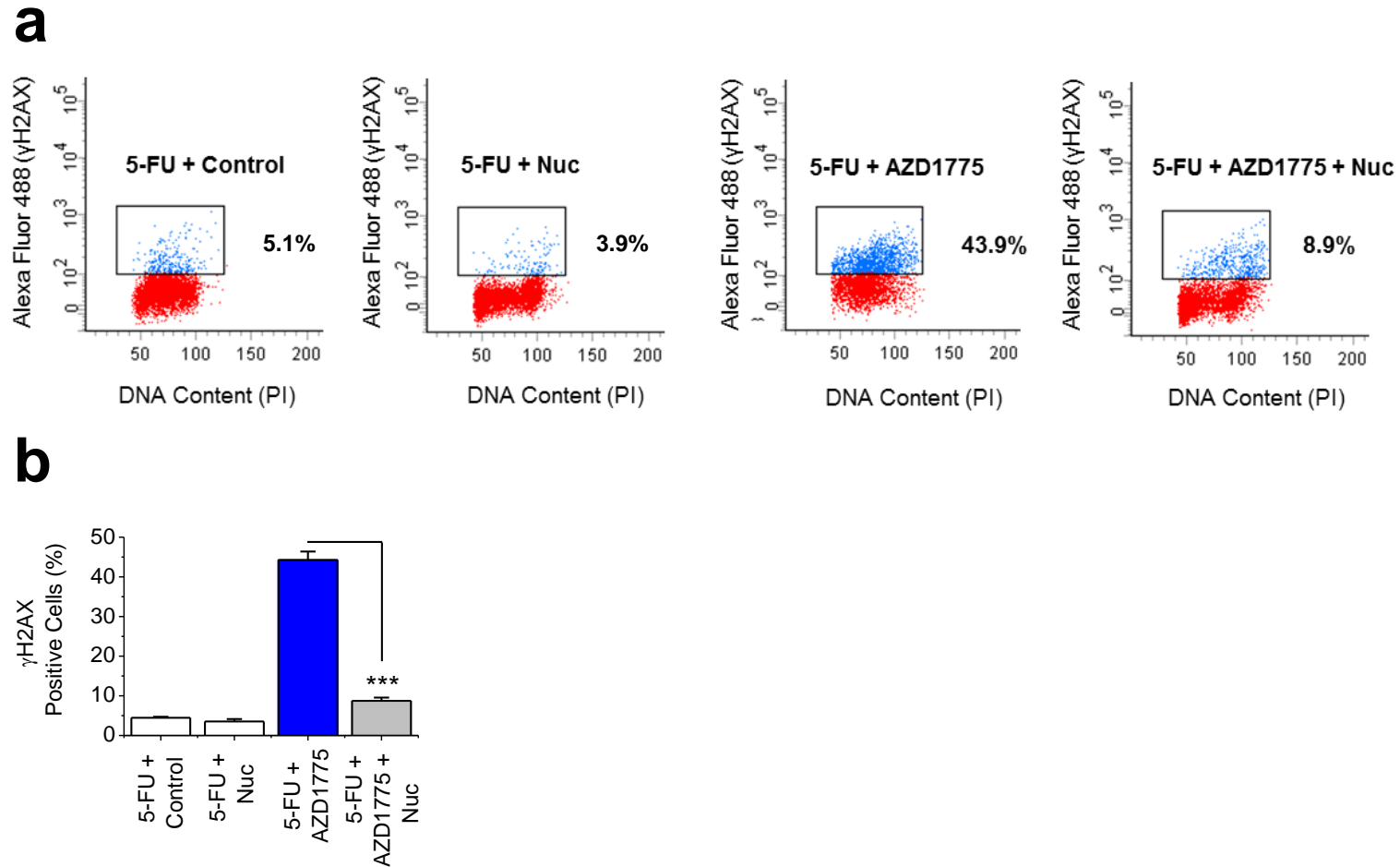
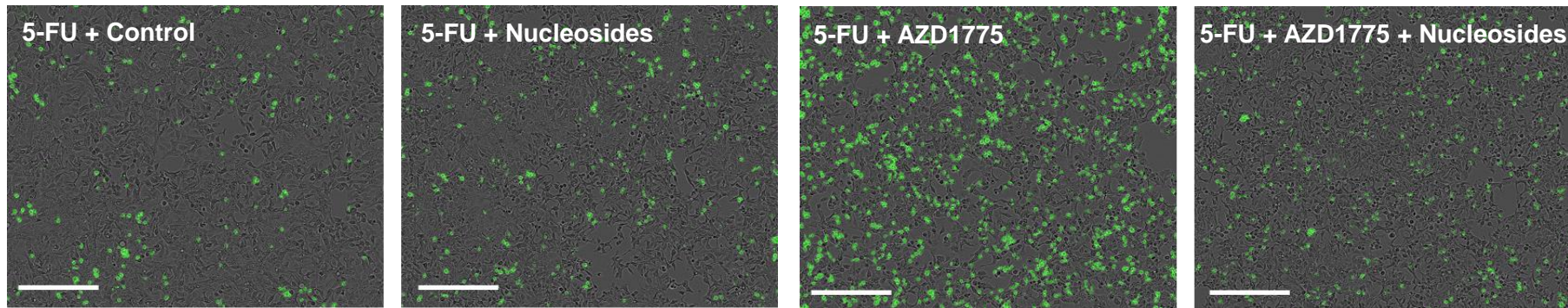


Figure 49 DS-DNA Breaks Caused by AZD1775 and 5-FU Combination Therapy can be Prevented by Adding Exogenous Nucleosides

a. Four example flow cytometry dot plots for unlabelled HT29 cells (red) and HT29 cells labelled with anti- γ H2AX antibody (blue). All cells received 24 hrs 5-FU (1 μ M) followed by either vehicle control (Control), exogenous nucleosides (Nuc, EmbryoMax[®], 1:5 dilution), AZD1775 (300 nM) or AZD1775 (300 nM) + exogenous nucleosides (EmbryoMax[®], 1:5 dilution) **b.** Mean data for the four groups in a (n=3 each).

a



b

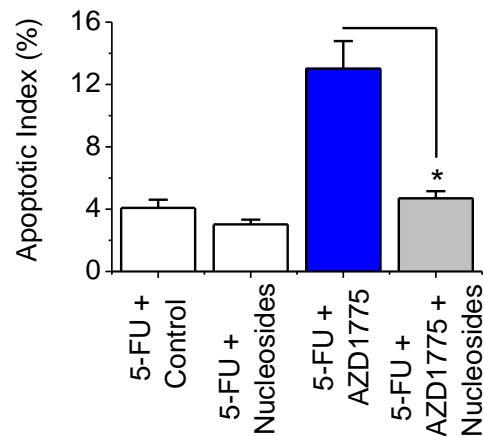


Figure 50 AZD1775 and 5-FU Combination Therapy Induces Caspase-3 Dependent Apoptosis, which can be Prevented with Exogenous Nucleoside Addition

a. Images of fluorescence from caspase-3 activity indicator in HT29 cells. All cells received 24 hrs 5-FU (1 μ M) followed by 24 hrs of either vehicle control, exogenous nucleosides (EmbryoMax®, 1:5 dilution), AZD1775 (300 nM) or AD1775 (300 nM) + exogenous nucleosides (EmbryoMax®, 1:5 dilution) **b.** Mean data for experiments of the type shown in a (n=3 each).

5.6 Summary of Findings

- AZD1775 decreases HT29 cell viability when used in combination with 5-FU
- AZD1775 only sensitises p53 mutated HT29 colorectal cancer cells to irinotecan or oxaliplatin at low concentrations.
- AZD1775 monotherapy causes DS-DNA breaks and inhibits HT29 proliferation with an IC₅₀ of 183 nM
- 5-FU and AZD1775 combination therapy causes an early increase in mitosis and progressive DS-DNA breaks in HT29 cells compared to 5-FU and vehicle control
- 5-FU and AZD1775 combination therapy causes increased Caspase-3 dependent apoptosis compared to 5-FU and vehicle control, which can be rescued with exogenous nucleoside supplementation

5.7 Discussion

The aim of this chapter was to determine the dominant mechanism of action of AZD1775 when used in combination with DNA-damaging agents. The rationale for this chapter stems from the lack of clarity within the literature about the dominant mechanism of action of AZD1775 and the importance of p53 status. In the majority of clinical trials AZD1775 is used as a DNA-damaging sensitiser, where cells with DNA damage (e.g. from chemotherapy) are forced into mitosis prematurely with lethal unrepaired DNA damage. However, AZD1775 can also have monotherapeutic activity by inducing DS-DNA breaks. In this chapter, AZD1775 did not fully sensitise HT29 cells (p53 mutated) to Irinotecan or Oxaliplatin. It did however improve the IC₅₀ of 5-FU. In combination with 5-FU, AZD1775 increased mitosis, DS-DNA breaks and apoptosis compared to 5-FU alone. Supplementation of 5-FU and AZD1775 treated HT29 cells with exogenous nucleosides reversed the increased caspase-3 dependent apoptosis, suggesting that DS-DNA breaks and nucleotide shortage are the dominant mechanism of action of AZD1775 when used in conjunction with DNA-damaging agents.

5.7.1 Dosing Strategies

The vast majority of ongoing clinical trials assessing AZD1775 efficacy are investigating it as a DNA-damage sensitising agent through its ability to cause premature mitosis. In general, the DNA-damaging agent is given on day 1, followed by several doses of AZD1775. Treatment is then repeated in a cycle every couple of weeks depending on the individual trial endpoints. For instance, in one clinical trial for relapsed or recurrent brain tumours, irinotecan hydrochloride is administered on day 1 and AZD1775 on days 1-5, with treatment repeating every 21 days (ClinicalTrials.gov Identifier: NCT02095132). In another clinical trial for

recurrent ovarian, primary peritoneal, or fallopian tube cancer, patients receive gemcitabine hydrochloride on days 1, 8, and 15 and AZD1775 on days 1, 2, 8, 9, 15, and 16. The cycle is then repeated every 28 days (ClinicalTrials.gov Identifier NCT02101775). The proliferation assays were designed to replicate this dosing pattern, with HT29 cells receiving 5-FU, irinotecan or oxaliplatin on day 1 and AZD1775 or vehicle control on day 2.

The dosing strategies used in this chapter are also based upon a previous study using colorectal cancer cell lines (Hirai et al., 2010). Hirai et al., tested a range of chemotherapies on colorectal cancer cell lines for 24 hrs and then treated with AZD1775 100 nM, AZD1775 300 nM or vehicle control for a further 24 hrs. As a sensitising effect had been seen using 300 nM AZD1775 this dose was used in the present studies.

5.7.2 AZD1775 Mechanism of Action

Work in this chapter shows that when AZD1775 is used in combination with 5-FU against a p53 mutated colorectal cancer cell line the enhanced cytotoxicity is due to AZD1775 causing increased DS-DNA breaks, not premature mitosis. AZD1775 appears to exert its own cytotoxic effects independent of chemotherapeutic agents.

In this chapter, the HT29 colorectal cancer cell line was studied specifically because it has a mutated p53 (Arg-273 to His). This means that both mechanisms of action (premature mitosis and DS-DNA breaks) were possible explanations for cytotoxicity seen with combination therapy. Three chemotherapeutic agents commonly used to treat colorectal cancer, 5-FU, oxaliplatin and irinotecan were investigated as it is clinically relevant to see if AZD1775 could improve their

sensitivity. In the proliferation assays AZD1775 significantly improved the IC₅₀ of 5-FU but not irinotecan or oxaliplatin. In all three cases AZD1775 greatly improved chemotherapy efficacy at lower doses, but had less effect at higher doses. This does not indicate increased sensitisation at lower chemotherapeutic doses, but likely reflects AZD1775 having independent cytotoxicity. AZD1775 has potent monotherapeutic action against HT29 cells and has been found to have more potent effects on cell viability than some DNA-damaging agents in other cancer cell lines (Kreahling et al., 2013). AZD1775 monotherapy was capable of inhibiting HT29 cell proliferation by causing DS-DNA breaks with an IC₅₀ of 183 nM. Therefore, a single dose of 300 nM AZD1775 is likely to cause some cytotoxicity independent of its interaction with chemotherapeutic agents.

5-FU was chosen for further investigation because AZD1775 addition significantly improved its IC₅₀. However, 5-FU monotherapy had limited effects on HT29 viability. Even at doses of 100 µM it only inhibited proliferation by 30% compared to vehicle control. Therefore the big improvement with AZD1775 addition likely reflected the independent cytotoxicity of AZD1775 and not a sensitisation effect. Hirai et al., previously reported that AZD1775 had a sensitisation effect with 5-FU against p53 deficient colorectal cancer cell lines (Hirai et al., 2010). Although they did not test HT29 cells, the IC₅₀ for 5-FU was improved with 100 nM and 300 nM AZD1775 addition in WiDr, S498, COLO205, and LS411N p53 deficient colorectal cancer cell lines. However, a review of their data shows similar concentration-response curves to those generated in this chapter, with AZD1775 addition greatly improving 5-FU toxicity at low concentrations (3 µM) and having much smaller improvements at higher concentrations of 5-FU (100 µM).

To clarify if AZD1775 could sensitise HT29 cells to 5-FU at low concentrations experiments investigating the mechanism of action for AZD1775 were performed. Doses of 1 μ M 5-FU and 300 nM AZD1775 were chosen because in the concentration-response curves this combination caused a big reduction in HT29 viability compared to 1 μ M 5-FU alone. As expected, both mitosis and DS-DNA breaks increased with AZD1775 addition. The increase in mitosis was quick, with a peak at 8hrs before almost returning back to control levels at 24 hrs. In contrast the increase in DS-DNA breaks occurred in a linear fashion and peaked at 24 hrs.

Both premature mitosis and DS-DNA breaks occur with AZD1775 treatment because of an increase in active CDK1 (reduction in pCDK1-Y15). However, only DS-DNA breaks occur as a consequence of critical nucleotide shortage. The addition of exogenous nucleosides to combination therapy could rescue the amount of DS-DNA breaks almost to the levels seen with 5-FU treatment alone. In chapter 4, it was shown that AZD1775 could cause apoptosis in CLMECs as a consequence of DS-DNA breaks. Therefore, caspase-3 dependent apoptosis was measured for 5-FU and AZD1775 combination therapy. As expected, there was a 3-fold increase in apoptosis when AZD1775 was added to 5-FU compared to 5-FU treatment alone. Importantly, this increased apoptosis could be rescued with exogenous nucleoside addition. This suggests that DS-DNA breaks are the cause of the increased apoptosis and although there is an increase in mitosis levels, it is not the cause of cytotoxicity. Obviously these findings contradict a number of previous studies in colorectal cancer cell lines that suggest WEE1 inhibition sensitises cells to DNA damaging agents through premature mitosis (Wang et al., 2001, Hirai et al., 2009, Hirai et al., 2010). However, these studies were published before the role of WEE1 in regulating DNA synthesis was discovered and so DS-DNA breaks were not investigated.

One interesting point to consider as a result of work in this chapter is whether 5-FU could actually sensitise HT29 cells to AZD1775. The mechanism of action of 5-FU is attributed to the inhibition of thymidine synthesis, which results in deoxynucleotide pool imbalances (Longley et al., 2003). As AZD1775 causes a critical nucleotide shortage the addition of 5-FU may further exacerbate the critical shortage of nucleotides. Further work on this hypothesis is necessary, initially in the form of in vitro studies.

5.7.3 Importance of p53 Status

The p53 status of a cancer has previously been reported to be important for the success of AZD1775 combination therapy. Numerous studies have reported that AZD1775 only sensitises DNA-damaging agents in p53 mutated cancer cells (Wang et al., 2001, Hirai et al., 2009, Hirai et al., 2010, Rajeshkumar et al., 2011). This is because p53 has an important role in maintaining G1/S phase arrest in response to DNA damage. ATM, ATR, CHK1 and CHK2 can phosphorylate p53 in response to DNA damage, which prevents its nuclear export and degradation (Sancar et al., 2004). Increased p53 targets the p21CIP/WAF1 gene, which encodes the p21 protein. p21 is capable of binding to and inhibiting the cyclin E/CDK2 and cyclin D/CDK4 complexes, preventing cell cycle progression into S phase and allowing DNA to be repaired (Sancar et al., 2004). It is thought that cancer cells that have a mutated non-functional p53 have a non-functional G1/S cell cycle checkpoint and therefore are much more reliant on the G2/M cell cycle checkpoint for DNA repair. If a cancer cell has a functioning p53 its G1/S checkpoint is intact and DNA damage can be repaired here, meaning that induced DNA damage is repaired before the cell enters mitosis. In 2012, evidence first emerged that AZD1775 can sensitise DNA-damaging agents independent of p53 status although the exact mechanism of

action was not clear (Kreahling et al., 2012, Van Linden et al., 2013, Guertin et al., 2013, Muller, 2014).

As the main mechanism of action of AZD1775 in combination therapy is the generation of DS-DNA breaks and critical nucleotide shortage, p53 status should have no impact upon efficacy. In agreement with this, AZD1775 has been shown to have single agent activity in 66 different colorectal cancer cell lines with varying p53 status (Guertin et al., 2013). If that is the case, then why have previous studies not seen a “sensitisation” effect in wildtype p53 cancer cell lines? One possibility is the dose of AD1775 necessary to induce DS-DNA breaks may be greater. Of the studies performed in cell lines, the maximum dose that has been used with combination therapy is 300 nM, often less (Wang et al., 2001, Hirai et al., 2009, Hirai et al., 2010, Mueller et al., 2014). This would also indicate why no monotherapy effects of AZD1775 are reported in these studies.

5.7.4 Implications for Ongoing Clinical Trials

As previously discussed, the vast majority of ongoing clinical trials investigating AZD1775 are doing so in the context of a DNA-damaging sensitiser. This usually involves a maximum tolerated dose of a DNA damaging agent (eg. chemotherapy) followed by several doses of AZD1775 to cause premature mitosis before DNA-damage is repaired. This is followed by a period of no treatment before the cycle is repeated. However, work in this chapter has demonstrated that AZD1775 exerts its own cytotoxic effects through DS-DNA breaks, independent of chemotherapeutic agents. Therefore, current dosing regimens may not be the most effective in terms of causing cytotoxicity. Further work is needed to calculate the optimum duration of AZD1775 treatment, but results from current clinical trials may be improved if

AZD1775 is used as an outright DNA-damaging agent alongside other DNA-damaging agents.

5.7.5 Conclusion

Despite the discovery of AZD1775 over seven years ago, its dominant mechanism of action has yet to be determined. In this chapter it has been shown that when AZD1775 is used in combination with 5-FU against a p53 mutated colorectal cancer cell line the enhanced cytotoxicity is due to AZD1775 causing increased DS-DNA breaks, not premature mitosis. AZD1775 exerts its own cytotoxic effects independent of chemotherapeutic agents by causing DS-DNA breaks and caspase-3 dependent apoptosis due to a critical nucleotide shortage. This has important implications in ongoing clinical trials investigating AZD1775, where current dosing strategies may not be optimised to derive maximal oncological benefit from WEE1 inhibition.

Chapter 6: Identifying New Anti-Angiogenic Targets in Colorectal Cancer Liver Metastases using a Proteomics Screen

Tumour endothelial cells are distinct from normal endothelial cells. For instance, in Chapter 3 it was shown that CLMECs have reduced expression of CD31 and VEGFR-2 compared with matched LECs. Identifying proteins that are up- or down-regulated in tumour endothelial cells and ascertaining their importance in tumour angiogenesis would be of great value for the development of future anti-angiogenic agents. However, a number of issues have prevented this from being a straightforward process. As eluded to in Chapter 3, the isolation and culture of human endothelial cells can be technically challenging. Pure endothelial cell cultures can be difficult to obtain and may become contaminated with other cell types, such as fibroblasts. The lack of a specific endothelial marker also makes culture confirmation difficult. Furthermore, identifying important differences in protein expression can be a prolonged process, not least because investigators are “hunting in the dark”.

Quantitative proteomics is a powerful technique used to analyse global protein expression within a cell. It involves the isotopic labelling of proteins or peptides, which can then be separated and identified by mass spectrometry. Comparisons of protein or peptide abundance can be made between matched samples and therefore can be used to identify differentially expressed proteins between groups.

The aim of this chapter was to identify differentially expressed proteins in matched LECs and CLMECs using proteomic studies.

6.1 LECs and CLMECs Express Numerous Endothelial Cell Markers

Matched LECs and CLMECs from five patients were expanded in culture and submitted for proteomic analysis to identify any differences in protein expression. The patient characteristics are summarised in Table 8. There were two male patients and three female patients ranging in age from 63 to 81 years old. There were a range of co-morbidities, but four of the five patients had cardiovascular disease. This included three patients with hypertension (receiving medication), one patient with Type II diabetes mellitus (tablet-controlled) and one patient with Type I diabetes mellitus. There was one current smoker. Only one patient had no co-morbidities and took no medication.

The specific details of each patient's primary colorectal cancer, diagnosis of CLM, subsequent surgery and pathological outcomes are summarised in Table 9. Three patients had primary rectal adenocarcinoma and two patients had primary colonic adenocarcinoma. Four patients had metachronous liver metastases and one patient had synchronous metastases who had the primary colorectal cancer and liver metastases resected at separate surgeries. The number, size and location of the metastases were variable. Four of the five CLM resections showed moderately differentiated adenocarcinoma, with one being well differentiated adenocarcinoma. Unfortunately three resections had positive margins (R1). At the time of writing (26th October 2016) two patients are alive with no recurrent disease, two patients are alive with recurrent disease not amenable to surgical intervention and one patient has died.

As endothelial cells display heterogeneity in different organs and endothelial cells of CLM have never been characterised before, a panel of 23 endothelial cell markers was generated to assess LECs and CLMECs against (Garlanda and Dejana, 1997). Proteomics detected 16 out of the 23 markers, including the well-recognised endothelial cell markers CD31, vWF, VE-Cadherin, eNOS and endoglin (Figure 51). Three endothelial markers had significant differences in expression levels between LECs and CLMECs. Both VEGFR-1 and fibronectin (isoform 17) were significantly up-regulated in CLMECs and vWF was significantly down-regulated in CLMECs. Despite western blotting showing a significant reduction in CD31 expression in CLMECs (Figure 21), this was not confirmed with the proteomics data. There was an obvious reduction in CD31 intensity in CLMECs, however, the p-value was 0.06. Likewise, western blotting clearly showed VEGFR-2 to be significantly down-regulated in CLMECs (Figure 23), however it wasn't detected in either the LECs or CLMECs with proteomics. To distinguish vascular endothelial cells from lymphatic endothelial cells a panel of 3 markers was generated, podoplanin (PDPN), prospero homeobox protein 1 (PROX1) and lymphatic vessel endothelial hyaluronan receptor 1 (LYVE-1) (Podgrabinska et al., 2002) . None of the lymphatic endothelial cell markers were identified in LECs or CLMECs.

Unique ID	Sex (M/F)	Age	Co-Morbidities	Medications
74	M	66	Nil	Nil
75	M	67	Type II Diabetes Mellitus	Metformin, Simvastatin
78	F	80	Transient Ischaemic Attack, Atrial Fibrillation, Anorexia, Smoker, Hypertension, Bladder Cancer	Atorvastatin, Clopidogrel, Codeine, Folic Acid, Loperamide, Morphine Sulphate, Ramipril, Lactulose
79	F	81	Type I Diabetes Mellitus, Hypertension, Cholecystectomy, Appendectomy	Clopidogrel, Creon, Enalapril, Loperamide, Insulin, Omeprazole, Simvastatin, Prednisolone
80	F	63	Hypertension, Idiopathic Thrombocytopenic Purpura	Amlodipine

Table 8 Patient Characteristics of the Matched LEC and CLMEC Samples Submitted for Proteomic Studies

Patient age, sex, co-morbidities and current medication are listed for each patient analysed in the LEC vs. CLMEC proteomic studies.

Unique ID	Primary Colorectal Cancer	Colorectal Liver Metastases	Date of Operation	Nature of Operation	Histology of Colorectal Liver Metastases
74	Caecal Adenocarcinoma pT3, N0, M0, R0	Metachronous 1 large lesion spanning segments 8/5/6/4/1	16/06/2015	Right hepatic trisectionectomy with caudate lobectomy	Moderately differentiated adenocarcinoma R1
75	Rectal Adenocarcinoma pT3, N1, M1, R0	Synchronous 1 lesion in segment 2, 1 lesion in segment 5	14/07/2015	Laparoscopic Right hemi-hepatectomy	Moderately differentiated adenocarcinoma R0
78	Rectal Adenocarcinoma pT3, N0, M0, R0	Metachronous 1 lesion in segment 2/3	06/10/2015	Laparoscopic left lateral sectionectomy	Well differentiated adenocarcinoma R0
79	Rectal Adenocarcinoma pT1, N1, M0, R0	Metachronous 1 lesion in segment 4	20/10/2015	Laparoscopic segment 2/3/4 metastasectomy	Moderately differentiated adenocarcinoma R1
80	Colonic Adenocarcinoma pT3 N0 M0, R0	Metachronous (3 rd recurrence) 1 lesion in segment 7, 1 lesion in segment 8	03/11/2015	Re-do (third) liver resection - segment 7 and 8 metastasectomies	Moderately differentiated adenocarcinoma R1

Table 9 Colorectal Cancer History for Each Patient Investigated with Proteomic Studies

Pathological data for each patient analysed in the LEC vs. CLMEC proteomic studies. Primary colorectal cancer has been staged according to the TNM classification system. The nature, surgical treatment and pathological details for the CLM are also stated.

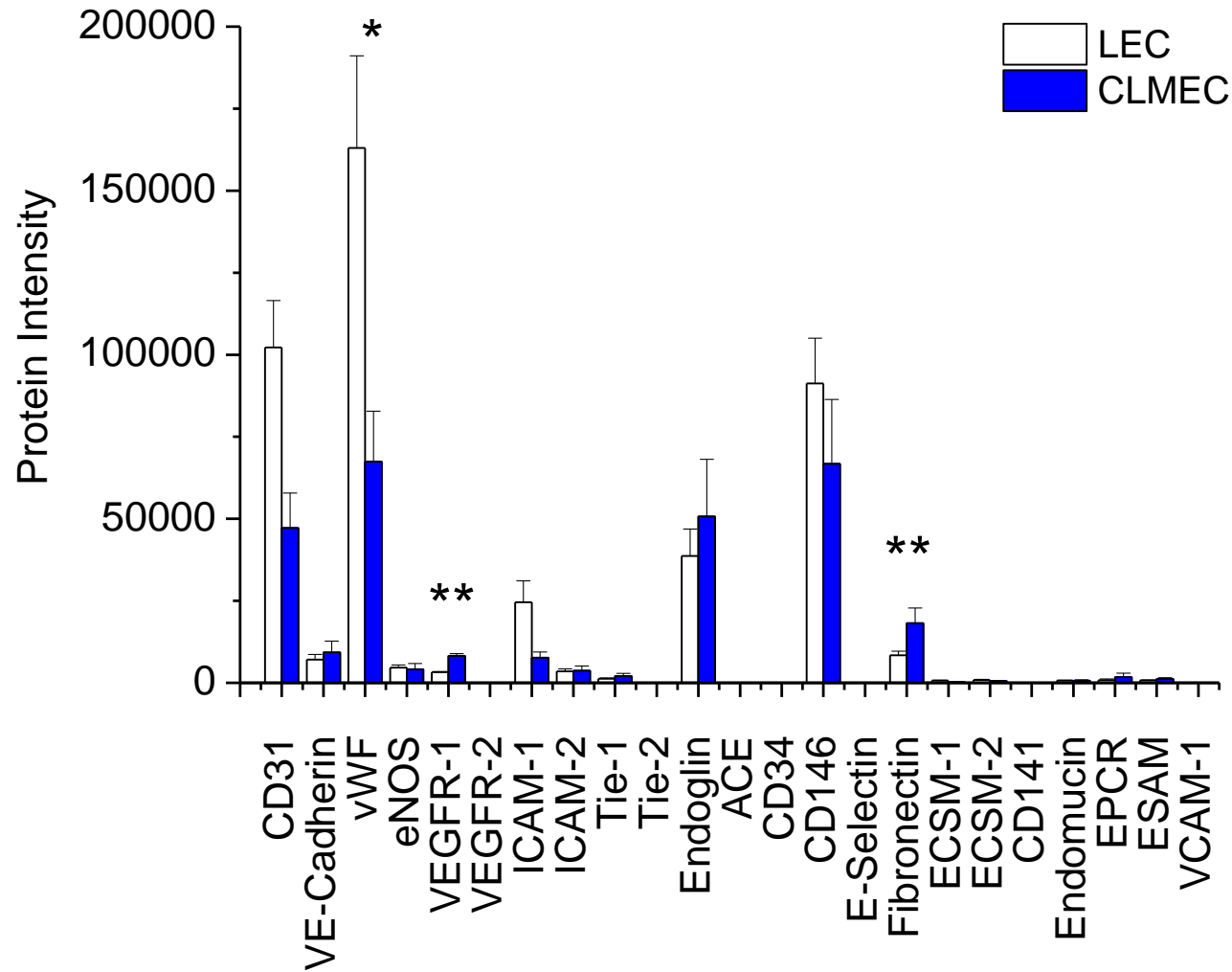


Figure 51 LECs and CLMECs Express a Range of Endothelial Markers

A comparison of relative protein intensity for 23 endothelial cell markers in LECs and CLMECs. For each endothelial marker the mean protein intensity for LECs has been statistically compared with CLMECs (n=5 each), * (p<0.05) and ** (p<0.01)

6.2 Quantitative Proteomics Reveals Differentially Expressed Proteins in CLMECs and LECs

The total proteome for each patient is displayed in the heat map in Figure 52. Within each matched patient sample, protein abundance in CLMECs has been compared to LECs and assigned a colour based on its Z-score. For the majority of proteins there was no difference in expression between LECs and CLMECs, indicated by a yellow band, reflecting a Z-score of ~ 0 . In total, 4,767 proteins were detected in both LECs and CLMECs and 157 proteins had a significantly different expression level between the two groups (Appendix I). The top 15 differentially expressed proteins (ranked according to their p-value) are displayed in Table 10. The most significantly up-regulated protein was thrombospondin-1 (TSP-1), a known endogenous inhibitor of angiogenesis (Lawler, 2002). The mean expression of TSP-1 was 2.8 times higher in CLMECs compared to LECs. VEGFR-1, another endogenous inhibitor of angiogenesis was also significantly upregulated in CLMECs, expressed 2.5 times higher compared to LECs. Unsurprisingly, for the vast majority of the 157 proteins that had a significant difference in expression between LECs and CLMECs, little is known about their role in endothelial cells, angiogenesis or cancer.

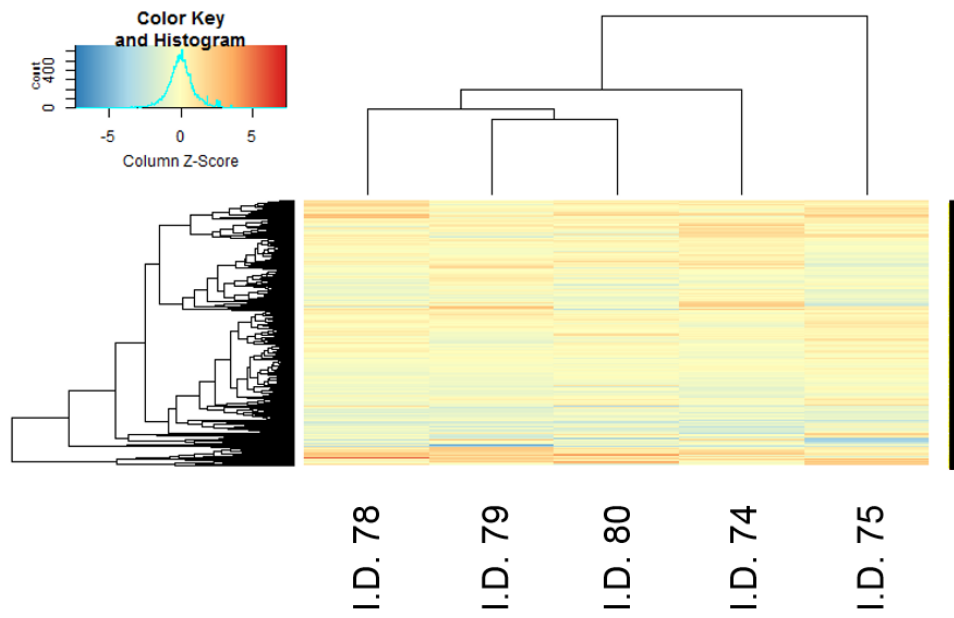


Figure 52 Heat Map of the Total LEC and CLMEC Proteome Determined by Proteomic Studies

Z-scores are plotted for the relative protein expression determined by proteomic studies. For each patient, CLMEC protein intensity has been compared to LEC protein intensity and assigned a colour based on its Z-score.

Protein	Mean LEC Intensity	Mean CLMEC Intensity	LEC/CLMEC Ratio	LEC vs. CLMEC p value
Thrombospondin-1	47508.6	134408	0.356179697	0.00025449
cAMP-Dependent Protein Kinase Type I-Beta Regulatory Subunit	1234.5	392.45	3.368114727	0.000697796
Rho GTPase-Activating Protein 7	664.164	2519.78	0.267445423	0.001026153
Vascular Endothelial Growth Factor Receptor 1	3265.7	8222.44	0.403526385	0.001088631
60S Ribosomal Protein L37	2103.42	4174.36	0.480491872	0.001879499
Tubulin Alpha-4A Chain	9472.1	4342.2	2.781709713	0.001927656
LIM Domain Only Protein 7	1345.32	5934.74	0.231716048	0.002053259
Solute Carrier Family 2, Facilitated Glucose Transporter Member 1	1141.878	2887.7	0.397928842	0.002208671
E3 Ubiquitin-Protein Ligase RBBP6	210.436	803.504	0.253763778	0.002245187
Transforming Growth Factor Beta-2	1313.032	12818.66	0.116912767	0.00273289
Neuronal Growth Regulator 1	305.332	770.166	0.400242361	0.002752091
Lysosome-Associated Membrane Glycoprotein 2	2604.78	3397.5	0.740762045	0.003172724
LIM and Cysteine-Rich Domains Protein 1	320.98	1872.46	0.186101686	0.003259361
Cyclin-Dependent Kinase Inhibitor 1	587.758	1255.236	0.455710266	0.003761478
Fibronectin Isoform 17	56968.2	192440	0.308406416	0.003766208

Table 10 Differentially Expressed Proteins in LECs and CLMECs

The top 15 differentially expressed proteins in LECs and CLMECs in proteomic studies ranked according to their p-value

6.3 Validation of Proteomic Results

To validate the proteomic study results, western blotting was performed on the same samples for all endothelial cell markers that showed statistically different levels of expression between LECs and CLMECs. In the proteomic studies, vWF expression was reduced in all CLMEC samples compared to LECs, although the difference was much less in patient sample 75 (Figure 53a,b). Western blotting also confirmed vWF to be down-regulated in CLMECs (Figure 53c). Quantification of the vWF band intensity relative to the β -actin loading control in matched samples revealed the expression of vWF to be 64% lower in CLMECs (Figure 53d).

VEGFR-1 expression was significantly increased in CLMECs in all patient samples analysed with proteomics (Figure 54a,b). Western blotting for VEGFR-1 revealed two bands, one at ~180 kDa and a separate band at ~110 kDa that were both visibly more intense in CLMECs (Figure 54c). The band ~180kDa in size corresponds to the full length VEGFR-1. The band ~110 kDa in size corresponds to the shorter soluble VEGFR-1 (sVEGFR-1). Both the VEGFR-1 and sVEGFR-1 band intensity were increased in CLMECs relative to the β -actin control. VEGFR-1 was found to be up-regulated by 52% and s-VEGFR-1 by 65% (Figure 54d).

Fibronectin isoform 17 was significantly up-regulated in CLMECs in all patient samples analysed in the proteomic studies (Figure 55a,b). However, western blotting showed fibronectin to be down-regulated in CLMECs (Figure 55c). Quantification of the fibronectin band intensity relative to the β -actin loading control in matched samples revealed the expression of fibronectin to be 53% lower in CLMECs (Figure 55d).

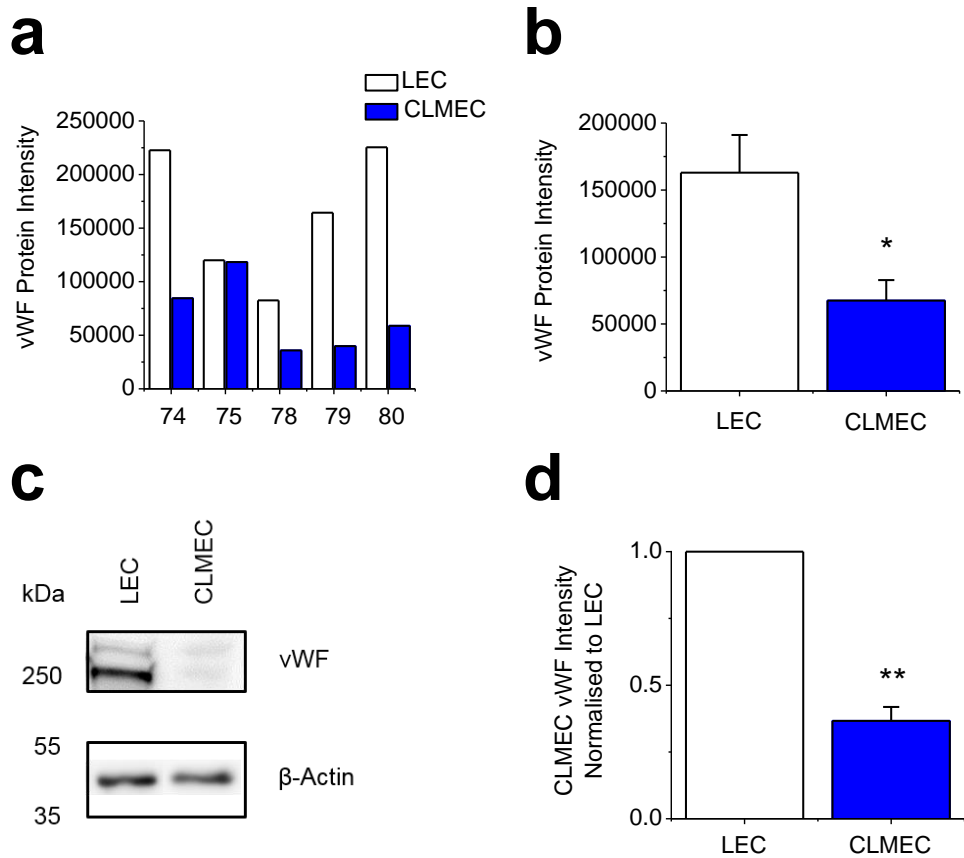


Figure 53 vWF is Down-Regulated in CLMECs

a. vWF protein intensity in LECs and CLMECs determined by proteomic studies in five matched patient samples (n=5) **b.** Mean vWF intensity in all matched LEC and CLMEC samples shown in **a** **c.** Example western blot labelled with anti-vWF and anti- β -actin antibodies for LECs and CLMECs **d.** Quantification of the CLMEC vWF band intensity relative to β -actin and normalised to LEC (n=3 each).

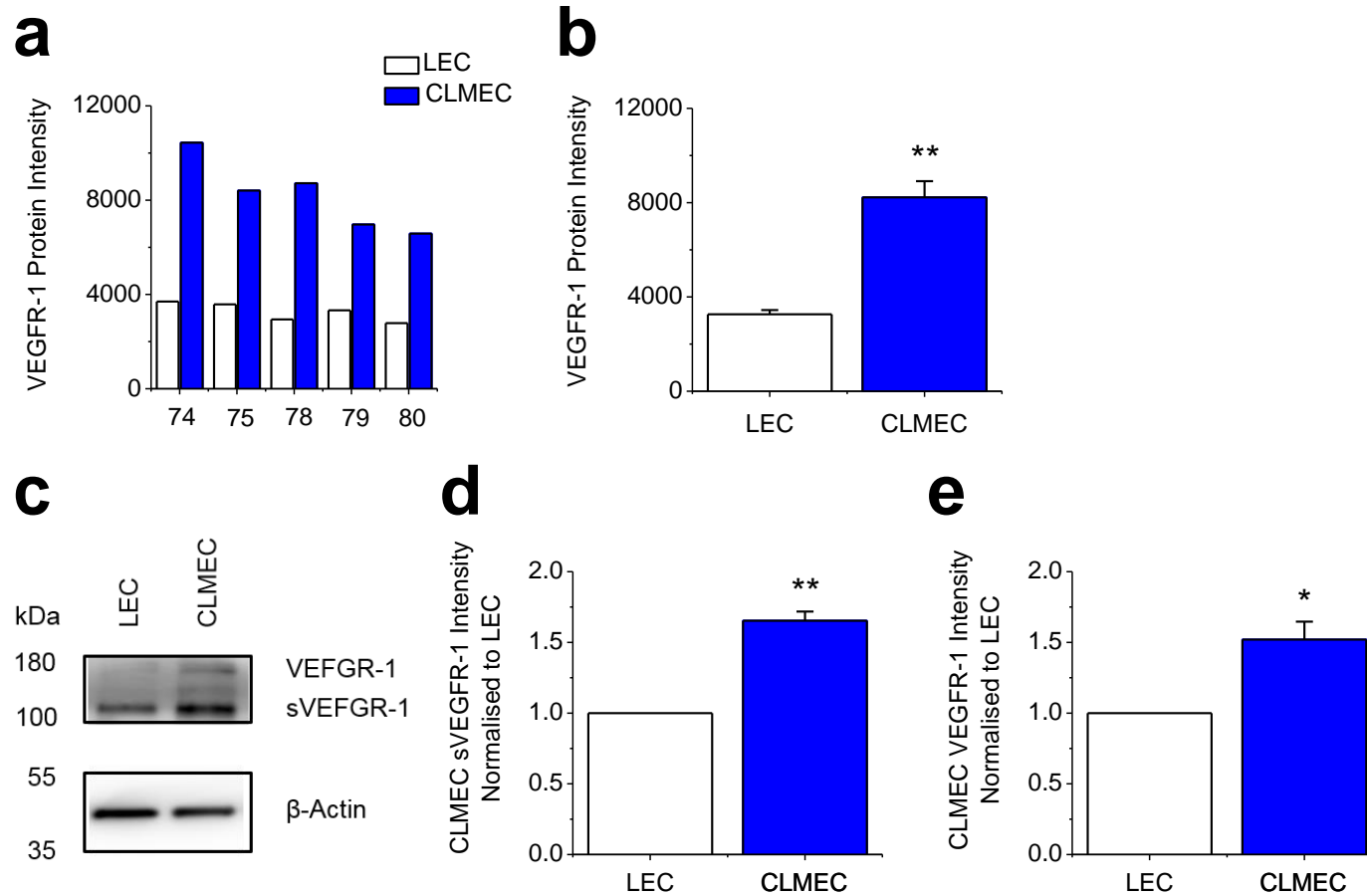


Figure 54 VEGFR-1 and sVEGFR-1 are Up-Regulated in CLMECs

a. VEGFR-1 protein intensity in LECs and CLMECs determined by proteomic studies in five matched patient samples (n=5) **b.** Mean VEGFR-1 intensity in all matched LEC and CLMEC samples shown in **a**. **c.** Example western blot labelled with anti-VEGFR-1 and anti- β -actin antibodies for LECs and CLMECs **d.** Quantification of the CLMEC sVEGFR-1 band intensity relative to β -actin and normalised to LEC (n=3 each) **e.** Quantification of the CLMEC VEGFR-1 band intensity relative to β -actin and normalised to LEC (n=3 each).

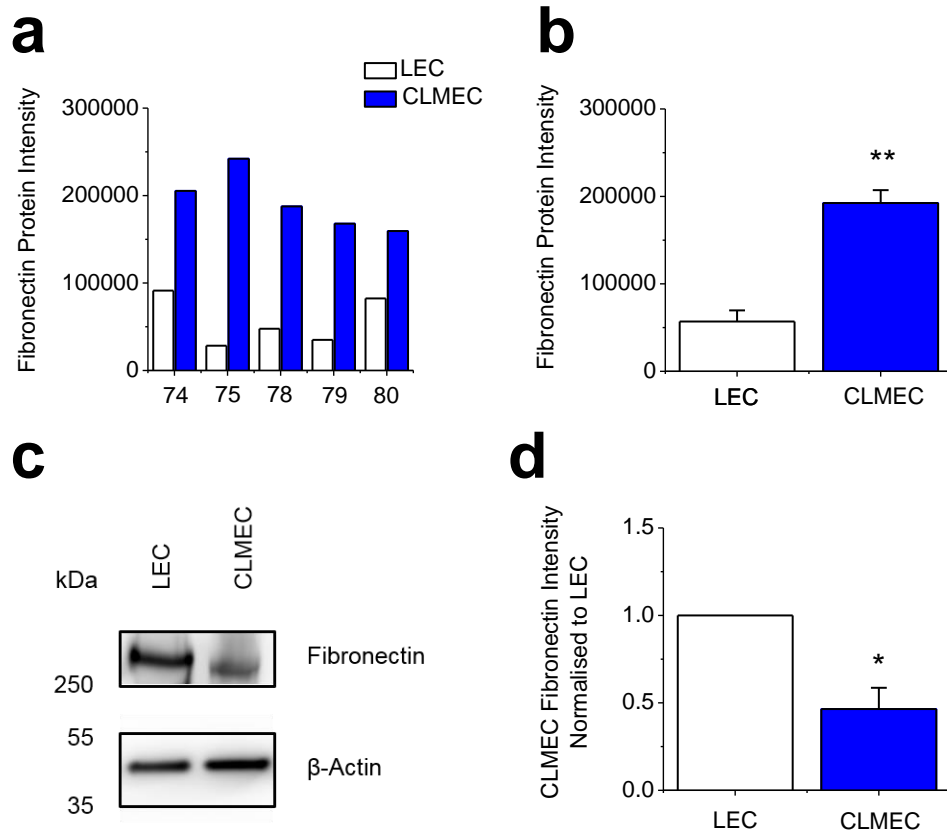


Figure 55 Fibronectin is Down-Regulated in CLMECs

a. Fibronectin isoform 17 protein intensity in LECs and CLMECs determined by proteomic studies in five matched patient samples (n=5) **b.** Mean fibronectin isoform 17 intensity in all matched LEC and CLMEC samples shown in **a**. **c.** Example western blot labelled with anti-fibronectin and anti- β -actin antibodies for LECs and CLMECs **d.** Quantification of the CLMEC fibronectin band intensity relative to β -actin and normalised to LEC (n=3 each).

6.4 Thrombospondin-1 as an Anti-Angiogenic Target

TSP-1 is a known endogenous inhibitor of angiogenesis and was the most significantly upregulated protein in CLMECs (Table 10). In the proteomic studies, TSP-1 expression was increased in all CLMEC samples compared to LECs (Figure 56a,b). Western blotting also confirmed TSP-1 to be up-regulated in CLMECs (Figure 56c). Quantification of the TSP-1 band intensity relative to the β -actin loading control in matched samples revealed the expression of TSP-1 to be 2.4 fold higher in CLMECs (Figure 56d).

TSP-1 inhibits endothelial cell proliferation and migration in HUVECs (Lawler, 2002). To assess the functional relevance of TSP-1 in CLMECs, pooled siRNA targeted against TSP-1 was used to knockdown TSP-1 (Figure 57a). Quantification of the TSP-1 band intensity relative to the β -actin loading control revealed the expression of TSP-1 to be 51% lower in CLMECs transfected with TSP-1 siRNA compared to scrambled siRNA (Figure 57b). Proliferation was measured 48 hrs after transfection using the nuclear dye Vybrant[®] Green (Figure 57c). Knockdown of TSP-1 increased CLMEC proliferation by 24% compared to scrambled siRNA (Figure 57d). To investigate the effect of TSP-1 knockdown on CLMEC migration a scratch wound assay was performed (Figure 58a). At 20 hrs the RWD in CLMECs transfected with TSP-1 siRNA was 95%, whereas in CLMECs transfected with scrambled siRNA the RWD was 78% (Figure 58b), indicating that knockdown of TSP-1 increased migration in CLMECs.

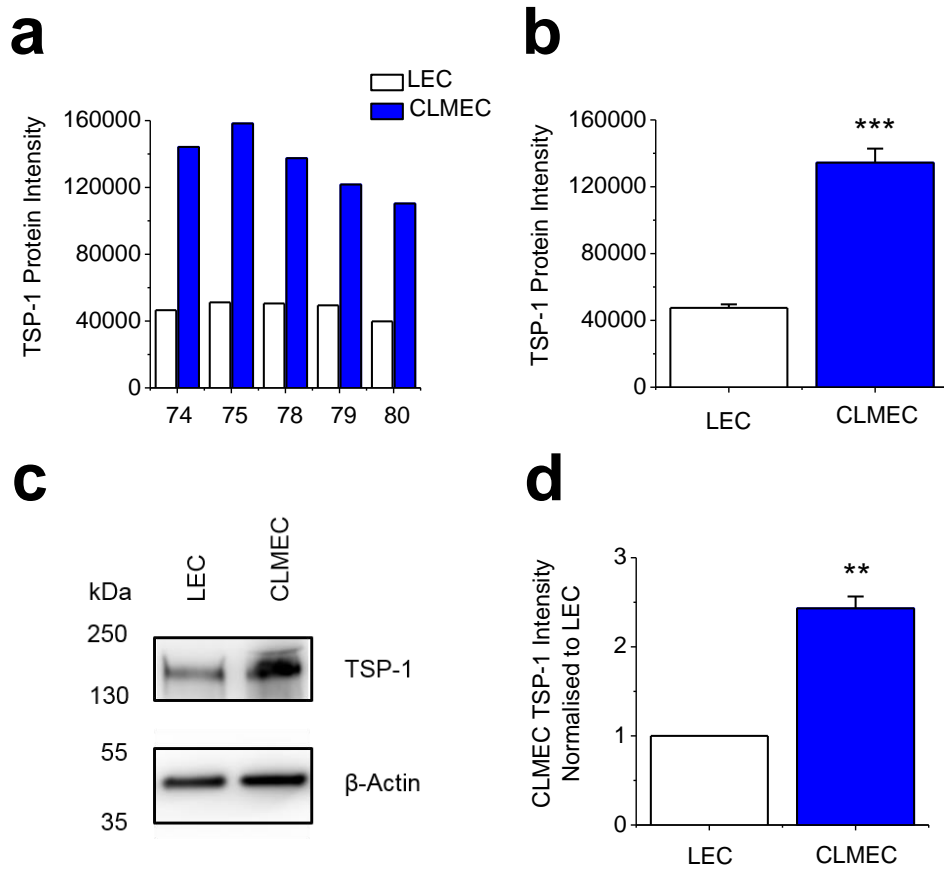


Figure 56 Thrombospondin-1 is Up-Regulated in CLMECs

a. TSP-1 protein intensity in LECs and CLMECs determined by proteomic studies in five matched patient samples (n=5) **b.** Mean TSP-1 intensity in all matched LEC and CLMEC samples shown in **a** **c.** Example western blot labelled with anti-TSP-1 and anti-β-actin antibodies for LECs and CLMECs **d.** Quantification of the CLMEC TSP-1 band intensity relative to β-actin and normalised to LEC (n=3 each).

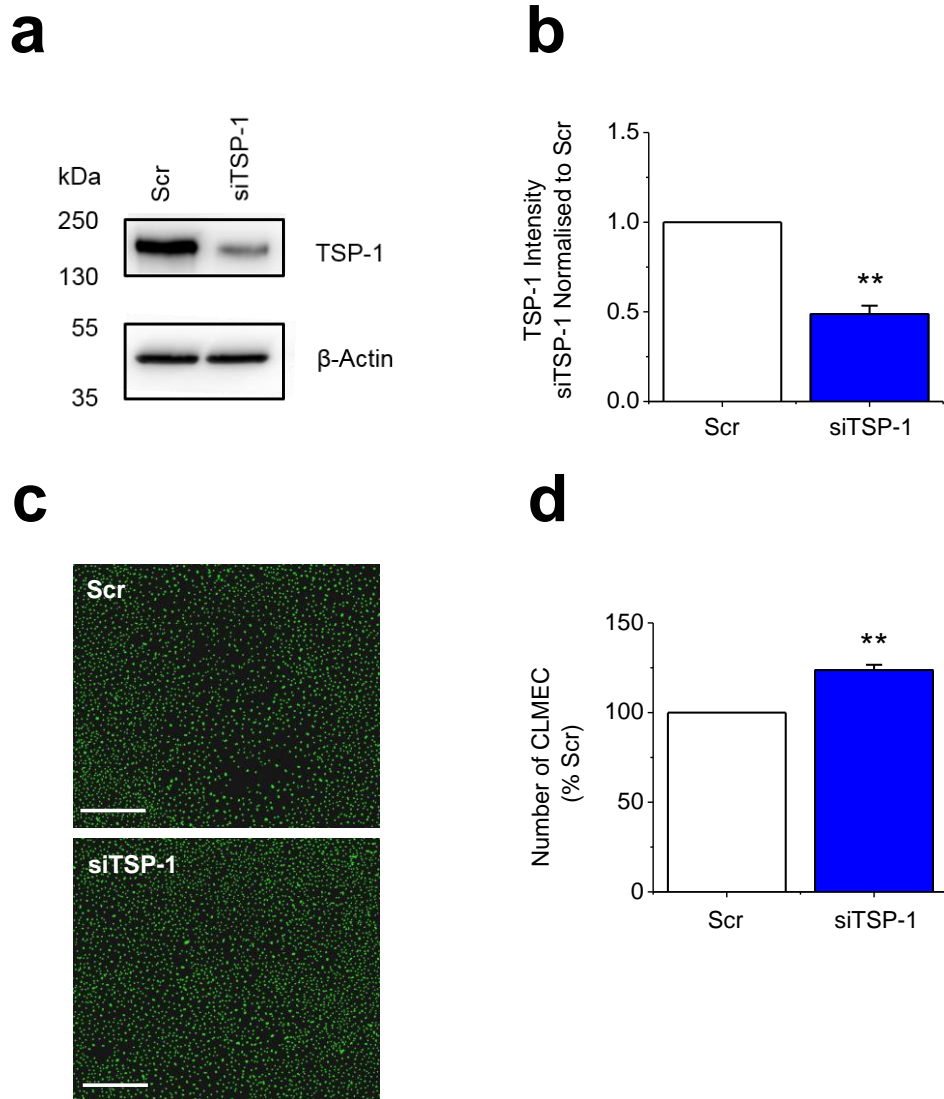
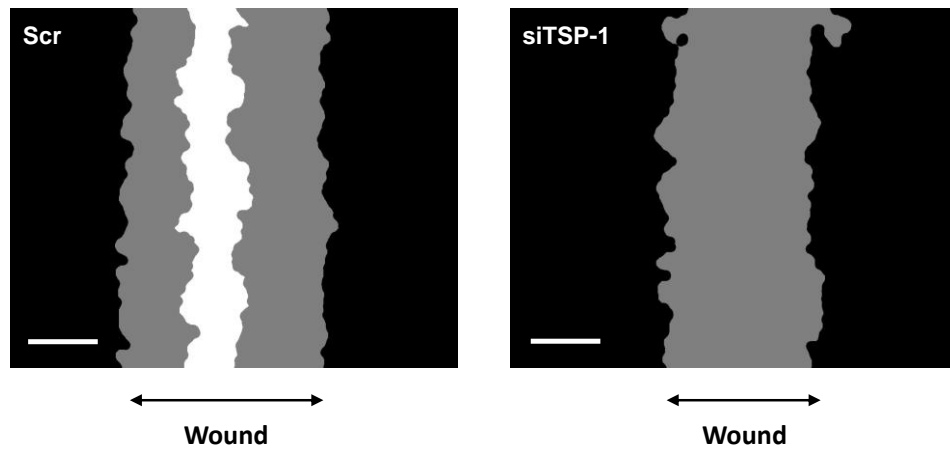


Figure 57 TSP-1 Knockdown Increases Proliferation in CLMECs

a. Example western blot labelled with anti-TSP-1 and anti- β -actin antibodies for CLMECs transfected with scrambled siRNA (Scr) or ON-TARGETplus TSP-1 siRNA (siTSP-1) **b.** Quantification of the siTSP-1 group TSP-1 band intensity relative to β -actin and normalised to the Scr group (n=3 each) **c.** Fluorescence images of CLMECs 48 hrs after transfection with scrambled siRNA (Scr) or ON-TARGETplus TSP-1 siRNA (siTSP-1). Fluorescence was from cell nuclei stained with Vybrant[®] Dye Cycle[™] (green). Scale bars 400 μ m **d.** Quantification of the number of CLMECs seen in the images of the type shown in c. The siTSP-1 group has been normalised to the Scr group (n=3, N=9).

a



b

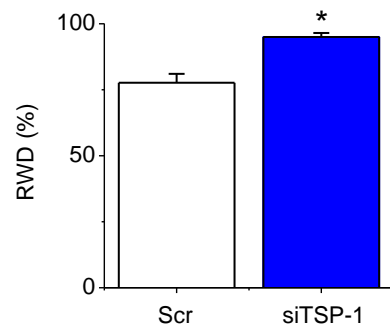


Figure 58 TSP-1 Knockdown Increases Migration in CLMECs

a. Example linear wound mask images after 20 hr migration in CLMECs transfected with scrambled siRNA (Scr) or ON-TARGETplus TSP-1 siRNA (siTSP-1). Black represents cells outside the linear wound, grey represents cells which have migrated into the wound, and white represents no cells. Scale bars 200 μ m **b.** Relative wound density at 20 hrs in CLMECs transfected with ON-TARGETplus TSP-1 siRNA (siTSP-1) or scrambled siRNA (Scr) (n=3, N=9).

6.5 Piezo1 as an Anti-Angiogenic Target

Analysis of the proteomics data revealed that Piezo1 was present in both LECs and CLMECs (Figure 59a). Our laboratory has a special interest in Piezo1 which is a Ca^{2+} permeable mechanosensitive ion channel. In endothelial cells it serves as a sensor of frictional force (shear stress) and determinant of vascular structure in both developmental and adult physiology (Li et al., 2014). There was no difference in Piezo1 expression between LECs and CLMECs (Figure 59b).

Validation of the proteomic results proved difficult with western blotting due, in part, to the lack of a specific antibody against Piezo1. Therefore, an alternative approach was adopted to prove the presence of Piezo1. Although physiologically activated by shear stress, the first chemical activator of Piezo1, Yoda1, was discovered in 2015 (Syeda et al., 2015). Activation of Piezo1 by shear stress causes intracellular Ca^{2+} entry (Li et al., 2014), therefore, intracellular concentrations of Ca^{2+} were measured in response to a range of Yoda1 concentrations in matched LECs and CLMECs. In LECs, Yoda1 could activate Ca^{2+} entry between a range of concentrations (0.05 - 10 μM) (Figure 60a). A concentration-response curve was created for Yoda1 in LECs (Figure 60b) and the calculated EC_{50} was 1.85 μM . Yoda1 could also evoke Ca^{2+} entry in CLMECs at concentrations between 0.05 and 10 μM (Figure 60c). A concentration-response curve for Yoda1 was also created for CLMECs and the EC_{50} was calculated to be 2.47 μM (Figure 60d). Although this mean value was higher than in LECs, there was no statistically significant difference between the two groups (Figure 60e).

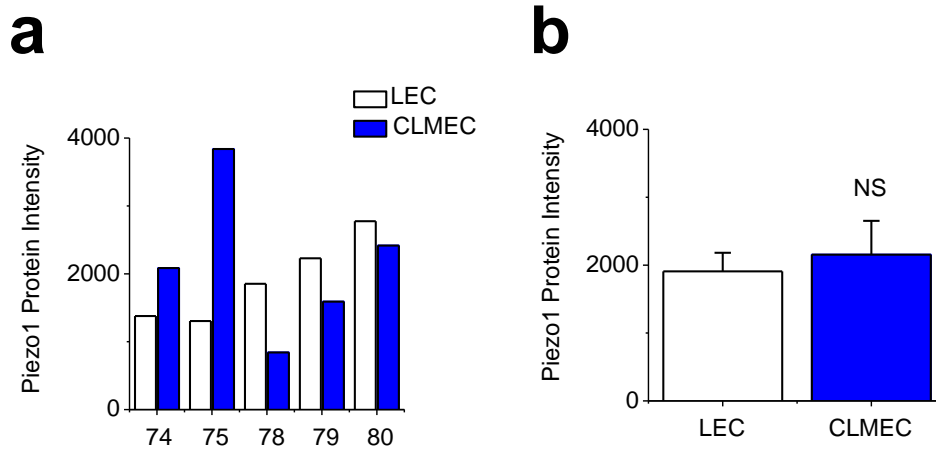


Figure 59 Piezo1 Expression is not Altered in CLMECs

a. Piezo1 protein intensity in LECs and CLMECs determined by proteomic studies in five matched patient samples (n=5) **b.** Mean Piezo1 intensity in all matched LEC and CLMEC samples shown in a

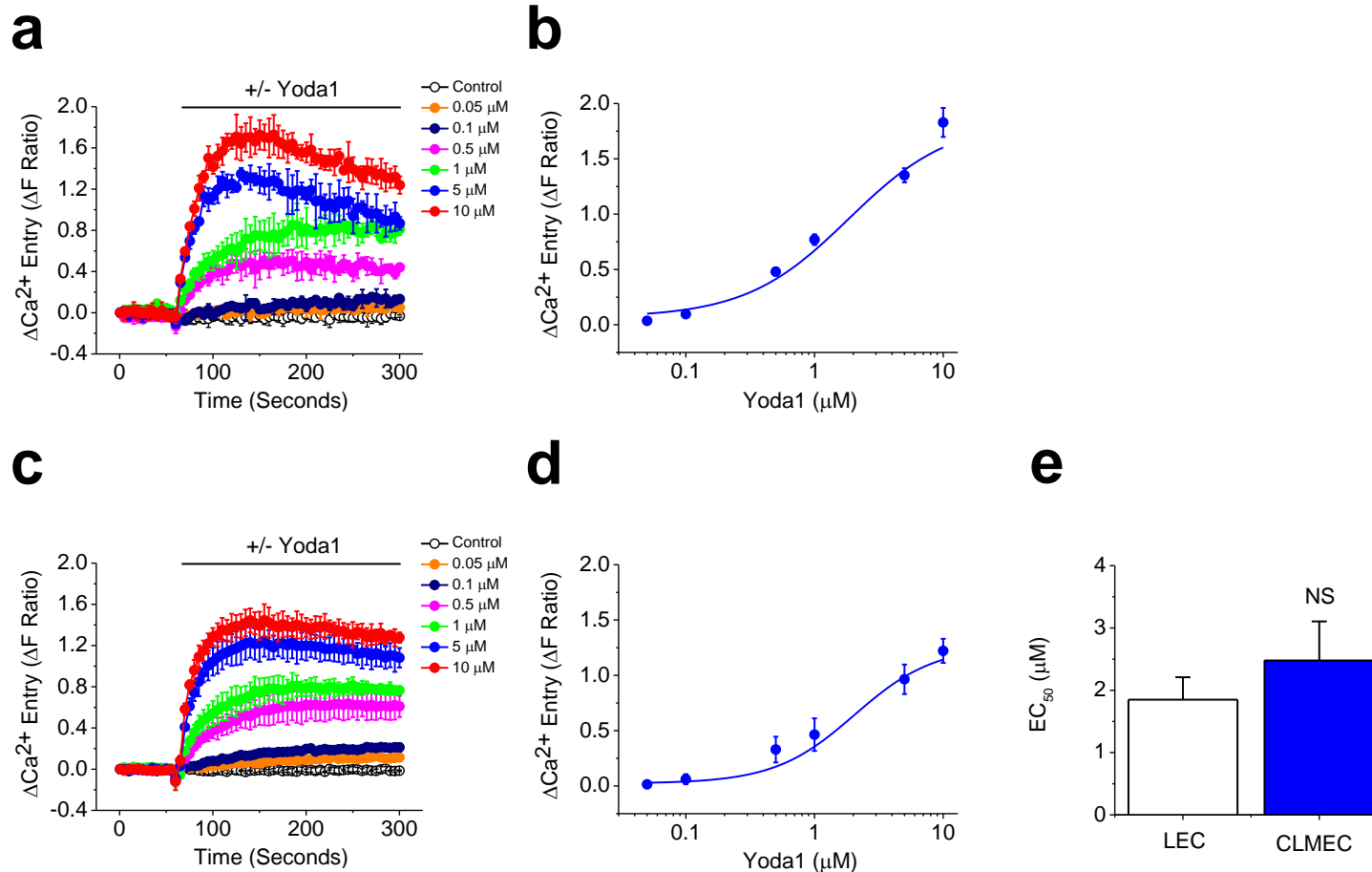


Figure 60 Yoda1 evokes Ca^{2+} Entry in LECs and CLMECs

a. Example Intracellular Ca^{2+} measurement data in LECs in response to a range of Yoda1 concentrations. Traces show averaged responses to a range of Yoda1 concentrations across multiple wells of a 96-well plate compared to control (N=3 wells each) **b.** Yoda1 concentration response curve in LECs measuring intracellular $[\text{Ca}^{2+}]$ at 150 secs (n=3) **c.** Example Intracellular Ca^{2+} measurement data in CLMECs in response to a range of Yoda1 concentrations. Traces show averaged responses to a range of Yoda1 concentrations across multiple wells of a 96-well plate compared to control (N=3 wells each) **d.** Yoda1 concentration response curve in CLMECs measuring intracellular $[\text{Ca}^{2+}]$ at 150 secs (n=3) **e.** Mean data for the derived EC_{50} values for Yoda1 in matched LECs and CLMECs (n=3 each).

6.5.1 Yoda1 Causes Ca²⁺ Entry Specifically Through Piezo1

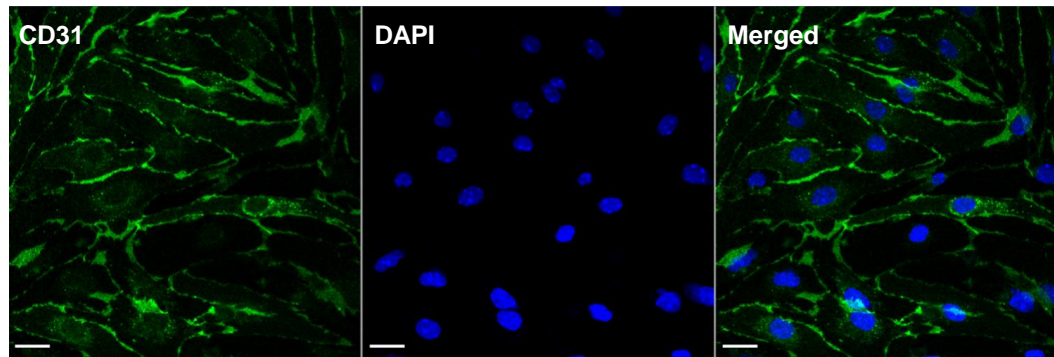
The specificity of Yoda1 to cause Ca²⁺ entry through the Piezo1 channel is unknown and therefore Yoda1 could be causing Ca²⁺ entry through other Ca²⁺ permeable ion channels. To answer this question, use was made of the tamoxifen-inducible endothelial-specific Piezo1 knockout mouse model we have in our laboratory. Generation of the murine model is described in chapter 2.

Mice livers were harvested by Dr Baptiste Rode (University of Leeds) and mouse liver endothelial cells (mLECs) were isolated using an IMS technique similar to that used for the human studies except the CD146 rather than CD31 antibody was used. Immunofluorescent staining of the isolated mLECs confirmed expression of CD31 (Figure 61a). PCR, performed by Dr Baptiste Rode (University of Leeds), confirmed an 88% knockdown of Piezo1 at the mRNA level in mLECs with deleted Piezo1 (Piezo1^{ΔEC}) compared to Control mLECs (Figure 61b). Application of 2 μM Yoda1 caused an increase in intracellular Ca²⁺ that peaked at 150 seconds and was maintained until at least 300 seconds in Control mLECs (Figure 61c). In stark contrast Yoda1 failed to cause any Ca²⁺ entry in Piezo1^{ΔEC} mLECs (Figure 61c,d).

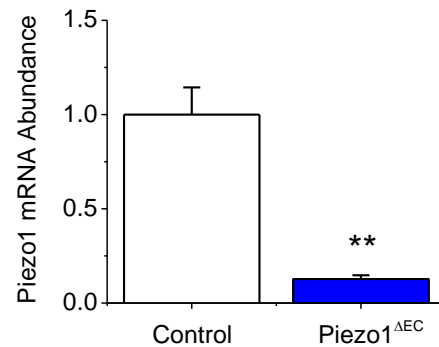
To ensure other mechanisms of Ca²⁺ entry were still functional in the Piezo1^{ΔEC} mLECs, Ca²⁺ entry in response to the physiological agonist ATP and the drug ionomycin was tested. In both Control and Piezo1^{ΔEC} mLECs, 20 μM ATP caused Ca²⁺ entry that peaked at 70 seconds before gradually returning back to baseline levels by 300 seconds (Figure 62a). There was no significant difference in the peak Ca²⁺ entry values between the two groups (Figure 62b). Ionomycin (1 μM) caused Ca²⁺ entry in both Control and Piezo1^{ΔEC} mLECs that peaked at 80 seconds followed by a sustained phase that stayed above the baseline for at least 300

seconds (Figure 62c). Although the mean peak Ca^{2+} entry was lower in the Piezo1^{ΔEC} mLECs, there was no significant difference between the two groups (Figure 62d).

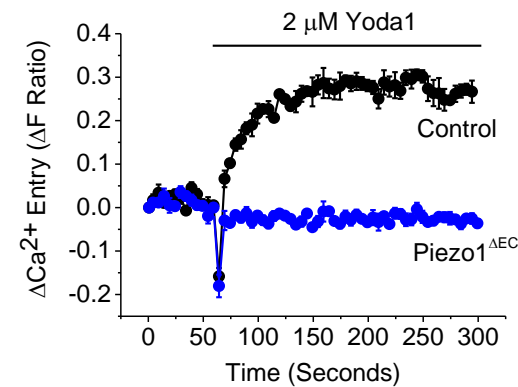
a



b



c



d

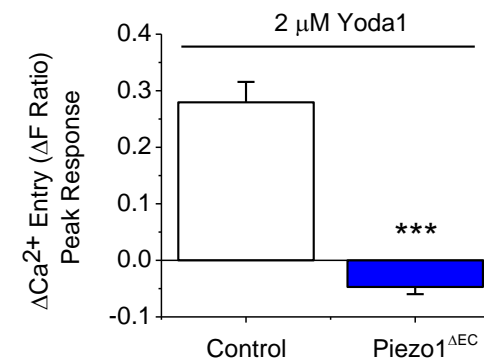


Figure 61 Yoda1 does not Evoke Ca²⁺ Entry in Mouse Liver Endothelial Cells with Piezo1 Knockout

a. Immunofluorescence images of mLECs stained with anti-CD31 antibody (green) and DAPI to label nuclei (blue). Scale bars 20 μm **b.** Piezo1 mRNA expression relative to β-actin in Piezo1 endothelial knockout (Piezo1^{ΔEC}) and Control (Control) mLECs (n=3 each performed by Dr Baptiste Rode, University of Leeds) **c.** Intracellular Ca²⁺ measurement data from Piezo1^{ΔEC} and Control mLECs. Traces show averaged responses to 2 μM Yoda1 across multiple wells of a 96-well plate **d.** Mean data for the peak (200 s) responses to Yoda1 of the type exemplified in c (n=6, N=20 each).

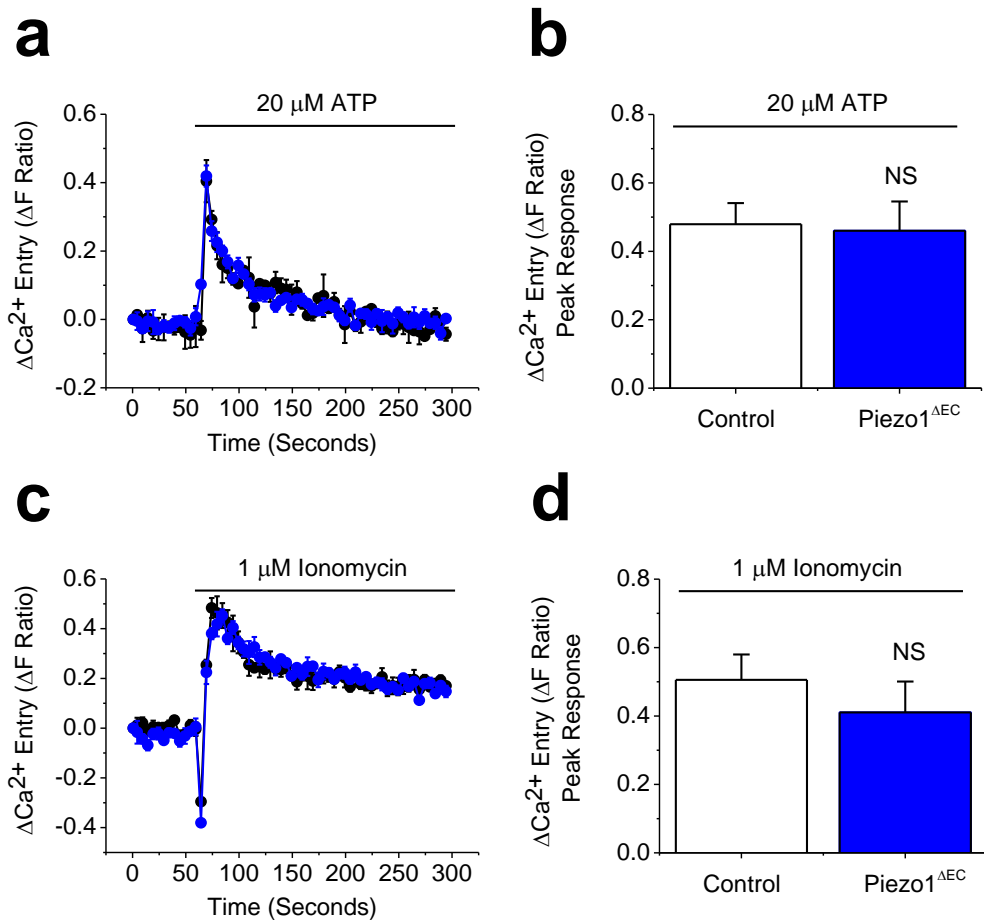


Figure 62 Endothelial Piezo1 Knockout Does Not Effect ATP and Ionomycin Evoked Ca^{2+} Entry in Mouse Liver Endothelial Cells

a. Intracellular Ca^{2+} measurement data from Piezo1 $^{\Delta\text{EC}}$ (blue) and Control (black) mLECs. Traces show averaged responses to 20 μM ATP across multiple wells of a 96-well plate **b.** Mean data for the peak (70 s) responses to ATP of the type exemplified in a (Piezo1 $^{\Delta\text{EC}}$: n=6, N=16, Control: n=4, N=10) **c.** Intracellular Ca^{2+} measurement data from Piezo1 $^{\Delta\text{EC}}$ (blue) and Control (black) mLECs. Traces show averaged responses to 1 μM Ionomycin across multiple wells of a 96-well plate **d.** Mean data for the peak (80 s) responses to Ionomycin of the type exemplified in c (Piezo1 $^{\Delta\text{EC}}$: n=6, N=16, Control: n=4, N=10).

6.5.2 Yoda1 Causes eNOS Phosphorylation in CLMECs

Shear stress causes intracellular Ca^{2+} entry through Piezo1 and is able to induce phosphorylation of eNOS at Ser-1177 (Li et al., 2014). eNOS is responsible for nitric oxide (NO) synthesis, which is able to regulate angiogenesis (Cooke and Losordo, 2002). To see if Yoda1 was also capable of inducing phosphorylation of eNOS at Ser-1177, CLMECs were treated with Yoda1 (2 μM) or vehicle control for 1 minute and levels of eNOS and peNOS-S1177 were measured using western blotting. Yoda1 clearly induced phosphorylation of eNOS at Ser-1177, whereas its vehicle control did not (Figure 63a). Quantification of the peNOS-S1177 band intensity relative to the eNOS band intensity revealed peNOS-S1177 to be up-regulated 2.2 fold with Yoda1 treatment (Figure 63b).

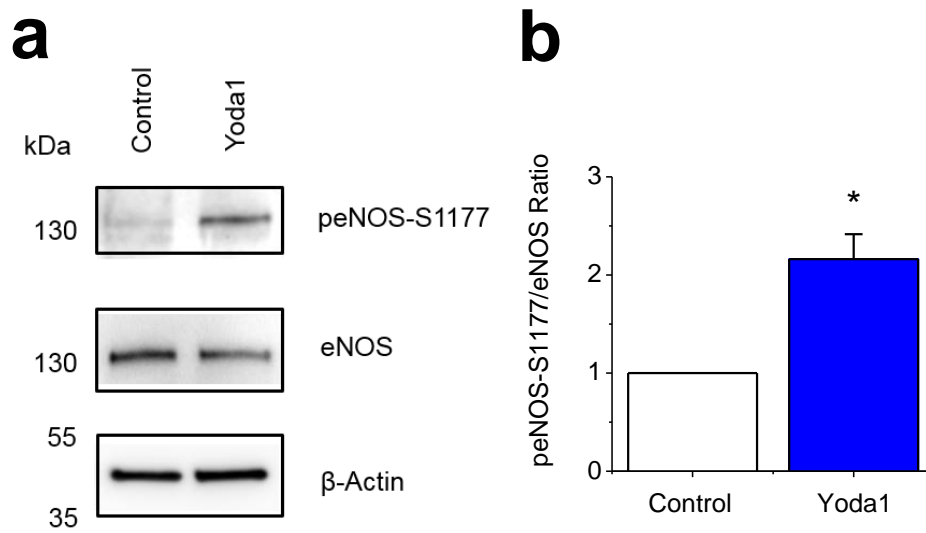


Figure 63 Yoda1 Induces Phosphorylation of eNOS at Ser-1177 in CLMECs

a. Example western blot labelled with anti-peNOS-S1177, anti-eNOS and anti-β-actin antibodies for CLMECs treated with Yoda1 (2 μM) or vehicle control **b.** Quantification of the Yoda1 peNOS-S1177 band intensity relative to eNOS and normalised to vehicle control (n=3 each).

6.6 Summary of Findings

- Proteomics studies have identified 157 proteins that are differentially expressed in LECs and CLMECs
- LECs and CLMECs express a wide range of endothelial cell markers
- CLMECs up-regulate VEGFR-1 and down-regulate vWF
- TSP-1, an endogenous inhibitor of angiogenesis, is the most significantly up-regulated protein in CLMECs
- siRNA mediated knockdown of TSP-1 increases CLMEC proliferation and migration
- LECs and CLMECs both express Piezo1
- Yoda1 evokes intracellular Ca²⁺ entry in LECs and CLMECs
- Yoda1 causes Ca²⁺ entry specifically through Piezo1 in endothelial cells
- Yoda1 causes eNOS phosphorylation in CLMECs

6.7 Discussion

The aim of this chapter was to identify differentially expressed proteins in matched LECs and CLMECs using proteomic studies. In total, 157 proteins were found to be differentially expressed between the two groups. Both LECs and CLMECs positively expressed a broad range of endothelial markers with significant down-regulation of vWF and up-regulation of VEGFR-1 in CLMECs. CLMECs also significantly up-regulated TSP-1, a known endogenous anti-angiogenic substance. Genetic knockdown of TSP-1 with pooled siRNA significantly increased proliferation and migration in CLMECs. For the first time, Piezo1 was shown to be expressed in LECs and CLMECs. Modulation of the Piezo1 channel with Yoda1 lead to Ca²⁺ entry and phosphorylation of eNOS.

6.7.1 Validation of LECs and CLMECs

Proteomic studies of matched LECs and CLMECs provided a further opportunity to validate the endothelial nature of the cells that were being isolated. As previously discussed, no specific endothelial marker exists that is expressed by all types of endothelial cells. Therefore, in chapter 3, CLMECs were characterised by testing for the expression of several well established endothelial markers (CD31, vWF, VEGFR-2, eNOS, VE-Cadherin) and for functional properties of endothelial cells (alignment, tube formation). In this chapter, a list of 23 endothelial markers was generated based upon a previous study (Garlanda 1997). Proteomics revealed that LECs and CLMECs expressed 16 out of the 23 markers. VEGFR-2, Tie-2, CD34, ACE, E-Selectin, CD141 and VCAM-1 were not detected. This could be because the isolated endothelial cells truly do not express these markers, or it could be because of the proteomics methodology. A case for the latter point is VEGFR-2, which was easily detectable by western blot in LECs and CLMECs, but was not

detected in the proteomics study. This could be for a number of reasons including the digestion method used to break up the protein into peptides which are then detected by mass spectrometry. Failure of the digestion process to break up the protein or digestion that results in unrecognisable peptide sequences will mean peptides are not detected by mass spectrometry. For this reason, all potential “hits” were confirmed by performing western blots. For the remaining six endothelial markers that were not detected by proteomics, it would be important to confirm their absence with western blot.

6.7.2 Results of The Proteomics Study

The proteomics study revealed 157 proteins that were differentially expressed between LECs and CLMECs (Appendix I). A small number of these proteins are known to have roles in angiogenesis, however the vast majority are not.

Several endothelial markers showed different expression levels in LECs and CLMECs. There was up-regulation of VEGFR-1 and Fibronectin (isoform 17) and down-regulation of vWF in CLMECs. vWF is a blood glycoprotein that has a role in haemostasis and is synthesised in endothelial cells and stored in Weibel-Palade bodies. The presence of vWF in CLMECs was confirmed in Chapter 3, with immunofluorescent staining clearly revealing the presence of Weibel-Palade bodies that could be seen as peri-nuclear rod-shaped granules. Western blotting also confirmed the proteomics result. The reason for vWF down-regulation is unclear, however, several studies support this finding. Firstly, vWF has been reported to be significantly down-regulated in primary colorectal cancer endothelial cells compared to matched healthy colon endothelial cells (Schellerer et al., 2007). Therefore, this could be an important mechanism for both primary and metastatic colorectal cancer

angiogenesis. Secondly, apart from its major role as a platelet adhesion molecule, endothelial vWF also has a role in leucocyte adhesion and the regulation of inflammation (Pendou et al., 2006). Therefore, down-regulation may be a form of tumour defence against the host immune system. Furthermore, angiogenesis increases in HUVECs depleted of vWF by siRNA in vitro and it is also increased in vWF deficient mice in vivo (Starke et al., 2011). This is thought to be due to the essential role of vWF in forming Weibel-Palade bodies, which also store Ang-2. With vWF deficiency and reduced Weibel-Palade bodies Ang-2 cannot be stored, resulting in its dysregulated release. Ang-2 is known to promote VEGF-dependent stimulation of endothelial cells to migrate and sprout.

Isoform 17 of fibronectin was upregulated in all CLMEC patient samples in the proteomics study, however, western blotting for fibronectin found the opposite result, that it was down-regulated in CLMECs. This may mean that the specific isoform 17 of fibronectin has importance in CLMEC angiogenesis. Unfortunately there is no commercial antibody available against isoform 17 of fibronectin so the proteomics result could not be validated. Fibronectin is an extracellular matrix protein and known endogenous inhibitor of angiogenesis that acts through integrin signalling (Avraamides et al., 2008). Unlike other endogenous inhibitors of angiogenesis identified in the proteomics (VEGFR-1, TSP-1), fibronectin was down-regulated in CLMECs. Targeted down-regulation of fibronectin maybe an angiogenesis promoting mechanism in CLMECs. Further work will be needed to determine the significance of this result.

In chapter 3, CD31 was found to be down-regulated in CLMECs with western blotting. This was not confirmed in the proteomics study. Although it was clearly

down-regulated in four out of five samples, it was up-regulated in one sample resulting in an overall p-value of 0.06. Interestingly, when the patient characteristics of each sample are reviewed, CD31 is down-regulated in all patients with metachronous CLM but up-regulated in the only patient with synchronous metastases. Similarly, ICAM-1, another adhesion molecule, is clearly down-regulated in four out of five samples with an overall p-value of 0.06. The only sample it was up-regulated in was again the patient with synchronous CLM. Adhesion molecules such as ICAM-1 and VCAM-1, have previously been reported to be down-regulated in the tumour endothelium (Griffioen et al., 1996, Alessandri et al., 1999). This is thought to be a form of tumour defence because leucocytes are less able to bind to these adhesion molecules and leave the circulation to attack the tumour. Although impossible to determine based upon one synchronous tumour, these results may suggest a difference in biology between synchronous and metachronous CLM, specifically in terms of ability to evade the host's immune system.

A number of studies have been performed comparing the proteome of TECs with that of healthy endothelial cells. To date, four studies have analysed protein expression in matched culture-expanded endothelial cells from colorectal cancer and healthy colon tissue (van Beijnum et al., 2006, Schellerer et al., 2007, Jayasinghe et al., 2009, Mesri et al., 2013) and no study has looked at differences in endothelial cell protein expression in CLM. As previously mentioned, work in this chapter supports that of Schellerer et al., in that vWF is down-regulated in CLMECs. Jayasinghe et al., reported VEGFR-1 and s-VEGFR-1 to be non-significantly reduced in colorectal cancer endothelial cells compared to healthy colon endothelial cells. Although not significant, this is the opposite effect to what has been observed in LECs and CLMECs. van Beijnum et al., identified seventeen

genes up-regulated in colorectal cancer endothelial cells. Nine of these proteins were detected in the proteomics study and one was significantly up-regulated in CLMECs, insulin-like growth factor binding protein 7. This is also in agreement with other studies (St Croix et al., 2000). Mesri et al., identified 56 proteins overexpressed in colorectal cancer endothelial cells. Thirty-three of these were detected in the current proteomic study and one of these proteins was significantly up-regulated in CLMECs, lysosomal-associated membrane protein 2.

In 2000 St Croix et al., reported nine transcripts thought to be specific markers for tumour endothelial cells. Termed Tumour Endothelial Markers (TEM 1-9), these genes showed a 10-fold up-regulation compared to healthy endothelial cells (St Croix et al., 2000). None of the TEMs were detected in the current proteomic study. However, it is important to note that the validity of these markers has been questioned, as they are also expressed in a number of different cell types (MacFadyen et al., 2007, Halder et al., 2009). Only two proteins were exclusively expressed in CLMECs, Tumour necrosis factor receptor superfamily member 10D and Mediator of RNA polymerase II transcription subunit 6. Unfortunately expression levels in CLMECs were low and both proteins are widely expressed in a range of other cell types.

Unfortunately the proteomic study did not detect WEE1. This is most likely due to the digestion process used to prepare the sample as in chapters 3 and 4 WEE1 could be clearly detected with western blotting in LECs and CLMECs. Furthermore, the target protein of WEE1, CDK1, was detected in the proteomics study and its expression was unchanged.

6.7.3 Identification of Further Anti-Angiogenic Targets in CLM

6.7.3.1 Thrombospondin-1

Thrombospondins are a family of five multidomain, Ca²⁺-binding extracellular glycoproteins found in a wide variety of cell types. TSP-1 was the first family member identified and has been studied the most intensively. TSP-1 was the first protein to be shown to play a critical role as a naturally occurring inhibitor of angiogenesis (Zhang and Lawler, 2007). TSPs interact with a wide range of other proteins and as such, their functions are dynamic and diverse.

TSP-1 antagonizes VEGF in several ways, via inhibition of VEGF release from the extracellular matrix, direct interaction, and inhibition of VEGF signal transduction (Lawler and Lawler, 2012). Critical to the anti-angiogenic function of TSP-1 is a central domain containing three type 1 repeats (TSRs). Via its TSRs, TSP-1 is able to bind matrix metalloproteinases, suppressing their activity. This results in decreased release of VEGF from the extracellular matrix and suppression of angiogenesis (Rodriguez-Manzaneque et al., 2001). TSP-1 can bind directly to VEGF, which mediates its uptake and removal from the extracellular space (Greenaway et al., 2007). Finally TSRs can interfere with VEGF signal transduction through their interaction with CD36. The interaction of CD36 with TSP-1 down regulates the VEGFR-2 phosphorylation normally invoked by VEGF-A, the main regulator of angiogenesis (Primo et al., 2005). An association of CD36 with β 1 integrins also appears necessary for the inhibition of VEGFR-2 phosphorylation by TSP-1 (Primo et al., 2005). TSP-1 is an important antagonist of the VEGF-Nitric Oxide (NO) signalling pathway and powerfully counteracts the proangiogenic signals generated. Normally VEGF induces phosphorylation of Ser1177 on eNOS via both PI3K-AKT and PLC γ -AMPK pathways, which drives the production of NO.

NO then binds to the prosthetic heme on soluble guanylate cyclase to stimulate cyclic guanosine monophosphate synthesis, which acts to promote endothelial cell migration, proliferation, and survival, as well as vascular permeability (Isenberg et al., 2009).

In the proteomics study, TSP-1 was upregulated 2.8 times in CLMECs compared to LECs and this was validated with western blotting. This could be a consequence of prolonged exposure to high concentrations of VEGF found in the tumour microenvironment. Up-regulation of TSP-1 may therefore be an attempt to balance pro-angiogenic and anti-angiogenic factors. TSP-1 was shown to have a functional role in CLMEC proliferation and migration, with knockdown of TSP-1 increasing both these processes. However, synthetic analogues of TSP-1 have been unsuccessful in clinical trials (Markovic et al., 2007). This may be because TSP-1 is already significantly up-regulated and the addition of more TSP-1 is unable to inhibit angiogenesis any further. Alternatively, tumours may resort to angiogenic pathways independent of VEGF, meaning TSP-1 will have less effect. Promising results with TSP-1 in vitro have not translated to patient success. Further work is needed to determine why tumours appear to be resistant to TSP-1 targeted therapy.

6.7.3.2 VEGFR-1/sVEGFR-1

Proteomic studies demonstrated a 2.5 times increase in VEGFR-1 expression in CLMECs, with all five individual patient samples showing a higher expression in CLMECs compared to LECs. VEGFR-1 binds VEGF-A, VEGF-B and PGF and is thought to be a negative regulator of angiogenesis, either by acting as a decoy receptor for VEGF or by suppressing VEGF signalling through VEGFR-2 (Yang et

al., 2011). Homozygous deletion of VEGFR-1 in mice results in embryonic lethality due to the overgrowth of endothelial cells, resulting in disorganised and dysfunctional vasculature (Fong et al., 1995). VEGFR-1 expresses two types of mRNA, one which encodes the full length receptor and one which encodes a short soluble protein known as soluble (s)VEGFR-1. sVEGFR-1 has been shown to bind VEGF with high affinity and inhibit its mitogenic activity in endothelial cells (Kendall and Thomas, 1993). Expression of VEGF and sVEGFR-1 is induced by hypoxia, for instance, in the tumour microenvironment (Wu et al., 2010). A plethora of in vivo studies have demonstrated that gene transfer of sVEGFR-1 can inhibit tumour angiogenesis (Yang et al., 2011). In one such study, bone-marrow derived stromal cells were used to deliver sVEGFR-1 gene therapy to metastatic colon cancers. sVEGFR-1 gene therapy was shown to decrease metastatic disease and prolong survival time through inhibition of angiogenesis (Hu et al., 2008)

Targeting VEGFR-1 and sVEGFR-1 for the development of anti-angiogenic therapy has had promising results, but nevertheless research is in its infancy. Much work needs to be done to understand the exact anti-angiogenic mechanism of VEGFR-1/sVEGFR-1, consequences of anti-VEGF therapy for VEGFR-1/sVEGFR-1 expression and the role of VEGFR-1/sVEGFR-1 as prognostic markers. The data in this study encourage further investigation of VEGFR-1/sVEGFR1. Both VEGFR-1 and sVEGFR-1 were up-regulated in CLMECs which may be a consequence of prolonged exposure to high concentrations of VEGF in the tumour microenvironment. To combat the high expression of VEGF, the up-regulation of VEGFR-1 and sVEGFR-1 could serve to prevent excessive VEGFR-2 signalling and decrease angiogenesis.

6.7.3.3 Piezo1

Endothelial cells have pronounced sensitivity to the frictional force of shear stress. Physiologically, shear stress is generated by blood flow. The detection of shear stress by endothelial cells enables vascular development, however, the mechanisms that underlie this process have been unclear. Initially, important studies showed that shear stress evoked Ca^{2+} entry in endothelial cells (Schwarz et al., 1992). Although a number of ion channels have been reported to be important in shear stress sensing, recent work in our laboratory showed the mechanosensitive ion channel Piezo1 to be critical for shear-stress evoked Ca^{2+} signalling and non-selective cationic channel current activity in endothelial cells (Li et al., 2014). Piezo1 knockout was embryonic lethal in mice at E9.6-11.5, shortly after the time when the murine heart starts to beat and when important vascular structures should first emerge. Analysis of the embryonic yolk sacs revealed disrupted vascular structures. There were even disturbances in the vasculature of haploinsufficient mice, where endothelial cells failed to align in the direction of flow compared to wildtype animals. The critical role of Piezo1 in vascular development is of potential oncological interest, as tumours must develop their own blood supply for growth and metastatic spread. Could inhibition of Piezo1 be a potential anti-angiogenic treatment strategy? Genetic knockdown of Piezo1 in HUVECs inhibits tube formation in vitro and in vivo (Li et al., 2014). However, at present there are no specific inhibitors of Piezo1. Non-specific blockers of Piezo1 include ruthenium red and the spider toxin *Grammostola spatulata* (Coste et al., 2010, Bae et al., 2011).

Proteomic studies showed no difference in expression of Piezo1 between LECs and CLMECs. Western blotting to detect Piezo1 was unsuccessful due to the lack of a specific antibody. Fortunately the first chemical activator of Piezo1, Yoda1, was

discovered in 2015 (Syeda et al., 2015) and this was used to indirectly confirm Piezo1 expression through measurements of intracellular Ca^{2+} entry. Yoda1 was able to induce Ca^{2+} entry in both LECs and CLMECs and although the mean EC_{50} for Yoda1 was higher in CLMECs, it was not statistically significant, suggesting no difference in channel expression. To prove that Yoda1 caused Ca^{2+} entry specifically through Piezo1 and not through another ion channel, experiments were performed on liver endothelial cells isolated from mice with a tamoxifen-inducible endothelial specific Piezo1 knockout. Phenotypically there was no difference in culture between Piezo1 $^{\Delta\text{EC}}$ and Control mLECs. Strikingly, Yoda1-evoked Ca^{2+} entry was completely abolished in the Piezo1 knockout endothelial cells. This suggests that Yoda1-evoked Ca^{2+} entry is specifically through Piezo1 and indirectly confirms the presence of Piezo1 channels in LECs and CLMECs. Ca^{2+} entry in response to ionomycin and ATP were unaffected with Piezo1 knockout.

The tumour vasculature is highly abnormal and is functionally and morphologically distinct from healthy blood vessels. Tumour blood vessels are chaotic in nature. They are tortuous, dilated, elongated and leaky with many vessels ending blindly (Dudley, 2012). There is also considerable variability in vessel diameter. This results in a heterogeneous rate of blood flow throughout the tumour, with areas of high and low shear stress. The effects of shear stress on tumour vessel angiogenesis are not fully understood. At low levels of shear stress, indicative of a poorly-perfused vessel, endothelial cells sprout to seek new sources of blood flow (Jain et al., 2014). At the other end of the spectrum, high shear stress is capable of inducing vessel branching through intussusceptive angiogenesis (Djonov et al., 2002). Shear stress induces Ca^{2+} entry through Piezo1 leading to calpain activation, proteolytic cleavage of actin cytoskeletal and focal adhesion proteins and endothelial cell reorganisation (Li et al., 2014). Piezo1 channels could represent a

therapeutic target whereby chemical inhibition of Piezo1 abolishes angiogenesis signalling pathways caused by shear stress.

A completely contrasting concept is that activation of Piezo1 in the tumour vasculature could encourage vessel normalization and be beneficial. Vessel normalization improves tumour blood flow, reducing hypoxia and VEGF secretion leading to decreased sprouting angiogenesis through VEGF/VEGFR-2 signalling. Furthermore, as argued by Jain, vessel normalization could improve drug delivery to the tumour enhancing the efficacy of current therapeutic agents (Carmeliet and Jain 2011).

eNOS is capable of synthesising NO, a key regulator of blood pressure, vascular remodelling and angiogenesis, from the amino acid L-arginine. In endothelial cells, NO regulates a number of cellular processes including proliferation, migration, extracellular matrix degradation, and angiogenesis (Cooke and Losordo, 2002). eNOS is a 1,203 amino acid, 133 kDa protein which has a bi-domain structure and functions as a dimer. It consists of an N-terminal oxygenase domain containing binding sites for heme, L-arginine and tetrahydrobiopterin (BH₄) and a COOH-terminal reductase domain with binding sites for nicotinamide adenine dinucleotide phosphate (NADPH), flavin mononucleotide (FMN), flavin adenine dinucleotide (FAD) and Ca²⁺/Calmodulin (CaM) (Fleming, 2010). During the synthesis of NO, NADPH derived electrons are transferred to FAD, FMN and then to the heme located in the oxygenase domain of the opposing monomer. This allows the heme iron to bind oxygen and catalyse the stepwise synthesis of NO from L-arginine. It was originally thought that eNOS was a CaM dependent enzyme (Fleming, 2010). In basal conditions caveolin (Cav) maintains eNOS in an inactivated state.

Increases in intracellular $[Ca^{2+}]$, lead to disruption of the eNOS-Cav interaction by Ca^{2+} bound CaM. Association of CaM with its binding site is generally accepted to activate NO synthesis by enabling the reductase domain to transfer electrons to the oxygenase domain (Fleming, 2010).

A number of studies have shown that eNOS activity can be regulated without increasing intracellular $[Ca^{2+}]$, for instance by glycosylation, phosphorylation and protein partners (Fleming, 2010). eNOS can be phosphorylated at multiple sites, but most research has focussed on two residues, Ser-1177, which increases eNOS activity and Thr-495, which decreases eNOS activity. Ser-1177 is rapidly phosphorylated in HUVECs following application of shear stress (Dimmeler et al., 1999) or VEGF (Dimmeler et al., 2000). The kinases involved in phosphorylation of Ser-1177 vary based upon the stimulant, for instance, shear stress elicits phosphorylation via protein kinase A (PKA) whereas VEGF acts via AKT. Phosphorylation of Ser-1177 is thought to disable an inhibitory control element that normally interferes with the interaction between the two flavin moieties and attenuates electron transfer in a CaM-independent manner (Balligand et al., 2009).

Yoda1 was able to induce phosphorylation of the Ser-1177 residue of eNOS in CLMECs. This site was investigated because shear stress acting through Piezo1 is able to cause Ser-1177 phosphorylation (Li et al., 2014) and therefore as a Piezo1 activator, the same would be expected of Yoda1. Exactly how Yoda1 causes Ser-1177 phosphorylation is unclear, but the response is relatively quick, as cells were treated for 1 minute with Yoda1. Phosphorylation of Ser-1177 could occur through PKA as is the case with shear stress activation or as Yoda1 causes an increase in intracellular Ca^{2+} it could act through Ca^{2+} /calmodulin-dependent protein kinase II

(CaMKII) to cause Ser-1177 phosphorylation (Fleming et al., 2001). Further work is needed to determine the exact mechanism by which Yoda1 causes eNOS Ser-1177 phosphorylation. However, this result further supports that inhibition of Piezo1 could have anti-angiogenic effects by reducing eNOS phosphorylation and NO production.

Piezo1 is a potentially interesting target for the development of future anti-angiogenic therapeutics. Initial work will need to focus on the benefit of activating or inhibiting Piezo1 for the reasons discussed above. The discovery of Yoda1 has certainly helped better understand the properties of Piezo1. Work in this chapter has, for the first time, shown Yoda1 to specifically cause intracellular Ca^{2+} entry through Piezo1 in CLMECs. Yoda1 will therefore be integral to the development of small molecule Piezo1 inhibitors.

6.7.4 Conclusion

Proteomic analysis has shown both LECs and CLMECs to express a plethora of endothelial markers. Furthermore 157 proteins have been identified that are differentially expressed in CLMECs and LECs. These represent potential treatment targets that may be critical to the survival and expansion of CLMECs. The established endogenous angiogenesis inhibitor TSP-1 was the most significantly up-regulated protein in CLMECs and has been shown to have a role in CLMEC proliferation and migration. For the first time, the mechanosensitive, Ca^{2+} permeable ion channel Piezo1 has been shown to be expressed in CLMECs. Modulation of the Piezo1 channel with Yoda1 evokes intracellular Ca^{2+} entry and eNOS phosphorylation and therefore it may be a potential anti-angiogenic target for the treatment of CLM.

Chapter 7: Conclusions and Future Work

The aim of this study was to identify novel protein targets in CLMECs that could be used in the future for the development of anti-angiogenic therapies for the treatment of CLM. For the first time CLMECs have been isolated, cultured and characterised from patients undergoing curative surgery for CLM. CLMECs behave similar to other endothelial cell types, but harbor differences in expression levels of a number of proteins compared to matched LECs (Table 11). WEE1 has been identified as a potential anti-angiogenic target that is up-regulated in CLMECs. AZD1775, a small molecule WEE1 inhibitor, inhibits CLMEC proliferation, migration and tube formation in vitro by causing DS-DNA breaks and caspase-3 dependent apoptosis due to a critical nucleotide shortage. Known endogenous inhibitors of angiogenesis, TSP-1 and VEGFR-1 have been confirmed to be present and up-regulated in CLMECs. Finally, Piezo1 has been confirmed to be present in CLMECs. This protein, which has a critical role in vasculature development in both embryogenesis and adult physiology, is a mechanosensitive Ca^{2+} permeable ion channel. Yoda1 has been confirmed to be a specific activator of Piezo1 in endothelial cells resulting in eNOS phosphorylation. Future work will, in part, involve investigating the importance of this channel in tumour angiogenesis.

7.1 Summary of Key Findings

- Isolated CLMECs behave similarly to other endothelial cells; they grow in a cobblestone appearance in vitro, they form lattice like structures on Matrigel® and they align in response to shear stress.
- CLMECs express a number of common endothelial cell markers including CD31, VEGFR-2, VE-Cadherin, vWF and eNOS.
- CLMECs have decreased expression of VEGFR-2 and VEGF evokes significantly less Ca²⁺ entry compared to matched LECs.
- WEE1 is up-regulated in CLMECs and AZD1775 is able to inhibit CLMEC proliferation, migration and tube formation in vitro.
- AZD1775 causes DS-DNA breaks and caspase-3 dependent apoptosis in CLMECs as a result of critical nucleotide shortage (Figure 64).
- The dominant mechanism of action of AZD1775, either as a monotherapy or part of a combination therapy, is through its ability to cause DS-DNA breaks rather than premature mitosis.
- Proteomic screening has identified 157 proteins that are differentially expressed between matched LECs and CLMECs giving rise to potential further anti-angiogenic targets (Table 11).

- Known endogenous inhibitors including VEGFR-1 and TSP-1 have been confirmed to be up-regulated in CLMECs.
- Piezo1 is expressed in CLMECs and activation by Yoda1 causes Ca^{2+} entry and eNOS phosphorylation

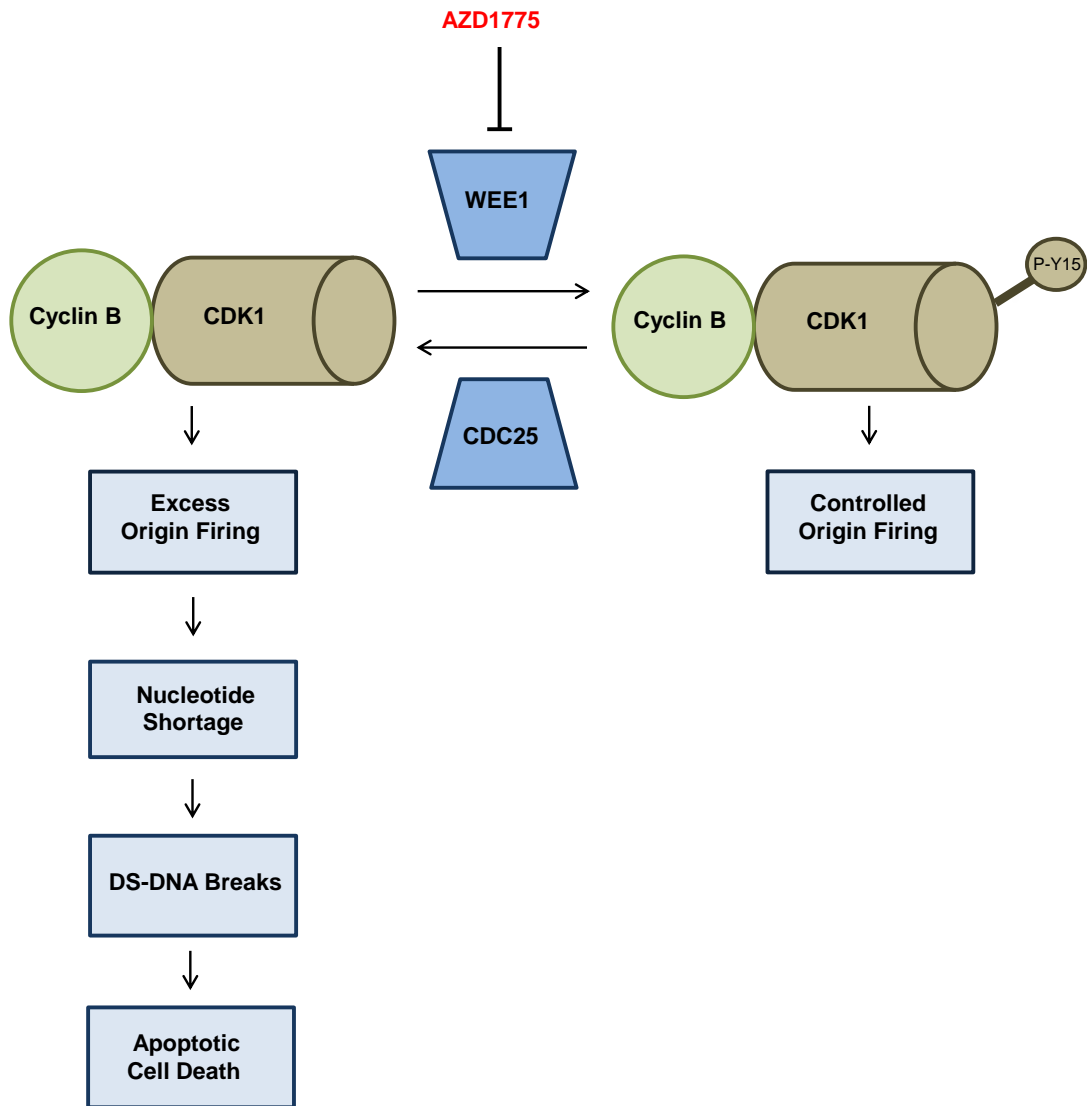


Figure 64 Proposed Mechanism of Action of AZD1775 in CLMECs

CDK1 is regulated by WEE1 and controls origin firing during DNA synthesis. WEE1 inhibition with AZD1775 prevents the inhibitory phosphorylation of cyclin B bound CDK1 at its Tyr15 residue. This results in increased active CDK1 and excessive origin firing. Nucleotide stores are exhausted due to increased DNA replication rates which leads to replication fork stalling and DS-DNA breaks. This results in caspase-3 dependent apoptotic cell death.

Protein	Up- or Down-Regulated in CLMECs	Fold Change	P Value
CD31	↓	0.36	0.001
vWF	↓	0.37	0.006
Thrombospondin-1	↑	2.43	0.009
sVEGFR-1	↑	1.65	0.009
VEGFR-2	↓	0.46	0.017
VEGFR-1	↑	1.52	0.020
WEE1	↑	1.74	0.029
Fibronectin	↓	0.46	0.047

Table 11 Validated Alterations in Protein Expression in CLMECs

Summarised data for changes in protein expression in matched LECs and CLMECs. All changes in protein expression have been confirmed with western blot and ranked according to their p value.

7.2 Future Directions

7.2.1 The Functional Importance of WEE1 in the Endothelium in vivo

Work in chapters 3 and 4 demonstrated clearly that WEE1 is upregulated in CLMECs and that targeted inhibition of WEE1 with AZD1775 blocked several angiogenic processes. Although AZD1775 is currently being investigated in clinical trials for its anti-cancer activity, none of these trials are set-up to review anti-angiogenic activity. Furthermore, determining true anti-angiogenic activity may be difficult as AZD1775 can also kill tumour cells. What these trials can determine however, is cardiovascular complications that may arise due to the anti-angiogenic activity of AZD1775. Existing trials have reported minimal cardiovascular complications (Do et al., 2015) but it is important that studies look for these adverse events, particularly in patients with pre-existing cardiovascular disease.

A murine model of CLM already exists in the University of Leeds (Hawcroft et al., 2012). In this, 11 week old female BALB/c mice are injected with 1×10^6 viable Mouse Colon-26 (MC26) cells percutaneously into the spleen under ultrasound guidance. This reliably generates liver metastases within two weeks. AZD1775 could be delivered orally to these mice to determine the efficacy of WEE1 inhibition as a treatment for CLM. Although, it would be difficult to differentiate between anti-angiogenic and anti-tumour effects it would provide valuable insight into the overall oncological benefit of AZD1775 treatment in CLM patients.

One way of investigating anti-angiogenic activity in vivo would be the generation of a tamoxifen-inducible, endothelial specific, WEE1 knockout murine model. This would follow the same principles of the Piezo1 murine model used in this report.

After induction of endothelial WEE1 knockout, colorectal cancer cells could be implanted subcutaneously and after a set time period tumours could be harvested and vessel micro-density could be measured to assess vascularisation of tumours compared to controls. Alternatively, MC26 cells could be injected into the splenic vein to generate CLM. Using this approach, WEE1 could be knocked out after CLM are established to see if it prevents their growth, or alternatively, prior to tumour cell injection to see if this prevents CLM generation. Although these latter studies could provide important information about when WEE1 inhibition is most effective, it is a genetic model and therefore is not 100% representative of what will happen with AZD1775 treatment.

7.2.2 Optimal Dosing Strategy for AZD1775

In chapters 4 and 5, AZD1775 was demonstrated to cause cytotoxicity through its ability to induce DS-DNA breaks. As CDK1 regulates origin firing during DNA synthesis, WEE1 inhibition causes excess origin firing, exhausting nucleotide stores, leading to DS-DNA breaks and caspase-3 dependent apoptosis. This is the case whether it is used as a monotherapy or in combination with DNA-damaging agents. This finding has implications upon a number of ongoing clinical trials that are using AZD1775 as a DNA-damaging sensitiser, suggesting that the dosing schedule for AZD1775 may not be optimal.

The mechanism of action of AZD1775 in combination with other DNA-damaging agents needs to be validated in other colorectal cancer cell lines as well as other types of cancer. To begin with this can be investigated using the in vitro techniques used within this thesis. Furthermore, cancer cell types with varying p53 status should be investigated to confirm that this does not impact upon AZD1775 efficacy.

Further in vivo studies could be undertaken to determine the optimal dosing schedule for AZD1775 in combination with DNA-damaging agents.

7.2.3 Investigation of Piezo1 as an Anti-Angiogenic Target

In chapter 6, Piezo1 was confirmed to be expressed by CLMECs. This mechanosensitive, Ca²⁺ permeable ion channel has an important role in the determination of vascular structure in developmental embryology and adult physiology (Li et al., 2014). Its role in the generation of the tumour vasculature is unknown, however, a logical hypothesis would be that inhibition of Piezo1 could disrupt tumour angiogenesis. Work in our laboratory has already shown that targeted siRNA knockdown of Piezo1 in HUVECs can inhibit angiogenesis in vivo (Li et al., 2014).

To determine the anti-angiogenic effect of Piezo1 blockade, in vitro assays could be performed in CLMECs to assess the importance of Piezo1 in CLMEC proliferation, migration and tube formation. Advantage could be taken of the tamoxifen-inducible, endothelial specific, Piezo1 knockout murine model in our laboratory. Piezo1 could be knocked down prior to subcutaneous or intra-splenic injection of colorectal cancer cells. Tumour weight/growth and vessel micro-density could be measured to determine anti-angiogenic activity compared to control mice.

At present there is no specific chemical inhibitor of Piezo1. However, work in this thesis has shown that Yoda1 is a specific chemical activator of Piezo1. Therefore, knowledge about the chemical structure of Yoda1 can be used to design and test chemical inhibitors of Piezo1. Work in our laboratory is underway to discover the

first specific chemical inhibitor of Piezo1. If discovered, this could be used as an alternative to genetic inhibition of Piezo1 to assess its functional relevance in tumour angiogenesis.

7.2.4 Interrogation of Proteomic Data and Investigation of Further Hits

The proteomic screen in chapter 6 generated 157 protein targets that are differentially expressed between LECs and CLMECs. Many of these proteins are not known to have a function in endothelial cells, angiogenesis or cancer. Although this is a valuable dataset revealing proteins that may be critical to CLMEC survival and angiogenesis, determining which proteins to investigate will be a difficult and lengthy process. There is very little known about some proteins and no specific antibodies, targeted siRNA, small molecule inhibitors or activators exist. Nevertheless, work has begun on rationalising this list of protein targets. A literature search is being performed to determine what is known about each protein and whether antibodies/inhibitors/activators for the protein exist. To begin with, proteins that are known to play a role in angiogenesis will be investigated alongside proteins that have existing antibodies and inhibitors/activators for ease of investigation.

7.2.4 Future Clinical Implications

Characterising and experimenting on isolated CLMECs is a significant step away from cell line based assays and helps better predict clinical responses. The proteomic screening has identified a number of protein targets which can be used to develop clinically relevant anti-angiogenic agents in the future. Considering the cost and time-scale required to develop a drug, this research is undoubtedly in its infancy. However, as has been demonstrated in this thesis, targets can be identified

that already have a role in cancer treatment such as WEE1. These targets, for which small molecule inhibitors may exist and already be in use or in clinical trials, are already well along the drug discovery pathway and the time-frame to clinical use will be much shorter.

Since the concept was proposed by Judah Folkman in the 1970s, inhibition of tumour angiogenesis has proven an attractive anti-cancer treatment strategy. In the last decade anti-angiogenic agents have been clinically licensed for the treatment of metastatic colorectal cancer. However, despite extensive research and great promise in pre-clinical studies, these therapies have only led to a modest improvement in patient survival rates. Much is still to learn about tumour angiogenesis including what mechanisms are critical to tumour endothelial cell survival and how tumours develop resistance to anti-angiogenic agents. By targeting direct mechanisms critical to tumour endothelial cell function and survival, resistance to current anti-angiogenic agents, which indirectly target endothelial cells, may be overcome. Clinically, this could lead to meaningful improvements in survival rates for patients with inoperable CLM. It could also lead to an increase in conversion rates of patients with initially inoperable CLM who are subsequently able to undergo curative surgery. Finally, it may reduce the high recurrence rate associated with CLM resections.

7.3 Conclusion

Tumour angiogenesis is critical for the growth of CLM and CLMECs form a genetically distinct population of endothelial cells. Better understanding of the cellular mechanisms critical for CLMEC survival will help overcome the problems associated with anti-angiogenic therapy resistance. In this research study, CLMECs have been successfully isolated and characterised for the first time. The WEE1 protein has been identified as an anti-angiogenic target that is significantly upregulated in CLMECs. Inhibition of WEE1 with AZD1775 has been demonstrated to have clear anti-angiogenic effects in CLMECs. Furthermore, 157 proteins have been identified that are differentially expressed in CLMECs. This includes the established endogenous inhibitors of angiogenesis TSP-1 and VEGFR-1. The mechanosensitive, Ca²⁺ permeable ion channel Piezo1 has also been identified as another potential anti-angiogenic target in CLMECs. Modulation of the Piezo1 channel with Yoda1 has been demonstrated for the first time in CLMECs and shown to induce phosphorylation of eNOS.

References

ABDALLA, E. K., VAUTHEY, J. N., ELLIS, L. M., ELLIS, V., POLLOCK, R., BROGLIO, K. R., HESS, K. & CURLEY, S. A. 2004. Recurrence and outcomes following hepatic resection, radiofrequency ablation, and combined resection/ablation for colorectal liver metastases. *Ann Surg*, 239, 818-27.

ADAIR, R. A., YOUNG, A. L., COCKBAIN, A. J., MALDE, D., PRASAD, K. R., LODGE, J. P. & TOOGOOD, G. J. 2012. Repeat hepatic resection for colorectal liver metastases. *Br J Surg*, 99, 1278-83.

ADAIR, T. H. & MONTANI, J. P. 2010. *Angiogenesis*. San Rafael (CA): Morgan & Claypool Life Sciences.

ADAM, R., DELVART, V., PASCAL, G., VALEANU, A., CASTAING, D., AZOULAY, D., GIACCHETTI, S., PAULE, B., KUNSTLINGER, F., GHEMARD, O., LEVI, F. & BISMUTH, H. 2004. Rescue surgery for unresectable colorectal liver metastases downstaged by chemotherapy: a model to predict long-term survival. *Ann Surg*, 240, 644-58.

ADAMS, R. H. & ALITALO, K. 2007. Molecular regulation of angiogenesis and lymphangiogenesis. *Nat Rev Mol Cell Biol*, 8, 464-78.

AIRD, W. C. 2009. Molecular heterogeneity of tumor endothelium. *Cell Tissue Res*, 335, 271-81.

ALESSANDRI, G., CHIRIVI, R. G., FIORENTINI, S., DOSSI, R., BONARDELLI, S., GIULINI, S. M., ZANETTA, G., LANDONI, F., GRAZIOTTI, P. P., TURANO, A., CARUSO, A., ZARDI, L., GIAVAZZI, R. & BANI, M. R. 1999. Phenotypic and functional characteristics of tumour-derived microvascular endothelial cells. *Clin Exp Metastasis*, 17, 655-62.

ALVER, R. C., CHADHA, G. S. & BLOW, J. J. 2014. The contribution of dormant origins to genome stability: from cell biology to human genetics. *DNA Repair (Amst)*, 19, 182-9.

ANDRE, T., BONI, C., NAVARRO, M., TABERNERO, J., HICKISH, T., TOPHAM, C., BONETTI, A., CLINGAN, P., BRIDGEWATER, J., RIVERA, F. & DE GRAMONT, A. 2009. Improved overall survival with oxaliplatin, fluorouracil, and leucovorin as adjuvant treatment in stage II or III colon cancer in the MOSAIC trial. *J Clin Oncol*, 27, 3109-16.

ARNAOUTOVA, I., GEORGE, J., KLEINMAN, H. K. & BENTON, G. 2009. The endothelial cell tube formation assay on basement membrane turns 20: state of the science and the art. *Angiogenesis*, 12, 267-274.

AVRAAMIDES, C. J., GARMY-SUSINI, B. & VARNER, J. A. 2008. Integrins in angiogenesis and lymphangiogenesis. *Nat Rev Cancer*, 8, 604-17.

BAE, C., SACHS, F. & GOTTLIEB, P. A. 2011. The mechanosensitive ion channel Piezo1 is inhibited by the peptide GsMTx4. *Biochemistry*, 50, 6295-300.

BALA, M. M., RIEMSMA, R. P., WOLFF, R. & KLEIJNEN, J. 2013. Cryotherapy for liver metastases. *Cochrane Database Syst Rev*, CD009058.

BALLIGAND, J. L., FERON, O. & DESSY, C. 2009. eNOS activation by physical forces: from short-term regulation of contraction to chronic remodeling of cardiovascular tissues. *Physiol Rev*, 89, 481-534.

BAUTCH, V. L. 2009. Endothelial cells form a phalanx to block tumor metastasis. *Cell*, 136, 810-2.

BECK, H., NAHSE-KUMPF, V., LARSEN, M. S., O'HANLON, K. A., PATZKE, S., HOLMBERG, C., MEJLVANG, J., GROTH, A., NIELSEN, O., SYLJUASEN, R. G. & SORENSEN, C. S. 2012. Cyclin-dependent kinase suppression by WEE1 kinase protects the genome through control of replication initiation and nucleotide consumption. *Mol Cell Biol*, 32, 4226-36.

BECK, H., NAHSE, V., LARSEN, M. S., GROTH, P., CLANCY, T., LEES, M., JORGENSEN, M., HELLEDAY, T., SYLJUASEN, R. G. & SORENSEN, C. S. 2010. Regulators of cyclin-dependent kinases are crucial for maintaining genome integrity in S phase. *J Cell Biol*, 188, 629-38.

BENSON, A. B., 3RD 2005. Adjuvant chemotherapy of stage III colon cancer. *Semin Oncol*, 32, S74-7.

BENVENUTI, S., SARTORE-BIANCHI, A., DI NICOLANTONIO, F., ZANON, C., MORONI, M., VERONESE, S., SIENA, S. & BARDELLI, A. 2007. Oncogenic activation of the RAS/RAF signaling pathway impairs the response of metastatic

colorectal cancers to anti-epidermal growth factor receptor antibody therapies. *Cancer Res*, 67, 2643-8.

BIKFALVI, A., CRAMER, E. M., TENZA, D. & TOBELEM, G. 1991. Phenotypic modulations of human umbilical vein endothelial cells and human dermal fibroblasts using two angiogenic assays. *Biol Cell*, 72, 275-8.

BIOTIUM. 2016. Apoptosis and Viability Assays for Flow Cytometry [Online]. Available: <https://biotium.com/> [Accessed 12th August 2016].

BOCCI, G., NICOLAOU, K. C. & KERBEL, R. S. 2002. Protracted low-dose effects on human endothelial cell proliferation and survival in vitro reveal a selective antiangiogenic window for various chemotherapeutic drugs. *Cancer Res*, 62, 6938-43.

BOKEMEYER, C., BONDARENKO, I., HARTMANN, J. T., DE BRAUD, F., SCHUCH, G., ZUBEL, A., CELIK, I., SCHLICHTING, M. & KORALEWSKI, P. 2011. Efficacy according to biomarker status of cetuximab plus FOLFOX-4 as first-line treatment for metastatic colorectal cancer: the OPUS study. *Ann Oncol*, 22, 1535-46.

BOLTON, J. S., O'CONNELL, M. J., MAHONEY, M. R., FARR, G. H., JR., FITCH, T. R., MAPLES, W. J., NAGORNEY, D. M., RUBIN, J., FULORIA, J., STEEN, P. D. & ALBERTS, S. R. 2012. Hepatic arterial infusion and systemic chemotherapy after multiple metastasectomy in patients with colorectal carcinoma metastatic to the liver: a North Central Cancer Treatment Group (NCCTG) phase II study, 92-46-52. *Clin Colorectal Cancer*, 11, 31-7.

BROWDER, T., BUTTERFIELD, C. E., KRALING, B. M., SHI, B., MARSHALL, B., O'REILLY, M. S. & FOLKMAN, J. 2000. Antiangiogenic scheduling of chemotherapy improves efficacy against experimental drug-resistant cancer. *Cancer Res*, 60, 1878-86.

BUJKO, K., GLYNNE-JONES, R. & BUJKO, M. 2010. Does adjuvant fluoropyrimidine-based chemotherapy provide a benefit for patients with resected rectal cancer who have already received neoadjuvant radiochemotherapy? A systematic review of randomised trials. *Ann Oncol*, 21, 1743-50.

CADUFF, J. H., FISCHER, L. C. & BURRI, P. H. 1986. Scanning electron microscope study of the developing microvasculature in the postnatal rat lung. *Anat Rec*, 216, 154-64.

CAMILLERI-BRENNAN, J. & STEELE, R. J. 2001. The impact of recurrent rectal cancer on quality of life. *Eur J Surg Oncol*, 27, 349-53.

CANCER RESEARCH UK. 2016. *Bowel Cancer Incidence Statistics* [Online]. Available: <http://www.cancerresearchuk.org> [Accessed 11 July 2016].

CARMELIET, P. 2003. Angiogenesis in health and disease. *Nat Med*, 9, 653-60.

CARMELIET, P. 2005. Angiogenesis in life, disease and medicine. *Nature*, 438, 932-6.

CARMELIET, P. & JAIN, R. K. 2011. Principles and mechanisms of vessel normalization for cancer and other angiogenic diseases. *Nat Rev Drug Discov*, 10, 417-27.

CARRATO, A., SWIEBODA-SADLEJ, A., STASZEWSKA-SKURCZYNSKA, M., LIM, R., ROMAN, L., SHPARYK, Y., BONDARENKO, I., JONKER, D. J., SUN, Y., DE LA CRUZ, J. A., WILLIAMS, J. A., KORYTOWSKY, B., CHRISTENSEN, J. G., LIN, X., TURSI, J. M., LECHUGA, M. J. & VAN CUTSEM, E. 2013. Fluorouracil, leucovorin, and irinotecan plus either sunitinib or placebo in metastatic colorectal cancer: a randomized, phase III trial. *J Clin Oncol*, 31, 1341-7.

CHAPMAN, W. C. 2013. Liver transplantation for unresectable metastases to the liver: a new era in transplantation or a time for caution? *Ann Surg*, 257, 816-7.

CHAUDHURY, P., HASSANAIN, M., BOUGANIM, N., SALMAN, A., KAVAN, P. & METRAKOS, P. 2010. Perioperative chemotherapy with bevacizumab and liver resection for colorectal cancer liver metastasis. *HPB*, 12, 37-42.

CHEN, H. X. & CLECK, J. N. 2009. Adverse effects of anticancer agents that target the VEGF pathway. *Nat Rev Clin Oncol*, 6, 465-77.

CHOTI, M. A., SITZMANN, J. V., TIBURI, M. F., SUMETCHOTIMETHA, W., RANGSIN, R., SCHULICK, R. D., LILLEMOR, K. D., YEO, C. J. & CAMERON, J. L. 2002. Trends in long-term survival following liver resection for hepatic colorectal metastases. *Ann Surg*, 235, 759-66.

CHOW, J. P., POON, R. Y. & MA, H. T. 2011. Inhibitory phosphorylation of cyclin-dependent kinase 1 as a compensatory mechanism for mitosis exit. *Mol Cell Biol*, 31, 1478-91.

CHRISTOPHI, C., NIKFARJAM, M., MALCONTENTI-WILSON, C. & MURALIDHARAN, V. 2004. Long-term survival of patients with unresectable colorectal liver metastases treated by percutaneous interstitial laser thermotherapy. *World J Surg*, 28, 987-94.

CHUNG, A. S., LEE, J. & FERRARA, N. 2010. Targeting the tumour vasculature: insights from physiological angiogenesis. *Nat Rev Cancer*, 10, 505-14.

CIROCCHI, R., TRASTULLI, S., BOSELLI, C., MONTEDORI, A., CAVALIERE, D., PARISI, A., NOYA, G. & ABRAHA, I. 2012. Radiofrequency ablation in the treatment of liver metastases from colorectal cancer. *Cochrane Database Syst Rev*, CD006317.

COOKE, J. P. & LOSORDO, D. W. 2002. Nitric oxide and angiogenesis. *Circulation*, 105, 2133-5.

COSTE, B., MATHUR, J., SCHMIDT, M., EARLEY, T. J., RANADE, S., PETRUS, M. J., DUBIN, A. E. & PATAPOUTIAN, A. 2010. Piezo1 and Piezo2 are essential components of distinct mechanically-activated cation channels. *Science (New York, N.Y.)*, 330, 55-60.

CUNEO, K. C., MORGAN, M. A., DAVIS, M. A., PARCELS, L. A., PARCELS, J., KARNAK, D., RYAN, C., LIU, N., MAYBAUM, J. & LAWRENCE, T. S. 2016. Wee1

Kinase Inhibitor AZD1775 Radiosensitizes Hepatocellular Carcinoma Regardless of TP53 Mutational Status Through Induction of Replication Stress. *Int J Radiat Oncol Biol Phys*, 95, 782-90.

CUNNINGHAM, D., LANG, I., MARCUELLO, E., LORUSSO, V., OCVIRK, J., SHIN, D. B., JONKER, D., OSBORNE, S., ANDRE, N., WATERKAMP, D. & SAUNDERS, M. P. 2013. Bevacizumab plus capecitabine versus capecitabine alone in elderly patients with previously untreated metastatic colorectal cancer (AVEX): an open-label, randomised phase 3 trial. *Lancet Oncol*, 14, 1077-85.

DAVIES, R. J., MILLER, R. & COLEMAN, N. 2005. Colorectal cancer screening: prospects for molecular stool analysis. *Nat Rev Cancer*, 5, 199-209.

DE GRAMONT, A., FIGER, A., SEYMOUR, M., HOMERIN, M., HMISSI, A., CASSIDY, J., BONI, C., CORTES-FUNES, H., CERVANTES, A., FREYER, G., PAPAMICHAEL, D., LE BAIL, N., LOUVET, C., HENDLER, D., DE BRAUD, F., WILSON, C., MORVAN, F. & BONETTI, A. 2000. Leucovorin and fluorouracil with or without oxaliplatin as first-line treatment in advanced colorectal cancer. *J Clin Oncol*, 18, 2938-47.

DICKSON, P. V., HAMNER, J. B., SIMS, T. L., FRAGA, C. H., NG, C. Y., RAJASEKERAN, S., HAGEDORN, N. L., MCCARVILLE, M. B., STEWART, C. F. & DAVIDOFF, A. M. 2007. Bevacizumab-induced transient remodeling of the vasculature in neuroblastoma xenografts results in improved delivery and efficacy of systemically administered chemotherapy. *Clin Cancer Res*, 13, 3942-50.

DIMMELER, S., DERNBACH, E. & ZEIHNER, A. M. 2000. Phosphorylation of the endothelial nitric oxide synthase at ser-1177 is required for VEGF-induced endothelial cell migration. *FEBS Lett*, 477, 258-62.

DIMMELER, S., FLEMING, I., FISSLTHALER, B., HERMANN, C., BUSSE, R. & ZEIHNER, A. M. 1999. Activation of nitric oxide synthase in endothelial cells by Akt-dependent phosphorylation. *Nature*, 399, 601-5.

DJONOV, V., BAUM, O. & BURRI, P. H. 2003. Vascular remodeling by intussusceptive angiogenesis. *Cell Tissue Res*, 314, 107-17.

DJONOV, V. G., KURZ, H. & BURRI, P. H. 2002. Optimality in the developing vascular system: branching remodeling by means of intussusception as an efficient adaptation mechanism. *Dev Dyn*, 224, 391-402.

DO, K., WILSKER, D., JI, J., ZLOTT, J., FRESHWATER, T., KINDERS, R. J., COLLINS, J., CHEN, A. P., DOROSHOW, J. H. & KUMMAR, S. 2015. Phase I Study of Single-Agent AZD1775 (MK-1775), a Wee1 Kinase Inhibitor, in Patients With Refractory Solid Tumors. *J Clin Oncol*, 33, 3409-15.

DONOVAN, D., BROWN, N. J., BISHOP, E. T. & LEWIS, C. E. 2001. Comparison of three in vitro human 'angiogenesis' assays with capillaries formed in vivo. *Angiogenesis*, 4, 113-21.

DREVS, J., FAKLER, J., EISELE, S., MEDINGER, M., BING, G., ESSER, N., MARME, D. & UNGER, C. 2004. Antiangiogenic potency of various

chemotherapeutic drugs for metronomic chemotherapy. *Anticancer Res*, 24, 1759-63.

DUDLEY, A. C. 2012. Tumor Endothelial Cells. *Cold Spring Harbor Perspectives in Medicine*, 2, a006536.

DUDLEY, A. C., KHAN, Z. A., SHIH, S.-C., KANG, S.-Y., ZWAANS, B. M. M., BISCHOFF, J. & KLAGSBRUN, M. 2008. Calcification of multi-potent, prostate tumor endothelium. *Cancer cell*, 14, 201-211.

DUELAND, S., GUREN, T. K., HAGNESS, M., GLIMELIUS, B., LINE, P. D., PFEIFFER, P., FOSS, A. & TVEIT, K. M. 2015. Chemotherapy or liver transplantation for nonresectable liver metastases from colorectal cancer? *Ann Surg*, 261, 956-60.

DUFRAINE, J., FUNAHASHI, Y. & KITAJEWSKI, J. 2008. Notch signaling regulates tumor angiogenesis by diverse mechanisms. *Oncogene*, 27, 5132-7.

EDGE, S., BYRD, D. R., COMPTON, C. C., FRITZ, A. G., GREENE, F. L. & TROTTI, A. 2010. *AJCC (American Joint Committee on Cancer) Cancer Staging Manual 7th Edition*, New York, Springer.

EGELAND, E. V., FLATMARK, K., NESLAND, J. M., FLORENES, V. A., MAELANDSMO, G. M. & BOYE, K. 2016. Expression and clinical significance of Wee1 in colorectal cancer. *Tumour Biol*, 37, 12133-12140

EWING, J. 1928. *Neoplastic Diseases*, Philadelphia, W.B.Saunders.

FALCONE, A., RICCI, S., BRUNETTI, I., PFANNER, E., ALLEGRINI, G., BARBARA, C., CRINO, L., BENEDETTI, G., EVANGELISTA, W., FANCHINI, L., CORTESI, E., PICONE, V., VITELLO, S., CHIARA, S., GRANETTO, C., PORCILE, G., FIORETTO, L., ORLANDINI, C., ANDREUCETTI, M. & MASI, G. 2007. Phase III trial of infusional fluorouracil, leucovorin, oxaliplatin, and irinotecan (FOLFOXIRI) compared with infusional fluorouracil, leucovorin, and irinotecan (FOLFIRI) as first-line treatment for metastatic colorectal cancer: the Gruppo Oncologico Nord Ovest. *J Clin Oncol*, 25, 1670-6.

FEARON, E. R. & VOGELSTEIN, B. 1990. A genetic model for colorectal tumorigenesis. *Cell*, 61, 759-67.

FERNANDEZ, F. G., DREBIN, J. A., LINEHAN, D. C., DEHDASHTI, F., SIEGEL, B. A. & STRASBERG, S. M. 2004. Five-year survival after resection of hepatic metastases from colorectal cancer in patients screened by positron emission tomography with F-18 fluorodeoxyglucose (FDG-PET). *Ann Surg*, 240, 438-47; discussion 447-50.

FEROCI, F., VANNUCCHI, A., BIANCHI, P. P., CANTAFIO, S., GARZI, A., FORMISANO, G. & SCATIZZI, M. 2016. Total mesorectal excision for mid and low rectal cancer: Laparoscopic vs robotic surgery. *World Journal of Gastroenterology*, 22, 3602-3610.

FERRARA, N., GERBER, H. P. & LECOUTER, J. 2003. The biology of VEGF and its receptors. *Nat Med*, 9, 669-76.

FIDLER, I. J. 1970. Metastasis: quantitative analysis of distribution and fate of tumor emboli labeled with ^{125}I -5-iodo-2'-deoxyuridine. *J Natl Cancer Inst*, 45, 773-82.

FIDLER, I. J. 1990. Critical factors in the biology of human cancer metastasis: twenty-eighth G.H.A. Clowes memorial award lecture. *Cancer Res*, 50, 6130-8.

FIDLER, I. J. 2003. The pathogenesis of cancer metastasis: the 'seed and soil' hypothesis revisited. *Nat Rev Cancer*, 3, 453-8.

FIORENTINI, G., ALIBERTI, C., TILLI, M., MULAZZANI, L., GRAZIANO, F., GIORDANI, P., MAMBRINI, A., MONTAGNANI, F., ALESSANDRONI, P., CATALANO, V. & COSCHIERA, P. 2012. Intra-arterial infusion of irinotecan-loaded drug-eluting beads (DEBIRI) versus intravenous therapy (FOLFIRI) for hepatic metastases from colorectal cancer: final results of a phase III study. *Anticancer Res*, 32, 1387-95.

FIORIO PLA, A. & MUNARON, L. 2014. Functional properties of ion channels and transporters in tumour vascularization. *Philosophical Transactions of the Royal Society B: Biological Sciences*, 369, 20130103.

FLEMING, I. 2010. Molecular mechanisms underlying the activation of eNOS. *Pflugers Arch*, 459, 793-806.

FLEMING, I., FISSALTHALER, B., DIMMELER, S., KEMP, B. E. & BUSSE, R. 2001. Phosphorylation of Thr(495) regulates Ca^{2+} /calmodulin-dependent endothelial nitric oxide synthase activity. *Circ Res*, 88, E68-75.

FOLKMAN, J. 1971. Tumor angiogenesis: therapeutic implications. *N Engl J Med*, 285, 1182-6.

FONG, G. H., ROSSANT, J., GERTSENSTEIN, M. & BREITMAN, M. L. 1995. Role of the Flt-1 receptor tyrosine kinase in regulating the assembly of vascular endothelium. *Nature*, 376, 66-70.

FREVERT, U., ENGELMANN, S., ZOUGBÉDÉ, S., STANGE, J., NG, B., MATUSCHEWSKI, K., LIEBES, L. & YEE, H. 2005. Intravital Observation of Plasmodium berghei Sporozoite Infection of the Liver. *PLoS Biology*, 3, e192.

GALLER, A. S., PETRELLI, N. J. & SHAKAMURI, S. P. 2011. Rectal cancer surgery: a brief history. *Surg Oncol*, 20, 223-30.

GARLANDA, C. & DEJANA, E. 1997. Heterogeneity of endothelial cells. Specific markers. *Arterioscler Thromb Vasc Biol*, 17, 1193-202.

GERHARDT, H., GOLDING, M., FRUTTIGER, M., RUHRBERG, C., LUNDKVIST, A., ABRAMSSON, A., JELTSCH, M., MITCHELL, C., ALITALO, K., SHIMA, D. & BETSHOLTZ, C. 2003. VEGF guides angiogenic sprouting utilizing endothelial tip cell filopodia. *J Cell Biol*, 161, 1163-77.

GIANTONIO, B. J., CATALANO, P. J., MEROPOL, N. J., O'DWYER, P. J., MITCHELL, E. P., ALBERTS, S. R., SCHWARTZ, M. A. & BENSON, A. B., 3RD 2007. Bevacizumab in combination with oxaliplatin, fluorouracil, and leucovorin (FOLFOX4) for previously treated metastatic colorectal cancer: results from the Eastern Cooperative Oncology Group Study E3200. *J Clin Oncol*, 25, 1539-44.

GIORGIO, A., TARANTINO, L., MARINIELLO, N., DE STEFANO, G., PERROTTA, A., ALOISIO, V., DEL VISCOVO, L. & ALAIA, A. 1998. [Ultrasonography-guided percutaneous ethanol injection in large an/or multiple liver metastasis]. *Radiol Med*, 96, 238-42.

GIOVANNINI, M. & SEITZ, J. F. 1994. Ultrasound-guided percutaneous alcohol injection of small liver metastases. Results in 40 patients. *Cancer*, 73, 294-7.

GOEL, H. L. & MERCURIO, A. M. 2013. VEGF targets the tumour cell. *Nature reviews. Cancer*, 13, 871-882.

GOLDBERG, R. M., SARGENT, D. J., MORTON, R. F., FUCHS, C. S., RAMANATHAN, R. K., WILLIAMSON, S. K., FINDLAY, B. P., PITOT, H. C. & ALBERTS, S. R. 2004. A randomized controlled trial of fluorouracil plus leucovorin, irinotecan, and oxaliplatin combinations in patients with previously untreated metastatic colorectal cancer. *J Clin Oncol*, 22, 23-30.

GOLDSTEIN, N. S. & ARMIN, M. 2001. Epidermal growth factor receptor immunohistochemical reactivity in patients with American Joint Committee on Cancer Stage IV colon adenocarcinoma: implications for a standardized scoring system. *Cancer*, 92, 1331-46.

GRAHAM, J., MUHSIN, M. & KIRKPATRICK, P. 2004. Oxaliplatin. *Nat Rev Drug Discov*, 3, 11-12.

GRANT, D. S., LELKES, P. I., FUKUDA, K. & KLEINMAN, H. K. 1991. Intracellular mechanisms involved in basement membrane induced blood vessel differentiation in vitro. *In Vitro Cell Dev Biol*, 27A, 327-36.

GREEN, B. L., MARSHALL, H. C., COLLINSON, F., QUIRKE, P., GUILLOU, P., JAYNE, D. G. & BROWN, J. M. 2013. Long-term follow-up of the Medical Research Council CLASICC trial of conventional versus laparoscopically assisted resection in colorectal cancer. *Br J Surg*, 100, 75-82.

GREENAWAY, J., LAWLER, J., MOOREHEAD, R., BORNSTEIN, P., LAMARRE, J. & PETRIK, J. 2007. Thrombospondin-1 inhibits VEGF levels in the ovary directly by binding and internalization via the low density lipoprotein receptor-related protein-1 (LRP-1). *J Cell Physiol*, 210, 807-18.

GRIFFIOEN, A. W., DAMEN, C. A., MARTINOTTI, S., BLIJHAM, G. H. & GROENEWEGEN, G. 1996. Endothelial intercellular adhesion molecule-1 expression is suppressed in human malignancies: the role of angiogenic factors. *Cancer Res*, 56, 1111-17.

GROTHEY, A., VAN CUTSEM, E., SOBRERO, A., SIENA, S., FALCONE, A., YCHOU, M., HUMBLET, Y., BOUCHE, O., MINEUR, L., BARONE, C., ADENIS, A., TABERNERO, J., YOSHINO, T., LENZ, H. J., GOLDBERG, R. M., SARGENT, D. J., CIHON, F., CUPIT, L., WAGNER, A. & LAURENT, D. 2013. Regorafenib monotherapy for previously treated metastatic colorectal cancer (CORRECT): an international, multicentre, randomised, placebo-controlled, phase 3 trial. *Lancet*, 381, 303-12.

GUERTIN, A. D., LI, J., LIU, Y., HURD, M. S., SCHULLER, A. G., LONG, B., HIRSCH, H. A., FELDMAN, I., BENITA, Y., TONIATTI, C., ZAWEL, L., FAWELL, S. E., GILLILAND, D. G. & SHUMWAY, S. D. 2013. Preclinical evaluation of the WEE1 inhibitor MK-1775 as single-agent anticancer therapy. *Mol Cancer Ther*, 12, 1442-52.

HAGNESS, M., FOSS, A., LINE, P. D., SCHOLZ, T., JORGENSEN, P. F., FOSBY, B., BOBERG, K. M., MATHISEN, O., GLADHAUG, I. P., EGGE, T. S., SOLBERG, S., HAUSKEN, J. & DUELAND, S. 2013. Liver transplantation for nonresectable liver metastases from colorectal cancer. *Ann Surg*, 257, 800-6.

HAIER, J. & NICOLSON, G. L. 2001. Tumor cell adhesion under hydrodynamic conditions of fluid flow. *APMIS*, 109, 241-62.

HALDER, C., OSSENDORF, C., MARAN, A., YASZEMSKI, M., BOLANDER, M. E., FUCHS, B. & SARKAR, G. 2009. Preferential expression of the secreted and membrane forms of tumor endothelial marker 7 transcripts in osteosarcoma. *Anticancer Res*, 29, 4317-22.

HANAHAAN, D. & WEINBERG, R. A. 2000. The hallmarks of cancer. *Cell*, 100, 57-70.

HARJI, D. P., GRIFFITHS, B., MCARTHUR, D. R. & SAGAR, P. M. 2012. Current UK management of locally recurrent rectal cancer. *Colorectal Dis*, 14, 1479-82.

HART, I. R. & FIDLER, I. J. 1980. Role of organ selectivity in the determination of metastatic patterns of B16 melanoma. *Cancer Res*, 40, 2281-7.

HAWCROFT, G., VOLPATO, M., MARSTON, G., INGRAM, N., PERRY, S. L., COCKBAIN, A. J., RACE, A. D., MUNARINI, A., BELLUZZI, A., LOADMAN, P. M., COLETTA, P. L. & HULL, M. A. 2012. The omega-3 polyunsaturated fatty acid eicosapentaenoic acid inhibits mouse MC-26 colorectal cancer cell liver metastasis via inhibition of PGE2-dependent cell motility. *British Journal of Pharmacology*, 166, 1724-1737.

HEALD, R. J. & RYALL, R. D. 1986. Recurrence and survival after total mesorectal excision for rectal cancer. *Lancet*, 1, 1479-82.

HECHT, J. R., TRARBACH, T., HAINSWORTH, J. D., MAJOR, P., JAGER, E., WOLFF, R. A., LLOYD-SALVANT, K., BODOKY, G., PENDERGRASS, K., BERG, W., CHEN, B. L., JALAVA, T., MEINHARDT, G., LAURENT, D., LEBWOHL, D. & KERR, D. 2011. Randomized, placebo-controlled, phase III study of first-line oxaliplatin-based chemotherapy plus PTK787/ZK 222584, an oral vascular endothelial growth factor receptor inhibitor, in patients with metastatic colorectal adenocarcinoma. *J Clin Oncol*, 29, 1997-2003.

HELFRICH, I., SCHEFFRAHN, I., BARTLING, S., WEIS, J., VON FELBERT, V., MIDDLETON, M., KATO, M., ERGUN, S., AUGUSTIN, H. G. & SCHADENDORF, D. 2010. Resistance to antiangiogenic therapy is directed by vascular phenotype, vessel stabilization, and maturation in malignant melanoma. *J Exp Med*, 207, 491-503.

HIDA, K., OHGA, N., AKIYAMA, K., MAISHI, N. & HIDA, Y. 2013. Heterogeneity of tumor endothelial cells. *Cancer Sci*, 104, 1391-5.

HILLEN, F. & GRIFFIOEN, A. W. 2007. Tumour vascularization: sprouting angiogenesis and beyond. *Cancer Metastasis Rev*, 26, 489-502.

HIRAI, H., ARAI, T., OKADA, M., NISHIBATA, T., KOBAYASHI, M., SAKAI, N., IMAGAKI, K., OHTANI, J., SAKAI, T., YOSHIZUMI, T., MIZUARAI, S., IWASAWA, Y. & KOTANI, H. 2010. MK-1775, a small molecule Wee1 inhibitor, enhances anti-tumor efficacy of various DNA-damaging agents, including 5-fluorouracil. *Cancer Biology & Therapy*, 9, 514-522.

HIRAI, H., IWASAWA, Y., OKADA, M., ARAI, T., NISHIBATA, T., KOBAYASHI, M., KIMURA, T., KANEKO, N., OHTANI, J., YAMANAKA, K., ITADANI, H., TAKAHASHI-SUZUKI, I., FUKASAWA, K., OKI, H., NAMBU, T., JIANG, J., SAKAI, T., ARAKAWA, H., SAKAMOTO, T., SAGARA, T., YOSHIZUMI, T., MIZUARAI, S. & KOTANI, H. 2009. Small-molecule inhibition of Wee1 kinase by MK-1775 selectively sensitizes p53-deficient tumor cells to DNA-damaging agents. *Mol Cancer Ther*, 8, 2992-3000.

HLUSHCHUK, R., RIESTERER, O., BAUM, O., WOOD, J., GRUBER, G., PRUSCHY, M. & DJONOV, V. 2008. Tumor recovery by angiogenic switch from sprouting to intussusceptive angiogenesis after treatment with PTK787/ZK222584 or ionizing radiation. *Am J Pathol*, 173, 1173-85.

HOLASH, J., MAISONPIERRE, P. C., COMPTON, D., BOLAND, P., ALEXANDER, C. R., ZAGZAG, D., YANCOPOULOS, G. D. & WIEGAND, S. J. 1999. Vessel cooption, regression, and growth in tumors mediated by angiopoietins and VEGF. *Science*, 284, 1994-8.

HOLMGREN, L., O'REILLY, M. S. & FOLKMAN, J. 1995. Dormancy of micrometastases: balanced proliferation and apoptosis in the presence of angiogenesis suppression. *Nat Med*, 1, 149-53.

HONG, K. S., KIM, H. S., KIM S. H., LIM D. J., PARK J. Y. & KIM S. D. 2011 Hypoxia induces Wee1 expression and attenuates hydrogen peroxide-induced endothelial damage in MS1 cells. *Experimental & molecular medicine*, 43, 653-659.

HOUGHTON JA, TILLMAN DM & FG, H. 1995. Ratio of 2'-Deoxyadenosine-5'-triphosphate/Thymidine-5'-triphosphate Influences the Commitment of Human Colon Carcinoma Cells to Thymineless Death. *Clinical Cancer Research*, 1, 723-730.

HOUSE, M. G., KEMENY, N. E., GONEN, M., FONG, Y., ALLEN, P. J., PATY, P. B., DEMATTEO, R. P., BLUMGART, L. H., JARNAGIN, W. R. & D'ANGELICA, M. I. 2011. Comparison of adjuvant systemic chemotherapy with or without hepatic arterial infusional chemotherapy after hepatic resection for metastatic colorectal cancer. *Ann Surg*, 254, 851-6.

HU, M., YANG, J. L., TENG, H., JIA, Y. Q., WANG, R., ZHANG, X. W., WU, Y., LUO, Y., CHEN, X. C., ZHANG, R., TIAN, L., ZHAO, X. & WEI, Y. Q. 2008. Anti-angiogenesis therapy based on the bone marrow-derived stromal cells genetically engineered to express sFlt-1 in mouse tumor model. *BMC Cancer*, 8, 306-306.

HUGHES, C. C. 2008. Endothelial-stromal interactions in angiogenesis. *Curr Opin Hematol*, 15, 204-9.

HURWITZ, H., FEHRENCACHER, L., NOVOTNY, W., CARTWRIGHT, T. & HAINSWORTH, J. 2004. Bevacizumab plus Irinotecan, Fluorouracil, and Leucovorin for Metastatic Colorectal Cancer. *NEJM*, 350, 2335-2342.

IORNS, E., LORD, C. J., GRIGORIADIS, A., MCDONALD, S., FENWICK, K., MACKAY, A., MEIN, C. A., NATRAJAN, R., SAVAGE, K., TAMBER, N., REIS-FILHO, J. S., TURNER, N. C. & ASHWORTH, A. 2009. Integrated functional, gene expression and genomic analysis for the identification of cancer targets. *PLoS One*, 4, e5120.

ISENBERG, J. S., MARTIN-MANSO, G., MAXHIMER, J. B. & ROBERTS, D. D. 2009. Regulation of nitric oxide signalling by thrombospondin 1: implications for anti-angiogenic therapies. *Nat Rev Cancer*, 9, 182-94.

IVAN, M., KONDO, K., YANG, H., KIM, W., VALIANDO, J., OHH, M., SALIC, A., ASARA, J. M., LANE, W. S. & KAELIN, W. G., JR. 2001. HIF α targeted for VHL-mediated destruction by proline hydroxylation: implications for O₂ sensing. *Science*, 292, 464-8.

JAFFE, E. A., NACHMAN, R. L., BECKER, C. G. & MINICK, C. R. 1973. Culture of human endothelial cells derived from umbilical veins. Identification by morphologic and immunologic criteria. *J Clin Invest*, 52, 2745-56.

JAIN, R. K. 2005. Normalization of tumor vasculature: an emerging concept in antiangiogenic therapy. *Science*, 307, 58-62.

JAIN, R. K., MARTIN, J. D. & STYLIANOPOULOS, T. 2014. The role of mechanical forces in tumor growth and therapy. *Annu Rev Biomed Eng*, 16, 321-46.

JAYASINGHE, C., SIMIANTONAKI, N., MICHEL-SCHMIDT, R. & KIRKPATRICK, C. J. 2009. Comparative study of human colonic tumor-derived endothelial cells (HCTEC) and normal colonic microvascular endothelial cells (HCMEC): Hypoxia-induced sVEGFR-1 and sVEGFR-2 levels. *Oncol Rep*, 21, 933-9.

KENDALL, R. L. & THOMAS, K. A. 1993. Inhibition of vascular endothelial cell growth factor activity by an endogenously encoded soluble receptor. *Proc Natl Acad Sci U S A*, 90, 10705-9.

KHAZAEI, M., MOIEN-AFSHARI, F. & LAHER, I. 2008. Vascular endothelial function in health and diseases. *Pathophysiology*, 15, 49-67.

KHEIRELSEID, E. A. H., MILLER, N. & KERIN, M. J. 2013. Molecular biology of colorectal cancer: Review of the literature. *Am J Mol Bio*, 3, 72-80.

KIRAN, R. P., KIRAT, H. T., BURGESS, A. N., NISAR, P. J., KALADY, M. F. & LAVERY, I. C. 2012. Is adjuvant chemotherapy really needed after curative surgery for rectal cancer patients who are node-negative after neoadjuvant chemoradiotherapy? *Ann Surg Oncol*, 19, 1206-12.

KONERDING, M. A., MALKUSCH, W., KLAPTHOR, B., ACKERN, C. V., FAIT, E., HILL, S. A., PARKINS, C., CHAPLIN, D. J., PRESTA, M. & DENEKAMP, J. 1999. Evidence for characteristic vascular patterns in solid tumours: quantitative studies using corrosion casts. *British Journal of Cancer*, 80, 724-732.

KREHLING, J. M., FOROUTAN, P., REED, D., MARTINEZ, G., RAZABDOUSKI, T., BUI, M. M., RAGHAVAN, M., LETSON, D., GILLIES, R. J. & ALTIOK, S. 2013. Wee1 inhibition by MK-1775 leads to tumor inhibition and enhances efficacy of gemcitabine in human sarcomas. *PLoS One*, 8, e57523.

KREHLING, J. M., GEMMER, J. Y., REED, D., LETSON, D., BUI, M. & ALTIOK, S. 2012. MK1775, a selective Wee1 inhibitor, shows single-agent antitumor activity against sarcoma cells. *Mol Cancer Ther*, 11, 174-82.

KUEBLER, J. P., WIEAND, H. S., O'CONNELL, M. J., SMITH, R. E., COLANGELO, L. H., YOTHERS, G., PETRELLI, N. J., FINDLAY, M. P., SEAY, T. E., ATKINS, J. N., ZAPAS, J. L., GOODWIN, J. W., FEHRENBACHER, L., RAMANATHAN, R. K., CONLEY, B. A., FLYNN, P. J., SOORI, G., COLMAN, L. K., LEVINE, E. A., LANIER, K. S. & WOLMARK, N. 2007. Oxaliplatin combined with weekly bolus fluorouracil and leucovorin as surgical adjuvant chemotherapy for stage II and III colon cancer: results from NSABP C-07. *J Clin Oncol*, 25, 2198-204.

LAFERRIERE, J., HOULE, F., TAHER, M. M., VALERIE, K. & HUOT, J. 2001. Transendothelial migration of colon carcinoma cells requires expression of E-selectin by endothelial cells and activation of stress-activated protein kinase-2 (SAPK2/p38) in the tumor cells. *J Biol Chem*, 276, 33762-72.

LAWLER, J. 2002. Thrombospondin-1 as an endogenous inhibitor of angiogenesis and tumor growth. *J Cell Mol Med*, 6, 1-12.

LAWLER, P. R. & LAWLER, J. 2012. Molecular Basis for the Regulation of Angiogenesis by Thrombospondin-1 and -2. *Cold Spring Harbor Perspectives in Medicine*, 2, a006627.

LEE, H. K., BAE, H. R., PARK, H. K., SEO, I. A., LEE, E. Y., SUH, D. J. & PARK, H. T. 2005. Cloning, characterization and neuronal expression profiles of tumor endothelial marker 7 in the rat brain. *Brain Res Mol Brain Res*, 136, 189-98.

LI, J., BRUNS, A.-F., HOU, B., RODE, B., WEBSTER, P. J., BAILEY, M. A., APPLEBY, H. L., MOSS, N. K., RITCHIE, J. E., YULDASHEVA, N. Y., TUMOVA, S., QUINNEY, M., MCKEOWN, L., TAYLOR, H., PRASAD, K. R., BURKE, D., O'REGAN, D., PORTER, K. E., FOSTER, R., KEARNEY, M. T. & BEECH, D. J. 2015. Orai3 Surface Accumulation and Calcium Entry Evoked by Vascular Endothelial Growth Factor. *Arteriosclerosis, Thrombosis, and Vascular Biology*, 35, 1987-1994.

LI, J., HOU, B., TUMOVA, S., MURAKI, K., BRUNS, A., LUDLOW, M. J., SEDO, A., HYMAN, A. J., MCKEOWN, L., YOUNG, R. S., YULDASHEVA, N. Y., MAJEED, Y., WILSON, L. A., RODE, B., BAILEY, M. A., KIM, H. R., FU, Z., CARTER, D. A. L., BILTON, J., IMRIE, H., AJUH, P., DEAR, T. N., CUBBON, R. M., KEARNEY, M. T., PRASAD, K. R., EVANS, P. C., AINSCOUGH, J. F. X. & BEECH, D. J. 2014. Piezo1 integration of vascular architecture with physiological force. *Nature*, 515, 279-282.

LONGLEY, D. B., HARKIN, D. P. & JOHNSTON, P. G. 2003. 5-Fluorouracil: mechanisms of action and clinical strategies. *Nat Rev Cancer*, 3, 330-338.

LORENZ, M., MULLER, H. H., SCHRAMM, H., GASSEL, H. J., RAU, H. G., RIDWELSKI, K., HAUSS, J., STIEGER, R., JAUCH, K. W., BECHSTEIN, W. O. & ENCKE, A. 1998. Randomized trial of surgery versus surgery followed by adjuvant hepatic arterial infusion with 5-fluorouracil and folinic acid for liver metastases of colorectal cancer. German Cooperative on Liver Metastases (Arbeitsgruppe Lebermetastasen). *Ann Surg*, 228, 756-62.

LOUPAKIS, F., CREMOLINI, C., MASI, G., LONARDI, S., ZAGONEL, V., SALVATORE, L., CORTESI, E., TOMASELLO, G., RONZONI, M., SPADI, R., ZANIBONI, A., TONINI, G., BUONADONNA, A., AMOROSO, D., CHIARA, S., CARLOMAGNO, C., BONI, C., ALLEGRINI, G., BONI, L. & FALCONE, A. 2014. Initial therapy with FOLFOXIRI and bevacizumab for metastatic colorectal cancer. *N Engl J Med*, 371, 1609-18.

MACFADYEN, J., SAVAGE, K., WIENKE, D. & ISACKE, C. M. 2007. Endosialin is expressed on stromal fibroblasts and CNS pericytes in mouse embryos and is downregulated during development. *Gene Expr Patterns*, 7, 363-9.

MAGNUSSEN, G. I., HOLM, R., EMILSEN, E., ROSNES, A. K., SLIPICEVIC, A. & FLORENES, V. A. 2012. High expression of Wee1 is associated with poor disease-free survival in malignant melanoma: potential for targeted therapy. *PLoS One*, 7, e38254.

MAK, T. W. C., LEE, J. F. Y., FUTABA, K., HON, S. S. F., NGO, D. K. Y. & NG, S. S. M. 2014. Robotic surgery for rectal cancer: A systematic review of current practice. *World Journal of Gastrointestinal Oncology*, 6, 184-193.

MAKINO, Y., CAO, R., SVENSSON, K., BERTILSSON, G., ASMAN, M., TANAKA, H., CAO, Y., BERKENSTAM, A. & POELLINGER, L. 2001. Inhibitory PAS domain protein is a negative regulator of hypoxia-inducible gene expression. *Nature*, 414, 550-4.

MALIK, H., KHAN, A. Z., BERRY, D. P., CAMERON, I. C., POPE, I., SHERLOCK, D., HELMY, S., BYRNE, B., THOMPSON, M., PULFER, A. & DAVIDSON, B. 2015. Liver resection rate following downsizing chemotherapy with cetuximab in metastatic colorectal cancer: UK retrospective observational study. *Eur J Surg Oncol*, 41, 499-505.

MANIOTIS, A. J., FOLBERG, R., HESS, A., SEFTOR, E. A., GARDNER, L. M., PE'ER, J., TRENT, J. M., MELTZER, P. S. & HENDRIX, M. J. 1999. Vascular channel formation by human melanoma cells in vivo and in vitro: vasculogenic mimicry. *Am J Pathol*, 155, 739-52.

MARÇOLA, M. & RODRIGUES, C. E. 2015. Endothelial Progenitor Cells in Tumor Angiogenesis: Another Brick in the Wall. *Stem Cells International*, 2015, 832649.

MARKOVIC, S. N., SUMAN, V. J., RAO, R. A., INGLE, J. N., KAUR, J. S., ERICKSON, L. A., PITOT, H. C., CROGHAN, G. A., MCWILLIAMS, R. R., MERCHAN, J., KOTTSCHADE, L. A., NEVALA, W. K., UHL, C. B., ALLRED, J. & CREAGAN, E. T. 2007. A phase II study of ABT-510 (thrombospondin-1 analog) for the treatment of metastatic melanoma. *Am J Clin Oncol*, 30, 303-9.

MARTINS, P. N., MOVAHEDI, B. & BOZORGZADEH, A. 2015. Liver Transplantation for Unresectable Colorectal Cancer Liver Metastases: A Paradigm Change? *Ann Surg*, 262, e12.

MASAKI, T., SHIRATORI, Y., RENGIFO, W., IGARASHI, K., YAMAGATA, M., KUROKOHCHI, K., UCHIDA, N., MIYAUCHI, Y., YOSHIJI, H., WATANABE, S., OMATA, M. & KURIYAMA, S. 2003. Cyclins and cyclin-dependent kinases: comparative study of hepatocellular carcinoma versus cirrhosis. *Hepatology*, 37, 534-43.

MATHESON, C. J., BACKOS, D. S. & REIGAN, P. 2016. Targeting WEE1 Kinase in Cancer. *Trends Pharmacol Sci*, 37, 872-81

MAUGHAN, T. S., ADAMS, R. A., SMITH, C. G., MEADE, A. M., SEYMOUR, M. T., WILSON, R. H., IDZIASZCZYK, S., HARRIS, R., FISHER, D., KENNY, S. L., KAY, E., MITCHELL, J. K., MADI, A., JASANI, B., JAMES, M. D., BRIDGEWATER, J., KENNEDY, M. J., CLAES, B., LAMBRECHTS, D., KAPLAN, R. & CHEADLE, J. P. 2011. Addition of cetuximab to oxaliplatin-based first-line combination chemotherapy for treatment of advanced colorectal cancer: results of the randomised phase 3 MRC COIN trial. *Lancet*, 377, 2103-14.

MAZZONE, M., DETTORI, D., DE OLIVEIRA, R. L., LOGES, S., SCHMIDT, T., JONCKX, B., TIAN, Y.-M., LANAHAN, A. A., POLLARD, P., DE ALMODOVAR, C. R., DE SMET, F., VINCKIER, S., ARAGONÉS, J., DEBACKERE, K., LUTTUN, A., WYNS, S., JORDAN, B., PISACANE, A., GALLEZ, B., LAMPUGNANI, M. G., DEJANA, E., SIMONS, M., RATCLIFFE, P., MAXWELL, P. & CARMELIET, P.

2009. Heterozygous Deficiency of PHD2 Restores Tumor Oxygenation and Inhibits Metastasis via Endothelial Normalization. *Cell*, 136, 839-851.

MEDEMA, R. H. & MACUREK, L. 2012. Checkpoint control and cancer. *Oncogene*, 31, 2601-13.

MESRI, M., BIRSE, C., HEIDBRINK, J., MCKINNON, K., BRAND, E., BERMINGHAM, C. L., FEILD, B., FITZHUGH, W., HE, T., RUBEN, S. & MOORE, P. A. 2013. Identification and characterization of angiogenesis targets through proteomic profiling of endothelial cells in human cancer tissues. *PLoS One*, 8, e78885.

MILES, W. E. 1908. A method of performing abdomino-perineal excision for carcinoma of the rectum and of the terminal portion of the pelvic colon. *Lancet*, 2, 1812-1813.

MINA, L. A. & SLEDGE, G. W., JR. 2011. Rethinking the metastatic cascade as a therapeutic target. *Nat Rev Clin Oncol*, 8, 325-32.

MISIAKOS, E. P., KARIDIS, N. P. & KOURAKLIS, G. 2011. Current treatment for colorectal liver metastases. *World J Gastroenterol*, 17, 4067-75.

MITRY, E., FIELDS, A. L., BLEIBERG, H., LABIANCA, R., PORTIER, G., TU, D., NITTI, D., TORRI, V., ELIAS, D., O'CALLAGHAN, C., LANGER, B., MARTIGNONI, G., BOUCHE, O., LAZORTHES, F., VAN CUTSEM, E., BEDENNE, L., MOORE, M. J. & ROUGIER, P. 2008. Adjuvant chemotherapy after potentially curative resection

of metastases from colorectal cancer: a pooled analysis of two randomized trials. *J Clin Oncol*, 26, 4906-11.

MORIKAWA, S., BALUK, P., KAIDOH, T., HASKELL, A., JAIN, R. K. & MCDONALD, D. M. 2002. Abnormalities in pericytes on blood vessels and endothelial sprouts in tumors. *Am J Pathol*, 160, 985-1000.

MUELLER, S., HASHIZUME, R., YANG, X., KOLKOWITZ, I., OLOW, A. K., PHILLIPS, J., SMIRNOV, I., TOM, M. W., PRADOS, M. D., JAMES, C. D., BERGER, M. S., GUPTA, N. & HAAS-KOGAN, D. A. 2014. Targeting Wee1 for the treatment of pediatric high-grade gliomas. *Neuro Oncol*, 16, 352-60.

MULLER, A., HOMEY, B., SOTO, H., GE, N., CATRON, D., BUCHANAN, M. E., MCCLANAHAN, T., MURPHY, E., YUAN, W., WAGNER, S. N., BARRERA, J. L., MOHAR, A., VERASTEGUI, E. & ZLOTNIK, A. 2001. Involvement of chemokine receptors in breast cancer metastasis. *Nature*, 410, 50-6.

MULLER, W. A. 2014. How Endothelial Cells Regulate Transmigration of Leukocytes in the Inflammatory Response. *The American Journal of Pathology*, 184, 886-896.

NATIONAL INSTITUTE FOR HEALTH AND CARE EXCELLENCE 2010. *Bevacizumab in combination with oxaliplatin and either fluorouracil plus folinic acid or capecitabine for the treatment of metastatic colorectal cancer*, London, NICE.

NATIONAL INSTITUTE FOR HEALTH AND CARE EXCELLENCE 2012. *Cetuximab, bevacizumab and panitumumab for the treatment of metastatic*

colorectal cancer after firstline chemotherapy: Cetuximab (monotherapy or combination chemotherapy), bevacizumab (in combination with non-oxaliplatin chemotherapy) and panitumumab (monotherapy) for the treatment of metastatic colorectal cancer after firstline chemotherapy, London, NICE.

NATIONAL INSTITUTE FOR HEALTH AND CARE EXCELLENCE 2014. *Aflibercept in combination with irinotecan and fluorouracil-based therapy for treating metastatic colorectal cancer that has progressed following prior oxaliplatin-based chemotherapy*, London, NICE.

NICOLSON, G. L. 1988. Organ specificity of tumor metastasis: role of preferential adhesion, invasion and growth of malignant cells at specific secondary sites. *Cancer Metastasis Rev*, 7, 143-88.

NIELSEN, K., ROLFF, H. C., EEFSEN, R. L. & VAINER, B. 2014. The morphological growth patterns of colorectal liver metastases are prognostic for overall survival. *Mod Pathol*, 27, 1641-8.

NIELSEN, M. B., LAURBERG, S. & HOLM, T. 2011. Current management of locally recurrent rectal cancer. *Colorectal Dis*, 13, 732-42.

NOGUERA-TROISE, I., DALY, C., PAPADOPOULOS, N. J., COETZEE, S., BOLAND, P., GALE, N. W., LIN, H. C., YANCOPOULOS, G. D. & THURSTON, G. 2006. Blockade of Dll4 inhibits tumour growth by promoting non-productive angiogenesis. *Nature*, 444, 1032-7.

NYBERG, P., XIE, L. & KALLURI, R. 2005. Endogenous inhibitors of angiogenesis. *Cancer Res*, 65, 3967-79.

OLIPHANT, R., NICHOLSON, G. A., HORGAN, P. G., MOLLOY, R. G., MCMILLAN, D. C. & MORRISON, D. S. 2013. Deprivation and colorectal cancer surgery: longer-term survival inequalities are due to differential postoperative mortality between socioeconomic groups. *Ann Surg Oncol*, 20, 2132-9.

OPAVSKY, R., HAVIERNIK, P., JURKOVICOVA, D., GARIN, M. T., COPELAND, N. G., GILBERT, D. J., JENKINS, N. A., BIES, J., GARFIELD, S., PASTOREKOVA, S., OUE, A. & WOLFF, L. 2001. Molecular characterization of the mouse Tem1/endosialin gene regulated by cell density in vitro and expressed in normal tissues in vivo. *J Biol Chem*, 276, 38795-807.

PAGET, S. 1889. The distribution of secondary growths in cancer of the breast. *Lancet*, 133, 571-573.

PALMER, G., MARTLING, A., CEDERMARK, B. & HOLM, T. 2007. A population-based study on the management and outcome in patients with locally recurrent rectal cancer. *Ann Surg Oncol*, 14, 447-54.

PASCHOS, K. A., MAJEED, A. W. & BIRD, N. C. 2014. Natural history of hepatic metastases from colorectal cancer - pathobiological pathways with clinical significance. *World J Gastroenterol*, 20, 3719-37.

PECH, M., WIENERS, G., FREUND, T., DUDECK, O., FISCHBACH, F., RICKE, J. & SEEMANN, M. D. 2007. MR-guided interstitial laser thermotherapy of colorectal liver metastases: efficiency, safety and patient survival. *Eur J Med Res*, 12, 161-8.

PENDU, R., TERRAUBE, V., CHRISTOPHE, O. D., GAHMBERG, C. G., DE GROOT, P. G., LENTING, P. J. & DENIS, C. V. 2006. P-selectin glycoprotein ligand 1 and beta2-integrins cooperate in the adhesion of leukocytes to von Willebrand factor. *Blood*, 108, 3746-52.

PERRY, J. A. & KORNBLUTH, S. 2007. Cdc25 and Wee1: analogous opposites? *Cell Div*, 2, 12.

PEZZELLA, F., PASTORINO, U., TAGLIABUE, E., ANDREOLA, S., SOZZI, G., GASPARINI, G., MENARD, S., GATTER, K. C., HARRIS, A. L., FOX, S., BUYSE, M., PILOTTI, S., PIEROTTI, M. & RILKE, F. 1997. Non-small-cell lung carcinoma tumor growth without morphological evidence of neo-angiogenesis. *The American Journal of Pathology*, 151, 1417-1423.

PFISTER, S. X., MARKKANEN, E., JIANG, Y., SARKAR, S., WOODCOCK, M., ORLANDO, G., MAVROMMATI, I., PAI, C. C., ZALMAS, L. P., DROBNITZKY, N., DIANOV, G. L., VERRILL, C., MACAULAY, V. M., YING, S., LA THANGUE, N. B., D'ANGIOLELLA, V., RYAN A.J. & HUMPHREY, T. C. 2015. Inhibiting WEE1 Selectively Kills Histone H3K36me3-Deficient Cancers by dNTP Starvation. *Cancer Cell*, 28, 557-68.

PHNG, L. K. & GERHARDT, H. 2009. Angiogenesis: a team effort coordinated by notch. *Dev Cell*, 16, 196-208.

PODGRABINSKA, S., BRAUN, P., VELASCO, P., KLOOS, B., PEPPER, M. S., JACKSON, D. G. & SKOBE, M. 2002. Molecular Characterization of Lymphatic Endothelial Cells. *Proceedings of the National Academy of Sciences of the United States of America*, 99, 16069-16074.

POSTHUMADEBOER, J., WURDINGER, T., GRAAT, H. C., VAN BEUSECHEM, V. W., HELDER, M. N., VAN ROYEN, B. J. & KASPERS, G. J. 2011. WEE1 inhibition sensitizes osteosarcoma to radiotherapy. *BMC Cancer*, 11, 156.

PRIMO, L., FERRANDI, C., ROCA, C., MARCHIO, S., DI BLASIO, L., ALESSIO, M. & BUSSOLINO, F. 2005. Identification of CD36 molecular features required for its in vitro angiostatic activity. *FASEB J*, 19, 1713-5.

PUGH, C. W. & RATCLIFFE, P. J. 2003. Regulation of angiogenesis by hypoxia: role of the HIF system. *Nat Med*, 9, 677-84.

RAHBARI, N. N., BORK, U., SCHOLCH, S., REISSFELDER, C., THORLUND, K., BETZLER, A., KAHLERT, C., SCHNEIDER, M., ULRICH, A. B., BUCHLER, M. W., WEITZ, J. & KOCH, M. 2016. Metastatic Spread Emerging From Liver Metastases of Colorectal Cancer: Does the Seed Leave the Soil Again? *Ann Surg*, 263, 345-52.

RAJESHKUMAR, N. V., DE OLIVEIRA, E., OTTENHOF, N., WATTERS, J., BROOKS, D., DEMUTH, T., SHUMWAY, S. D., MIZUARAI, S., HIRAI, H., MAITRA, A. & HIDALGO, M. 2011. MK-1775, a potent Wee1 inhibitor, synergizes with gemcitabine to achieve tumor regressions, selectively in p53-deficient pancreatic cancer xenografts. *Clin Cancer Res*, 17, 2799-806.

RHODES, J. M. & SIMONS, M. 2007. The extracellular matrix and blood vessel formation: not just a scaffold. *J Cell Mol Med*, 11, 176-205.

RIDGWAY, J., ZHANG, G., WU, Y., STAWICKI, S., LIANG, W. C., CHANTHERY, Y., KOWALSKI, J., WATTS, R. J., CALLAHAN, C., KASMAN, I., SINGH, M., CHIEN, M., TAN, C., HONGO, J. A., DE SAUVAGE, F., PLOWMAN, G. & YAN, M. 2006. Inhibition of Dll4 signalling inhibits tumour growth by deregulating angiogenesis. *Nature*, 444, 1083-7.

RISAU, W., SARIOLA, H., ZERWES, H. G., SASSE, J., EKBLUM, P., KEMLER, R. & DOETSCHMAN, T. 1988. Vasculogenesis and angiogenesis in embryonic-stem-cell-derived embryoid bodies. *Development*, 102, 471-8.

RIVLIN, N., BROSH, R., OREN, M. & ROTTER, V. 2011. Mutations in the p53 Tumor Suppressor Gene: Important Milestones at the Various Steps of Tumorigenesis. *Genes & Cancer*, 2, 466-474.

RIVOIRE, M., DE CIAN, F., MEEUS, P., NEGRIER, S., SEBBAN, H. & KAEMMERLEN, P. 2002. Combination of neoadjuvant chemotherapy with cryotherapy and surgical resection for the treatment of unresectable liver metastases from colorectal carcinoma. *Cancer*, 95, 2283-92.

ROCHA, F. G. & HELTON, W. S. 2012. Resectability of colorectal liver metastases: an evolving definition. *HPB*, 14, 283-284.

RODRIGUEZ-MANZANEQUE, J. C., LANE, T. F., ORTEGA, M. A., HYNES, R. O., LAWLER, J. & IRUELA-ARISPE, M. L. 2001. Thrombospondin-1 suppresses

spontaneous tumor growth and inhibits activation of matrix metalloproteinase-9 and mobilization of vascular endothelial growth factor. *Proc Natl Acad Sci U S A*, 98, 12485-90.

ROSHAK, A. K., CAPPER, E. A., IMBURGIA, C., FORNWALD, J., SCOTT, G. & MARSHALL, L. A. 2000. The human polo-like kinase, PLK, regulates cdc2/cyclin B through phosphorylation and activation of the cdc25C phosphatase. *Cell Signal*, 12, 405-11.

SAINSON, R. C., AOTO, J., NAKATSU, M. N., HOLDERFIELD, M., CONN, E., KOLLER, E. & HUGHES, C. C. 2005. Cell-autonomous notch signaling regulates endothelial cell branching and proliferation during vascular tubulogenesis. *FASEB J*, 19, 1027-9.

SALTZ, L. B., CLARKE, S., DIAZ-RUBIO, E., SCHEITHAUER, W., FIGER, A., WONG, R., KOSKI, S., LICHINITSER, M., YANG, T. S., RIVERA, F., COUTURE, F., SIRZEN, F. & CASSIDY, J. 2008. Bevacizumab in combination with oxaliplatin-based chemotherapy as first-line therapy in metastatic colorectal cancer: a randomized phase III study. *J Clin Oncol*, 26, 2013-9.

SANCAR, A., LINDSEY-BOLTZ, L. A., UNSAL-KACMAZ, K. & LINN, S. 2004. Molecular mechanisms of mammalian DNA repair and the DNA damage checkpoints. *Annu Rev Biochem*, 73, 39-85.

SARCAR, B., KAHALI, S., PRABHU, A. H., SHUMWAY, S. D., XU, Y., DEMUTH, T. & CHINNAIYAN, P. 2011. Targeting radiation-induced G(2) checkpoint activation

with the Wee-1 inhibitor MK-1775 in glioblastoma cell lines. *Mol Cancer Ther*, 10, 2405-14.

SAUER, R., BECKER, H., HOHENBERGER, W., RODEL, C., WITTEKIND, C., FIETKAU, R., MARTUS, P., TSCHMELITSCH, J., HAGER, E., HESS, C. F., KARSTENS, J. H., LIERSCH, T., SCHMIDBERGER, H. & RAAB, R. 2004. Preoperative versus postoperative chemoradiotherapy for rectal cancer. *N Engl J Med*, 351, 1731-40.

SAUER, R., LIERSCH, T., MERKEL, S., FIETKAU, R., HOHENBERGER, W., HESS, C., BECKER, H., RAAB, H. R., VILLANUEVA, M. T., WITZIGMANN, H., WITTEKIND, C., BEISSBARTH, T. & RODEL, C. 2012. Preoperative versus postoperative chemoradiotherapy for locally advanced rectal cancer: results of the German CAO/ARO/AIO-94 randomized phase III trial after a median follow-up of 11 years. *J Clin Oncol*, 30, 1926-33.

SCALTRITI, M. & BASELGA, J. 2006. The epidermal growth factor receptor pathway: a model for targeted therapy. *Clin Cancer Res*, 12, 5268-72.

SHELLERER, V. S., CRONER, R. S., WEINLANDER, K., HOHENBERGER, W., STURZL, M. & NASCHBERGER, E. 2007. Endothelial cells of human colorectal cancer and healthy colon reveal phenotypic differences in culture. *Lab Invest*, 87, 1159-70.

SCHLESSINGER, J. 2000. Cell signaling by receptor tyrosine kinases. *Cell*, 103, 211-25.

SCHWARZ, G., DROOGMANS, G. & NILIUS, B. 1992. Shear stress induced membrane currents and calcium transients in human vascular endothelial cells. *Pflügers Archiv*, 421, 394-396.

SEAMAN, S., STEVENS, J., YANG, M. Y., LOGSDON, D., GRAFF-CHERRY, C. & ST. CROIX, B. 2007. Genes that Distinguish Physiological and Pathological Angiogenesis. *Cancer cell*, 11, 539-554.

SEMENZA, G. L. 1999. Regulation of mammalian O₂ homeostasis by hypoxia-inducible factor 1. *Annu Rev Cell Dev Biol*, 15, 551-78.

SHIBATA, T., NIINOBU, T., OGATA, N. & TAKAMI, M. 2000. Microwave coagulation therapy for multiple hepatic metastases from colorectal carcinoma. *Cancer*, 89, 276-84.

SHIMIZU, S., YAMADA, N., SAWADA, T., IKEDA, K., NAKATANI, K., SEKI, S., KANEDA, K. & HIRAKAWA, K. 2000. Ultrastructure of early phase hepatic metastasis of human colon carcinoma cells with special reference to desmosomal junctions with hepatocytes. *Pathol Int*, 50, 953-9.

SMEDSRD, B., LE COUTEUR, D., IKEJIMA, K., JAESCHKE, H., KAWADA, N., NAITO, M., KNOLLE, P., NAGY, L., SENOO, H., VIDAL-VANACLOCHA, F. & YAMAGUCHI, N. 2009. Hepatic sinusoidal cells in health and disease: update from the 14th International Symposium. *Liver Int*, 29, 490-501.

ST CROIX, B., RAGO, C., VELCULESCU, V., TRAVERSO, G., ROMANS, K. E., MONTGOMERY, E., LAL, A., RIGGINS, G. J., LENGAUER, C., VOGELSTEIN, B.

& KINZLER, K. W. 2000. Genes expressed in human tumor endothelium. *Science*, 289, 1197-202.

STARKE, R. D., FERRARO, F., PASCHALAKI, K. E., DRYDEN, N. H., MCKINNON, T. A., SUTTON, R. E., PAYNE, E. M., HASKARD, D. O., HUGHES, A. D., CUTLER, D. F., LAFFAN, M. A. & RANDI, A. M. 2011. Endothelial von Willebrand factor regulates angiogenesis. *Blood*, 117, 1071-80.

STATON, C. A., REED, M. W. R. & BROWN, N. J. 2009. A critical analysis of current in vitro and in vivo angiogenesis assays. *International Journal of Experimental Pathology*, 90, 195-221.

STEEGMAIER, M., HOFFMANN, M., BAUM, A., LENART, P., PETRONCZKI, M., KRSSAK, M., GURTLER, U., GARIN-CHESA, P., LIEB, S., QUANT, J., GRAUERT, M., ADOLF, G. R., KRAUT, N., PETERS, J. M. & RETTIG, W. J. 2007. BI 2536, a potent and selective inhibitor of polo-like kinase 1, inhibits tumor growth in vivo. *Curr Biol*, 17, 316-22.

SUN, Y., WANG, J. W., LIU, Y. Y., YU, Q. T., ZHANG, Y. P., LI, K., XU, L. Y., LUO, S. X., QIN, F. Z., CHEN, Z. T., LIU, W. C., ZHOU, Q. H., CHEN, Q., NAN, K. J., LIU, X. Q., LIU, W., LIANG, H. J., LU, H. S., WANG, X. W., WANG, J. J., SONG, S. P., TU, Y. R., ZHOU, J. M. & LI, W. L. 2013. Long-term results of a randomized, double-blind, and placebo-controlled phase III trial: Endostar (rh-endostatin) versus placebo in combination with vinorelbine and cisplatin in advanced non-small cell lung cancer. *Thoracic Cancer*, 4, 440-448.

SURVEILLANCE EPIDEMIOLOGY AND END RESULTS (SEER) PROGRAM. 2016. *SEER Stat Fact Sheets: Colon and Rectum Cancer* [Online]. Surveillance Epidemiology and End Results (SEER) Program, . Available: <http://seer.cancer.gov/statfacts/html/colorect.html> [Accessed 22 August 2016].

SYEDA, R., XU, J., DUBIN, A. E., COSTE, B., MATHUR, J., HUYNH, T., MATZEN, J., LAO, J., TULLY, D. C., ENGELS, I. H., PETRASSI, H. M., SCHUMACHER, A. M., MONTAL, M., BANDELL, M. & PATAPOUTIAN, A. 2015. Chemical activation of the mechanotransduction channel Piezo1. *eLife*, 4, e07369.

TABERNERO, J., YOSHINO, T., COHN, A. L., OBERMANNOVA, R., BODOKY, G., GARCIA-CARBONERO, R., CIULEANU, T. E., PORTNOY, D. C., VAN CUTSEM, E., GROTHEY, A., PRAUSOVA, J., GARCIA-ALFONSO, P., YAMAZAKI, K., CLINGAN, P. R., LONARDI, S., KIM, T. W., SIMMS, L., CHANG, S. C. & NASROULAH, F. 2015. Ramucirumab versus placebo in combination with second-line FOLFIRI in patients with metastatic colorectal carcinoma that progressed during or after first-line therapy with bevacizumab, oxaliplatin, and a fluoropyrimidine (RAISE): a randomised, double-blind, multicentre, phase 3 study. *Lancet Oncol*, 16, 499-508.

TABUSE, K. 1979. A new operative procedure of hepatic surgery using a microwave tissue coagulator. *Nihon Geka Hokan*, 48, 160-72.

TAMANDL, D., GRUENBERGER, B., KLINGER, M., HERBERGER, B., KACZIREK, K., FLEISCHMANN, E. & GRUENBERGER, T. 2010. Liver resection remains a safe procedure after neoadjuvant chemotherapy including bevacizumab: a case-controlled study. *Ann Surg*, 252, 124-30.

THERMOFISHER SCIENTIFIC 2016. Introduction to Flow Cytometry [Online]. Thermofisher Scientific Inc. Available: <http://www.thermofisher.com> [Accessed 22nd August 2016]

THURSTON, G. & KITAJEWSKI, J. 2008. VEGF and Delta-Notch: interacting signalling pathways in tumour angiogenesis. *British Journal of Cancer*, 99, 1204-1209.

TIAN, H., MCKNIGHT, S. L. & RUSSELL, D. W. 1997. Endothelial PAS domain protein 1 (EPAS1), a transcription factor selectively expressed in endothelial cells. *Genes Dev*, 11, 72-82.

TOL, J. & PUNT, C. J. 2010. Monoclonal antibodies in the treatment of metastatic colorectal cancer: a review. *Clin Ther*, 32, 437-53.

TOMLINSON, J. S., JARNAGIN, W. R., DEMATTEO, R. P., FONG, Y., KORNPAT, P., GONEN, M., KEMENY, N., BRENNAN, M. F., BLUMGART, L. H. & D'ANGELICA, M. 2007. Actual 10-year survival after resection of colorectal liver metastases defines cure. *J Clin Oncol*, 25, 4575-80.

TORRE, L. A., BRAY, F., SIEGEL, R. L., FERLAY, J., LORTET-TIEULENT, J. & JEMAL, A. 2015. Global cancer statistics, 2012. *CA: A Cancer Journal for Clinicians*, 65, 87-108.

TVEIT, K. M., GUREN, T., GLIMELIUS, B., PFEIFFER, P., SORBYE, H., PYRHONEN, S., SIGURDSSON, F., KURE, E., IKDAHL, T., SKOVLUND, E., FOKSTUEN, T., HANSEN, F., HOFSLI, E., BIRKEMEYER, E., JOHANSSON, A.,

STARKHAMMAR, H., YILMAZ, M. K., KELDSEN, N., ERDAL, A. B., DAJANI, O., DAHL, O. & CHRISTOFFERSEN, T. 2012. Phase III trial of cetuximab with continuous or intermittent fluorouracil, leucovorin, and oxaliplatin (Nordic FLOX) versus FLOX alone in first-line treatment of metastatic colorectal cancer: the NORDIC-VII study. *J Clin Oncol*, 30, 1755-62.

VAN BEIJNUM, J. R., DINGS, R. P., VAN DER LINDEN, E., ZWAANS, B. M., RAMAEKERS, F. C., MAYO, K. H. & GRIFFIOEN, A. W. 2006. Gene expression of tumor angiogenesis dissected: specific targeting of colon cancer angiogenic vasculature. *Blood*, 108, 2339-48.

VAN BEIJNUM, J. R., ROUSCH, M., CASTERMANS, K., VAN DER LINDEN, E. & GRIFFIOEN, A. W. 2008. Isolation of endothelial cells from fresh tissues. *Nat. Protocols*, 3, 1085-1091.

VAN CUTSEM, E., KOHNE, C. H., LANG, I., FOLPRECHT, G., NOWACKI, M. P., CASCINU, S., SHCHEPOTIN, I., MAUREL, J., CUNNINGHAM, D., TEJPAR, S., SCHLICHTING, M., ZUBEL, A., CELIK, I., ROUGIER, P. & CIARDIELLO, F. 2011. Cetuximab plus irinotecan, fluorouracil, and leucovorin as first-line treatment for metastatic colorectal cancer: updated analysis of overall survival according to tumor KRAS and BRAF mutation status. *J Clin Oncol*, 29, 2011-9.

VAN CUTSEM, E., TABERNERO, J., LAKOMY, R., PRENEN, H., PRAUSOVA, J., MACARULLA, T., RUFF, P., VAN HAZEL, G. A., MOISEYENKO, V., FERRY, D., MCKENDRICK, J., POLIKOFF, J., TELLIER, A., CASTAN, R. & ALLEGRA, C. 2012. Addition of aflibercept to fluorouracil, leucovorin, and irinotecan improves

survival in a phase III randomized trial in patients with metastatic colorectal cancer previously treated with an oxaliplatin-based regimen. *J Clin Oncol*, 30, 3499-506.

VAN LINDEN, A. A., BATURIN, D., FORD, J. B., FOSMIRE, S. P., GARDNER, L., KORCH, C., REIGAN, P. & PORTER, C. C. 2013. Inhibition of Wee1 sensitizes cancer cells to antimetabolite chemotherapeutics in vitro and in vivo, independent of p53 functionality. *Mol Cancer Ther*, 12, 2675-84.

VASSILEV, L. T., TOVAR, C., CHEN, S., KNEZEVIC, D., ZHAO, X., SUN, H., HEIMBROOK, D. C. & CHEN, L. 2006. Selective small-molecule inhibitor reveals critical mitotic functions of human CDK1. *Proceedings of the National Academy of Sciences of the United States of America*, 103, 10660-10665.

VASUDEV, N. S. & REYNOLDS, A. R. 2014. Anti-angiogenic therapy for cancer: current progress, unresolved questions and future directions. *Angiogenesis*, 17, 471-94.

VATANDOUST, S., PRICE, T. J. & KARAPETIS, C. S. 2015. Colorectal cancer: Metastases to a single organ. *World J Gastroenterol*, 21, 11767-76.

VENNIX, S., PELZERS, L., BOUVY, N., BEETS, G. L., PIERIE, J. P., WIGGERS, T. & BREUKINK, S. 2014. Laparoscopic versus open total mesorectal excision for rectal cancer. *Cochrane Database Syst Rev*, CD005200.

VERMEULEN, P. B., COLPAERT, C., SALGADO, R., ROYERS, R., HELLEMANS, H., VAN DEN HEUVEL, E., GOOVAERTS, G., DIRIX, L. Y. & VAN MARCK, E.

2001. Liver metastases from colorectal adenocarcinomas grow in three patterns with different angiogenesis and desmoplasia. *J Pathol*, 195, 336-42.

VERMEULEN, P. B., GASPARINI, G., FOX, S. B., COLPAERT, C., MARSON, L. P., GION, M., BELIEN, J. A., DE WAAL, R. M., VAN MARCK, E., MAGNANI, E., WEIDNER, N., HARRIS, A. L. & DIRIX, L. Y. 2002. Second international consensus on the methodology and criteria of evaluation of angiogenesis quantification in solid human tumours. *Eur J Cancer*, 38, 1564-79.

VOGL, T. J., STRAUB, R., EICHLER, K., SOLLNER, O. & MACK, M. G. 2004. Colorectal carcinoma metastases in liver: laser-induced interstitial thermotherapy--local tumor control rate and survival data. *Radiology*, 230, 450-8.

WANG, Y., LI, J., BOOHER, R., KRAKER, A., LAWRENCE, T., LEOPOLD, W. & SUN, Y. 2001. Radiosensitization of p53 Mutant Cells by PD0166285, a Novel G2 Checkpoint Abrogator. *Cancer Res*, 61, 8211-8217.

WATANABE, N., BROOME, M. & HUNTER, T. 1995. Regulation of the human WEE1Hu CDK tyrosine 15-kinase during the cell cycle. *The EMBO Journal*, 14, 1878-1891.

WEISS, L. 2000. Metastasis of cancer: a conceptual history from antiquity to the 1990s. *Cancer Metastasis Rev*, 19, I-XI, 193-383.

WELEN, K., JENNBACHEN, K., TESAN, T. & DAMBER, J. E. 2009. Pericyte coverage decreases invasion of tumour cells into blood vessels in prostate cancer xenografts. *Prostate Cancer Prostatic Dis*, 12, 41-6.

WILHELM, S. M., DUMAS, J., ADNANE, L., LYNCH, M., CARTER, C. A., SCHUTZ, G., THIERAUCH, K. H. & ZOPF, D. 2011. Regorafenib (BAY 73-4506): a new oral multikinase inhibitor of angiogenic, stromal and oncogenic receptor tyrosine kinases with potent preclinical antitumor activity. *Int J Cancer*, 129, 245-55.

WONG, S. L., MANGU, P. B., CHOTI, M. A., CROCENZI, T. S., DODD, G. D., 3RD, DORFMAN, G. S., ENG, C., FONG, Y., GIUSTI, A. F., LU, D., MARSLAND, T. A., MICHELSON, R., POSTON, G. J., SCHRAG, D., SEIDENFELD, J. & BENSON, A. B., 3RD 2010. American Society of Clinical Oncology 2009 clinical evidence review on radiofrequency ablation of hepatic metastases from colorectal cancer. *J Clin Oncol*, 28, 493-508.

WU, F. T. H., STEFANINI, M. O., GABHANN, F. M., KONTOS, C. D., ANNEX, B. H. & POPEL, A. S. 2010. A systems biology perspective on sVEGFR1: its biological function, pathogenic role and therapeutic use. *Journal of Cellular and Molecular Medicine*, 14, 528-552.

XIONG, Y. Q., SUN, H. C., ZHANG, W., ZHU, X. D., ZHUANG, P. Y., ZHANG, J. B., WANG, L., WU, W. Z., QIN, L. X. & TANG, Z. Y. 2009. Human hepatocellular carcinoma tumor-derived endothelial cells manifest increased angiogenesis capability and drug resistance compared with normal endothelial cells. *Clin Cancer Res*, 15, 4838-46.

YANG, K.Y., LIU, K.T., CHEN, Y.C., CHEN, C.S., LEE, Y.C., PERNG, R.P. & FENG, J.Y. 2011. Plasma soluble vascular endothelial growth factor receptor-1

levels predict outcomes of pneumonia-related septic shock patients: a prospective observational study. *Critical Care*, 15, R11-R11.

YONENAGA, Y., MORI, A., ONODERA, H., YASUDA, S., OE, H., FUJIMOTO, A., TACHIBANA, T. & IMAMURA, M. 2005. Absence of smooth muscle actin-positive pericyte coverage of tumor vessels correlates with hematogenous metastasis and prognosis of colorectal cancer patients. *Oncology*, 69, 159-66.

YOSHIDA, T., TANAKA, S., MOGI, A., SHITARA, Y. & KUWANO, H. 2004. The clinical significance of Cyclin B1 and Wee1 expression in non-small-cell lung cancer. *Ann Oncol*, 15, 252-6.

YU, J. L., RAK, J. W., COOMBER, B. L., HICKLIN, D. J. & KERBEL, R. S. 2002. Effect of p53 status on tumor response to antiangiogenic therapy. *Science*, 295, 1526-8.

ZHANG, X. & LAWLER, J. 2007. Thrombospondin-based Antiangiogenic Therapy. *Microvascular research*, 74, 90-99.

Appendix I: Differentially Expressed Proteins in the Proteomics Screen

On the following eleven pages are the 157 differentially expressed proteins in LECs and CLMECs as determined by proteomic studies. In each case, the protein intensity in LECs and CLMECs is reported along with the LEC to CLMEC intensity ratio and p-value. Proteins are ranked according to their p-value.

Protein	Mean LEC Intensity	Mean CLMEC Intensity	LEC/CLMEC Ratio	LEC vs. CLMEC p value
Thrombospondin-1	47508.6	134408	0.356179697	0.00025449
cAMP-Dependent Protein Kinase Type I-Beta Regulatory Subunit	1234.5	392.45	3.368114727	0.000697796
Rho GTPase-Activating Protein 7	664.164	2519.78	0.267445423	0.001026153
Vascular Endothelial Growth Factor Receptor 1	3265.7	8222.44	0.403526385	0.001088631
60S Ribosomal Protein L37	2103.42	4174.36	0.480491872	0.001879499
Tubulin Alpha-4A Chain	9472.1	4342.2	2.781709713	0.001927656
LIM Domain Only Protein 7	1345.32	5934.74	0.231716048	0.002053259
Solute Carrier Family 2, Facilitated Glucose Transporter Member 1	1141.878	2887.7	0.397928842	0.002208671
E3 Ubiquitin-Protein Ligase RBBP6	210.436	803.504	0.253763778	0.002245187
Transforming Growth Factor Beta-2	1313.032	12818.66	0.116912767	0.00273289
Neuronal Growth Regulator 1	305.332	770.166	0.400242361	0.002752091
Lysosome-Associated Membrane Glycoprotein 2	2604.78	3397.5	0.740762045	0.003172724
LIM and Cysteine-Rich Domains Protein 1	320.98	1872.46	0.186101686	0.003259361
Cyclin-Dependent Kinase Inhibitor 1	587.758	1255.236	0.455710266	0.003761478
Fibronectin Isoform 17	56968.2	192440	0.308406416	0.003766208

Protein	Mean LEC Intensity	Mean CLMEC Intensity	LEC/CLMEC Ratio	LEC vs. CLMEC p value
Coiled-coil domain-containing protein 86	724.718	957.854	0.713252433	0.004068168
Isoform 2 of Sodium-coupled neutral amino acid transporter 2	1434.508	3904.14	0.373888007	0.004344309
Biglycan	391.128	1421.578	0.295381739	0.00478014
Importin-8	2483.78	4928.94	0.520507138	0.005825925
Isoform 8 of Double-stranded RNA-binding protein Staufen homolog 2	5958.24	17718.8	0.345370839	0.005835435
Isoform 4 of Receptor-type tyrosine-protein phosphatase alpha	1144.052	629.182	1.848735337	0.006215804
Isoform 2 of Aldo-keto reductase family 1 member C3	3652.16	758.426	5.605668297	0.006699675
Protein kinase C and casein kinase substrate in neurons protein 3	111.2834	739.054	0.1441083	0.006723402
Isoform 2 of EGF-like repeat and discoidin I-like domain-containing protein 3	670.978	11905.32	0.063406126	0.007037614
Alpha- and gamma-adaptin-binding protein p34	653.164	1463.968	0.455146068	0.007106586
Glutathione peroxidase 7	497.4486	1661.4	0.316800311	0.007569646
Isoform 5 of Neuron navigator 1	2328.84	8991.92	0.284549309	0.007720948
Protein phosphatase methyltransferase 1	3141.22	12605.84	0.274688454	0.007742732
Isoform 2 of Protein tweety homolog 3	6522.38	20097.4	0.3268724	0.007788754
Growth/differentiation factor 15	3585.68	6403.74	0.562366421	0.008076002

Protein	Mean LEC Intensity	Mean CLMEC Intensity	LEC/CLMEC Ratio	LEC vs. CLMEC p value
Ribosome biogenesis regulatory protein homolog	1254.12	3212.46	0.407326644	0.009056148
Vesicle-associated membrane protein 5	3807.78	1785.064	2.539389755	0.009316384
Endothelial cell-specific molecule 1	662.816	198.1932	4.235193186	0.009962981
Isoform PDE2A1 of cGMP-dependent 3,5-cyclic phosphodiesterase	5686.98	663.948	9.505616533	0.010206262
Ubiquitin-associated and SH3 domain-containing protein B	1003.138	5196.4	0.210718166	0.010831017
Glia maturation factor gamma	3104.86	1467.74	2.252407349	0.012125557
Isoform 11 of Dysferlin	59041.6	27907.8	2.517517756	0.012231579
Histone H1.3	2456.88	10645.16	0.26712756	0.012661688
Adhesion G protein-coupled receptor F5	19118.4	3424.18	6.607238943	0.012899255
Isoform 2 of Protein CDV3 homolog	1613.21	2189.96	0.641224705	0.012997302
Isoform 2 of CB1 cannabinoid receptor-interacting protein 1	1637.028	2869.1	0.580130921	0.013357121
rRNA-processing protein UTP23 homolog	191.166	377.876	0.471870502	0.013370795
THUMP domain-containing protein 1	974.932	1671.416	0.596434161	0.013846194
Sterile alpha motif domain-containing protein 9-like	578.952	1560.64	0.406409526	0.014494289
Procollagen-lysine,2-oxoglutarate 5-dioxygenase 2	10332.6	44884.8	0.256392503	0.014525053

Protein	Mean LEC Intensity	Mean CLMEC Intensity	LEC/CLMEC Ratio	LEC vs. CLMEC p value
Isoform 2 of 72 kDa type IV collagenase	752.012	2600.32	0.315606825	0.014552779
Isoform 5 of Multiple C2 and transmembrane domain-containing protein 1	313.352	1014.872	0.339140308	0.014685317
HLA class I histocompatibility antigen, A-3 alpha chain	2855.078	6975.92	0.349464243	0.014795925
Mesencephalic astrocyte-derived neurotrophic factor	6546.78	12655.4	0.525883654	0.015628764
Isoform 3 of RNA-binding protein Musashi homolog 2	449.416	1721.66	0.288453547	0.01579305
Alpha-2-macroglobulin	1256.654	164.17	7.65458975	0.016088913
Isoform 2 of Peptidyl-prolyl cis-trans isomerase FKBP11	5558.88	8482.02	0.666936853	0.016828787
Paladin	5884.22	1256.704	6.726440925	0.017044863
Transmembrane 4 L6 family member 18	531.04	75.234	7.05851078	0.017504998
Adenosine deaminase	2939.02	9036.32	0.369328104	0.017669589
Low density lipoprotein receptor adapter protein 1	16.2066	138.0532	0.098658306	0.017746818
Isoform 2 of Vacuolar protein sorting-associated protein 51	2074.66	1532.58	1.433633286	0.018305016
Latent-transforming growth factor beta-binding protein 1	323.992	2306.8	0.167137338	0.018410987
Guanylate kinase	2340.52	3965.68	0.609399433	0.018738363

Protein	Mean LEC Intensity	Mean CLMEC Intensity	LEC/CLMEC Ratio	LEC vs. CLMEC p value
Phospholipid scramblase 4	3251.36	7061.78	0.477115651	0.018954935
Isoform 4 of Band 4.1-like protein 3	6370.74	26672	0.269830675	0.019073238
28S ribosomal protein S6, mitochondrial	348.234	1063.456	0.293886526	0.019183599
Isoform 2 of Extracellular sulfatase Sulf-2	6545.5	2391.78	3.004041572	0.020063103
EGF-containing fibulin-like extracellular matrix protein 2	484.396	1304.78	0.402407864	0.020491576
Isoform 2 of Insulin-like growth factor-binding protein 7	9492.88	23337.8	0.433569375	0.020584888
Isoform 3 of Mediator of RNA polymerase II transcription subunit 12	325.338	1108.048	0.345616678	0.020645689
High mobility group protein B3	4658.58	9523.2	0.461054208	0.020652251
Dual specificity protein phosphatase 23	2186.3	10055.38	0.248739991	0.021088999
Sulfide:quinone oxidoreductase, mitochondrial	23645.6	7662.86	4.099915442	0.021202375
Isoform 3 of Apoptosis-associated speck-like protein containing a CARD	589.38	291.726	2.02032044	0.021212955
Isoform 4 of Nucleoporin NDC1	1396.198	4185.14	0.367382492	0.021420395
Follistatin-related protein 1	2727.814	9737.66	0.317876958	0.02199752
Polypeptide N-acetylgalactosaminyltransferase 2	8360.1	18723.6	0.480791793	0.022494818
Isoform 5 of Growth arrest-specific protein	297.55	598.082	0.501837117	0.022504674

Protein	Mean LEC Intensity	Mean CLMEC Intensity	LEC/CLMEC Ratio	LEC vs. CLMEC p value
Splicing factor 45	1542.554	1979.9	0.76870575	0.022669355
Isoform 2 of Ras-specific guanine nucleotide-releasing factor RalGPS2	209.26	483.94	0.361121318	0.022690513
Protein-methionine sulfoxide oxidase	4464.02	8847.58	0.532623888	0.02388848
Isoform 3 of Cell adhesion molecule 3	12.2186	610.938	0.03306972	0.024022651
Isoform LMP2.S of Proteasome subunit beta type-9	3877.78	2081.62	2.134099819	0.024940775
Heme oxygenase 1	12563.08	3411.8	4.197901738	0.02502463
Tryptophan--tRNA ligase, cytoplasmic	71986.4	28934.4	2.936182895	0.025026045
TGF-beta receptor type-2	19308	11591.8	1.76429087	0.025102754
Isoform 3 of Phosphatidylinositol 5-phosphate 4-kinase type-2 gamma	190.6484	462.646	0.455904701	0.025417738
Alpha-crystallin B chain	5854.966	25054.6	0.28549153	0.025609345
Sulfotransferase family cytosolic 1B member 1	3541.42	15411.48	0.249970933	0.027371235
Isoform 3 of NAD(P)H dehydrogenase [quinone] 1	34462.6	18410.56	2.272456824	0.028238465
Isoform 3 of Tetraspanin-3	146.842	475.832	0.284169326	0.028797587
Isoform 2 of Splicing factor, arginine/serine-rich 15	43.6264	215.6516	0.174707439	0.029021641
Uridine phosphorylase 1	10801.38	2327.78	6.23766498	0.029217897

Protein	Mean LEC Intensity	Mean CLMEC Intensity	LEC/CLMEC Ratio	LEC vs. CLMEC p value
Nucleoredoxin	802.22	2646.66	0.326288602	0.029362216
Transmembrane protein 263	4958.08	12674.94	0.427565822	0.029607408
Isoform 2 of Kinesin-like protein KIF2A	7241.94	12031.1	0.613482771	0.030807409
Guanylate-binding protein 2	8374.56	3034	3.357548483	0.030870993
Isoform 4 of Collagen alpha-1(XII) chain	9407.94	24902.8	0.434297779	0.03163561
Isoform 4 of Nexilin	4277.32	9970.6	0.447643386	0.031794821
40S ribosomal protein S19	13087.7	34889.4	0.383927191	0.031856666
Histone H1.2	999.87	5057.66	0.257122448	0.032100085
BAG family molecular chaperone regulator 2	3955.08	7967.12	0.523075759	0.032387614
Ankyrin repeat domain-containing protein 1	1126.252	2238.98	0.54060452	0.032408486
Ribonucleoside-diphosphate reductase large subunit	7522.56	17145.74	0.451666451	0.032994065
Isoform 3 of Galectin-9	5556.38	1026.924	7.100114932	0.03394191
Isoform BIN1-10-13 of Myc box-dependent-interacting protein 1	687.214	1781.41	0.414670863	0.035386312
V-type proton ATPase subunit F	2344.66	4068.08	0.587194382	0.035388671
Isoform 3 of Centrosomal protein POC5	1532.854	3565.58	0.479514364	0.035531842

Protein	Mean LEC Intensity	Mean CLMEC Intensity	LEC/CLMEC Ratio	LEC vs. CLMEC p value
COMM domain-containing protein 8	921.056	1665.534	0.610585206	0.035581682
von Willebrand factor	162997.4	67449.4	2.782607533	0.035950566
Isoform 2 of Regulation of nuclear pre-mRNA domain-containing protein 1A	731.156	1670.224	0.475753818	0.036116789
Isoform 3 of Acidic leucine-rich nuclear phosphoprotein 32 family member E	1142.92	1872.2	0.632178902	0.03613275
Lamina-associated polypeptide 2, isoform alpha	541.86	1745.326	0.340324002	0.036133592
DNA damage-binding protein 2	818.614	1868.26	0.495396854	0.037647896
Spermine synthase	3412.62	5310.52	0.680469675	0.0378676
Transgelin	15101.68	78022.8	0.306995577	0.038056208
Claudin-5	7378.44	1868.702	5.122690124	0.038142047
2-5-oligoadenylate synthase 3	4750.98	1681.79	4.102135698	0.038293601
Ras GTPase-activating protein-binding protein 2	2482.4	5288.98	0.511259811	0.038795691
mRNA export factor	94.4354	341.322	0.329786579	0.039748566
Connective tissue growth factor	19785.64	38894.2	0.541921167	0.039769657
Inhibitor of nuclear factor kappa-B kinase-interacting protein	15260.9	27825.8	0.552701271	0.03988357
Secretory carrier-associated membrane protein 2	1283.336	899.99	1.538070059	0.040455832

Protein	Mean LEC Intensity	Mean CLMEC Intensity	LEC/CLMEC Ratio	LEC vs. CLMEC p value
Tumor necrosis factor receptor superfamily member 10D	0	178.3018	0	0.040663093
Mitogen-activated protein kinase kinase kinase 11	895.922	628.936	1.621222102	0.04128939
Isoform 3 of UPF0585 protein C16orf13	1240.668	3428.92	0.430651527	0.041736248
Isoform 2 of RAB6A-GEF complex partner protein 1	230.552	598.546	0.443864927	0.042220921
Nucleolar protein 7	2157.16	4533.62	0.518457542	0.042709036
Isoform 2 of Serine/threonine-protein phosphatase 2A 56 kDa regulatory subunit alpha isoform	937.066	564.376	2.059221955	0.042747168
Synaptotjanin-2-binding protein	1393.518	3377.86	0.435966767	0.042764676
Leucine-rich repeat-containing protein 32	373.188	94.404	3.95301047	0.043072243
Succinate dehydrogenase [ubiquinone] iron-sulfur subunit, mitochondrial	1931.06	3063.1	0.649018494	0.043153129
Nuclear cap-binding protein subunit 2	2073.96	4860.66	0.486492686	0.043279389
Isoform 5 of Nuclear valosin-containing protein-like	263.074	726.68	0.41145959	0.044625389
Isoform 10 of Dystrophin	20.88	178.4382	0.060539989	0.044872151
Isoform 2 of Endothelial differentiation-related factor 1	5596.74	16804.4	0.356734071	0.04550145
Isoform 3 of Protein enabled homolog	3822.3	9065.86	0.469157909	0.045591055

Protein	Mean LEC Intensity	Mean CLMEC Intensity	LEC/CLMEC Ratio	LEC vs. CLMEC p value
Isoform HERA-B of GTPase Era, mitochondrial	674.06	1332.954	0.504290318	0.045859992
Proteasome activator complex subunit 3	5227.58	11243.8	0.513701169	0.045950975
40S ribosomal protein S9	25967.6	38288.4	0.70246054	0.046311414
40S ribosomal protein S13	22107	44003	0.55423787	0.046357047
Myosin regulatory light polypeptide 9	791.25	1746.58	0.486356918	0.046793222
Bisphosphoglycerate mutase	5101.28	11880.58	0.449100315	0.04718663
Endoplasmic reticulum aminopeptidase 1	29302	15853.82	2.154151925	0.047383219
CDGSH iron-sulfur domain-containing protein 2	2042.8	5036.18	0.469280201	0.047809018
U1 small nuclear ribonucleoprotein C	357.738	548.0312	0.448393024	0.047980957
Ubiquitin-conjugating enzyme E2 G1	550.918	879.012	0.636043993	0.048011806
Isoform 2 of FERM domain-containing protein 6	311.562	763.636	0.448617643	0.048121889
Isoform 3 of Fatty acid desaturase 2	3939.44	11112.04	0.355048732	0.048394822
BTB/POZ domain-containing protein KCTD12	35262.8	14004.64	3.53397243	0.048490204
Isoform 3 of Collagen alpha-1(XVIII) chain	31967	16556.3	2.245111246	0.048584924
Isoform 2 of Transcription elongation regulator 1	1940.64	3928.28	0.549316694	0.048780593

Protein	Mean LEC Intensity	Mean CLMEC Intensity	LEC/CLMEC Ratio	LEC vs. CLMEC p value
Hexokinase-2	3069.36	9633.66	0.36631215	0.049376501
Uncharacterized protein C7orf50	75.792	192.3832	0.233871039	0.049402254
Histone H2B type 2-E	8493.54	23213.2	0.42159489	0.049423362
Isoform 2 of Mitogen-activated protein kinase kinase kinase MLT	667.948	2052.34	0.36756853	0.049543028
Monocarboxylate transporter 4	17263.2	33808.4	0.558376968	0.049651447
Mimitin, mitochondrial	1774.7	4065.46	0.508129698	0.049767666
Tapasin-related protein	682.39	148.432	4.59732403	0.049834907